SCREENING AND CHARACTERIZATION OF ARABIDOPSIS THALIANA MUTANTS WITH ALTERED CAROTENOID PROFILE

A Thesis Submitted to the College of Graduate

Studies and Research

In Partial Fulfillment of the Requirements

For the Degree of Doctor of Philosophy

In the Department of Food and Bioproduct

Sciences

University of Saskatchewan

Saskatoon

By

Karthikeyan Narayanan

PERMISSION TO USE

In presenting this thesis in partial fulfilment of the requirements for a Postgraduate degree from the University of Saskatchewan, I agree that the Libraries of this University may make it freely available for inspection. I further agree that permission for copying of this thesis in any manner, in whole or in part, for scholarly purposes may be granted by the professor or professors who supervised my thesis work or, in their absence, by the Head of the Department or the Dean of the College in which my thesis work was done. It is understood that any copying or publication or use of this thesis or parts thereof for financial gain shall not be allowed without my written permission. It is also understood that due recognition shall be given to me and to the University of Saskatchewan in any scholarly use which may be made of any material in my thesis.

Requests for permission to copy or to make other use of material in this thesis in whole or part should be addressed to:

Head of the Department of Food and Bio-product Sciences
College of Agriculture and Bioresources
University of Saskatchewan
Room: 3E08, Agriculture Building
51 Campus Drive, Saskatoon,
Saskatchewan, S7N 5A8

ABSTRACT

Carotenoids are organic pigments that are mainly found in the chloroplasts and chromoplasts of plants and other photosynthetic organisms. Carotenoid molecules containing oxygen, such as lutein, violaxanthin and zeaxanthin are called xanthophylls and the rest containing un-oxygenated carotenoids are known as carotenes. Carotenoids form the integral part of the photosystem II LHC. Xanthophylls mainly aid in light harvesting and dissipation of harmful excess energy from excited chlorophyll molecules, thereby protecting chlorophyll from photo-degradation. The biosynthesis of carotenoids has been widely studied using plant and algae. However, the regulatory mechanisms involved in carotenoid metabolism need better understanding.

This thesis identified novel regulatory mechanisms involved in the carotenoid biosynthetic pathway using activation-tagged Arabidopsis mutants. Two screening methods, red seed coat screening and norflurazon resistance screening, were used in this study. Fourteen mutants were screened using red seed coat screening but a successful mutant characterization could not be performed due to the unavailability of mutants with a single copy T-DNA insertion.

Norflurazon screening identified eight mutants, out of which two mutants, KN203 and KN231, were characterized. The KN203 mutant had a defective keto-acyl CoA synthase 19 gene. KN203 mutant had lower carotenoid levels in the leaves and increased carotenoid levels in the mature seeds; the mutant was able to revert back to wild type phenotype after complementation of a functional KCS19 gene copy driven by native promoter. The fatty acid analysis indicated that the mutant KN203 had decreased MGDG and increased lysoPG, lysoPC and lysoPE content. Reduced carotenoid content in KN203 leaves was attributed to changes in fatty acid composition of chloroplast envelope membrane.

Mutant KN231 had a T-DNA insertion in a gene encoding a RNA binding protein (*RBP47C*). KN231 leaf carotenoid levels were similar to wild type but their levels were significantly higher in their seeds. Two allelic mutants were selected to characterize the mutants. Overexpression of functional RBP47C in the mutants reverted to wild type phenotype in some overexpression mutants. A tandem repeat homologue of RBP47C, RBP47C'was identified. *In-silico* analysis predicted *RBP47C* to be a potential candidate for chloroplast localization.

ACKNOWLEDGEMENT

I would never have been able to finish my Thesis and this program without the guidance of my committee members, help from friends, and support from my family and wife.

I would like to express my deepest gratitude to my advisors, Dr. Margie Gruber and Dr. George Khachatourians, for his excellent guidance, caring, patience, and providing me with an excellent atmosphere for doing research and learning.

I would like to thank Dr. Abdelali Hannoufa, for selecting me to experience the research of carotenoids in Arabidopsis issues beyond the textbooks and financially supported my research.

I thank Dr. Dwayne Hegedus, and Dr. Gordon Gray for patiently correcting my writing and I would also like to thank them along with Dr. Xiao Qiu for guiding my research for the past several years and helping me to develop my background in plant physiology, biochemistry, and molecular genetics.

Special thanks go to Dr. John Thompson, who was willing to participate in my final defense committee as an external examiner.

I would also like to thank Dr. Darren Korber and Ann Harley for their timely help in keeping me in line with the milestones for completing my degree requirements.

I would like to thank Mr. Delwin Epp, Dr. Shu Wei, and Dr. Bianyun Yu, as good friends were always willing to help and give their best suggestions for successful plant transformations and laboratory management. It would have been a lonely lab without them.

I would like to extend my gratitude to my Parents, family and friends as they were always supporting me and encouraging me with their best wishes.

I would like to thank my wife, Kalaivani. She was always there cheering me up and stood by me through the good times and bad.

Finally, I like to thank all researchers and students for dedicating and sharing their observations and resources for the advancement of science and knowledge.

TABLE OF CONTENTS

LIST OF TABLES

LIST OF FIGURES

LIST OF ABBREVIATIONS

ABA	Abscisic acid
ACP	Acyl carrier protein
ACT	Actin (At3g18780)
AO	Aldehyde oxidase
CCD	Carotenoid deoxygenase
CRTISO	Carotenoid isomerase
DA	Dark-adapted
DAP	Days after pollination
DBMIB	2,5-Dibromo-6-isopropyl-3-methyl-1,4-benzoquinone
DCMU	3-(3,4-Dichlorophenyl)-1,1-dimethylurea
DGDG	Di galactosyl diacyl glycerol
DXS	1-deoxy-D-xylulose 5-phosphate synthase
ESI-MS/MS	electrospray ionization/multi-stage mass spectrometry
ET	Etiolated
GGPP	Geranyl geranyl pyrophosphate
GL	Galactolipid
HPLC	High pressure liquid chromatography
IPP	Isopentyl pyrophosphate
LHC	Light harvesting complex
MEP	Methylerythritol phosphate
MGDG	Mono galactosyl diacyl glycerol
NCED	9-*cis*-epoxycarotenoid dioxygenase
NPQ	Non photochemical quencing
PA	Phosphotidic acid
PAT	Phosphinotricin acetyltransferase
PC	Phosphotidyl choline
LCR14	Pollen coat protein
PCR	Polymerase chain reaction
PDS	Phytoene desaturase
PE	Phosphotidyl ethanolamine
PET	Photosynthetic electron transfer
PEX4	At5g25760
PG	Phosphotidyl glycerol
PI	Phosphotidyl ionositol
PL	Phospholipid
PQH2	Reduced plastoquinone
PS	Phosphotidyl serine
PSI	Photosystem I

PSII	Photosystem II
PSY	Phytoene synthase
PTOX	Plastid-targeted alternative oxidase
qPCR	Quantitative polymerase chain reaction
RBP	RNA binding protein
ROS	Reactive oxygen species
RRM	RNA recognition motif
RSC	Red seed coat
RT-PCR	Reverse trancription - polymerase chain reaction
SLR1-BP	S locus related glycoprotein 1 - binding protein
SQDG	Sulpho quinovosyl diacyl glycerol
TAIL-PCR	Thermal asymmetric interlaced polymerase chain reaction
VDE	Violaxanthin de epoxidase
ZDS	ζ carotene desaturase
ZEP	Zeaxanthin epoxidase
βHYD	β carotene hydroxylase
βLYC	β lycopene cyclase
εHYD	ε carotene hydroxylase
εLYC	ε lycopene cyclase

1 GENERAL INTRODUCTION

Carotenoids represent one of the most fascinating, abundant, and widely distributed classes of natural pigments. They are a class of tetraterpenoid organic pigments that naturally occur in the chloroplasts and chromoplasts of plants and other photosynthetic organisms like algae, some bacteria and fungi. However, they are also found in other living organisms via food uptake (Biehler and Bohn, 2010). Among higher plants, these pigments accumulate in flowers, fruits, and storage roots and are represented by the bright yellow, orange, and red pigments of daffodils, carrots (Castenmiller and West, 1997) and tomatoes (Riso et al., 2004), respectively. In green plant tissues, carotenoids become evident only during the annual degradation of chlorophyll in the autumn. Both unmodified and metabolized dietary carotenoids serve as natural colorants in organisms that do not synthesize carotenoids themselves, such as crustaceans (Matsuno, 2001), insects (Sloan and Moran, 2012), fish (Torrissen and Naevdal, 1988), and birds (McGraw, 2005).

Wackenroder in 1831 isolated and crystallized a compound (β-carotene) from carrot roots which he named “Carotin” (Wackenroder, 1831). Berzelius in 1837 extracted a more polar yellow pigment from senescent autumn leaves and named it "Xanthophyll". Tswett in 1911 recognized the chemically related nature of the two compounds carotin and xanthophyll through chromatography and coined the term “carotenoids” to encompass both classes of pigments (Armstrong and Hearst, 1996). Today, “carotene” is used to refer to a hydrocarbon carotenoid, and xanthophyll denotes a carotene derivative with one or more oxygen-containing functional groups. Currently, about 750 structurally distinct carotenoids and their glycosides have been chemically characterized (Maoka, 2009). This makes carotenoids the second most abundant pigment in nature, behind only chlorophyll (De Spirt et al., 2010). Most carotenoid pigments are C_{40} polyenes and all are derived from phytoene. They are essential components of the photosynthetic machinery, where they are involved in the assembly of the photosystems and play a role in light harvesting, where they absorb light in a broader range of the blue spectrum than chlorophyll and then transfer the energy to chlorophyll. Carotenoids also play a critical role as photoprotective compounds by quenching triplet chlorophyll and singlet oxygen derived from excess light energy, thus limiting membrane damage (Havaux, 1998).

1.1 Carotenoid biosynthesis in plants

Studies on the biosynthesis of carotenoids in plants dating back to the mid-1960s have relied heavily on analyzing intermediates from naturally occurring carotenoid mutants, simulating certain environmental conditions and using herbicides that inhibit carotenoid biosynthesis (Cunningham and Gantt, 1998; Eisenreich et al., 2004). In plants, carotenoids are synthesized and accumulated in plastids, chloroplasts, chromoplasts and elaioplasts. They are lipid soluble byproducts of isoprenoid biosynthesis, where the 5 carbon compound, isopentyl pyrophosphate (IPP) forms the skeleton for the majority of the carotenoids and other isoprenoids. The carotenoid biosynthetic pathway can be divided into three components; 1) synthesis of the carotenoid C_{40} backbone, 2) synthesis of the branching carotenoid lycopene, 3) synthesis of xanthophylls (Armstrong and Hearst, 1996; Cunningham and Gantt, 1998; Cazzonelli and Pogson, 2010).

Carotenoid biosynthesis starts with the sequential assembly and linear addition of isopentyl pyrophosphate compounds to form C_{20} geranyl geranyl-pyrophosphate (GGPP), catalyzed by isopentyl pyrophosphate isomerase (Cunningham and Gantt, 1998; Eisenreich et al., 2004) (Figure 1-1). Phytoene synthase (PSY) condenses two GGPP molecules to form 15-*cis* phytoene (C_{40}) in the first step of the carotenoid pathway. PSY is a rate limiting enzyme of carotenoid biosynthesis in ripening tomato fruits (Bramley, 2002), in canola seeds (Shewmaker et al., 1999) and in marigold flowers (Moehs et al., 2001). The next step is the conversion of phytoene to lycopene via ζ-carotene by two structurally and functionally similar enzymes phytoene desaturase (PDS) and ζ-carotene desaturase (ZDS) (Dong et al., 2007; Li et al., 2007; Qin et al., 2007). Cyclization of lycopene is the branching point in the carotenoid pathway. One branch leads to β-carotene and the other leads to lutein synthesis. β-carotene is produced by a two-step reaction catalyzed by β-lycopene cyclase (β-LYC) that creates one β-ionone ring at each end of the lycopene molecule, while ε-lycopene cyclase (ε-LYC) creates one ε-ring to give δ-carotene (Cunningham and Gantt, 2001; Cheng, 2006).

Hydroxylation of cyclic carotenes at the 3C, 3'C positions is carried out by two types of enzymes, one specific for β-rings and the other for ε-rings. The hydroxylation enzymes catalyze the synthesis of xanthophylls, namely lutein and zeaxanthin. The β-carotene hydroxylase (β-

HYD) converts β-carotene to zeaxanthin via β-cryptoxanthin (Bouvier et al., 1998; Fiore et al., 2006). Two β-carotene hydroxylases have been found in both *Arabidopsis thaliana* (Arabidopsis) and tomato, with one expressed in green leaves and the other in flowers (Hirschberg, 2001). Zeaxanthin epoxidase (ZEP) catalyses the conversion of zeaxanthin to violaxanthin via antheraxanthin (Barrero et al., 2005). It introduces 5, 6-epoxy groups into the 3-hydroxy- β-rings in a redox reaction that requires ferredoxin. In leaves, violaxanthin can be converted back to zeaxanthin by violaxanthin deepoxidase (VDE). VDE is activated by low pH upon ascorbic acid accumulation, and is amassed in the chloroplast lumen under strong light (Bratt et al., 1995; Müller-Moulé et al., 2002). This inter-conversion of zeaxanthin and violaxanthin via antheraxanthin is known as the "xanthophyll cycle". Zeaxanthin is effective in dissipating excess thermal energy in the light-harvesting antennae, thereby protecting the photosynthetic system from damage by intense light.

Many biologically active compounds are breakdown products of carotenoids in plants and precursors in animals and other organisms. The hormone abscisic acid (ABA) is synthesized by two enzymes, 9-cis-epoxycarotenoid dioxygenase (NCED) and aldehyde oxidase (AO) (Hirschberg, 2001). The degradation of β-carotene by carotene-deoxygenase (CCD) is involved in the biosynthesis of strigolactone (reviewed in Holbrook, 1992) , a hormone involved in germination of parasitic seeds and inhibition of shoot branching (Carey and Smale, 2000). In mammals, ingested β-carotene forms the precursor of retinal or Vitamin A. In algae, lycopene and γ-carotene are the precursors to okenone (Hsieh et al., 1999) and myxol biosynthesis (Peers et al., 2009), respectively.

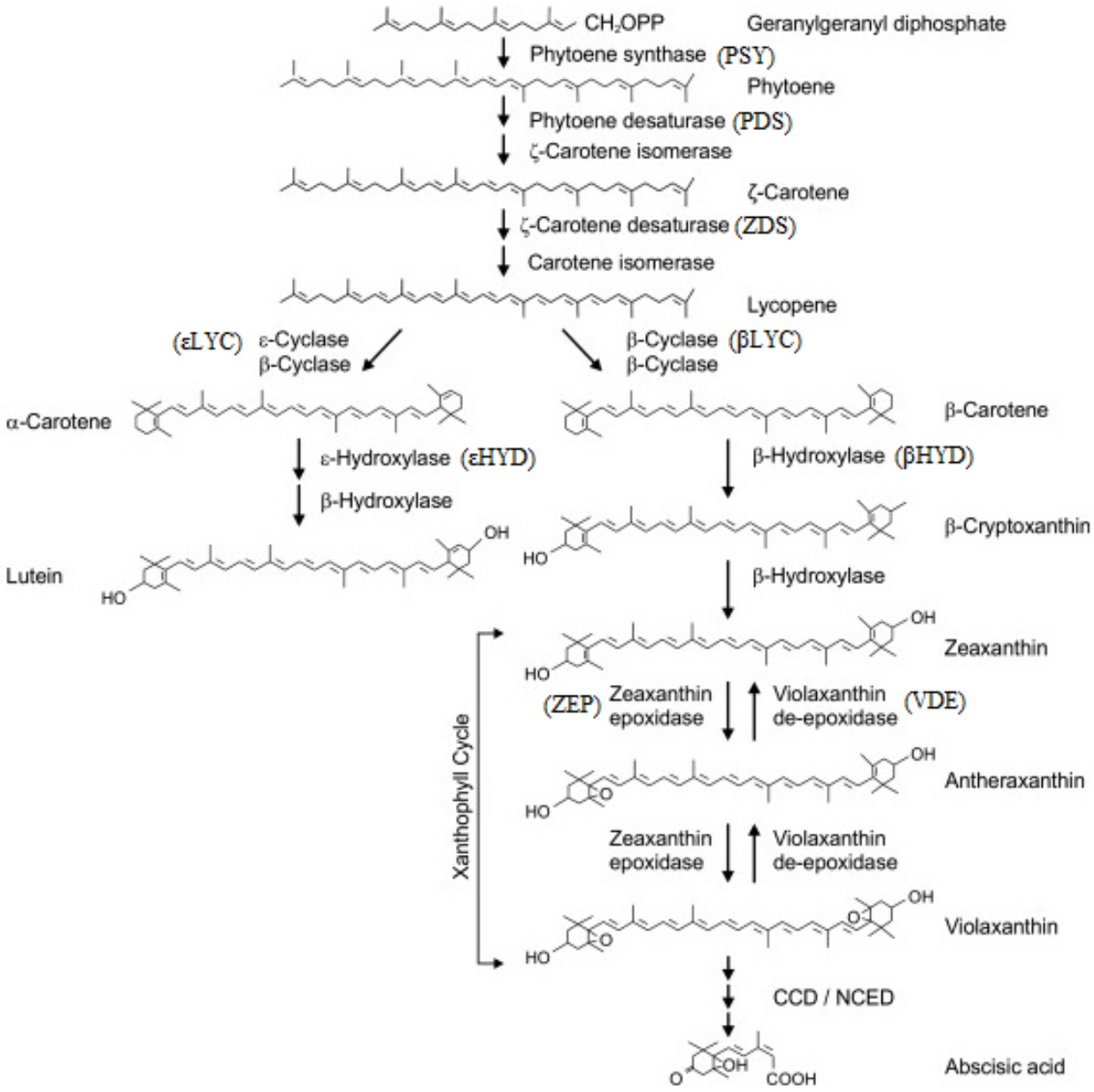

Figure 1-1: Carotenoid biosynthesis pathway in plants. 9-*cis*-epoxycarotenoid dioxygenase (NCED) and carotene-deoxygenases (CCD) are shown in abbreviated forms. Reprinted with permission from Hannoufa (2012).

1.2 Functions of carotenoids

Photosynthesis is the basic source of energy supporting a myriad of life forms on earth. One of the major functions of carotenoids is to protect the photosynthetic machinery. Carotenoids form the integral part of the photosystem II (PSII) light harvesting complex (LHC) (Horn and Paulsen, 2004). Carotenoids (mainly xanthophylls) aid in light harvesting and dissipation of harmful excess energy from excited chlorophyll molecules, thereby protecting chlorophyll from photo-degradation (reviewed in Demmig-Adams, 2002). The role of lutein in photo-protection by deactivation of the triplet chlorophyll molecule and pigment-induced protein folding has been reported in Arabidopsis (Fiore et al., 2006; Jahns and Holzwarth, 2012). Carotenoids have the ability to quench excited sensitizer molecules, as well as quench singlet oxygen ($^1O_2$) (Mozzo et al., 2008; James D, 2009). Zeaxanthin molecules act as direct quenchers of excess excitation by accepting singlet oxygen transferred from chlorophyll (Jahns and Holzwarth, 2012). It has also been observed that at least three chlorophyll molecules are in the proximity of zeaxanthin and violaxanthin, which aids in efficient singlet excitation electron transfer from chlorophylls (Liu et al., 2004).

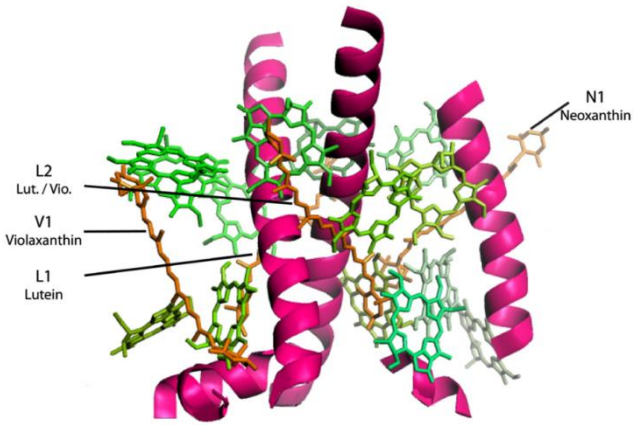

Figure 1-2: Molecular model of light harvesting complex II (LHC II) with carotenoids. Photosystem II light harvesting complex polypeptide monomers with chlorophyll and xanthophyll chromophores bound to different binding sites (L1, L2, V1 and N1). The model has been drawn based on the crystal structures of LHCII trimer. Pink, polypeptide; green, chlorophylls; orange, carotenoids. Reprinted with permission from Triantaphylidès (2009).

Carotenoids were reported to possess antioxidant properties due to their ability to interact with and quench various oxidative molecules that are generated within cells (Abdel-Aal and Akhtar, 2006). β-carotene was shown to act synergistically with α-tocopherol (Vitamin E) and ascorbic acid (Vitamin C) to enhance their antioxidant properties (Hsieh and Goodman, 2006). Lycopene activates the expression of reporter genes fused with antioxidant responsive element sequences in transiently transfected cancer cells, whereas other carotenoids such as phytoene, phytofluene, β-carotene, and astaxanthin did not have a significant effect (Ben-Dor et al., 2005). Lutein protects skin from UV-induced damage and helps reduce the risk of cardiovascular diseases (Alves-Rodrigues and Shao, 2004). In a study involving human hepatoma HepG2 cells, accumulation of β-carotene and astaxanthin suppressed lipid peroxidation and lycopene displayed antioxidant properties *in vitro* (Huang and Kadonaga, 2001).

β-carotene serves as the precursor for vitamin A, retinal, and retinoic acid in mammals, thereby playing essential roles in nutrition, vision, and cellular differentiation, respectively (Olson, 1989). Lutein and zeaxanthin are distributed in various body tissues, but are uniquely concentrated in the retina and lens, indicating a possible specific function in these two vital ocular tissues (Ma and Lin, 2010). Zeaxanthin has been proposed to serve as a blue light photoreceptor in coleoptiles of *Zea mays* (Gyula et al., 2003). Similarly, it was proposed that the protective effects of carotenoids are due to the powerful blue-light filtering activities and antioxidant properties of zeaxanthin (Ma and Lin, 2010). Cleavage of specific cyclic epoxy-xanthophylls serves as the starting point for the biosynthesis of ABA, an important plant hormone (Millar et al., 2006).

Carotenoids are ubiquitous and essential components of photosynthetic tissues in plants, algae and cyanobacteria where they serve two major functions; they provide stability to the light harvesting apparatus (Figure 1-3) and prevent photooxidative damage of the photosynthetic apparatus (Baroli et al., 2003).

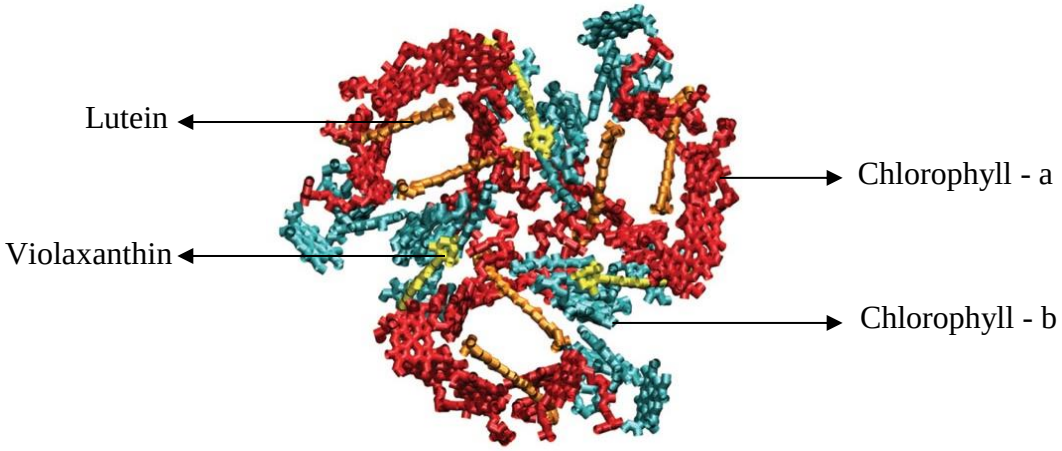

Figure 1-3: Lumenal view of the membrane of the light harvesting complex II. The figure shows only the chromophores. Chlorophyll-a is red and chlorophyll-b is cyan, lutein is orange and violaxanthin is yellow. The image is reused with permission from Scholes, 2011.

Xanthophylls are oxidized carotenoid derivatives of α- and β-carotenes, and include lutein, zeaxanthin, neoxanthin, violaxanthin, and β-cryptoxanthin. During the light reaction of photosynthesis, zeaxanthin epoxidase (ZEP) catalyses the conversion of zeaxanthin within photosystem II (PSII) to violaxanthin via antheraxanthin by introducing 5, 6-epoxy groups using singlet O_2 into the two 3, 5-hydroxy rings (Figure 1-4) in a reduction reaction that accepts electrons from reduced ferredoxin and regenerates oxidized ferredoxin to prevent excess electrons from being passed to photosystem I (PSI). When energy dissipation is no longer required by the photosystem, violaxanthin is re-synthesized from zeaxanthin by zeaxanthin epoxidase (ZEP) on the opposite side of the thylakoid membrane in the stroma (Frechijia et al., 1999; Jahns and Holzwarth, 2012) (Figure 1-4). The xanthophylls, lutein, violaxanthin and zeaxanthin, are physically integrated into the PSII photo complex, since they are essential for the energy dissipating photoprotective function in PSII. While the role of lutein is mainly restricted to its unique function in the deactivation of excited triplet chlorophyll (^{3}Chl) states, zeaxanthin is a major player in the deactivation of excited singlet chlorophyll (^{1}Chl) state by accepting an electron and thus participating in non-photochemical quenching (NPQ) (Mozzo et al., 2008; Jahns and Holzwarth, 2012).

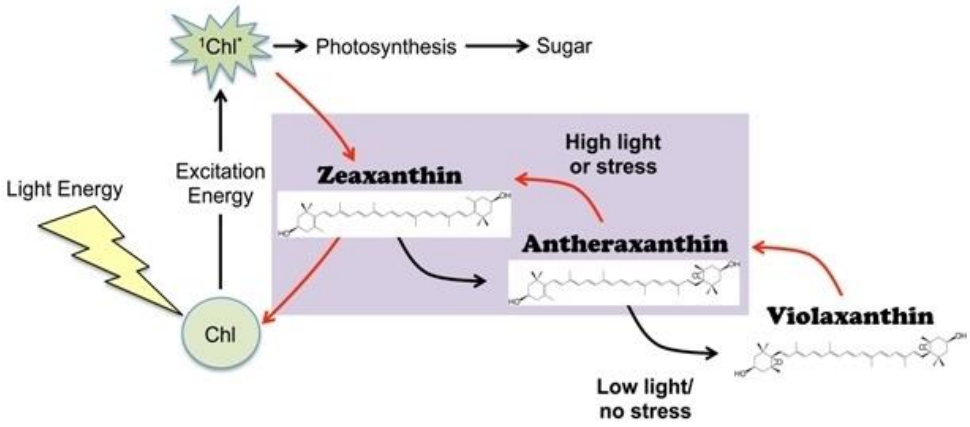

Figure 1-4: Xanthophyll cycle of carotenoids in plants. Xanthophyll cycle aids in photoprotection by dissipation of excess light energy. The xanthophyll violaxanthin is converted to zeaxanthin (via the intermediate antheraxanthin) whenever chloroplasts absorb excess light. Zeaxanthin acts as a key facilitator of the dissipation of excess $^{1}Chl^{*}$. Conversely, when light is not in excess, zeaxanthin is disengaged from energy dissipation and converted back to violaxanthin, thereby returning to efficient utilization of light energy in photosynthesis. Re-used with permission from Demmig-Adams, 2012.

The changes in reduction/oxidation (redox) state of components in the photosynthetic machinery act as signal carriers. These signal carriers regulate the expression of proteins in both chloroplasts and the nucleus (Pfannschmidt, 2003). The transcription of proto-chlorophyllide oxidoreductase, an enzyme involved in the key regulatory step in the synthesis of chlorophyll is repressed in liverworts upon treatment with electron transport inhibitor herbicide 2, 5-dibromo-3-methyl-6-isopropyl-p-benzoquinone (DBMIB) (Eguchi et al., 2002). It is also determined that the DBMIB binds to the Qo-site of the cytochrome Cyt b_6f; thereby inhibiting electron flow to plastocyanin. The inhibition of electron flow to plastocyanin results in the accumulation of reduced plastoquinone (PQH_2) in the thylakoid (Eguchi et al., 2002). In the cyanobacterium, *Synechococcus*, the inverse occurs when the plastoquinone pool is oxidized by PSI harvested light or when the herbicide 3-(3',4'—dichlorophenyl)—1,1'-dimethyl urea (DCMU) binds to the Q_B-site of the PSII D1 protein and prevents oxidized plastoquinone from accepting PSII electron flow (Figure 1-5) (Pfannschmidt, 2003). DCMU treatment increased transcription for the cyanobacterial genes *PSBA*, *PSBD*, *PSAA* and *PSAB*, which encode the PSII reaction-centre proteins D1, D2, PSAA and PSAB (Ronen et al., 2000).

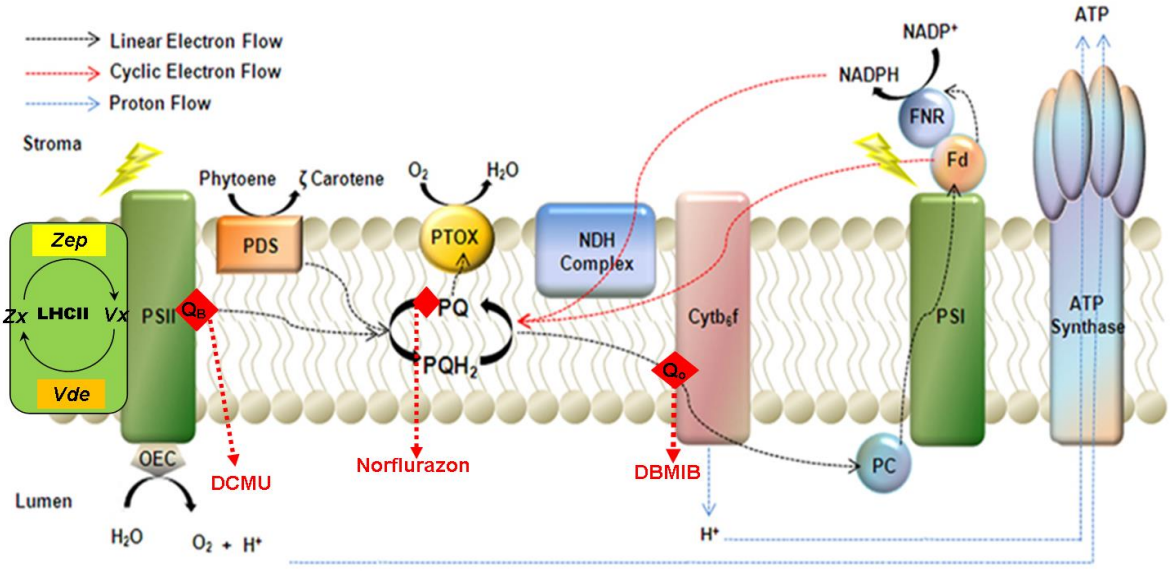

Figure 1-5: The thylakoid membranes and their domains, and the dynamics of the photosynthetic electron-flow machinery. Several dynamic processes regulate the absorption of light: thermal dissipation in the photosystem II (PSII) outer antenna light-harvesting complex II (LHCII) is modulated by the xanthophyll cycle (Zx – zeaxanthin; Vx – violaxanthin; Zep – zeaxanthin epoxidase; Vde – violaxanthin de epoxidase). This dynamic regulation of photosynthesis also involves electron transport. Alternative electron carriers can be recruited depending on nutrient availability for the operation of the electron transport chain; Fd, ferredoxin; FNR, Fd:NADP+ reductase; PQ, plastoquinone; PQH_2, plastoquinol. PTOX is a plastoquinol terminal oxidase that regulates the redox state of the plastoquinone pool during early chloroplast biogenesis. PDS, Phytoene desaturase regulating the flow of electrons to the PQ pool is also shown. The red diamonds indicate the blocking sites; namely, Q_B at the PSII, PQ molecule and Q_o at the $Cytb_6f$ for herbicides DCMU, Norflurazon and DBMIB, respectively. Image adapted and reused with permission from Foudree, 2012.

1.3 Regulation of carotenoid biosynthesis in plants

In 1961, Francois Jacob and Jacques Monod proposed a general model for bacterial gene regulation, providing evidence that genes are controlled at the level of transcription by the products of other genes encoding regulators and that these regulators act through binding at specific sites on DNA near the genes they control (Jacob and Monod, 1961). Five decades later, a large number of DNA-binding proteins with the ability to activate or repress transcription were characterized in both plant and animal models (Farrell, 2007). Furthermore, recent emergence of RNA interference (RNAi)-related mechanisms indicates that RNA can also directly participate in the regulation of gene expression (reviewed by Lauria, 2011). The advent of molecular

characterization and complementation studies using bacterial carotenoid genes have helped to identify the various carotenoid biosynthetic genes in plants (Farré et al., 2010). However, few molecular mechanisms that regulate the synthesis or degradation of carotenoids and sustain the total carotenoid content in photosynthetic and other plant tissues are known (Hannoufa and Hossain, 2012). In plants, carotenoids are synthesized in plastids and their regulation has been studied in chromoplasts and chloroplasts (reviewed in Hirschberg, 2001). So far, it is known that the regulation of carotenoid biosynthesis in plants is accomplished by metabolic flux, stress signalling, and/or epigenetic mechanisms.

Metabolic flux-mediated regulation of carotenogenesis in chromoplasts has been extensively studied using the colour changes that occur in ripening tomato fruit (reviewed in Hirschberg, 2001). The carotenoid composition in the green stages of tomato fruit development is similar to that of leaf tissue. The increase in the level of carotenoids (especially lycopene) occurs at the "breaker" stage when the colour changes from green to orange (Jiang et al., 2008). This color change is due to the degradation of chlorophyll pigments in the green fruit, and also due to the down regulation of both lycopene β-cyclase and lycopene ε-cyclase genes in ripening tomatoes (Ronen et al., 1999; Johansen and Carrington, 2001). Two transcription factors, NOR and NIR, combined with ethylene play a major role in tomato ripening by regulating the phytoene synthase gene (Osorio et al., 2011). Transgenic tobacco seedlings treated with inhibitors of carotenoid and chlorophyll biosynthesis indicated that carotenoid and chlorophyll levels are tightly co-regulated in green tissues. Furthermore, a chemically-induced arrest in pigment biosynthesis resulted in the activation of the *PDS* promoter, suggesting that in green tissues *PDS* transcription may respond to end-product regulation (Corona et al., 1996). In the *cla-1* mutant, chloroplast development is affected leading to an albino leaf phenotype (Mandel et al., 1996). It was later discovered that the *cla* locus encodes the gene for 1-deoxy-D-xylulose 5-phosphate synthase (DXS), the first enzyme of the 2-C-methyl-D-erythritol 4-phosphate (MEP) pathway that leads to the synthesis of carotenoid precursor GGPP (Crowell et al., 2003). DXS (define) is a key rate-limiting step for carotenoid biosynthesis in tomato fruit and was proposed to play a synchronizing role with PSY in the control of carotenoid synthesis during fruit ripening (Lois et al., 2000).

Many carotenoid genes are known to be regulated by various environmental stimuli. In crocus, the zeaxanthin 7,8(7′,8′)-cleavage dioxygenase gene (*CsZCD*) encodes a chromoplast

enzyme that initiates the biogenesis of the crocetin glycosides, picrocrocin, and safranal. It has been reported that the *CsZCD* expression is enhanced under dehydration stress (Bouvier et al., 2003). It is well known that carotenoid biosynthesis occurs in leaves upon light stimulation. Increase in *PSY* mRNA levels correlated with photomorphogenesis due to phytochrome-mediated regulation; however, the expression of *PDS* and geranyl geranyl pyrophosphate synthase (*GGPS*) remained constant (von Lintig et al., 1997). Studies on developing mustard seedlings showed that enzymatically inactive PSY in thylakoid prolamellar body became active upon illumination with white light. Therefore, it was proposed that a similar light-mediated regulation is possible for both carotenoid and chlorophyll biosynthesis (Welsch et al., 2000). Two allelic Arabidopsis mutants, spontaneous cell death1-1 (*spc1-1*) and *spc1-2A,* shown to have a defective ζ-carotene desaturase, displayed bleached leaves and a seedling-lethal phenotype. This gene was further found to be a part of a retrograde signalling system that indicated chloroplast health (Dong et al., 2007). A NCED belonging to the subclass of a carotenoid cleavage dioxygenase (CCD) family was up-regulated by drought and salt stress in a maize vivipary mutant *vp14* (Tan et al., 1997). The Arabidopsis *ZEP* gene was induced by drought, salt, and polyethylene glycol (Xiong et al., 2002). Two genes, β-carotene hydroxylase 1 and β-carotene hydroxylase 3` were induced in rice during dehydration and cold stress (Chaudhary et al., 2010). Similarly, an allele of *PSY* in rice, OsPSY3, increased in roots after salt and drought treatment (Heinzel et al., 1997; Chaudhary et al., 2010).

Several studies involving the epigenetic regulation of carotenoid biosynthesis have been reported. A mutant *ccr1* in Arabidopsis has been reported to encode a histone methyltransferase, Set Domain Group 8 (SDG8) (Cazzonelli et al., 2009). The *ccr1* mutant is not an allelic mutant for any carotenoid structural genes; however, it appears to regulate the carotenoid isomerase (*CRTISO)* gene (involved in the lutein synthesis) since *CRTISO* transcript levels decreased by up to 90% in the *ccr1* mutant (Cazzonelli et al., 2010). A de-etiolating mutant *det1* identified in tomato was shown to be a negative regulator of light-mediated responses in plants (Davuluri et al., 2004) and enhanced carotenoid and flavonoid levels in tomatoes and *Brassica napus* (Davuluri et al., 2005; Wei et al., 2009). *det1* is also shown to regulate lutein, β-carotene and zeaxanthin levels in *B. napus* (Wei et al., 2009), whereas only lycopene and β-carotene in tomatoes (Davuluri et al., 2005).

AtRAP2.2 is a member of the *APETALA2* (AP2)/ethylene-responsive element-binding protein transcription factor family that binds to the ATCTA element. Arabidopsis lines overexpressing *AtRAP2.2* displayed noticeable changes in phytoene synthase and phytoene desaturase transcripts in root-derived calli, which consequently showed a reduction in carotenoid content (Diretto et al., 2007). Constitutive expression of *OsAP2-39* (a member of *AP2* family) in rice led to pleiotropic phenotypes and down-regulation of zeaxanthin epoxidase (*OsZEP-1*), as well as up-regulation of *OsNCED-1* (Os3g0645900) and *OsNCED-3* (Os07g0154100) which encode 9-cis-epoxycarotenoid dioxygenases (Yaish et al., 2010). Recently, a micro-RNA, miR156b, was characterized in Arabidopsis (Wei et al., 2012) and its over-expression led to enhanced lutein and β-carotene in *B. napus* (Wei et al., 2010).

1.4 Norflurazon affects carotenoid biosynthesis

Studies on norflurazon-resistant cyanobacterium, *Synechococcus* , identified a single-base pair substitution (T to G) at position 1313 of *PDS* that led to a valine-to-glycine change at amino acid residue 403 (Chamovitz et al., 1991). It was speculated that the mutation affecting the norflurazon-binding site and the catalytic site for dehydrogenation of phytoene are either overlapping or in close proximity to each other on the PDS polypeptide. Evolution of resistance to norflurazon through somatic mutations was also reported in the aquatic plant Hydrilla (Michel et al., 2004; Arias et al., 2006). Transgenic Arabidopsis plants showed significant resistance to norflurazon when the Hydrilla PDS was substituted at arginine 304 with serine, histidine, cysteine and threonine (Arias et al., 2006). In tomato, PDS promoter activity increased in response to norflurazon (Corona et al., 1996). Although carotenoid accumulation was previously shown to be correlated with fatty acid biosynthesis in both algae (Leóna et al., 2007; Lamers et al., 2008; Ye et al., 2008; Lemoine and Schoefs, 2010) and plant systems(Ayala et al., 1992; Hannoufa et al., 1993; McNevin Jp, 1993; Abrous et al., 1998; Shewmaker et al., 1999), the detailed interdependence between both processes has not been investigated. Norflurazon was shown inhibit fatty acid desaturation by affecting the Δ6 desaturation in rat liver cells (Hagve et al., 1985). In soybean plants, norflurazon treatment led to a decrease in 18:3/18:3 molecular species and an increase in its precursors 18:2/18:3 and 18:2/18:2, suggesting that the ω3 FAD7 desaturase activity was inhibited by norflurazon (Abrous-Belbachir et al., 2009).

1.5 Fatty Acids and carotenoids

Plant mitochondria contribute to fatty acid synthesis in a very minor way by harboring a few fatty acid synthase enzymes on their membrane (Schwertner and Biale, 1973). However, the bulk of fatty acid synthesis in plant cells takes place in the chloroplast stroma. The thylakoids, which constitute the bulk of the membrane surface in a mature chloroplast (approximately 90 mol% of the membrane lipids) are composed of four different lipid classes, the galactolipids, monogalactosyldiacylglycerol (MGDG) and digalactosyldiacylglycerol (DGDG), and the two anionic lipids, phosphatidylglycerol (PG) and sulphoquinovosyldiacylglycerol (SQDG) (Harwood, 1997). The primary function of the chloroplast membrane lipids is to provide a structural environment for photosynthetic membrane protein complexes and a barrier for the different solutes present in the thylakoid lumen and chloroplast stroma (Kieselbach et al., 1998) This barrier is also a prerequisite for the establishment of the photosynthetic proton gradient. In addition, particular lipids are also found in very close association with or embedded into the photosynthetic membrane protein complexes and linked to specific biochemical functions (Palsdottir and Hunte, 2004).

Fatty acid synthesis involves successive elongation of a growing acyl chain with C2 units derived from malonyl-CoA. In plants, fatty acid synthetase carrying out the necessary condensing reactions is localized in the plastids (Schwertner and Biale, 1973; Journet and Douce, 1985). Three enzymes involved in the condensing reaction exhibit different substrate specificities; namely, acetoacetyl-[acyl carrier protein] (ACP) synthase that is most active with C2-C4 substrates, β-ketoacyl-ACP synthase I that prefers C2-C14 substrates, and β-ketoacyl-ACP synthase II that shows specificity for C10-C16 substrates (Shimakata and Stumpf, 1982). These enzymes are also differentially sensitive to cerulenin, a specific β-ketoacyl-ACP-synthase inhibiting antibiotic produced by the fungus *Cephalosporium caerulens*. The acetoacetyl synthase is insensitive, synthase II moderately sensitive, and synthase I highly sensitive (Siggaard-Andersen et al., 1991).

Several studies indicated that carotenoids contribute to the stability of lipid bilayers in the thylakoid membranes of the chloroplast. The exact amount of carotenoids freely dissolved in the thylakoid lipid bilayer is not known and the contribution of carotenoids to the thylakoid

membrane stability remains an open question. It has, however, been suggested that the xanthophyll cycle participates in regulating thylakoid membrane stability (Macko et al., 2002). Some of the parameters affecting the relationship between fatty acid metabolism and carotenoid accumulation have been reported in algae (Zhekisheva et al., 2005; Ye et al., 2008; Vidhyavathi et al., 2009; Lamers et al., 2010; Lemoine and Schoefs, 2010) and in higher plants (Schwertner and Biale, 1973; Ayala et al., 1992; Shewmaker et al., 1999; Galleschi et al., 2002). For example, in *Haematococcus pluvialis*, oleic acid (18:1) levels decreased to up to 40% as astaxanthin levels decreased under high light stress; at the same time, the proportion of other major fatty acids, 16:0 and 18:2, did not change (Zhekisheva et al., 2005). In transgenic *B. napus* seeds, the relative percentage of oleic acid (18:1) increased linoleic acid (18:2) and linolenic acid (18:3) decreased when *PSY* was over-expressed (Shewmaker et al., 1999). This difference in fatty acyl composition held over several generations and under both greenhouse and field conditions, although the magnitude of the change varied with growth conditions.

1.6 RNA binding proteins in Arabidopsis

In plants, carotenoids are synthesized in the plastids and their regulation can be best observed in chormoplasts and chloroplasts (Hirschberg, 2001). The regulation of carotenogenesis in chromoplasts has been extensively studied using the color changes that occur in tomato fruits upon ripening (Hirschberg, 2001). It has been established that the accumulation of lycopene during the breaker stage is controlled by transcriptional regulation (Ronen et al., 2000). In the *Delta* mutants of tomato the accumulation of δ-carotene was correlated with increased levels of *εLYC* gene expression (Ronen et al., 1999). Similarly in the *Beta* mutants, the *βLYC* gene was up-regulated leading to accumulation of β -carotene (Ronen et al., 1999).

The mRNAs coding for chlorophyll a/b binding protein of the photosystem II light harvesting complex failed to accumulate in high light-grown, carotenoid deficient plants, such as maize (*Zea mays*), barley (*Hordeum vulgare*) and mustard (*Sinapis alba*) (Sagar et al., 1988). As most of the research is based on the regulation of carotenoids in chromoplasts, little is known about the regulation of their biosynthesis in the chloroplast. It is well known that carotenoid biosynthesis occurs in the leaves upon light stimulation. Studies on developing mustard seedlings showed that enzymatically inactive PSY in the prolamellar body in the thylakoids became active

upon illumination with white light. Therefore, it was proposed that a similar regulatory mechanism could underlie the coordination between carotenoid and chlorophyll biosynthesis in developing seeds (Welsch et al., 2000). Studies involving *nox* (no xanthophylls) mutants of Arabidopsis indicate that xanthophylls, besides their role in photoprotection and light harvesting complex assembly, also play an important role in photosystem I core translation and stability (Dall'Osto et al., 2013). The *BPG2* (Brassinazole-insensitive-pale green 2) encodes a chloroplast-localized protein with a zinc finger motif and four GTP-binding domains that are necessary for normal chloroplast biogenesis (Komatsu et al., 2010). The direct physical interaction of the nuclear encoded BPG2 protein with the plastid rRNAs indicates that BPG2 mediates light-regulated ribosomal RNA processing functions in chloroplast development and its photosynthetic apparatus (Kim et al., 2012).

The regulation of gene expression during development is achieved through transcriptional regulation and post-transcriptional control of RNAs, which in turn is governed by RNA-binding proteins (RBPs). Most RBPs contain one or more conserved domains, such as the RNA-recognition motif (RRM), the K-homology (KH) motif, RGG (Arg-Gly-Gly) boxes, and double-stranded RNA-binding domains (dsRBDs) (Burd and Dreyfuss, 1994). RBPs are classified into; poly(A)-binding proteins, Ser/Arg (SR) and spliceosomal RRM- containing proteins, oligouridylate-specific RRM proteins, hnRNPs-like proteins, chloroplast RRM-containing proteins (cpRNPs), glycine-rich and small RRM-containing proteins, 30K- RRM proteins, and RRM proteins containing an NTF-like domain (Lorkovic and Barta, 2002).

1.7 Activation Tagging in Arabidopsis

Generation of a mutant population is one of the methods used to dissect complex biological processes in plants. Mutations, resulting from T-DNA insertion, transposon tagging or chemical mutagenesis usually cause loss of function and are therefore recessive; hence, mutant phenotypes can only be observed following two generations of selfing of the mutated plants. This requires a substantial amount of effort and may not be feasible for all plants. Also, it has been estimated that fewer than 10% of the genes tagged in the Arabidopsis genome are likely to generate a visible phenotypic change (Jeon and An, 2001). Therefore, an alternative approach called activation-tagging was developed to overcome these disadvantages (Hayashi et al., 1992).

Current activation-tagging T-DNA vectors contain four copies of an enhancer element from the constitutively active promoter of the cauliflower mosaic virus (CaMV) 35S gene (Weigel et al., 2000). These enhancers cause transcriptional activation of nearby genes; therefore, this approach has become known as activation-tagging.

Some of the main advantages of T-DNA activation tagging are as follows: (i) A gene that is disrupted by the T-DNA can be easily isolated from the mutant by plasmid rescue or by TAIL-PCR; (ii) It is easy to determine if the phenotype is an activation tag or insertion mutant by segregation analysis (since activation-tagged phenotypes are dominant); iii) It becomes easy to recapture the mutant phenotype by introduction of the candidate genes into the wild type under the control of a strong promoter; and (iv) A member of a gene family can be represented by a mutant phenotype without interference from other members of the family (Nakazawa et al., 2003). In Arabidopsis, two T-DNA activation tagging binary vectors pSKI015 (Figure 1-6) and pSKI074 were developed (Weigel et al., 2000). Several mutants have been isolated and characterized using the pSKI015 activation tagging binary vector. A recessive *pid-9* mutant was isolated from a T2 population of plants transformed with pSKI015 and characterization of the mutant indicated its role in the regulation of auxin-mediated responses (Christensen et al., 2000). A *demeter* mutant was isolated and characterized from the same set of mutagenized lines created using pSKI015 (Choi et al., 2002). The mutant was characterized as encoding a defective DNA glycosidase protein that plays a vital role in embryo gene imprinting and seed viability in Arabidopsis. A photosensitive riboflavin related mutant *phs1* (Ouyang et al., 2010) and in 2011 a freezing tolerance mutant (*ftl1-1D*) was isolated from the same pSKI015 activation-tagged population of Arabidopsis (Kang et al., 2011). The *ftl/ddf1* gene encodes an AP2 domain-containing transcription factor. The overexpression of this gene leads to enhanced tolerance to drought, heat, salt and freezing stresses, and increased transcription of abiotic stress-induced genes (Kang et al., 2011).

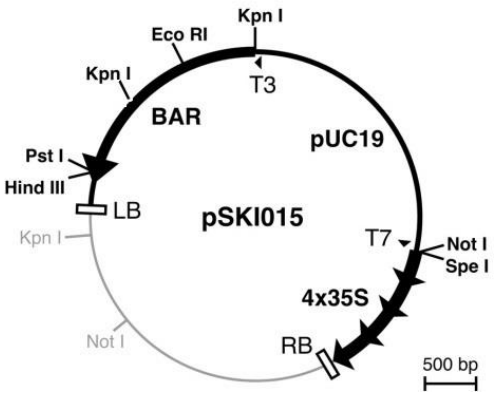

Figure 1-6: Map of the activation-tagging binary vector pSKI015. Restriction enzyme sites in T-DNA internal sequences to aid in plasmid rescue are shown. (Weigel et al., 2000).

A population of almost 50,000 activation-tagged Arabidopsis lines, called the SK population, has been developed and archived as individual T_3 generation lines (Robinson et al., 2009). The population provides an excellent tool for both reverse and forward genetic screens and has been used to identify a number of novel mutants. A new dominant Arabidopsis *transparent testa* mutant, *sk21-D*, had increased expression of two *KAN4* transcript splice variants with identical MYB-like B-motifs, large, light- and dark-colored patches on seed coat, and also reduced expression of gene transcripts involved in flavonoid biosynthesis (Xu et al., 2009). Two novel genes involved in the carotenoid pathway have also been discovered using this Arabidopsis population. A *cbd* mutant was isolated based on its yellow cotyledons, yellow-first true leaves, and stunted growth (Yu et al., 2012). The *cbd* mutant phenotype was recessive, involved in retrograde signaling and affected the *cpSRP54* gene encoding the 54kDa subunit of the chloroplast signal recognition particle. Expression in *B. napus* led to increased carotenoid and abscisic acid (ABA) biosynthesis (Yu et al., 2012). Another mutant, *sk156*, was isolated and characterized from the same population; this mutant had enhanced expression of a *miR156b* which led to increased seed carotenoid levels and enhanced branching (Wei et al., 2012).

The recent findings detailed above have broadened our understanding of how carotenoids are synthesised and accumulated in plants; however, this limited knowledge can be largely attributed to the discoveries in a small number of novel carotenoid mutants in tomatoes, oranges, Arabidopsis, and maize. Therefore, to dissect the networks that regulate carotenoid biosynthesis, many more mutants that affect carotenoids in plants need to be identified. Our understanding of

carotenoid biosynthetic pathway will expand if we can determine more of the metabolic regulations that affect carotenoid enzymes, the interactions between the carotenoid pathway and other metabolic pathways, and especially the molecular components that control the expression of carotenoid genes. Discovering and characterizing a much larger set of mutants will give us a better understanding of this important pathway and improve our ability to manipulate carotenoid accumulation in crop plants.

Our understanding of carotenoid metabolism and regulation can grow from the discovery of mutants that affect carotenoid biosynthesis. Therefore, this thesis has identified carotenoid mutants from an activation tagged Arabidopsis population as a means of discovering the complex networks that regulate carotenoid biosynthesis in Arabidopsis. Novel regulatory mechanisms involved in carotenoid metabolism can be discovered by identifying new activation-tagged Arabidopsis mutants with altered carotenoid level. In order to test this hypothesis, in this thesis an activation-tagged mutant Arabidopsis population was screened using seed coat color and for norflurazon tolerance to determine mutants with altered carotenoid contents. Molecular characterization and complementation studies of the screened Arabidopsis mutants were performed to understand the mechanisms involved in regulation of carotenoid biosynthesis in Arabidopsis.

2 SCREENING AND CHARACTERIZATION OF RED SEED COAT ARABIDOPSIS MUTANTS

2.1 Introduction

Carotenoids accumulate in all types of plastids of fruits, flowers, roots and seed, except in the undifferentiated progenitor of plastids, the proplastid. This includes chromoplasts (colored plastids), amyloplasts (starch-storing plastids), elaioplasts (lipid-storing plastids), leucoplasts (colorless plastids) and etioplasts (dark-grown precursors of the chloroplast) (Howitt and Pogson, 2006). Carotenoids accumulate in specialized lipoprotein-sequestering structures inside the chromoplasts which store carotenoids as sheets, ribbons and crystals (Vishnevetsky et al., 1999). These structures are known to be packed densely in the tissues of yellow, orange and red fruits and flowers (Li et al., 2001), but are poorly characterized in seeds. Additionally, elaioplasts can store more carotenoids than amyloplasts which store only starch (Shewmaker et al., 1999; Wise, 2006). Elaioplasts are specialized lipid-storing plastids in oilseeds, such as canola and sunflower. Sunflower seeds primarily accumulate lutein (McGraw et al., 2001). Pumpkin seeds primarily accumulate lutein (53%), as well as α-carotene and small amounts of β-carotene (10%) (Matus et al., 1993). Canola seeds predominantly accumulate lutein and traces of β-carotene (Shewmaker et al., 1999) and Arabidopsis seeds contain 60% lutein and 4% β-carotene (Lindgren et al., 2003).

Carotenoid production in developing seeds has several roles primarily leading to the production of ABA and eventually leading to ABA-dependent seed dormancy (Cunningham and Gantt, 1998; DellaPenna, 1999). Therefore, reduction in carotenoids could cause reduction in dormancy leading to vivipary, which was used as a screening method to identify carotenoid mutants in rice (Wurtzel et al., 2001). Furthermore, carotenoids contribute to the antioxidant system in seeds, which functions to limit free radical-induced membrane deterioration and seed ageing (Calucci et al., 2004). Several lines of evidence suggest that ABA is synthesized *in situ* in the seed, rather than imported. In wheat, the grain contains eight times more ABA than the remainder of the ear, which would not be expected if imported from the xylem (King, 1976). Furthermore, transgenic tobacco over-expressing the carotenoid *ZEP* gene under the influence of

a 35S promoter resulted in increased ABA levels in the seed and delayed seed germination (Frey et al., 1999).

Studies on carotenoid regulation and biosynthesis in plants have relied heavily on analyzing intermediates from naturally occurring carotenoid mutants, using color variations in different tissues such as leaves (Pogson et al., 1998), fruits (Alquezar et al., 2008), flowers (Cunningham and Gantt, 2005), and seed (Janick-Buckner et al., 1999), or using carotenoid biosynthesis-inhibiting herbicides (Cunningham and Gantt, 1998; Yu et al., 2007). Wild-type maize seed, which is bright yellow in color primarily accumulates lutein, followed by zeaxanthin, a xanthophyll monoester and trace amounts of β-carotene (Janick-Buckner et al., 1999). Lutein is the major carotenoid in white millet, while zeaxanthin is the major carotenoid in red millet seed (McGraw et al., 2001). Lutein, which accounts for 75% of the total carotenoid pool in wild-type Arabidopsis seed, was reduced to 57% in *lut1* mutant seeds (Tian et al., 2003). The *lut1* mutant of Arabidopsis has a pale yellow seedling phenotype and a defective cytochrome P450-type monooxygenase, which functions as a ε-hydroxylase (Tian et al., 2004). The wild-type maize seed has a red bran color and accumulates lutein, zeaxanthin and a xanthophyll monoester, as well as trace amounts of β-carotene, whereas the *y10* mutant seed is pale yellow and has markedly reduced lutein and, to a lesser extent, zeaxanthin (Janick-Buckner et al., 1999). However, no significant reduction of β-carotene was observed in the *y10* kernel. Furthermore, the *y10* mutation is thought to occur at a step prior to the synthesis of phytoene, suggesting a preferential maintenance of β-carotene production in the *y10* mutant (Janick-Buckner et al., 1999). Two rice mutants, one accumulating phytoene and other with no detectable carotenoids were identified by screening for seed vivipary combined with an albino seedling phenotype (Wurtzel et al., 2001). Carotenoid mutants in algae were also identified using altered color profiles (Chen et al., 2003).

This study focuses on determining the levels of major carotenoids in the seedlings and mature seeds of Arabidopsis and identifying carotenoid mutants with altered carotenoid profiles from seed color variants of the SK population of Arabidopsis mutants (Robinson et al., 2009). As carotenoids are known to impart color to tissues, the efficiency of screening for activation tagged mutants in Arabidopsis with red seed color is determined.

2.2 Materials and Methods

2.2.1 Plant material, growth conditions and screening

Seeds of wild-type (WT) Arabidopsis (ecotype Columbia) and activation-tagged Arabidopsis mutant lines were obtained from the laboratory of Dr. Isobel Parkin at Agriculture and Agri-Food Canada (AAFC, Saskatoon, Canada). These lines have been developed and described earlier (Robinson et al., 2009). Two Salk allelic mutant lines with a disruption at At2g25344 encoding a pollen coat protein (LCR14) were obtained from the Arabidopsis Biological Resource Center (ABRC). The two Salk mutants were SALK_011157C and SAIL_895_A01 were renamed RSC-1 and RSC-2 respectively. The *Brassica napus* L. cv. spring, seeds were obtained from the laboratory of Dr. Margie Gruber at Agriculture and Agri-Food Canada (AAFC, Saskatoon, Canada).

Seeds from WT Arabidopsis and mutants were sown in 10- cm plastic pots filled with RediEarth (Sungro Horticulture) medium at a density of 5 plants per pot. The *B. napus* seeds were sown in 22 cm pots filled with RediEarth (Sungro Horticulture) medium at a density of 1 plant per pot. A slow release fertilizer (N:P:K, 20:20:20) (Scotts Company LLC) and water were provided regularly as needed. Plants were grown in a greenhouse at constant temperature of 20°C with 16/8 h (light/dark) cycle. Ambient light provided a photosynthetic photon flux density (PPFD) of 240 to 250 μmol photons m^{-2} s^{-1}. Various tissues were collected throughout the growth cycle which spanned seed germination to seed production.

The activation-tagged lines were used to screen for putative carotenoid mutants by comparing seed color with the WT Arabidopsis seed. Visual screening of the seeds of T_3 mutant lines of Arabidopsis was performed by Min Yu in Dr. Margie Gruber's lab (AAFC, SK, CA) and red seed coat color lines were kindly provided for this study. The mutants were initially screened visually using light microscopy for changes in color to the seed coat (red compared to the golden brown color of WT seed).

2.2.2 Carotenoid extraction

Carotenoids were extracted from 200 mg fresh weight tissue of 10-day-old seedlings, leaves (14 day old), flowers, developing siliques (3 to7 days after pollination; DAP), developing and

mature seeds from WT Arabidopsis and mutants using the protocol adapted from (Yu et al., 2007). Briefly, the tissues were pulverized by rapid shaking in a scintillation vial containing a steel rod and 3 ml of hexane:acetone:ethanol (50:25:25) extraction solvent (Shewmaker et al., 1999). The sample was then centrifuged for 10 min at 1,800 g and the supernatant collected. The pellet was then washed with another 3 ml of extraction solvent and the supernatant collected and pooled. The solvent was removed from the supernatant by evaporation at room temperature under a stream of nitrogen gas. The triacylglycerides were saponified by heating at 80°C for 1 h in 5 ml methanolic-KOH (10% [w/v] KOH in 80:20 methanol:water [v/v]). Carotenoids were partitioned using a mixture containing 2 ml of H_2O and petroleum ether. The carotenoids were extracted in the petroleum ether phase twice. The carotenoid-rich ether phases from the two 3 ml ether washes were collected, pooled and the solvent evaporated off at room temperature under a nitrogen gas stream. The residue was suspended in 200 µl of acetonitrile/methylene chloride/methanol (50:40:10 [v/v]) containing 0.5% (w/v) butylated hydroxytoluene and filtered through a 0.2 µm pore size Whatman® Mini-UniPrep® nitrocellulose syringe filter (Sigma-Aldrich) into a dark HPLC sample vial and stored at -20°C until analysis.

Due to the small size of Arabidopsis seed, dissecting seed coat from the developing and mature seeds was technically challenging. Therefore, carotenoids were extracted from manually dissected embryo and seed coat from developing *B. napus* seeds (20 DAP).The embryo and seed coat from mature *B. napus* seeds were separated by de-hulling and then used for carotenoid extraction

2.2.3 HPLC determination of carotenoids

The carotenoid extracts were analyzed using the HPLC system described by Yu et al. (2007). A carotenoid standard test mix containing lutein, violaxanthin, β-carotene, cryptoxanthin and zeaxanthin (CaroteNature Inc) was dissolved in 100% methanol at a concentration of 1 mg ml^{-1}. A working standard of 50 µg $µl^{-1}$ was prepared by dilution in 100% methanol and 2 µl was injected for HPLC analyses. Extracts of tissue samples (20 µl) were loaded onto a 4.6 µm x 250 mm reverse-phase C_{30} YMC "Carotenoid Column" (Waters) at 35°C. Mobile phases consisted of 100% methanol and 100% *tert*-methyl butyl ether. A linear gradient starting at 95% (v/v) methanol and 5% (v/v) *tert*-methyl butyl ether and proceeding to 35% (v/v) methanol and 65%

(v/v) *tert*-methyl butyl ether over 25 min with a flow rate of 1.2 ml min^{-1} was used for elution. Compounds in the eluate were monitored at 450 nm using a photodiode array detector. Peaks were identified by their retention time and absorption spectra compared to those of known carotenoid standards. Quantification of carotenoids was conducted using standard curves; the R^2 values were greater than 0.99 when constructed using the known carotenoid standards.

2.2.4 Estimation of the number of T-DNA insertions using quantitative polymerase chain reaction (qPCR)

Genomic DNA from Arabidopsis mutant lines was isolated using a Qiagen DNeasy kit (Qiagen) following the manufacturer's protocol. The isolated genomic DNA was subjected to qPCR using Platinum® SYBR® Green qPCR SuperMix-UDG with ROX dye kit (Life Technologies). The gene encoding phosphinothricin acetyltransferase (*PAT*) was amplified to detect T-DNA copy number. A single copy gene *High Mobility Group-I/Y* (*HMG-I/Y*, AGI id: At1g14900) from Arabidopsis served as the internal control (Gupta et al., 1998). The gene-specific forward and reverse primers for *PAT* and *HMG-I/Y* were selected using Primer3 software (http://bioinfo.ut.ee/primer3/) (Untergasser et al., 2012) and are provided in Table 3-1. A confirmed Arabidopsis mutant (*sk156*) confirmed by Southern hybridization to contain a single copy T-DNA insert by Wei et al. (2012) was used as the reference for the estimation of the copy number. The reference was used to normalize any difference between the amplification efficiency of the *PAT* gene and *HMG-I/Y* gene fragments (Weng et al., 2004). qPCR was performed in a CFX96 Touch™ Real-Time PCR Detection System (Bio Rad Laboratories). Two dilutions (1X and 4X) of genomic DNA in triplicate technical replicates for each gene were used to determine the copy numbers of T-DNA. Plasmid standards containing *PAT* with $\log_4$ dilutions (1X, 4X, 16X, 64X) were also run simultaneously to estimate the threshold cycle (C_T) and the efficiency of the PCR using CFX Manager™ software (Bio Rad Laboratories). The copy number was estimated using the formula $2^{-\Delta\Delta CT}$ for the samples where the C_T standard deviations of the technical replicates were less than 0.3 (Livak and Schmittgen, 2001; Weng et al., 2004).

Table 2-1: Primers used in this study for qPCR and sqPCR

Primer	Primer Description/AGI Codes	Forward Primer 5' to 3'	Reverse Primer 5' to 3'
PAT	Phosphinothricin acetyltransferase	CGAGTCAACCGTGTACGTCT	GACAGCGACCACGCTCTT
HMG-I/Y	At1g14900	AACCGGTCAGCTAATCATGG	GATTCGGCCTGAGTCTTCTG
LCR14	At2g25344	ACTTTCAACCCTCGTTCGTC	GGAACGACACTCATCGTGAA
ACT2q	At3g18780	GTTCTACTTACCGAGGCTCCTCTT	CTCGTAGATAGGCACAGTGTGAGAC
ACT2sq	At3g18780	GATGAGGCAGGTCCAGGAATC	AACCCCAGCTTTTTAAGCCTTT
SKI1	pSKI015	AATTGGTAATTACTCTTTCTTTTCCTCCATATTGA	
LB1	T-DNA Left border	GTGGGCCCCAAATGAAGTGCAGGTCAAAC	
LB2	T-DNA Left border	GCCTTTTCAGAAATGGATAAATAGCCTTGCTTCC	
AD1	TAIL –PCR primer	NTCGASTWTSGWGTT	
AD2	TAIL –PCR primer	NGTCGASWGANAWGAA	
AD3	TAIL –PCR primer	WGTGNAGWANCANAGA	

2.2.5 Determination of T-DNA flanking regions

Genomic DNA flanking the T-DNA insertion site in mutants was determined using plasmid rescue (Weigel et al., 2000) or thermal asymmetric interlaced (TAIL)-PCR (McElver et al., 2001). For plasmid rescue, 5 µg of genomic DNA was digested overnight with *Kpn*I, *Eco*RI, and *Hin*dIII for rescue of sequences adjacent to the T-DNA right border, while *Bam*HI, *Spe*I and *Not*I was used for T-DNA left border rescue (Weigel et al., 2000). After restriction digestion, the successful digestion of the genomic DNA, visible as a smear, was confirmed by agarose gel electrophoresis. The digested fragments (2 µg μl^{-1}) were then self-ligated overnight using 10 U of T4 ligase (New England Biolabs) in an incubator at 16°C. Ligated DNA was purified using QIAquick PCR purification kit (Qiagen) and 400 ng of ligated DNA was used to transform into *Escherichia coli* DH10B electrocompetent cells by electroporation (Invitrogen). The transformed colonies were selected by growing on Luria-Bertani (LB) agar medium (Gibco; 10% [w/v] peptone 140, 5% [w/v] yeast extract and 5% [w/v] sodium chloride) containing 50 µg ml^{-1}

kanamycin. Plasmid extraction from five transformed clones per mutant was carried out using a Promega Wizard® Plus plasmid purification kit (Promega) and the rescued genomic DNA fragments were sequenced using respective left border primers (Table 3-1) at the DNA sequencing facility of the Plant Biotechnology Institute (Saskatoon, SK). Basic local alignment search tool (BLAST) analysis was performed on the identified sequences against the Arabidopsis information resource (TAIR) sequence database (Version 9) to determine homology to any known Arabidopsis nucleotide sequences. (http://www.arabidopsis.org/Blast/index.jspwebcite).

The border sequences were recovered in high-throughput manner using a modified TAIL-PCR protocol (McElver et al., 2001). The genomic sequence flanking the T-DNA insertion sites (FST) was amplified by TAIL-PCR as described in (Sessions et al., 2002). Initial linear amplification with one of the secondary T-DNA primers, SKI1, was carried out for 5 cycles (94°C, 10 sec; 64°C, 1 min; 72°C, 2.5 min), followed by 15 cycles (94°C, 10 sec; 64°C, 1 min; 72°C, 2.5 min; 94°C, 10 sec; 64°C 1 min; 72°C, 2.5 min; 94°C, 10 sec; 44°C, 1 min; 72°C, 2.5 min). Reactions were then subjected to a low annealing temperature PCR for 5 cycles (94°C, 10 sec; 44°C, 1 min; 72°C, 3 min). A final extension at 72°C for 5 min was followed by a hold at 4°C. The degenerate primer mix containing AD1, AD2, and AD3 (Table 3-1), was used in combination with T-DNA left border LB1or LB2 (Table 3-1). The TAIL-PCR reactions (10 µl) were incubated at 37°C for 1 h with 2 U of exonuclease I (Life Technologies) and 0.5 U of shrimp alkaline phosphatase (Life Technologies) was added to the reaction mix, followed by a 10 min heat inactivation step at 70°C. A 5 µl sample of each completed TAIL-PCR reaction was subjected to electrophoresis on a 2% (w/v) agarose gel to determine the amplified fragments containing the T-DNA flanking regions. Any amplified fragment was excised from the gel and purified using QIAquick gel extraction kit (Qiagen). The fragments were sequenced using respective left border primers (LB1 or LB2) (Table 3-1) at the DNA sequencing facility of the Plant Biotechnology Institute (Saskatoon, SK). Basic local alignment search tool (BLAST) analysis was performed on the identified sequences against the Arabidopsis information resource (TAIR) sequence database (Version 9) to determine homology to any known Arabidopsis nucleotide sequences. (http://www.arabidopsis.org/Blast/index.jspwebcite).

2.2.6 Total RNA extraction and cDNA synthesis

Tissues (rosette leaves, stems, flower buds, flowers, siliques and mature seeds) from WT Arabidopsis were harvested and frozen immediately in liquid nitrogen. The frozen tissues were then ground using a mortar and pestle to a fine powder. Approximately 500 mg of the ground tissues were placed in 2 ml centrifuge tubes and stored at -80°C for total RNA extraction. Total RNA from the samples was extracted using the RNeasy Plant Mini Kit (Qiagen) following the manufacturer's protocol. The isolated RNA was quantified using a Nanovue spectrophotometer (GE Healthcare Biosciences, PA, USA). The quality and purity of the examined total RNA was tested by electrophoresis using a 1% (w/v) agarose gel and ethidium bromide (20 µg ml^{-1}) staining. The presence of distinct 28S and 18S rRNA bands with a 2:1 ratio and the absence of any smearing caused by degradation indicated good quality RNA suitable for reverse transcription.

Single strand cDNA was synthesized from total RNA using AMV reverse transcriptase (Life Technologies) following the manufacturer's protocol. A 20 µl reverse transcription reaction was prepared by adding the following reagents: 4 µl of 25 mM $MgCl_2$, 2 µl of 10X reverse transcription buffer; 2 µl of 10 mM dNTP mixture; 0.5 µl of 10 U recombinant RNasin® ribonuclease inhibitor; 1 µl of 15 U AMV reverse transcriptase; 1 µl of 0.5 µg Oligo(dT)15 primer; 1 µg total RNA; and nuclease-free water to a final volume of 20 µl. The reaction was incubated at 42°C for 40 min for first strand cDNA synthesis. The sample was heated to 95°C for 5 min and stored at -20°C.

2.2.7 Polymerase chain reaction (PCR)

2.2.7.1 Semi-quantitative polymerase chain reaction (sqPCR)

Expression profiles in WT Arabidopsis tissues were generated using sqPCR. The gene-specific primers for *Actin2* (*ACT2sq;* AGI code: At3g18780) and *LCR14* which is similar to a pollen coat protein (AGI code: At2g25344), are provided in Table 2-1 and were selected using Primer3 software (http://bioinfo.ut.ee/primer3/) (Untergasser et al., 2012). A 25 µl PCR reaction using Taq DNA polymerase (Life Technologies) was set up by mixing the following: 1 µl of cDNA template, 5 µl of 10X PCR buffer, 1 µl of 10 mM dNTPs, 1 µl of 10 mM each forward and reverse *ACT2sq* or *LCR14*-specific primers and nuclease-free water to obtain a volume of 24

µl and 1 µl of Taq Polymerase (1 U) was added to obtain a final volume of 25 µl. The PCR amplification cycle (GeneAmp PCR System 9700 96 Well Thermocycler; Applied Biosystems) had an initial denaturation at 95°C for 5 min followed by 25 cycles at 95°C for 30 sec, 55°C for 30 sec and 72°C for 30 sec, followed by a final extension at 72°C for 7 min. The amplified products were then examined using 1% agarose gel electrophoresis for the presence of a gene-specific PCR product. The *ACT2sq* PCR product was used as an internal reference to account for differences in cDNA input.

2.2.7.2 Quantitative polymerase chain reaction (qPCR)

Relative expression levels of *LCR14* in flower buds from Arabidopsis WT and mutants were examined using qPCR. Gene-specific primers for *ACT2q* and *LCR14* (Table 2-2) were selected using Primer3 software (http://bioinfo.ut.ee/primer3/) (Untergasser et al., 2012). The qPCR reaction mix contained l0 µl of 2X SYBR Green master mix (Life Technologies), 0.5 µl of cDNA, 1 µl of 10 mM each forward and reverse *ACT2q* or *LCR14* -specific primers (Table 3-1) and the final volume was adjusted to 20 µl using nuclease free water. qPCR was performed using a CFX96 Touch™ Real-Time PCR Detection System (Bio-Rad Laboratories). The qPCR conditions were as follows; initial denaturation at 94°C for 5 min, followed by 40 cycles of denaturation at 94°C for l0 sec, annealing at 55°C for l0 sec and extension at 72°C for 15 sec. The amount of PCR products formed was quantified at the end of each extension cycle. A melt curve analysis was performed to determine the PCR efficiencies by increasing the temperature from 65°C to 94°C and measuring the fluorescence at 0.5°C increments. All qPCR reactions displayed efficiencies between 87 and 110% (data not shown). The data obtained from the qPCR was normalized and analyzed using the CFXI000 software (Bio-Rad Laboratories). Relative expression levels of the genes were computed using the $2^{-\Delta\Delta CT}$ method of relative quantification (Livak and Schmittgen, 2001). Expression values were calculated and normalized to the expression of *ACT2q*.

2.2.8 Experimental design and statistical analysis

Carotenoid extraction and HPLC determination were performed using three biological replicates and one technical replicate. Each biological replicate represents a pool of tissues

sampled from 10 individual plants. The mean and the standard deviation of the three biological replicates are presented. Total RNA was extracted from three biological replicates, where each replicate represents a pool of tissues sampled from 10 individual plants. A total of two cDNA were synthesized from each RNA sample. The cDNAs synthesized were used in qPCR for expression studies.

The data sets were tested for normal distribution at $p < 0.05$ using a chi-square test and the significance determined using a one-way analysis of variance (ANOVA) at $p < 0.05$ which indicates a 95% confidence level. A least significant difference (LSD) post-hoc test was performed to separate the differences among means ($p < 0.05$). All statistical analyses were performed using SPSS software (Version 17.0.1, IBM, USA).

2.3 Results

2.3.1 Carotenoid levels in different tissues of Arabidopsis

The analysis of carotenoid levels in Arabidopsis ecotype Columbia indicates that the major carotenoids (lutein, β-carotene, cyptoxanthin, zeaxanthin and violaxanthin) are present in all the tissue types analyzed, including 10-day-old seedlings, mature leaves, flowers, siliques and mature seeds (Figure 2-1). Lutein and β-carotene levels were the highest, together contributing up to 90% of the total carotenoids. Cryptoxanthin levels were the lowest among the five carotenoids determined. Statistical analysis indicated that 10-day-old seedlings and leaves had significantly higher levels of lutein and zeaxanthin compared to flowers, siliques or mature seed tissues. The β-carotene and violaxanthin levels were significantly higher in the flower tissues compared to 10-day-old seedlings, siliques and seeds; however, their levels were not significantly higher compared to leaves. Mature seed had significantly lower levels of all carotenoids compared to other tissues.

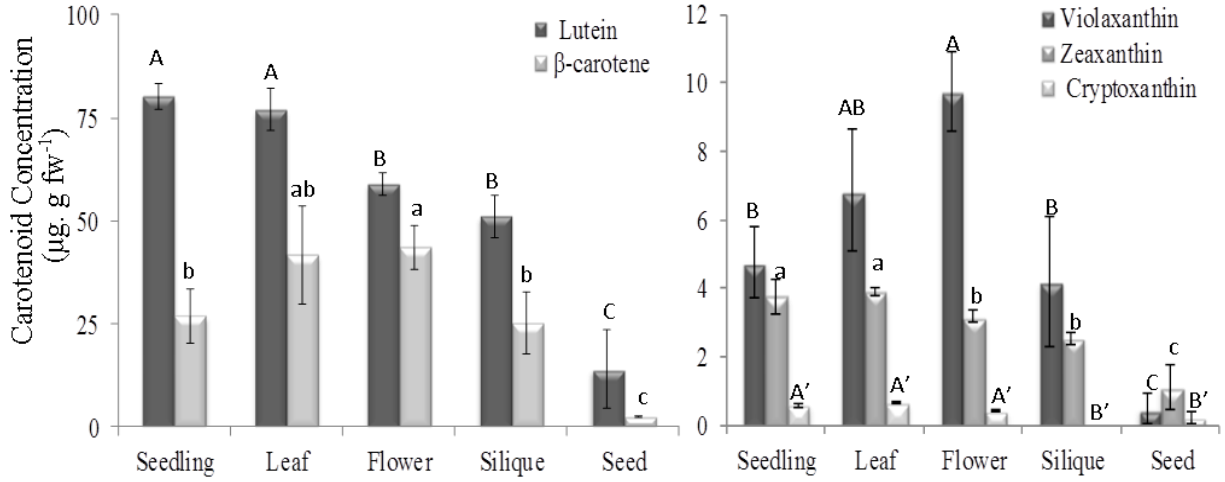

Figure 2-1: Carotenoid composition in various vegetative tissues of Arabidopsis. Values represent means ± SD (n = 3) and are expressed on a fresh weight (fw) basis. Different letters within each panel (uppercase for lutein and zeaxanthin; lower case for β-carotene and violaxanthin; upper case prime for cryptoxanthin) indicate statistical significance at $p < 0.05$. fw, fresh weight.

It was determined in Figure 2-1 that the mature seeds had decreased carotenoid levels; therefore, understanding the carotenoid distribution in the tissues of developing and mature seeds will be beneficial for screening Arabidopsis mutants for altered carotenoid profiles. *B. napus* was used to determine carotenoid distribution in developing and mature seeds due to its ease of handling, larger seed size, and that it also belongs to the *Brassicaceae* family. The seed coat and embryo tissues from *B. napus* developing seeds (20 DAP) were dissected and subjected to carotenoid analysis. Mature *B. napus* seeds were also milled to separate seed coat and embryo tissues prior to carotenoid analysis.

The analysis indicated the presence of four major carotenoids (lutein, β-carotene, violaxanthin and zeaxanthin) in both embryo and seed coat of developing *B. napus* seed (Figure 2-2). Only β-carotene was found to be significantly higher in the embryo of developing seed compared to the seed coat. Levels of all other carotenoids, namely lutein, violaxanthin and zeaxanthin, were not significantly different between the two tissues. Furthermore, the β-carotene level was relatively higher than the lutein level in the embryo.

Only lutein and β-carotene were detectable in the embryo and seed coat tissues of mature *B. napus* seeds (Figure 2-3). The lutein levels did not differ significantly between embryo and the mature seed coat, but the levels were 30-fold lower compared to the developing embryo tissues. β-carotene was barely detectable in the mature seed coat and not detectable in embryo, even though it was the predominant carotenoid in seed tissues.

2.3.2 Carotenoid levels in developing and mature seeds of *B. napus*

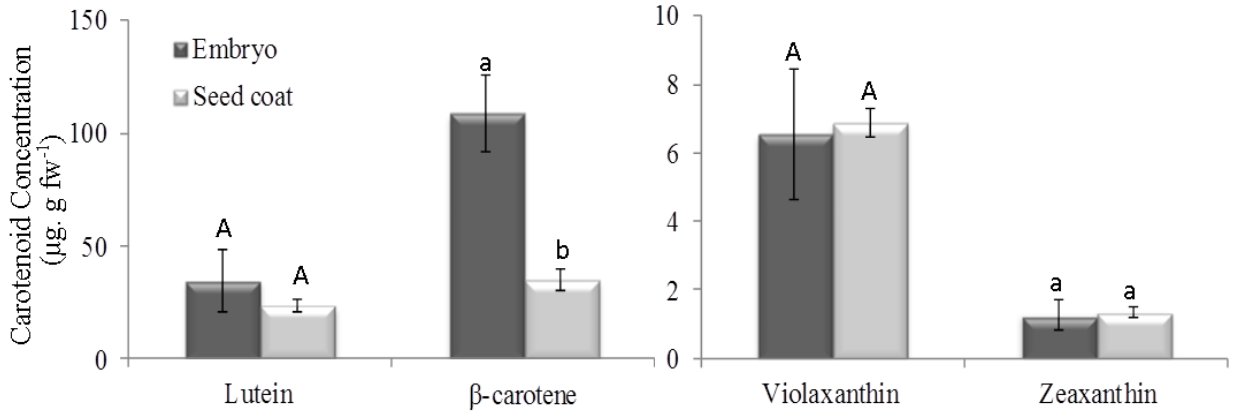

Figure 2-2: Carotenoid composition in the embryo and seed coat of developing *B. napus* seeds at 20 DAP. Values represent means ± SD (n = 3) and are expressed on a fresh weight (fw) basis. Different letters within each panel (uppercase for lutein and zeaxanthin; lower case for β-carotene and violaxanthin) indicate statistical significance at $p < 0.05$. DAP, days after pollination; fw, fresh weight.

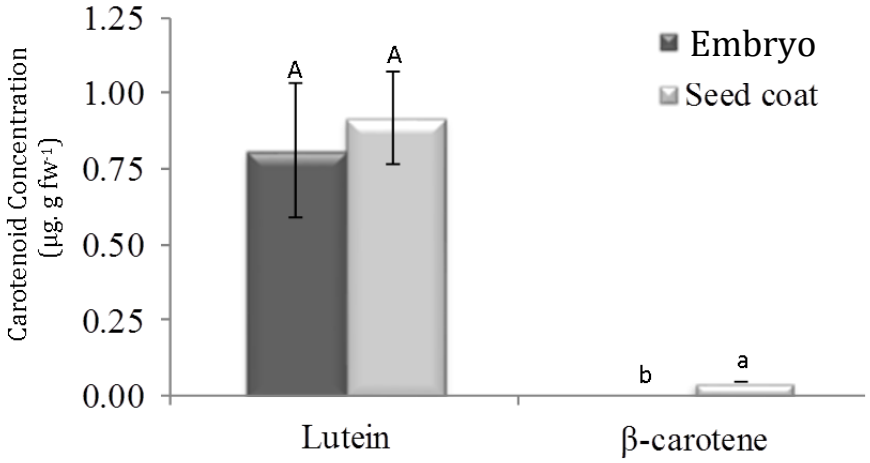

Figure 2-3: Carotenoid composition in the embryo and seed coat of mature *B. napus* seed. Values represent means ± SD (n = 3) and are expressed on a fresh weight (fw) basis. Different letters within each panel (uppercase for lutein; lower case for β-carotene) indicate statistical significance at $p < 0.05$. Violaxanthin and zeaxanthin could not be detected. fw, fresh weight.

2.3.3 Screening of activation-tagged Arabidopsis mutant lines for red seed coat color

The observations from the experiment on carotenoid distribution within *B. napus* seed tissues made it apparent that carotenoids accumulate in the seed coat both during seed development and maturation. Carotenoids are known to impart color in the tissues in which they accumulate and the major carotenoids present in the seed coat are lutein (yellow) and β-carotene (orange) (Ito et al., 2000). The two xanthophylls, zeaxanthin and violaxanthin, exhibit yellow and orange colors, respectively (Curl and Bailey, 1954). The precursor for both lutein and β-carotene is lycopene (red) (Kong et al., 2010). Therefore, screening of Arabidopsis mutants with red seed coat color was used to recover mutants with altered carotenoid profile (Figure 2-4). Fourteen mutants having red seed coats were identified from screening the activation-tagged T-DNA population of Arabidopsis.

Figure 2-4: Red seed coat mutants. Mutants (T_3) with red seed coat color selected from the activation-tagged Arabidopsis population compared to the wild-type seeds.

2.3.4 Carotenoid levels in red seed coat color mutant lines

The carotenoid levels of mature seeds of the mutants are presented in Figure 2-5. Of the fourteen mutants, only mutant SK21229 had significantly higher levels of lutein, β-carotene, zeaxanthin and violaxanthin in the mature seeds compared to the WT. Mutant SK20694 had significantly higher levels of lutein and violaxanthin in the seed compared to the WT seeds. Mutants SK21026 and SK22075 had significantly higher levels of violaxanthin and zeaxanthin, respectively in their seeds compared to WT. Mutant SK22446 had significantly lower levels of all analyzed carotenoids in the seed tissue compared to the WT. Mutant SK21931 and SK22484 had significantly lower levels of lutein, β-carotene and violaxanthin in the seed compared to the

WT. It is interesting to note that majority of the red seed coat mutants analyzed (8 out of 14; SK20676, SK21522, SK21559, SK21931, SK22078, SK22100, SK22446, and SK22484) had significantly decreased levels of lutein, β-carotene and/or violaxanthin in the seed compared to the WT. The carotenoid levels in the seeds of two mutants; namely, SK21470 and SK22046 were not significant compared to the WT seeds.

The carotenoid analysis on the 14-day old mature leaves was performed on the 14 Arabidopsis mutants to determine if the carotenoid distribution was comparable in the seeds and leaves (Figure 2-6). Mutant SK22446, which had significantly lower levels of all carotenoids in the seeds, also had significantly lower levels of lutein, β-carotene and violaxanthin in the leaves compared to the WT. In contrast, mutant SK21229, which had significantly higher levels of all carotenoids in the seeds, had significantly lower levels of lutein, β-carotene and violaxanthin in the leaves compared to the WT leaves. Mutant SK21522 had significantly lower levels β-carotene in both seeds and leaf tissues compared to the levels in the WT. Mutant SK22075 had significantly lower levels of all carotenoids analyzed in the leaves compared to the WT; however, the seed carotenoid profile indicated significantly higher zeaxanthin and significantly lower violaxanthin levels compared to the WT seeds.

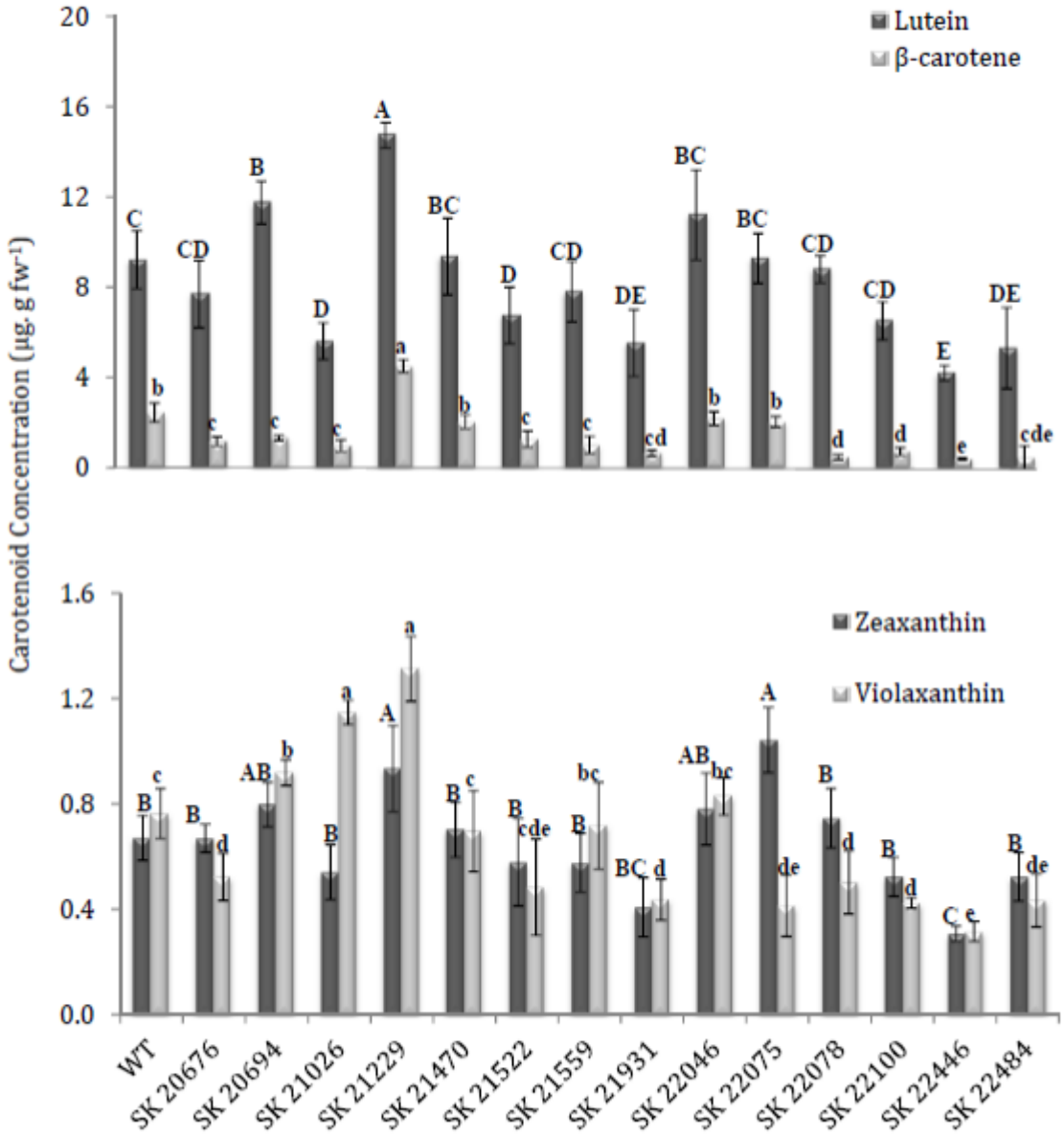

Figure 2-5: Carotenoid composition in mature seeds of Arabidopsis mutants lines (T_4) selected for their red seed coat. Values represent means ± SD (n = 3) and are expressed on a fresh weight (fw) basis. Different letters within each panel (uppercase for lutein and zeaxanthin; lower case for β-carotene and violaxanthin) indicate statistical significance at $p < 0.05$. fw, fresh weight.

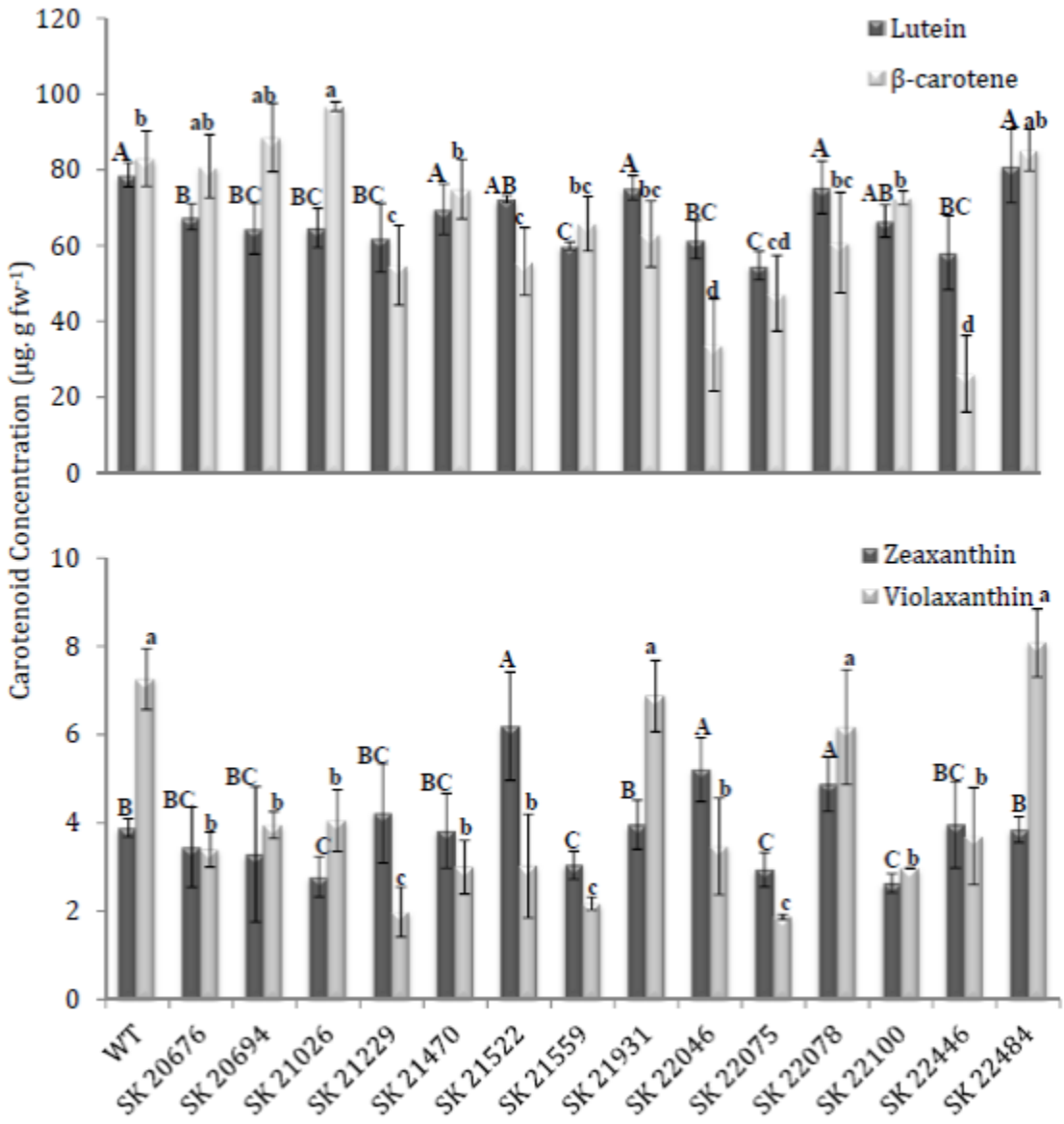

Figure 2-6: Carotenoid composition in 14-day-old leaves of Arabidopsis mutants lines (T_4) selected for their red seed coat. Values represent means ± SD (n = 3) and are expressed on a fresh weight (fw) basis. Different letters within each panel (uppercase for lutein and zeaxanthin; lower case for β-carotene and violaxanthin) indicate statistical significance at $p < 0.05$. fw, fresh weight.

2.3.5 Molecular analysis of red seed coat color mutant lines

The T-DNA copy numbers for the selected mutants were determined using qPCR (the $2^{-\Delta\Delta cT}$ method) by analyzing *PAT* copy number, representing T-DNA. The results indicated that only two (SK22075, and SK22446) mutant lines had a single T-DNA insertion. The other twelve mutants analyzed had multiple T-DNA insertions in their genomes (Table 2-2). The T-DNA insertion loci for select Arabidopsis mutants were determined using plasmid rescue or TAIL-PCR methods. The T-DNA insertion locus in SK20676, SK21229, SK21522 and SK22075 were identified using plasmid rescue. Although qPCR indicated two T-DNA insertions were present in SK21229 and SK21522, only one T-DNA insertion site for each mutant was determined. TAIL-PCR analysis was able to determine at least one T-DNA insertion site for each of eight mutant lines; four mutant lines identified in this study (SK20694, SK21559, SK21931, SK22484) and the other four determined by Dr. Parkin (SK21026, SK21470, SK22046, SK22078) (Table 2-2). Repeated TAIL-PCR and plasmid rescue experiments failed to provide T-DNA insertion locus information for two mutant lines SK22100 and SK22446. Furthermore, only one T-DNA insertion locus was determined using TAIL-PCR or plasmid rescue in mutant lines with multiple T-DNA copy numbers.

The genes flanking the T-DNA insertions in the mutants were distributed across all five Arabidopsis chromosomes and displayed a wide range of functions. Three genes, At3g05940, At3g26350 and At3g60760 were affected due to the T-DNA insertion in the mutants SK21229, SK21522 and SK22046, respectively. All these three genes coded for proteins of unknown functions (Table 2-2). The T-DNA insertion site data revealed genes involved in the following functions in at least two mutant lines with a red seed coat phenotype; pollen development, ribosomal structural proteins, embryo development, and zinc-ion binding. Genes encoding enzymes involved in lignin biosynthesis, root hair development, protein folding and signal transduction were also present in the T-DNA flanking regions in the red seed coat mutants. The mutant, SK22075, had two T-DNA copy number based on qPCR analysis and the insertion locus information were determined using plasmid rescue to be in At3g30415 and At2g25344. Therefore the mutant SK22075 was chosen for further characterization.

Table 2-2: T-DNA copy numbers and probable insertion sites with corresponding proteins and functions in Activation-tagged mutant lines of Arabidopsis displaying a red seed coat color phenotype.

Mutant	T-DNA Copy numbers	T-DNA Insertion	Coding protein name	Function
SK20676	2	Intergenic region of At5g56500 and At5g5610	Subunit of chloroplast chaperonins and glycine-rich protein /oleosin	Protein folding and lipid storage
SK20694	3	At4g30980	Encodes a basic helix-loop-helix (bHLH) protein	Regulates root hair development
SK21026#	2	At1g17145	RING/U-box superfamily protein	zinc ion binding
SK21229	2	At3g05940	Protein of unknown function	unknown
SK21470#	2	Intergenic region of At4g34050 and At4g24060	Caffeoyl coenzyme A O-methyltransferase 1 and Dof-type zinc finger DNA-binding family protein	Coumarin biosynthesis and zinc ion binding
SK21522	2	Intergenic region of At3g26350 and At3g26360	Unknown protein and ribosomal protein S21 family protein	Late embryogenesis abundant protein and structural constituent of ribosome
SK21559	2	At2g43480	Peroxidase superfamily protein	peroxidase activity, heme binding
SK21931	3	Intergenic region of At4g21745 and At4g21750	PAK-box/P21-Rho-binding family protein and encodes a homeobox protein similar to GL2	Unknown function and embryo development ending in seed dormancy
SK22046#	4	Intergenic region of At3g60760 and At3g60770	Unknown expressed protein and Ribosomal protein S13/S15	Unknown and structural constituent of ribosome
SK22075	2	At3g30415 At2g25344	Pseudogene, cysteine rich protein	unknown similarity to pollen coat protein
SK22100	2	Unknown	Unknown	Unknown
SK22446	1	Unknown	Unknown	Unknown
SK22078#	2	Intergenic region between At1g80090 and At1g80100	Cystathionine beta-synthase family protein and Histidine phospho-transfer protein 6	Pollen development, pollen tube guidance and cytokinin mediated signaling pathway
SK22484	3	At4g13460	Set domain group 22	histone-lysine N-methyltransferase activity

2.3.6 Characterization of mutant SK22075

The red seed coat mutant SK22075 (renamed RSC for Red Seed Coat) which was earlier determined to contain a single T-DNA insertion near the At2g25344 locus was found to contain

another T-DNA insertion based on additional information from Dr. Parkin, therefore SK22075 had two T-DNA insertion sites. The two genes flanking the T-DNA are At2g25344, which encodes a cysteine-rich protein (LCR14) similar to pollen coat protein and At3g30415, which is a pseudogene encoding an enzyme similar to that of the urophorphyrin III methylase family. Since both insertions were identified, it was hypothesized that either or both T-DNA insertions could impact carotenoid accumulation and/or red seed coat phenotype.

To determine if knockout mutants from the Salk library of either gene also exhibited a similar red seed coat phenotype, two allelic knockout mutants of At2g25344 were obtained. These two mutants SALK_011157C and SAIL_895_A01 were renamed RSC-1 and RSC-2, respectively. The At2g25344 gene encodes a 79 amino acid low molecular weight cysteine-rich protein (LCR14) showing similarity to a pollen coat protein. A protein BLAST search using the 8.95 kDa amino acid sequence of At2g25344 determined the protein to be an S locus-related glycoprotein-1 binding pollen coat protein (SLR1-BP). This family consists of a number of cysteine-rich SLR1 binding pollen coat like proteins. The At2g25344 gene organization is detailed in Figure 2-7A. The gene has two exons and an intron, the first exon is 61 bp long and the second exon is 179 bp long. The intron is 665 bp and forms the majority of the gene. The T-DNA insertion in two mutants RSC and RSC-2 were determined to be in exon 1, while the T-DNA insertion in the other mutant RSC-1 is located in the intron. Both RSC-1 and RSC-2 exhibited red seed color similar to RSC mutant (Figure 2-7B).

Unfortunately, Salk knockout lines were not available for the At3g30415 gene; therefore, the seed coat phenotype could not be determined. Furthermore, from the TAIR BLAST analysis, At3g30415 was determined to be a pseudogene, i.e. a dysfunctional gene that no longer encodes a complete protein or is no longer expressed (Vanin, 1985).

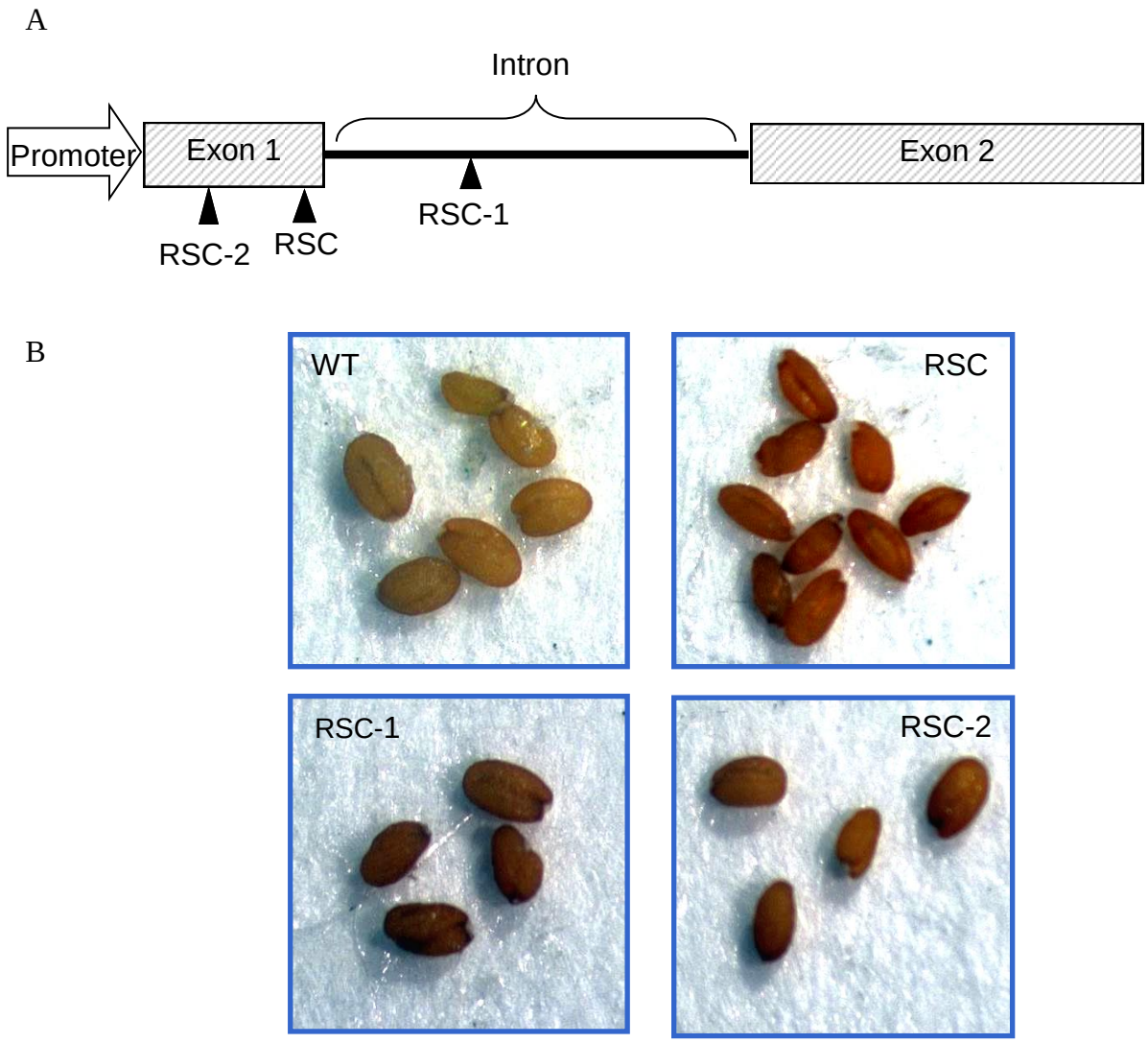

Figure 2-7: RSC mutant identification. A) Genomic structure of At2g25344 (*LCR14*) and T-DNA insertion positions. Shaded rectangles represent the exons, and lines represent introns. Triangles represent T-DNA insertions. B) Mature seeds of RSC (SK22075), RSC-1 and RSC-2 with red seed coat compared with WT.

2.3.7 Carotenoid analysis of WT and RSC mutants

The carotenoid analysis on the 10-day old seedlings of WT and mutants indicated that lutein levels were significantly reduced in the RSC mutant compared to that in RSC-1, RSC-2 and WT. The RSC-2 mutant had significantly higher β-carotene and violaxanthin levels in 10-day-old seedlings compared to mutants RSC, RSC-1 or the WT (Figure 2-8). The zeaxanthin level in the RSC mutant was significantly higher when compared to the WT seedlings. In contrast, the RSC-

1 and RSC-2 allelic mutants of RSC had significantly lower levels of zeaxanthin when compared to both RSC mutant and the WT seedlings (Figure 2-8).

Carotenoid analysis on the mature seeds indicated that the levels of lutein, violaxanthin and zeaxanthin were significantly higher in RSC and RSC-2 seeds compared to the WT seeds (Figure 2-9). However, the allelic SALK mutant RSC-1 did not show significant difference in mature seed lutein, violaxanthin and zeaxanthin levels when compared to the WT seeds. The seed β-carotene levels between the mutant lines and the WT were similar.

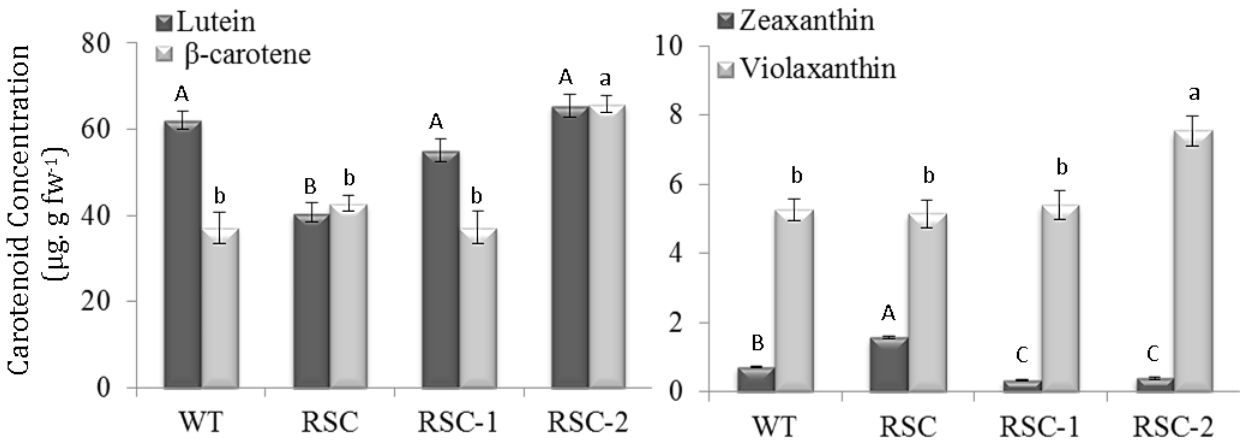

Figure 2-8: Carotenoid composition in 14-days old leaves of wild-type (WT) and RSC mutants of Arabidopsis. Values represent means ± SD (n = 3) and are expressed on a fresh weight (fw) basis. Different letters within each panel (uppercase for lutein and zeaxanthin; lower case for β-carotene and violaxanthin) indicate statistical significance at $p < 0.05$. fw, fresh weight; ND, non-detectable.

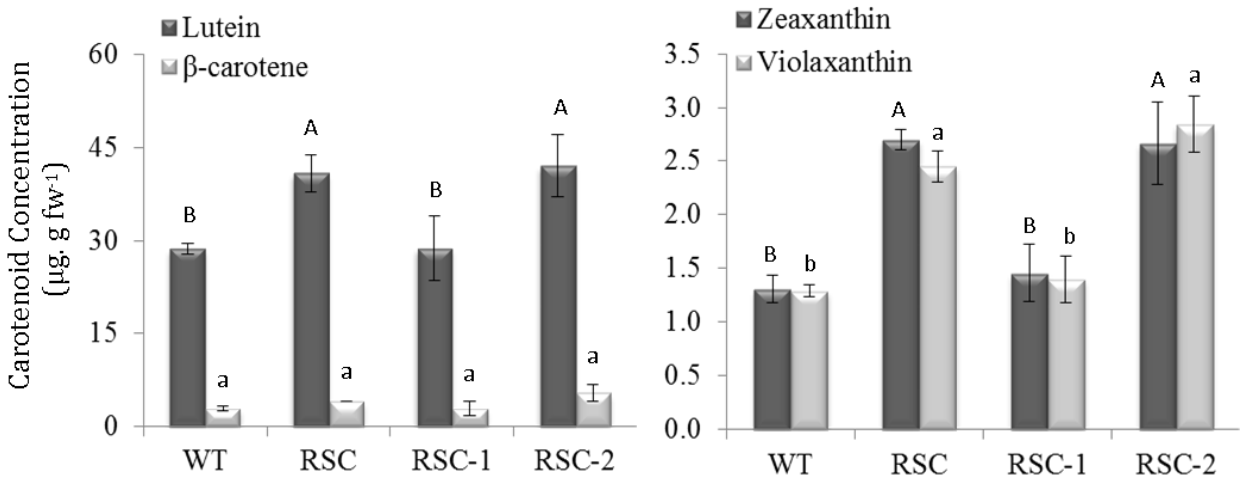

Figure 2-9: Carotenoid composition in mature seeds of wild-type (WT) and RSC mutants of Arabidopsis. Values represent means ± SD (n = 3) and are expressed on a fresh weight (fw) basis. Different letters within each panel (uppercase for lutein and zeaxanthin; lower case for β-carotene and violaxanthin) indicate statistical significance at $p < 0.05$. fw, fresh weight; ND, non-detectable.

2.3.8 Expression profiles of *LCR14*

sqPCR analysis was used to determine the expression of *LCR14* in leaves, stem, flower bud, flower, siliques and mature seeds. The results indicated that *LCR14* is expressed only in the floral buds and flowers as mRNA could not be detected in other tissues (Figure 2-10). It is to be noted that the *Actin2* levels for the mature seeds in Figure 2-10 were very low and therefore the presence of any LCR14 transcripts is not detectable. cDNA from total RNA obtained from the floral buds of mutants and WT were used to determine the expression levels of *LCR14* using qPCR. The qPCR results indicated that the *LCR14* expression levels in all the three RSC mutants were significantly reduced compared to the WT expression levels (Figure 2-11). Taken together, the carotenoid analysis and gene expression profiles suggest that the red seed coat phenotype may be associated with the defective *LCR14*, but that this does not correlate with carotenoid levels.

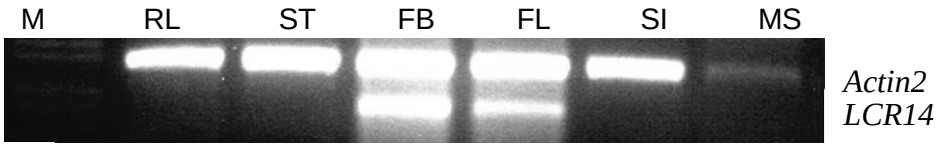

Figure 2-10: Detection of *LCR14* transcripts in different tissues of Arabidopsis. M-100bp DNA marker; RL, rosette leaves; ST, stem; FB, flower bud; FL, flower; SI, siliques; MS, mature seeds.

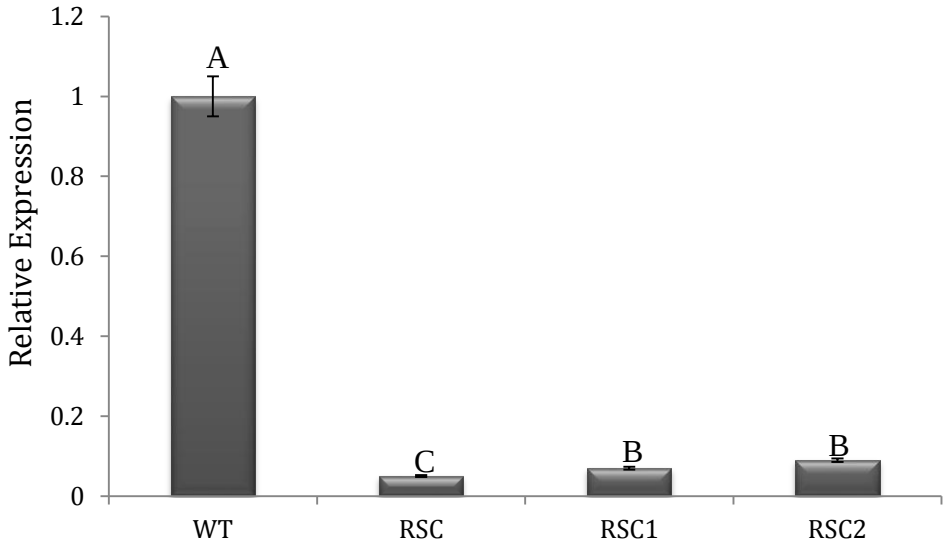

Figure 2-11: *LCR14* expression in flower bud tissues of wild-type (WT) and RSC mutants of Arabidopsis. The expression levels are normalized to the reference gene *ACT2* and relative to the WT set to a value of 1. Values represent means ± SD (n = 3). Different letters indicate statistical significance at $p < 0.05$.

2.4 Discussion

This study showed that lutein and β-carotene together account for up to 90% of the total carotenoid content in the leaves and seeds of Arabidopsis. The highest levels of lutein were found in 10-day-old seedlings and mature leaves compared to the reproductive tissues. The results also indicate that carotenoid levels in the seedlings were comparable with those in mature leaves. Therefore, using 10-day-old seedlings for carotenoid analysis should reduce the time required to screen for seedling mutants with altered carotenoid profiles. This study also demonstrated that Arabidopsis flowers contain significantly higher levels of violaxanthin compared to other tissues analyzed. In the tomato *wf*, mutant the pale white phenotype of the flower compared to yellow phenotype of the non-mutated tomato plants was associated with a sharp decrease in the violaxanthin and neoxanthin content (Galpaz et al., 2006). Although Arabidopsis flower petals are pale white, the other parts of the flower; namely, stamen, stigma and pollens are orange to yellow in color similar to the color of violaxanthin. Therefore, higher violaxanthin levels in Arabidopsis flowers could be attributed to the accumulation of violaxanthin in the stamen, stigma and pollen pellets.

Carotenoid analysis on young *B. napus* seeds indicated that the embryo had significantly higher levels of β-carotene and similar levels of lutein compared to the seed coat. However, mature *B. napus* embryo and seed coat had 30 times less lutein and β-carotene compared to the developing embryo and seed coat. The ABA levels in Arabidopsis seeds also increase during maturation and a major part of the ABA is synthesized both in the embryo and seed coat (Karssen et al., 1983). Similarly, reduction in carotenoid levels has been observed and attributed to the synthesis of ABA in the mature seeds of Arabidopsis (Howitt and Pogson, 2006). ABA-deficient mutants of *Nicotiana plumbaginifolia* show substantial seed abortion, reduced seed yield, and delayed growth of the remaining embryos (Frey et al., 2004). In the same study, it was shown that the ABA is synthesized in the seed coat and not transported from the phloem (Frey et al., 2004). Therefore, from these observations, reduction in the two major carotenoids occurs concomitantly with seed maturation and is correlated to an increase in ABA content. Although carotenoids in the seed coat of Arabidopsis were not measured in this thesis owing to small seed size, it is suggested from the *B. napus* study that the Arabidopsis seed coat might also contain carotenoids that are used during maturation for ABA biosynthesis.

In this study, SK activation-tagged Arabidopsis mutants with red seed coat were screened and analyzed for altered carotenoid profiles. The red color was in the screening to determine accumulation of lycopene carotenoid, which is red in color. Although some of the screened mutants had altered carotenoid profiles, not all the mutants had significantly altered carotenoid levels. A few of the screened mutants showed a red seed coat phenotype, but no alteration in their carotenoid content when compared to the WT. However, no lycopene content were determined in this study, therefore measuring lycopene levels in the seed would help to determine the any correlation of red seed coat to lycopene. The golden brown color of the WT seed coat is mainly attributed to the accumulation of phenolic compounds, such as anthocyanins and pro-anthocyanins (Tanaka et al., 2008). Mutants defective in pro-anthocyanidin biosynthesis were also characterized using altered seed coat phenotype, where the red seed color was found in a mutant with a defective anthocyanin reductase gene (Debeaujon et al., 2000). This indicates that the phenotype observed may not be solely attributed to the change in the carotenoid content.

The qPCR method used to identify the copy numbers of the screened SK Arabidopsis mutants was not an efficient technique, as mutant SK22075 had another copy of the T-DNA insertion in the genome. Therefore, the qPCR could be used as a high throughput screening method to determine T-DNA copy numbers; however, Southern hybridization needs to be performed to confirm the T-DNA copy numbers in the selected mutant. In this study, two methods were used to determine the genes flanking the T-DNA insertion site, namely, plasmid rescue and TAIL-PCR. Although both methods failed to determine all the T-DNA insertion sites, the methods were in successful in determining at least one T-DNA insertion locus. Furthermore, TAIL-PCR stood out to be a better method compared to plasmid rescue, as nine T-DNA insertion loci were determined by TAIL-PCR and only four T-DNA loci were identified by plasmid rescue.

Mutant SK22075 (RSC) was selected based on qPCR analysis that showed it to contain a single T-DNA insertion and the insertion site was determined using plasmid rescue. The seedling carotenoid profiles between the RSC and SALK mutants were not similar. The mature seed carotenoid analysis indicated that RSC and RSC-2 mutants had similar carotenoid profiles with significantly higher levels of lutein, violaxanthin and zeaxanthin content. Gene expression studies indicated that the *LCR14* is expressed only in floral parts of Arabidopsis, therefore, this

mutation is unlikely to be related to the carotenoid changes in the seedlings and mature seeds. Gene expression analysis on the RSC and Salk mutants (RSC-1 and RS-2) indicate that the red seed coat phenotype could be associated with the defective *LCR14* encoding a cysteine-rich protein with similarities to pollen coat protein belonging to the SLR1 family. Additionally, the gene is shown to be expressed only in the flower and flower buds indicating a close relationship between *LCR14* expression and reproductive stage in Arabidopsis. The adhesion of pollen grains to the stigmatic surface is a critical step during sexual reproduction in plants.

In Brassicas, S locus related glycoprotein 1 (SLR1), a stigma-specific protein belonging to the S gene family of proteins, has been shown to be involved in pollination (Murphy, 2006). SLR1-BP specifically binds SLR1 with high affinity. The *SLR1-BP* is specifically expressed in pollen at late stages of development and is a member of the class A pollen coat protein family, which includes LCR14-A1, an SLG (S locus glycoprotein)-binding protein (Takayama et al., 2000). However, more analysis involving ultra-structural studies with the mutant flower parts, the reproductive mechanism and the protein binding studies in the mutant will determine the role of the SLR1-BP protein encoded by *LCR14*. Gene complementation and antisense RNAi studies would be able to confirm the association of *LCR14* in red seed coat phenotype.

Screening of Arabidopsis mutants using red seed coat color did not prove to be an efficient screening method for identifying mutants related to carotenoid biosynthesis. Although mutants with altered carotenoid profile were identified and the RSC mutant characterized; sufficient relationship between the carotenoid profile and the affected gene function cannot be established. Furthermore, since the affected *LCR14* in the RSC mutant is related to pollen coat protein family and its allelic mutants (RSC-1 and RSC-2) did not display a similar carotenoid profile, any direct or indirect relationship to carotenoid biosynthesis is questionable. Since, the scope of this thesis is to identify Arabidopsis mutants with altered carotenoid profiles to discover novel regulatory genes involved in the carotenoid biosynthesis, further characterization of the RSC mutant was withheld. Therefore, a new methodology is required to identify mutants with altered carotenoid profiles.

3 LIGHT AND REDOX MEDIATED REGULATION OF CAROTENOID BIOSYNTHESIS IN ARABIDOPSIS

3.1 Introduction

Carotenoids play a vital role in photoprotection and are integrated in protein complexes of the photosynthetic mechanism (Scholes et al.). Light is a very important environmental factor for all photosynthetic organisms. Not only is it essential for photosynthesis, but it is also involved in the regulation of many aspects of plant growth and development. In higher plants, light plays a key role in the process of de-etiolation, the transition from growth in the dark to growth in the light. During de-etiolation, several developmental responses to light have been observed, such as the opening of the apical hook, expansion of the cotyledons, chloroplast development, gene expression and accumulation of photosynthetic pigments (Bohne and Linden, 2002).

A significant increase in lutein content occurs when leaves are exposed to sunlight, indicating that specific carotenoids play a significant role in photosynthesis in plants (Czeczuga, 1987). However, under high intensity illumination (~60,000 lux) carotenoids are rapidly destroyed (Horváth et al., 1972). The basic chemical function of carotenoids is the quenching of triplet-state chlorophyll and singlet oxygen (Perez-Martin, 1999). Three xanthophylls (lutein, zeaxanthin and violaxanthin) participate in the dissipation of excess light energy as heat, a process termed non-photochemical quenching (NPQ) (Mozzo et al., 2008; Nowicka et al., 2009). Thermal dissipation of excess light energy represents a basic photoprotective mechanism in photosynthetic eukaryotes. NPQ is generally based on light-regulated and xanthophyll-dependent specific antenna proteins whose conformations are affected by pH or light. Therefore, the xanthophyll-dependent antenna proteins act as sensors of lumen pH or light and thereby activate or deactivate NPQ through light-induced and pH-dependent conformational changes (Baroli et al., 2003; North et al., 2005; Johnson et al., 2007). Zeaxanthin has also been reported to have an antioxidant function independent of binding to photosystem II (PSII) antenna proteins (Havaux et al., 2007).

In *Synechocystis* sp. the redox state of one of the electron carriers, Cytb6f, between the plastoquinone pool and photosystem I was shown to influence not only the expression of the

PSBA gene, but also that of two other photosynthetic genes, *PSAE* (encoding a small subunit of PSI) and *CPCBA* (encoding the β- and α-subunits of the phycocyanin) (Alfonso et al., 2000). The redox state of a photosynthetic electron carrier activates PSBA in its oxidized state and PSAE in its reduced state, supporting redox regulation of PSI and PSII genes. However, the origin of the signal in *Synechocystis* was located between the plastoquinone pool and PSI (Dahnhardt et al., 2002).

From the present literature in plants, transcriptional regulation by redox seems to work only under low- or mid-light conditions (Pfannschmidt et al., 2003). In addition, little is known about how the model of transcriptional regulation fits with that of translational regulation and whether and how these regulating mechanisms cooperate (2001; 2001; Pfannschmidt et al., 2003). To address this issue and to determine which xanthophyll carotenoid genes are regulated by light, redox changes or both at the transcriptional level, the expression profiles of Arabidopsis genes involved in the xanthophyll cycle and carotenoid biosynthesis were determined in response to light and redox stress. These findings will be used to evaluate the role of the plastoquinone pool and redox regulation in carotenoid biosynthesis. This will provide an alternative strategy for screening new carotenoid mutants in Arabidopsis.

3.2 Materials and Methods

3.2.1 Plant material and growth conditions

Seed of wild-type (WT) Arabidopsis (ecotype Columbia) were obtained from the laboratory of Dr. Isobel Parkin at Agriculture and Agri-Food Canada (AAFC, Saskatoon, Canada). Seeds were surface sterilized using a solution of 70% (v/v) ethanol and 30% (v/v) sodium hypo chlorite followed by three washes in distilled water and then suspended in sterile water containing 0.1% agar. The suspended seeds were deposited using a pipette on to a group of 18 sterile Petri dishes containing ½ × Moorashige and Skoog MS media (Sigma Aldrich) in 0.8% (w/v) agar with 2% (w/v) sucrose. The Petri dishes were divided into three sets containing 6 plates each and placed in grow room set at 22°C with a PPFD of 250 μmol photons m^{-2} s^{-1}. The first set of plates (control) were placed at 16/8 h (light:dark) conditions for 12 days. The second set of plates (dark-adapted) were placed under 16/8 h (light:dark) conditions for 10 days and then covered using thick aluminum foil to create a dark-adapted environment for two days. The third sets of plates (etiolated) were covered using thick aluminum foil creating a continuous dark environment for the entire 12 days. All seedlings were sampled on day 12, flash frozen in liquid nitrogen and stored at -20°C until used for carotenoid or gene expression analyses.

3.2.2 Treatment with Photosynthetic Inhibitors

The photosynthetic inhibitors 2,5-dibromo-3-methyl-6-isopropyl-p-benzoquinone (DBMIB) and 3-(3',4'-dichlorophenyl)-1,1'-dimethyl urea (DCMU) were used to examine the redox state of the plastoquinone pool. Arabidopsis plants (ecotype Columbia) were grown from seed under greenhouse conditions as described in section 3.2.1. The 20 day old rosette leaves from a group of 15 plants were excised 2 to 3 h after the onset of the day period. The leaf tissues were divided into 9 groups representing three biological replicates for each treatment and control (DBMIB, DCMU and ethanol). Stock solutions of DBMIB (1 M) and DCMU (100mM) (Sigma aldrich) were prepared by dissolving the chemicals in 100% (v/v) ethanol. The working solutions of the herbicides were prepared by diluting appropriate amount of stock solutions in distilled water. Each group of leaves were placed in a beaker containing the 100 μM DBMIB, 10 μM DCMU or 1% ethanol and vacuum infiltrated using a vacuum chamber for 5 min. After vacuum infiltration,

the leaf tissues were placed under low light conditions (40 to 50 μmol photons m^{-2} s^{-1}) at 25°C. Samples from each group were collected at 5 and 30 min, as well as 1, 2, 3 and 4 h after infiltration. The samples were immediately ground in liquid nitrogen and stored at -80°C until used for gene expression studies.

3.2.3 Carotenoid extraction and determination

Carotenoid extraction and HPLC analyses from control, dark-adapted and etiolated seedlings (all 12 days old) were carried out as described in sections 3.2.2 and 3.2.3 respectively.

3.2.4 Total RNA extraction and cDNA synthesis

The extraction of total RNA and cDNA synthesis from control, dark-adapted and etiolated seedlings (all 12 days old), as well as two-week-old leaves treated with photosynthetic inhibitors occurred as described in section 3.2.6.

3.2.5 qPCR

Relative expression levels of carotenoid biosynthetic genes were examined using qPCR. Gene-specific primers (Table 2-1 and Table 3-1) were selected using Primer3 software (http://bioinfo.ut.ee/primer3/) (Untergasser et al., 2012). qPCR and determination of relative expression levels occurred as described in section 2.2.7.2. Expression values were calculated and normalized to the expression of *PEROXIN 4*, a suitable endogenous reference gene because of its stable and low level expression in Arabidopsis (Czechowski et al., 2005).

Table 3-1: Gene-specific primers used in qPCR for the examination of carotenoid biosynthetic genes.

Gene	AGI code	Forward primer (5′to 3′)	Reverse primer (5′ to 3′)
PSY	At5g17230	TGCGGTGAAGTTTGCGCTGA	TGAAGCATTTGGCCCATCCA
PDS	At4g14210	GTCGGTCACGCGCTCAGGTA	CGAGATGCTGACATGGCCAGA
ZDS	At3g04870	CCATCGTCACGAGGCCTAGAA	TGTGTATGAACCGGCGAGGA
βLYC	At3g10230	TGGTAGCGCTGCTCTTTTGGA	ACCAGCAGGACCACCACCAA
εLYC	At5g57030	GTCATGGAGTTGTCGAAGGA	CGAAATCTTCTCTCACCGCTAC
βHYD	At4g25700	GGCACGCTTCTCTATGGAATATGCATGA	GAATCCATAAGAGAGGAGACCAATCGCT
εHYD	At3g53130	CGAAATCCCAATCATGGGTCA	GCACCTCCGAGGAGATCAGC
ZEP	At5g67030	ATGACCGGCTTCGAGAGTGG	TTCCGACGATGCAAGGTTGA
VDE	At1g08550	ACCGCTCCGCTGTTGCTAAA	TGGCAATGCACTTTGCGAGT
PEX4	At5g25760	TGCTTGGAGTCCTGCTTGGA	TGTGCCATTGAATTGAACCCTCT

PSY, phytoene synthase; *PDS*, Phytoene desaturase; *ZDS*, ζ-Carotene desaturase; *βLYC*, β-Lycopene cyclase; *εLYC*, ε-Lycopene cyclase; *βHYD*, β-ring hydroxylase; *εHYD*, ε-ring hydroxylase; *ZEP*, Zeaxanthin epoxidase; *VDE*, Violaxanthin de- epoxidase; *PEX4*, peroxin 4.

3.2.6 Experimental design and statistical analyses

Sampling for carotenoid determination and qPCR, as well as statistical analyses of the data occurred as described in section 2.2.8.

3.3 Results

3.3.1 Carotenoid levels in dark-adapted and etiolated seedlings

The levels of three carotenoids; β-carotene, violaxanthin and zeaxanthin, decreased significantly in Arabidopsis seedlings after a 48 h dark-adaptation (Figure 3-1). Similarly, the etiolated seedlings did not contain detectable levels of carotenoids except for lutein. The lutein level was unaffected in the dark-adapted seedlings, but significantly lower in the etiolated seedlings when compared to the normal light/dark grown (control) seedlings. Zeaxanthin was not detectable in either dark-adapted or etiolated seedlings. Interestingly, the violaxanthin level in the dark-adapted seedlings was significantly lower compared to the control. These results indicate a relationship between the levels of these carotenoids and light.

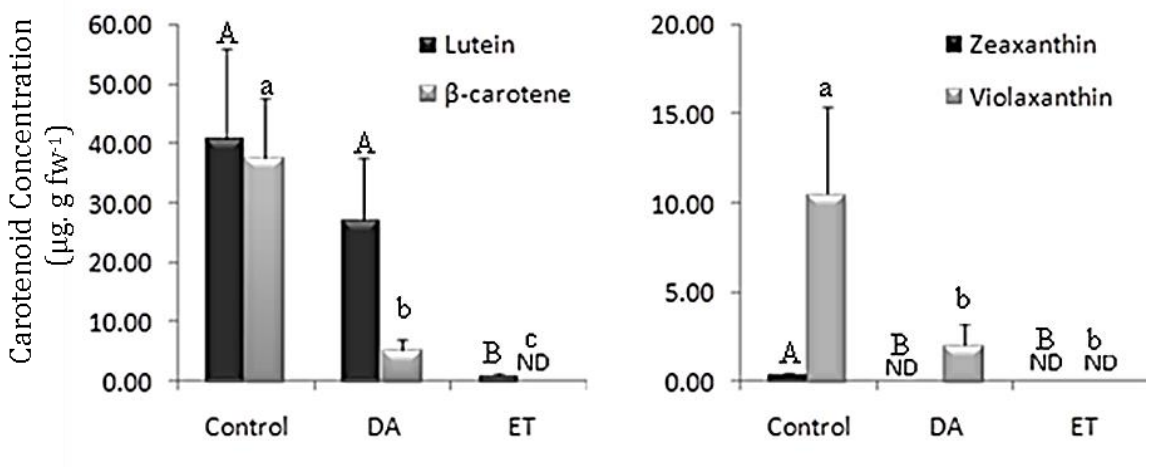

Figure 3-1: Carotenoid composition in seedlings of Arabidopsis. Seedlings were grown under varying light/dark regimes which included control, dark-adapted (DA) and etiolated (ET) conditions. Values represent means ± SD (n = 3) and are expressed on a fresh weight (fw) basis. Different letters within each panel (uppercase for lutein and zeaxanthin; lower case for β-carotene and violaxanthin) indicate statistical significance at $p < 0.05$. fw, fresh weight; ND, non-detectable.

3.3.2 Carotenoid gene expression in dark-adapted and etiolated seedlings

qPCR was used to determine if the expression of genes encoding carotenoid biosynthetic enzymes was affected by dark-adaptation and etiolation (Figure 3-2). The gene expression analysis revealed distinct expression profiles for carotenoid biosynthetic genes with the different

treatments. The first expression profile where gene expression was significantly lower in both dark-adapted and etiolated seedlings compared to control was displayed by five genes, namely, phytoene synthase (*PSY)*, phytoene desaturase (*PDS*), β-lycopene cyclase (*βLYC*), β-hydroxylase (*βHYD*) and zeaxanthin epoxidase (*ZEP*). The second expression profile where the gene expression was significantly lower only in the etiolated seedlings, but unchanged in dark-adapted seedlings compared to control was displayed by two genes, namely, ζ-carotene desaturase (*ZDS*) and vioxanthin deepoxidase (*VDE*). The third expression profile where the gene expression was significant decreased in dark-adapted compared to both etiolated and control seedlings was displayed by two genes, namely, ε-lycopene cyclase (*εLYC*), and ε-hydroxylase (*εHYD*). The expression levels of these two genes (*εLYC* and *εHYD*) were significantly lower in etiolated seedlings compared to control; however, significantly higher when compared to dark-adapted seedlings.

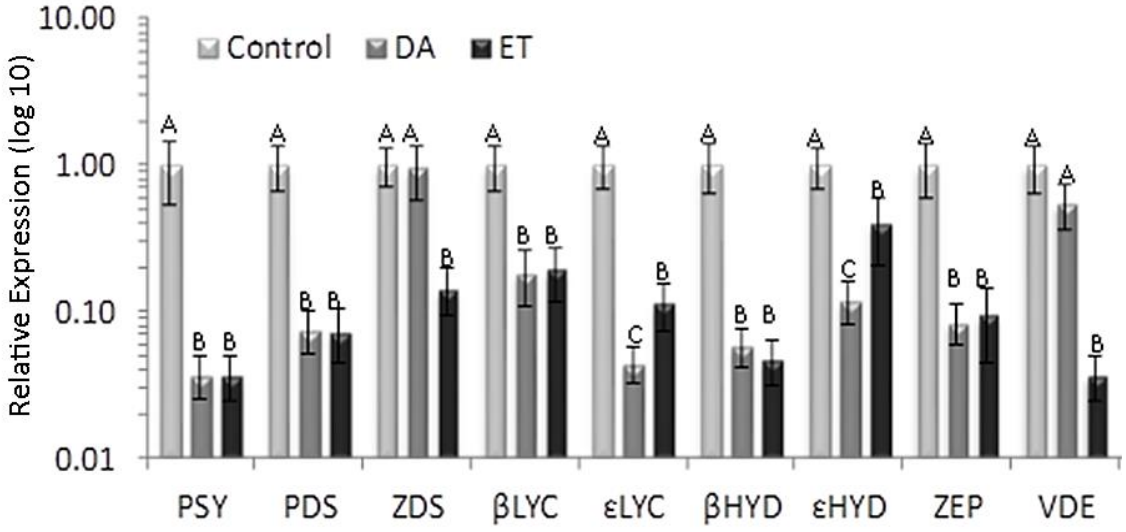

Figure 3-2: Expression profile of carotenoid biosynthetic genes in seedlings of Arabidopsis. Seedlings were grown under varying light/dark regimes which included control, dark-adapted (DA) and etiolated (ET) conditions. The expression levels are normalized to the reference gene *PEX4* and relative to the control light regime set to a value of 1. Values represent means ± SD (n = 3). Different letters within genes indicate statistical significance at $p < 0.05$. *PSY*, Phytoene synthase; *PDS*, Phytoene desaturase; *ZDS*, ζ-Carotene desaturase; *βLYC*, β-Lycopene cyclase; *εLYC*, ε-Lycopene cyclase; *βHYD*, β-ring hydroxylase; *εHYD*, ε-ring hydroxylase; *ZEP*, Zeaxanthin epoxidase; *VDE*, Violaxanthin de- epoxidase.

3.3.3 Carotenoid gene expression upon treatment with photosynthetic inhibitors

The normalized relative expression profiles for various carotenoid biosynthetic genes in response to DBMIB and DCMU treatments are shown in Figure 3-3 (upper-carotenoid pathway) and Figure 3-4 (lower carotenoid pathway). The DBMIB treatment inhibits the oxidation of plastoquinol to plastoquinone. The gene expression analysis indicated that the transcripts of all genes involved in carotenoid biosynthesis increased significantly at 2 h after treatment with DBMIB when compared to the control sample that was treated only with 1% ethanol. PSY the first enzyme involved in the biosynthesis of carotenoids had the quickest response and transcript levels increased 3.1-fold within 30 min of DBMIB treatment (Figure 3-3). Three genes, *εLYC*, *βLYC*, and *VDE*, were moderately responsive with their highest transcript levels reaching 4.3-, 3.5- and 3.0- folds, respectively, after 1 h of DBMIB treatment. In the case of *εHYD*, significantly higher transcript level (3.5-fold) was reached 2 h after DBMIB treatment. Four genes, namely, *ZEP, βHYD, PDS* and *ZDS*, were expressed at high levels up to 13-, 9-, 7- and 5-fold increase in their transcript levels, respectively. All the four genes (*ZEP, βHYD, PDS* and *ZDS*) had significantly higher levels of transcripts at 2 h when compared to the control (Figure 3-3 and Figure 3-4.

DCMU treatment of Arabidopsis leaves inhibits the reduction of plastoquinone to plastoquinol. DCMU treatment led to a significant decrease in the transcript levels of five genes, namely, *PDS, εLYC, βLYC, εHYD,* and *βHYD* within 30 min to 1 h. Four genes, namely, *PSY*, *ZDS*, *ZEP* and *VDE*, did not show significant changes in the transcript levels upon DCMU treatment when compared to the control. It is also interesting to note that the two genes involved in the xanthophyll cycle, *ZEP* and *VDE*, did not show significant changes in their transcript levels during DCMU treatment, but responded to DBMIB treatment.

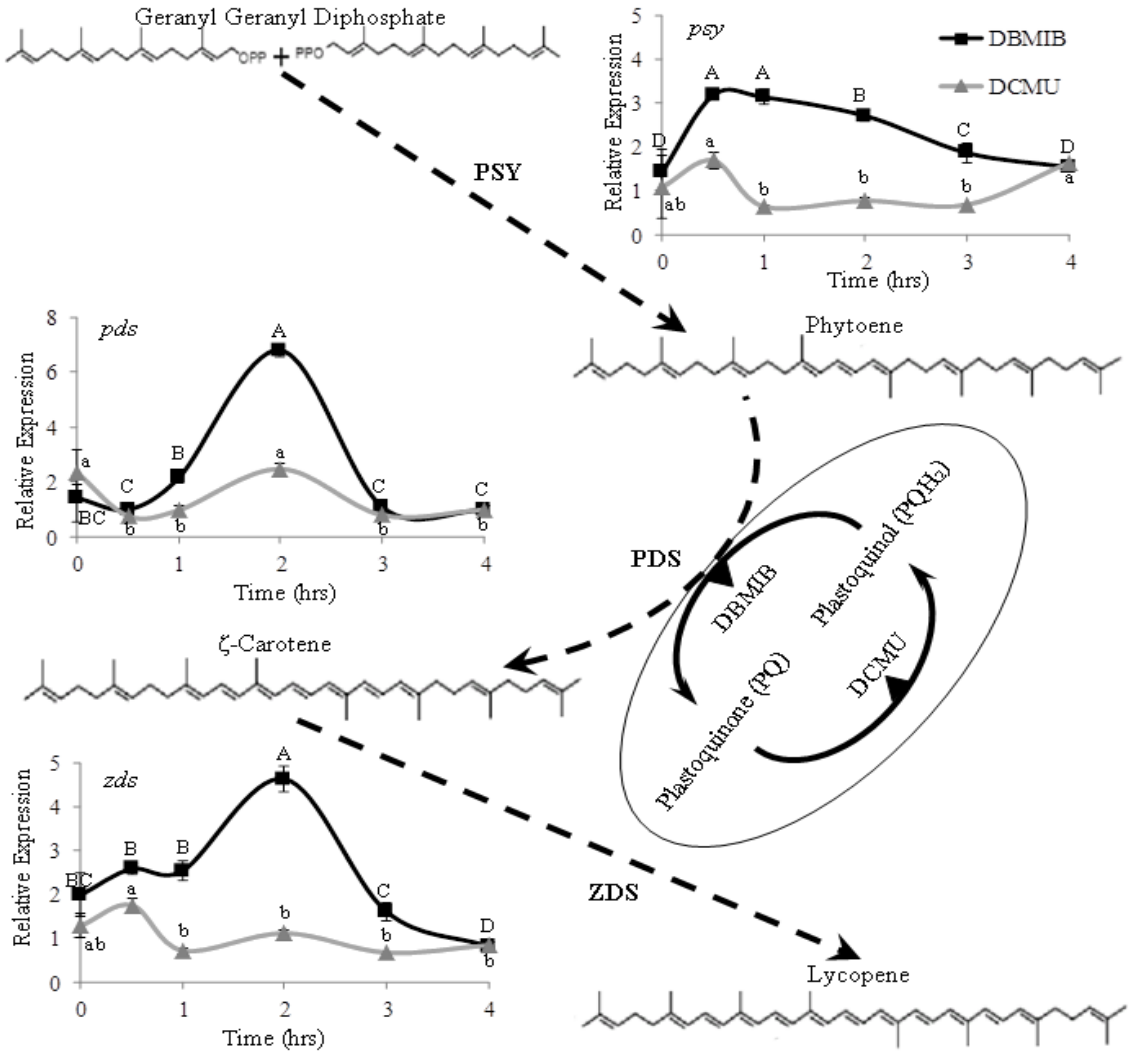

Figure 3-3: Expression profiles of upper carotenoid pathway genes in leaves of Arabidopsis treated with photosynthetic inhibitors. Mature leaves (20-days-old) were treated with 100 µM DBMIB (■) or 10 µM DCMU (▲) and sampled over 4 hours. The expression levels are normalized to the reference gene *PEX4* and relative to a 1% ethanol control set to a value of 1. Values represent means ± SD (n = 3). Different letters within treatments (uppercase for DBMIB; lowercase for DCMU) indicate statistical significance at $p < 0.05$. The figure also shows the interaction of PDS, DBMIB, DCMU and the plastoquinone pool. *PSY*, Phytoene synthase; *PDS*, Phytoene desaturase; *ZDS*, ζ-Carotene desaturase.

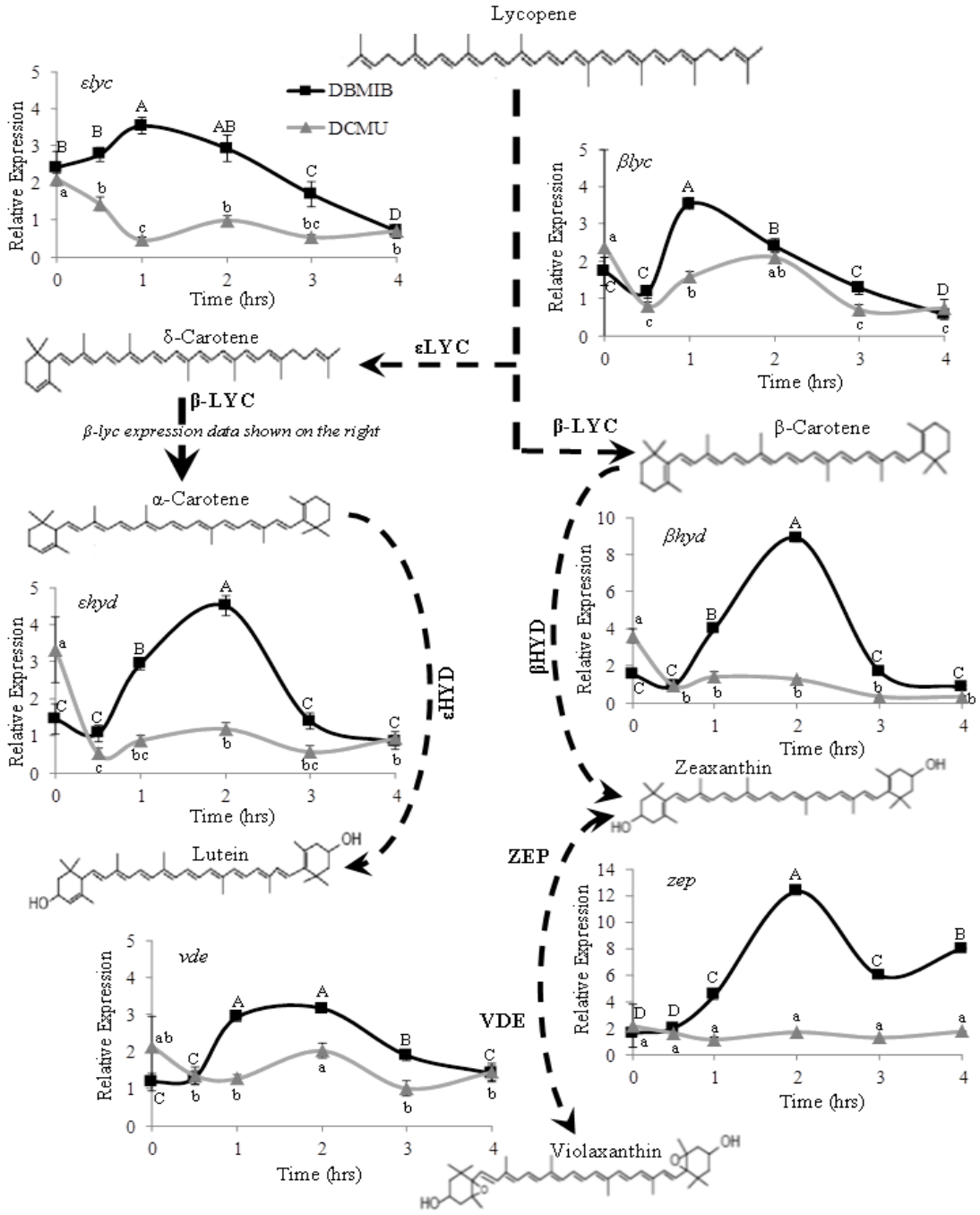

Figure 3-4: Expression profiles of lower carotenoid pathway genes in leaves of Arabidopsis treated with photosynthetic inhibitors. Mature leaves (20-days-old) were treated with 100 µM DBMIB (■) or 10 µM DCMU (▲) and sampled over 4 hours. The expression levels are normalized to the reference gene *PEX4* and relative to a 1% ethanol control set to a value of 1. Values represent means ± SD (n = 3). Different letters within treatments (uppercase for DBMIB; lowercase for DCMU) indicate statistical significance at $p < 0.05$. *βLYC*, β-Lycopene cyclase; *εLYC*, ε-Lycopene cyclase; *βHYD*, β-ring hydroxylase; *εHYD*, ε-ring hydroxylase; *ZEP*, Zeaxanthin epoxidase; *VDE*, Violaxanthin de- epoxidase.

3.4 Discussion

In this study, the light- and redox-mediated regulation of carotenoid genes was investigated using short term dark-adapted seedlings and site-specific electron transport chain inhibitors, respectively. While the vital role of carotenoids in photoprotection and quenching of triplet-state chlorophyll and singlet oxygen have been documented (Steiger et al., 1999; Pfannschmidt, 2003; Woitsch and Romer, 2003), very little is known about the light regulation of carotenogenesis on a molecular level. Only a few genes involved in the xanthophyll cycle, such as *β-HYD, ZEP* and *VDE* (Niyogi et al., 1998; North et al., 2005), and light-mediated regulation of *PSY* have been studied in detail. During short term dark-adaptation, a significant reduction in the levels of major carotenoids was observed. The reduced carotenoid levels under these conditions were similar to those observed in the etiolated seedlings, except for lutein. Similar observations have been reported in etiolated and low light treated maize seedlings (Horváth et al., 1972), and low light treatment studies in *Synechocystis* (Steiger et al., 1999). Transcripts of many carotenoid genes in short term dark-adapted seedlings displayed an expression profile that mimicked the etiolation state, indicating that the carotenoid genes are regulated by light. Photosynthetic organisms are also known to sense light in a more indirect way, namely via the redox states of the photosynthetic electron transport chain (Bennoun, 2001; Pfannschmidt et al., 2003; Oelze et al., 2008). During redox control, changes in the reduction/oxidation state of plastoquinone in PSII photosynthetic electron transport can occur due to a range of environmental conditions, such as light, drought, herbicides etc. (Pfannschmidt et al., 2001; Oelze et al., 2008). These can subsequently result in various responses, such as the modulation of enzyme activities in the chloroplast or the up-regulation of chloroplast and nuclear genes (Baroli et al., 2003; Pfannschmidt, 2003).

To dissect the role of redox mediated regulation of carotenoid biosynthesis, two site-specific electron transport chain inhibitors DCMU and DBMIB were used. The DCMU treatment should mimic a low light environment as it binds to the D1 protein of PSII and blocks the reduction of plastoquinone to plastoquinol leading to accumulation of plastoquinone in the lumen. The DBMIB treatment should mimic a high light environment as it binds to the Q_0 site of the cytb_6f (Roberts et al., 2004) and affects the oxidation of plastoquinol to plastoquinone, thereby leading

to the accumulation of reduced plastoquinone in the lumen and thereby starving the Q_0-site of plastoquinol.

In this study, *PSY* gene expression was significantly reduced during short term dark adaptation and etiolation of Arabidopsis seedlings; furthermore PSY displayed an immediate strong response to DBMIB treatment by increasing its transcript levels up to 3-fold compared to the control within 30 min of treatment. However, DCMU treatment did not affect the transcript levels when compared to the control treatment. Increases in PSY protein levels and enzymatic activity during de-etiolation in mature chloroplasts have been reported (Steiger et al., 1999; Welsch et al., 2000; Bohne and Linden, 2002). Similarly, in *Haematococcus pluvialis* high light led to increased PSY gene expression, which was prevented upon treatment with DCMU (Steinbrenner and Linden, 2001). Together, these results and the supporting literature suggest that *PSY* gene expression is activated by the accumulation of the plastoquinol in the lumen. Further analysis on the measurement of the plastoquinol pool should be able to confirm these observations.

The transition from phytoene to ζ-carotene is achieved by PDS through oxidation of plastoquinol to plastoquinone. Similarly, conversion of ζ-carotene to lycopene is also carried out by another desaturase enzyme ZDS. It is proposed that ZDS might also use the electron transport chain to facilitate the oxidation of plastoquinol to plastoquinone (Dong et al., 2007). From a thermodynamic point of view, the desaturation step is made possible because they are coupled with plastoquinol oxidation. This coupling can take place because both the carotenoid desaturase reactions and the photosynthetic machinery share the plastoquinone pool as a common intermediate (Bennoun, 2001). In this study, both *PDS* and *ZDS* expression were significantly higher 2 h after DBMIB treatment. This could be attributed to the accumulation of plastoquinol in the lumen upon treatment with DBMIB. However, short term dark-adaptation and DCMU treatment had contrasting effects on *PDS* and *ZDS* expression levels. *PDS* transcript level was significantly lower in both short term dark-adapted seedlings and DCMU treatment (mimicking low light) compared to control. In contrast, *ZDS* expression was not affected by dark-adapted conditions or DCMU treatment when compared to the control. This suggests that *PDS* and *ZDS* genes are regulated independently; *PDS* expression is directly regulated by the redox pool (both high and low light), while *ZDS* expression is regulated only by accumulation of plastoquinol

(high-light). It has been demonstrated that the redox state of the plastoquinone pool is a potent initiator of retrograde signaling, although the nature of the signaling pathway(s) is unclear (Pfannschmidt et al., 2003).

The εLYC, βLYC and εHYD enzymes sequentially catalyze the conversion of lycopene to lutein via α-carotene. Lutein is one of the xanthophylls that functions in photoprotection and its accumulation can substitute for the loss of NPQ by zeaxanthin in Arabidopsis (Li et al., 2009). Furthermore, it is one of the major carotenoids present in Arabidopsis seedlings. In this study, lutein was the only carotenoid detectable in the etiolated seedlings; furthermore, the expression levels of *εLYC* and *εHYD* were significantly higher in the etiolated seedlings when compared to dark-adapted seedlings. This indicates that lutein has an important role to play during etiolation. Enhanced accumulation of protochlorophyllide was correlated with increased levels of lutein in etiolated Arabidopsis seedlings suggesting a cross-regulation between chlorophyll and carotenoid biosynthetic pathways (Myśliwa-Kurdziel et al., 2012). The lutein level in the dark-adapted seedlings was not significantly different compared to the control. However, the expression levels of *εLYC* and *εHYD* were significantly reduced at 1 h and 30 min, respectively upon DCMU treatment (mimicking low light stress) and short term dark-adapted seedlings compared to the control. Taken together these results indicate that εLYC and εHYD could be regulated by the redox pool.

βLYC is an important enzyme in carotenoid pathway as it catalyzes the production of both α- and β-carotene. Although the lutein levels were unaffected, the β-carotene levels were significantly reduced in in the dark-adapted seedlings when compared to control. Similarly, *βLYC* expression was also significantly affected in both dark-adapted seedlings and DCMU treated samples compared to control treatments. In DBMIB treated Arabidopsis leaves, the induction time for βLYC was 1 h compared to 2 h, with most genes. In higher plants, β-carotene binds to reaction center subunits of both PSI and PSII, while pigments of the xanthophyll cycle pool are both accessory pigments and structural elements of light-harvesting complexes. The xanthophylls (violaxanthin, antheraxanthin and zeaxanthin) with β-carotene as the chromophore function in photosynthetic electron transport, and as photoprotectants of the photosynthetic apparatus from reactive oxygen species (ROS) (Dall'osto et al., 2007). The role of βLYC gene in conferring tolerance to salt stress has been reported in Arabidopsis and tobacco (Chen et al.,

2003). These results suggest that the regulation of βLYC gene could be related to ROS stress created by the treatment of photosynthetic inhibitors.

βHYD catalyzes the synthesis of zeaxanthin, which participates in the photo-protection mechanism (Sun et al., 1996). The expression of *βHYD* increased upon DBMIB treatment, but 1 h later than *εLYC* and *βLYC*, indicating that its expression is regulated by the plastoquinone redox state. Similar results have been reported in a microarray study using high light-treated Arabidopsis seedlings (Rossel et al., 2002).

VDE gene expression did not change significantly upon short term dark-adaptation, but was lower in etiolated seedlings. Additionally, *VDE* expression was induced by DCMU and DBMIB treatment. A biphasic pattern of *VDE* transcript oscillation was reported in Arabidopsis leaves, indicating that the *VDE* expression was controlled by light and a second unidentified factor (North et al., 2005). In contrast, microarray analysis on high light-treated seedlings did not show significant changes in the *VDE* expression levels (Rossel et al., 2002). Since the induction of the xanthophyll cycle involves a pH-catalyzed post-translational activation of VDE, shifts in transcription may be unnecessary (Rossel et al., 2002). Activation of the xanthophyll cycle directly depends on the presence of ascorbate and indirectly depends on the electron transport activity and the plastoquinone pool that mediates acidification of the lumen. This indicates another linkage between the xanthophyll cycle and the chloroplast redox state through VDE activity (Oelze et al., 2008). Moreover, in another study the kinetics of epoxidation was found to be gradually retarded with increasing light stress leading to a gradual down-regulation of *ZEP* activity (Reinhold et al., 2008). However, complete understanding of redox regulation in photosynthesis and other chloroplast processes will depend on an integrated and systematic view of the complex interrelation between diverse redox parameters and the adjustment of non-photochemical quenching.

Research on redox-triggered signaling pathways from the chloroplast to the nucleus, on the transmission of information across the chloroplast envelope, and the integration of different signaling pathways to optimize the acclimation response, will increase our understanding of the complex regulation of carotenoid biosynthesis in plants. This study contributed to our understanding of redox signaling by determining the regulation of two carotenoid desaturase

genes (*PDS* and *ZDS*) by the plastoquinone pool. These results now suggest the possibility of obtaining carotenoid mutants using the herbicide norflurazon, since it binds to plastoquinone (Breitenbach et al., 2001) and likely will affect the desaturase activity of the two desaturase enzymes. Therefore screening of mutant population using such a method may lead to the discovery of new ways that chloroplasts control redox flux, including new genes involved in this process and in carotenogenesis.

4 IDENTIFICATION OF CAROTENOID MUTANTS BY SCREENING FOR NORFLURAZON TOLERANCE AND CHARACTERIZATION OF A MUTANT WITH A DEFECTIVE *KCS19* GENE

4.1 Introduction

Carotenoids are lipid soluble organic molecules containing a C40 polyene backbone that is often cyclized to generate terminal ionone rings. This structure allows carotenoids to absorb short-wave visible light and the wavelengths that are absorbed depend on the number and nature of the double bonds. Carotenoids are therefore pigments that range in color from yellow through orange to red. They are synthesized and accumulated in both chloroplasts and chromoplasts, imparting color to photosynthetic tissues as well as fruits, storage organs and flowers (Britton et al., 2004). In the chloroplast, practically all carotenoids are associated with chlorophyll-binding proteins, whereas chromoplasts have developed unique mechanisms to sequester carotenoids within specific lipoprotein structures (Vishnevetsky et al., 1999).

In the previous chapter it was determined that the plastoquinone redox pool can affect the regulation of carotenoid biosynthetic genes. The treatment of Arabidopsis leaves with DBMIB and DCMU affected carotenoid biosynthetic gene expression by mimicking high and low light stress, respectively. Similarly, norflurazon [4-chloro-5-(methylamino)-2-(α,α,α-trifluoro-m-tolyl)-3(2H)-pyridazinone] is a herbicide that affects the desaturase activity of carotenoid biosynthetic pathway by non-covalently binding to plastoquinone, a cofactor of the enzyme PDS, which converts phytoene into ζ-carotene via phytofluene (Breitenbach et al., 2001). Treating plants, algae or cyanobacteria with norflurazon results in the accumulation of phytoene and concurrent bleaching of the organism (Sagar et al., 1988; Linden et al., 1990; Wagner et al., 2002; Arias et al., 2006; Steinbrenner and Sandmann, 2006). Bleaching of the green tissue occurs due to the degradation of chlorophyll in the absence of carotenoids that protect the plants from high intensity light (Bramley, 2002). It was also reported that mRNAs coding for the chlorophyll a/b binding protein of photosystem II light harvesting complex failed to accumulate in high light-grown, carotenoid deficient *Zea mays* (Mayfield and Taylor, 1984) and *Hordeum vulgar* (Krol et al., 1995). Over-expression of the *Erwinia uredovora* phytoene desaturase gene in transgenic tobacco plants showed multiple resistances to both norflurazon and fluridone and led to alteration of xanthophyll metabolism of the transgenic plants (Misawa et al., 1994).

Based on the available literature, very little information is available on mutants that are resistant to norflurazon herbicide in plants. Also, the relationship between the carotenoid biosynthesis and other major pathways in plants, and how they are regulated needs further understanding. This study was aimed at screening Arabidopsis mutants using norflurazon for altered carotenoid profiles. One of the two selected mutants was characterized to understand the cross talk between very long chain fatty acid synthesis and carotenoid biosynthesis.

4.2 Materials and methods

4.2.1 Plant material and growth conditions

Seeds of wild-type (WT) Arabidopsis (ecotype Columbia) and activation-tagged Arabidopsis mutant lines were obtained from the laboratory of Dr. Isobel Parkin at Agriculture and Agri-Food Canada (AAFC, Saskatoon, Canada) and grown under greenhouse conditions essentially as described in section 2.2.1. However, all WT and mutant Arabidopsis plants were grown in 32-well flats containing Co-Co Mix soil mixture, consisting of compacted coconut fibre/peat moss/vermiculite (1/3/3, v/v/v) and 15-9-12 "Osmocote PLUS" controlled release fertilizer (Scotts Company LLC). For seed increase, selected mutant lines and WT were grown under greenhouse conditions as described in section 2.2.1. The T3 mutants and the WT plants were re-grown under identical conditions for advancement to the next T4 generation.

4.2.2 Screening Arabidopsis mutants using norflurazon

Initially, the minimum concentration of norflurazon which was not lethal to the plant was determined. The media was supplemented with varying concentrations of norflurazon (Sigma-Aldrich) (0, 1, 5 and 10 µM) prepared from a 1 mM stock in 100% ethanol. Wild-type (WT) Arabidopsis seeds were surface-sterilized as described in section 3.2.1and grown on Petri plates containing MS media supplemented with varying concentration of norflurazon. At 0.5 µM norflurazon concentration, the WT seedlings displayed an albino phenotype butwere able to survive in the medium. Therefore, 0.5 µM norflurazon was selected to screen the activation-tagged mutant lines. Approximately 200 T_2 pools (100 lines per pool out of 490 mutant pools, each containing 1000 seeds) were screened for resistance to norflurazon. Seeds were surface-sterilized and grown on Petri plates supplemented with 0.5 µM norflurazon. T_2 mutant lines showing resistance to norflurazon (by a green phenotype) were transferred to greenhouse conditions (described in section 2.2.1) to develop seed. The selected mutants in the T_3 generation were grown without norflurazon under greenhouse conditions (described in section 2.2.1).

4.2.3 Cerulenin sensitivity assay

Wild-type (WT) and mutant Arabidopsis seeds were surface-sterilized and grown on Petri plates as described in section 3.2.1. The media was supplemented with varying concentrations of cerulenin (Sigma-Aldrich) (0, 1, 5 and 10 μM) prepared from a 1 mM stock in 100% ethanol. A total of three individual plates for each treatment were prepared and kept randomized in the growth room. The 10-day old seedlings were sampled for carotenoid analysis and gene expression studies.

4.2.4 Carotenoid extraction and determination

Carotenoid extraction and HPLC analyses from two-week-old leaf tissues and mature seed was carried out as described in sections 2.2.2 and 2.2.3, respectively.

4.2.5 Estimation of the number of T-DNA insertions

T-DNA insertion copy number was determined by Southern hybridization (Sambrook, 2001). Genomic DNA was extracted as described in section 2.2.4 and 15 μg was digested overnight at 37°C using different restriction enzymes, namely *Eco*RI, *Hin*dIII, *Nco*I, *Pac*I, *Pme*I and *Swa*I. The digested genomic DNA was separated by electrophoresis on a 0.8% (w/v) agarose gel for 10 h at 20 V. After electrophoresis, the digested genomic DNA was transferred to a nitrocellulose membrane followed by denaturation and depurination using 0.25% (v/v) HCl and neutralization using 0.25% (w/v) NaOH. The denatured genomic DNA was cross-linked to the membrane using a UV cross-linker (Stratagene, Gemini BV, Apeldoorn, The Netherlands). The nitrocellulose membrane was pre-hybridized for 20 min at 65°C in a solution containing 1X SSC (0.15 M NaCl and 0.015 M sodium citrate, pH 7.0), 0.5% (w/v) sodium dodecyl sulphate (SDS), 10× Denhardt's solution (2g Ficoll, 2g Polyvinilpyrolidone and 2g bovine serum albumin in 1L of distilled water), and 0.05% (w/v) sodium pyrophosphate.

The radioactive probe for detecting the PAT gene in the mutants was generated using 800 bp DNA fragment of PAT gene obtained by PCR. The DNA template was heated in a microcentrifuge tube for 10 minutes at 95–100°C. The tube was rapidly chilled in an ice bath. To generate a single-stranded DNA probe, 500ng/ml denatured DNA template (25ng), 50mM Tris-

HCl (pH 8.0), 5mM $MgCl_2$, 2mM DTT, 0.2M HEPES (pH 6.6), 150 µg/ml random hexadeoxy ribonucleotides, 400 µg/ml BSA, 20 µM of each unlabeled dNTP, 333 nM [α-32P] dNTP (3,000 Ci/mmol) and 1 µl (5 U) of Klenow fragment was added. The reaction was incubated for 1 h at room temperature. The reaction was stopped and denatured by heating the mixture for 10 min at 95°C.

The hybridization was performed in the pre-hybridization solution containing ^{32}P labelled 800 bp fragments for 18 h at 55°C. The hybridized membrane was washed twice in a solution containing 2X SSC and 0.5% (w/v) SDS for 20 min each, and twice in 1X SSC solution for 20 min each at 55°C. After washing, the membrane was exposed overnight to an X-ray film (Bio-Rad Laboratories) and then developed using an automated X-ray film developer. The restriction enzymes were selected such that only a single restriction site was present on the T-DNA. Similarly the probe generated would bind specifically to the PAT gene and no restriction sites for the restriction enzymes used are present in the PAT gene. Therefore, the number of bands appearing on the X-ray film would be indicative of the copy number of the T-DNA insertion in the genome.

4.2.6 Determination of T-DNA flanking regions

The Genome Walker kit (Clontech Laboratories Inc., USA) was used to identify genomic DNA flanking the T-DNA insertion site according to the manufacturer's instructions. Genomic DNA was digested with each of three blunt-end restriction enzymes (*Dra*I, *Eco*RV, and *Pvu*II), ligated with adaptors, and flanking regions amplified by nested PCR with the T-DNA (Table 2-1). The experiment was repeated three times using different restriction enzymes. Two PCR products were obtained from independent Genome Walker experiments; each digested using *Eco*RV and *Pvu*II. The PCR products were cloned using the pGEM-T Easy vector (Promega Corporation, USA) as described by the manufacturer. Three colonies of each of the cloned products were selected for sequencing using the LB2 primer at the DNA sequencing facility of the Plant Biotechnology Institute (Saskatoon, CA). The T-DNA insertion site was determined from the sequence by BLAST analysis against the TAIR sequence database (Version 9) (http://www.arabidopsis.org/Blast/index.jspwebcite).

4.2.7 Total RNA extraction and cDNA synthesis

The extraction of total RNA from 14-day old leaf tissues was as described in section 2.2.6. Total RNA extractions from other tissues of Arabidopsis were performed following the protocol described by (Suzuki et al., 2004).

Single strand cDNA was synthesized from total RNA using Superscript reverse transcriptase III (Life Technologies) following the manufacturer's protocol. A 25 µl reverse transcription reaction was prepared by adding the following reagents: 5 µl of reaction buffer (5X), 1.25 µl of 0.1 M DTT, 1.25 µl of 10 mM dNTP mixture, 1 µl (10 U) RNAse inhibitor (Life Technologies), 0.5 µl each of random primers (10 µM) and oligo(dT) primers (10 µM), 1 µl (100 U) of Superscript reverse transcriptase III (Life Technologies), 1 µg total RNA, and nuclease-free water to a final volume of 25 µl. The reaction was incubated at 25°C for 5 min, followed by 50°C for 50 min and a final heat inactivation at 75°C for 15 min and stored at -20°C.

4.2.8 qPCR

Relative expression levels of carotenoid biosynthetic genes and members of the keto acyl-CoA synthase (KCS) gene family were examined using qPCR and the gene-specific primers presented in Tables 3-1 and 4-1, respectively. Primers were selected using Primer3 software (http://bioinfo.ut.ee/primer3/) (Untergasser et al., 2012). qPCR and determination of relative expression levels occurred as described in section 3.2.5.

Table 4-1: Primers used this study

Gene/Primer name	AGI ID	Forward Primer (5' to 3')	Reverse Primer (5' to 3')
KCS family qPCR primers			
KCS1	At1g01120	TCAAGACCGGAAGAAGTCAAA	CACCGATTGTTCCTCTCTCG
KCS2	At1g04220	GGTGACATCTTCCTCGGAATC	CCCCTTCGAGATTCCGTTAT
KCS3	At1g07720	GTGACTCAGGCAGCTCCAA	CGATAACCGCTTTACCTCCA
KCS4	At1g19440	TTAGCTTCGTTTGAGGAACTGT	TGAAAACATGAGCTCAAGAACTG
KCS5	At1g25450	GGTCGGATTGTATCGAACG	TGCAGTTTTCTCTATTTTCCCAAT
KCS6	At1g68530	TCTAGCTCGGTGAAGCTCAAG	AAGCTCAACGGCGACAATAG
KCS7	At1g71160	TGACATTGATTTCGCTGCTC	TGAAAGGTTGTTCCTACAATGC
KCS8	At2g15090	GGATAGATATCCGGTTGAGATTG	GCAAGTACCAAAACAAAGTTACCA
KCS9	At2g16280	TGCTTTCATCTTTCTCTCTGCTT	GAAGACTCTCCGGAGGAAGA
KCS10	At2g26250	TTTGGAAGAAGCTTTGGGACT	GAGCGAGGACGAGACATGAA
KCS11	At2g26640	CAGTTGAAGTCCCCAAGGTC	AAATTCACTGGGAAGACACAAAA
KCS12	At2g28630	CGCAAAAACAACACAAGGTG	TCCTTTCCAATCCATTTAAACAA
KCS13	At2g46720	CGCGTGTGAAGTCACGTTAT	CAAATAATACATATTTGTGGGGAAAA
KCS14	At3g10280	GAGGCTAAATGTCGGGTCAA	GTTAGCCGGAATCGTTCTCA
KCS15	At3g52160	CGTCTTGAGCCTTCCTTTGA	GCTCCAATGTCCGTCTTGAT
KCS16	At4g34250	CTTGGGAACAGTGTCTACACAAA	CGTCTCTATCTTCTTAATTCGTATCAT
KCS17	At4g34510	TGGGAACATTGCATCCATAG	GGTAAGCCTTCTGGTACATGG
KCS18	At4g34520	CCAAGTACAAGCTAGTTCACACG	ACTCCGATTTTGCCGCTCT
KCS19	At5g04530	GTGTTTGGGAGGTTCTAAAGGA	TCAACGAATGGATTAGGGATTC
KCS20	At5g43760	CGCAACAATCGCTAACCTCT	GGGACGGGTGGTGAAGTAAG
KCS21	At5g49070	GGCTAGCATGTGCAAGCAATA	TGTGAAAAGCGGTCTTTGTG
KCR	At1g67730	CTACTTCCTCCGACCATCCA	CTGGGTTACGAGCAACGAGT
ECR	At3g55360	CTGGAGCTTTGGTGCTTACA	CTGGGGTCCCTCAGATTCTT
KCS19 upstream and downstream primers			
At5g04480	At5g04480	TCCGTCTTTCCTCGAGTTTG	AGAACCCGGCAGTAACAATG
At5g04490	At5g04490	TCTCTGCGGTTTTCTTCTGG	TCCTGCCCAACTCTTTCTTG
At5g04500	At5g04500	CGTGTTGGTCAAGATTGTGG	CGACGCTTCCAAAGAGAAAG
At5g04510	At5g04510	GAAGAATCTAAGGTCCCAGACTCC	CAGAAGATGTAGGAGGAGCACTGT
At5g04520	At5g04520	GAGAGTGACGAAGGTGAAGAGAGT	ATATAGGGCACTCTCAGCCAGAC
At5g04540	At5g04540	GAGCTGCTCCAGACTTCTACTTTC	GTGCTCCCTTATGACCAGCTAA
At5g04550	At5g04550	ACTAGTGAAGCTCTCCAAGACGAC	CTTTCCGTACTCTGGTTTGGTC
At5g04560	At5g04560	AACTTCCCAAAGTGGTCGTG	GGCTGGCTTTTTAGTTGCTG
At5g04590	At5g04590	AATATGGGTAGCACGCTTGG	GAGAAAGAAGAGCCGCAATG
KCS19 Complementation and RNAi primers			
KCS19-FL	At5g04530	CACAATTCACTTAATTCTCACTCACTC	TAAATGCACCAACTTGAATACACAC
KCS19- RNAi	At5g04530	AATCTCTCGGGACTAGGGTGTAG	CCACATAGCGGATCAGTTCCTTGAC

4.2.9 Cloning of KCS19 binary complementation and RNAi vectors

A genomic fragment (1872 bp) of At5g04530 (*KCS19*) containing the full length open reading frame (1395 bp) and a promoter region (472 bp) was amplified from Arabidopsis WT genomic DNA using KCS19-FL primers (Table 4-1). The PCR reaction contained: 5 µl of 10X reaction buffer; 1 µl of (10 µM) gene-specific forward and reverse primers, 1 µl of 10 mM dNTP mixture; 100 ng of DNA; 1 µl (1 U) of Platinum® *Taq* High Fidelity DNA Polymerase (Life Technologies Inc.), and nuclease free water to a final volume made of 50 µl. The amplified genomic fragment was ligated into the pCR8/GW/TOPO-TA cloning vector (Life Technologies Inc.) following the manufacturer's protocol. The PCR amplification cycle had an initial denaturation at 95^{o}C for 5 min followed by 30 cycles at 95^{o}C for 30 sec, 55^{o}C for 30 sec and 72^{o}C for 45 sec, followed by a final extension at 72^{o}C for 7 min. The amplified products were then examined using 1% agarose gel electrophoresis for the presence of amplified PCR product.

To create the *KCS19* RNAi binary vector, a 430 bp fragment of *KCS19* was amplified using KCS19 –RNAi primers (Table 4-1) from Arabidopsis WT cDNA generated as described in section 3.2.4. The fragment was amplified using the same PCR conditions described above except 1 µl (10 U) of *Pfu* DNA polymerase (Life Technologies Inc.) was used to amplify blunt end DNA fragments to facilitate directional cloning into the pET100/D-TOPO (Life Technologies Inc.) entry vector. The amplified fragment was ligated into pET100/D-TOPO following the manufacturer's instructions. The ligated vectors were transformed into DH10B electro-competent *E. coli* cells (Sambrook, 2001). The transformed cells were selected on LB medium containing spectinomycin (100 µg ml^{-1}). The selected cells were cultured and the plasmid DNA was isolated using the Wizard® *Plus* SV Minipreps DNA Purification System (Promega Corporation) following the manufacturer's protocol. The purified plasmids were sequenced at the National Research Centre DNA sequencing facility (Saskatoon, CA).

Each Gateway^{TM} LR cloning reaction (Life Technologies Inc.) contains 4µl of LR 5X reaction buffer, ~50–300ng of the entry vector (pCR8/GW/TOPO-TA, containing full length genomic *KCS19* for complementation or pET100/D-TOPO, containing the 430 bp fragment of *KCS19* for RNAi), 100–250ng of destination vector (pMDC99 for *KCS19* complementation studies or pMDC32 for *KCS19* RNAi studies), 4µl of Gateway® LR Clonase mix (Life Technologies Inc.);

and 10 mM Tris-EDTA buffer to a final volume of 20µl. The reactions were incubated overnight at room temperature. The recombined plasmid DNA was transformed in to electrocompetent DH10B cells by electroporation (Sambrook, 2001) and selected for kanamycin resistance by growing the electroporated cells on a LB agar medium supplemented with Kanamycin (50 µg ml^{-1}). The selected positive transformants were cultured followed by plasmid purification and sequencing as described above. Plasmid from a positive clone (determined to contain the DNA fragment of interest) was used to transform electrocompetent *Agrobacterium tumefaciens* GV3101 cells by electroporation (Sambrook, 2001) and selected for transformants by growing the electroporated cells in LB agar medium supplemented with chloramphenicol (30 µg ml^{-1}) and kanamycin (50 µg ml^{-1}).

A) pMDC99

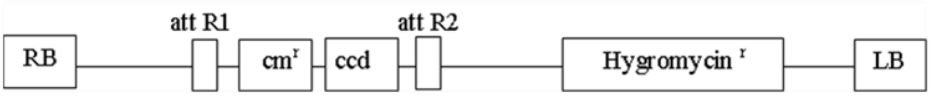

B) pMDC32

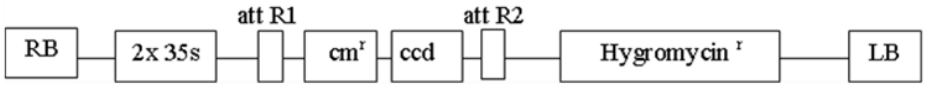

Figure 4-1: T-DNA organization of the destination vectors A) pMDC99 and B) pMDC32. The T-DNA in pMDC99 does not contain promoter region (used to create *KCS19* complementation binary vector), while pMDC32 contains dual 35S promoter (used to create overexpressing *KCS19* RNAi binary vector). Both T-DNA vectors confer hygromycin resistance to the transformed plant for selection. RB: T-DNA Right border, LB: T-DNA Left border, cm^r: chloramphenicol resistance, ccd: Cytotoxic protein, attR1, R2: Recombination cloning sites.

4.2.10 Plant transformation

Agrobacterium-mediated plant transformation was carried out using the floral dip method (Clough and Bent, 1998). Briefly, *Agrobacterium* cells harboring the vector of interest were grown to stationary phase at 25 to 28°C with shaking (250 rpm) in LB medium containing kanamycin (50 µg ml^{-1}) (Clough and Bent, 1998). Cultures were typically started from a 1:100 dilution of smaller overnight cultures and grown for roughly 18 to 24 h. Cells were harvested by centrifugation for 20 min at room temperature at 5,500 g and then suspended in infiltration

medium containing 5.0% (w/v) sucrose and 0.05% (v/v) Silwet L-77 (OSi Specialties, Inc., CT, USA).

The mutant and wild type Arabidopsis plants used for transformation using floral dip method were grown in a greenhouse at a 24/20°C (day/night) temperature with an 18/6 h (light/dark) cycle. Ambient and supplemental high-pressure sodium lighting provided a PPFD of 250 µmol photons m^{-2} s^{-1} PAR. To obtain more floral buds per plant, inflorescences were clipped after most plants had formed primary bolts, relieving apical dominance and encouraging synchronized emergence of multiple secondary bolts. Plants containing the flowers were dipped in the *Agrobacterium* culture 4 to 6 days after clipping (Clough and Bent, 1998), followed by vacuum infiltration in a vacuum chamber for 3 min. The transformed mutant and WT plants were covered using transparent plastic bags until harvest.

4.2.11 Selection of complemented mutants

Seeds of transformants were surface-sterilized with 95% ethanol for 30–60 sec, then with 50% (v/v) bleach (2.625% sodium hypochlorite, final volume) containing 0.05% Tween 20 for 5 min, followed by three rinses with sterile water. The seeds were suspended in 0.1% (w/v) sterile agarose solution and placed on selection plates containing ½ × MS media (Sigma Chemicals), 0.8% (w/v) agar (Sigma), 10 µg ml^{-1} glufosinate ammonium salt herbicide (Sigma) and 20 µg ml^{-1} hygromycin (Sigma) at a density of approximately 3000 seeds per 150 × 15 mm^2 plate. The plates were then transferred to a growth chamber with similar conditions mentioned in 4.2.2. Positive transformants were identified as seedlings resistant to both glufosinate and hygromycin that produced green leaves and well-established roots within the selective medium. Selected transformants were grown to maturity by transplanting into heavily moistened potting soil, preferably after the development of 3 to5 adult leaves until harvest. The seeds obtained from the transformants (T_0) were planted again in selection medium and then in greenhouse conditions for further analysis in the T_1 generation.

4.2.12 Lipid analyses

4.2.12.1 Fatty acid extraction

Fatty acid extraction from seeds was kindly performed by Dr. Rong Zhou at AAFC (Saskatoon, Canada). Mature seeds (100 mg fw^{-1}) from WT or mutant (T_4) Arabidopsis plants were dried at 103°C for 3 h and weighed again for dry weight (dw). The dried seeds were placed in 6.5 ml scintillation vials containing a steel rod. Heptane (1 ml) containing 1 mg ml^{-1} trinonadecanoin (C19:0) or tripentadecanoin (C15:0) was added to each vial. The samples were placed in an Eberbach shaker for 10 min at high speed. The vials were then centrifuged at 2,500 g for 15 min. A 50 µl aliquot of the supernatant was pipetted to auto-sampler vials. The heptane was then evaporated by placing the vials under a stream of nitrogen gas. An aliquot of 50 µl of hexane was added to the auto-sampler vials and then 100 µl of 30% (v/v) sodium methylate solution was added into each vial. The contents of the vials were mixed and incubated at room temperature for 30 min. A 50 µl aliquot of 0.1 M phosphate buffer (pH 7) was added to each sample containing vial and methanol was evaporated under a stream of nitrogen gas for < 2 min. Heptane (500 µl) was then added and the vials were capped and stored in -70°C.

4.2.12.2 Fatty acid determination

Fatty acid determination from seed extracts (Section 4.2.12.1) using gas chromatography was kindly performed by Dr. Rong Zhou at AAFC (Saskatoon, Canada). The auto-sampler was set to inject 3 µl of upper layer for gas chromatography. The gas chromatograph conditions were as follows: A NuChek Prep GLC 428 Flame standard solution was used to monitor gas chromatograph performance. A 7.5 m x 0.25 mm capillary column with 0.5 µm coating of fused silica was used with a HP Innowax coating, injector and detector temperature set at 300°C, initial temperature 190°C, and hydrogen as carrier gas at approximately 10 psi with a constant flow of ~60 cm sec^{-1} was used. The lipid species data obtained was then analysed statistically.

4.2.12.3 Lipid extraction from Arabidopsis leaves

Mature 14-day old leaves (200 mg fw) from WT or mutant (T_4) Arabidopsis plants were harvested and immersed in a 50 ml glass tube containing 3 ml of isopropanol (preheated at 75°C) with 0.01% (w/v) butylated hydroxytoluene (BHT; Sigma B1378). The samples were heated at

75ºC for 15 min and allowed to cool. An aliquot of 1.5 ml of chloroform and 0.6 ml of water was added to each tube and mixed using a vortex for 30 sec followed by agitating at room temperature for 1 h in a shaking incubator at 200 rpm.. The lipid extracts were transferred to 15 ml glass tubes with Teflon-lined screw-caps using glass Pasteur pipettes. A 4 ml aliquot of chloroform:methanol (2:1) with 0.01% (w/v) BHT was then added to the extract followed by shaking for 30 min. The extraction procedure was repeated three times or until the leaves became white. The leaf samples were dried at 105°C overnight after extraction to record their dry weight (dw). A 1 ml aliquot of 1 M KCl was added to the combined extract which was mixed with a vortex and centrifuged at 2500 g for 10 min. The upper phase was discarded. Nuclease free water (2 ml) was then added and the process repeated. The solvent was evaporated under a stream of nitrogen gas and stored in a -80°C.

4.2.12.4 Lipid extraction from Arabidopsis seeds

Mature seeds (200 mg fw) from WT or mutant (T_4) Arabidopsis plants were harvested and immersed in 50 ml tube containing 1 ml of isopropanol (preheated at 75°C) with 0.01% (w/v) BHT. The samples were heated at 75°C for 15 minutes and allowed to cool, followed by grinding in an agitator using stainless steel beads. The ground mixture was transferred to a 15 ml glass tube for extraction and 0.8 ml of nuclease free water was added. The tube was shaken vigorously and then 1 ml chloroform and 1 ml water were added followed by mixing. The samples were then centrifuged at 2,500 g for 10 min to separate the two phases and the lower layer containing chloroform and lipids was retained. The samples were re-extracted twice using 1 ml of chloroform, saving the lower layer. To the collected eluate 0.5 ml of 1 M KCl was added. The extracts were then mixed well and centrifuged at 2,500 g for 10 min. A thin water layer on top was pipetted off and then 1 ml of water was added to chloroform/lipids mixture, this was mixed, centrifuged at 2,500 g for 10 min and the top layer containing water removed. The sample was then transferred to a 2 ml vial with Teflon-lined screw cap, dried under a stream of nitrogen gas and stored in a -80°C.

4.2.12.5 Lipid profiling

Lipid profiling using ESI-MS/MS was performed at Kansas Lipidomics Research Center (Kansas State University, Manhattan, KS, USA). Dried lipid extracts were dissolved in 1 ml of

chloroform. The phospholipid standards were purchased from Avanti Polar Lipids, Inc. (Alabaster, AL, USA), except for di24:1-PE (phosphatidyl ethanolamine) and di24:1-PG (phosphatidyl glycerol) which was prepared by transphosphatidylation of di24:1-PC (phosphatidyl choline). Total phospholipids (PLs) were quantified by a phosphate assay performed at the Kansas Lipidomics Research Center (Kansas State University, Manhattan, KS, USA), except for the hydrogenated PI (phosphatidyl inositol) component, which were quantified by gas-liquid chromatography on a Supelco 30-meter Omegawax 250 capillary column (Sigma-Aldrich) as fatty acid methyl esters, using pentadecanoic acid as an internal standard, after derivatization in 1.5 M methanolic HCl. The hydrogenated galactolipid standards were purchased from Matreya Inc. (State College, PA, USA) and also quantified as fatty acid methyl esters by gas-liquid chromatography.

ESI-MS/MS was performed to determine individual PL and galactolipid (GL) classes based on the protocol provided by Welti (2002). Briefly, 1 ml of plant lipid extract was divided into two aliquots for mass spectrometry analysis: one sample for phospholipid analysis and one for GL analysis. For PL analysis, 150 µl of plant lipid extract in chloroform was combined with solvents and internal standards, such that the ratio of chloroform/methanol/ammonium acetate (300 mM) in water was 300:665:35 (v:v:v), the final volume was 1.8 ml. The phospholipid standard sample contained 6.6 nmol of di14:0-PC, 6.6 nmol of di24:1-PC, 6.6 nmol of 13:0-lysoPC, 6.6 nmol of 19:0-lysoPC, 3.6 nmol of di14:0-PE, 3.6 nmol of di24:1-PE, 3.6 nmol of 14:0-lysoPE, 3.6 nmol of 18:0-lysoPE, 3.6 nmol of di14:0-PG, 3.6 nmol of di24:1-PG, 3.6 nmol of 14:0-lysoPG, 3.6 nmol of 18:0-lysoPG, 3.6 nmol of di-14:0-PA, 3.6 nmol of di-20:0(phytanoyl)-PA, 2.4 nmol of di-14:0-PS, 2.4 nmol of di20:0(phytanoyl)-PS, 1.97 nmol of 16:0–18:0-PI, and 1.63 nmol of di-18:0-PI. For galactolipid analysis, 80 µl of plant lipid extract in chloroform was combined with solvent and internal standards, such that the ratio of chloroform/methanol/sodium acetate (50 mM) in water was 300:665:35, the final volume was 1.8 ml, and the sample contained 44.55 nmol of 16:0–18:0-MGDG, 35.45 nmol of di18:0-MGDG, 8.65 nmol of 16:0–18:0-DGDG, and 31.28 nmol of di-18:0-DGDG.

The samples were analyzed on a “triple” quadrupole tandem mass spectrometer (Micromass Ultima, Micromass Ltd., Manchester, UK) equipped for electrospray ionization. The source temperature was 100°C, the desolvation temperature was 250°C, ± 2.8 kV was applied to the

electrospray capillary, the cone energy was 40 V, and argon was used as the collision gas at 1.7 e^{-3} mBar as measured on the gauge in the collision cell line. The samples were introduced using an auto-sampler (LC Mini PAL, CTC Analytics AG, Zwingen, Switzerland) fitted with the required injection loop for the acquisition time and presented to the electrospray ionization needle at 30 µl/min. The mass analyzers were adjusted to a resolution of 0.6 atomic mass unit full width at half height. For each spectrum, 12 to 42 continuum scans were averaged in multiple channel analyzer modes. The phospholipid scanning modes were described by (Brügger et al., 1997). The GL product ions were reported by (Kim and Pfeiffer, 1999).

Data processing was performed using Masslynx software (Micromass Ltd.). Each head group-specific scan was collected as one continual spectrum. In each spectrum, the background was subtracted, and peak height determined with the centroiding routine. Corrections for overlap of isotopic variants (A + 2 peaks) in higher mass lipids were applied.

4.2.12.5.1 Lipid profiling data analysis

The lipids in each class were quantified relative to the internal standards using a correction curve determined between standards. The molar response of homologs within a head group is mass-dependent and largely dictated by collision energy. However, no collision energy was found that allowed spectral abundances to equal molar ratios. The shape of the mass-dependent correction curve between the internal standards was established for phospholipid content, including phosphotidyl glycerol (PG), phosphotidyl choline (PC), phosphotidyl ethanolamine (PE), phosphotidyl ionositol (PI), phosphotidyl serine (PS) and phosphotidic acid (PA), using standards of intermediate mass as described by Brügger et al. (1997). The data were fit with a second order polynomial.

4.2.13 Experimental design and statistical analyses

Sampling for lipid analysis consisted of four biological replications. Sampling for carotenoid determination and qPCR, as well as statistical analyses of the data occurred as described in section 3.2.8.

4.3 Results

4.3.1 Screening of activation tagged Arabidopsis mutants for norflurazon tolerance

Eight norflurazon-resistant mutants were selected by germinating the mutant T_2 seed pools on ½ strength MS solid media supplemented with 0.5 µM norflurazon. Figure 4-2 shows the norflurazon screening assay where the leaves of the resistant mutant lines appear green, while the sensitive lines have an albino phenotype. Carotenoid composition in the leaves and seeds was determined for the resistant lines in the absence of norflurazon and the results are shown in Figure 4-3 and Figure 4-4, respectively. Seven out of eight mutants showed significantly higher levels of lutein in the seeds compared to the WT. Five mutants (203, 227-3, 227-5, 231 and 232) had significantly lower lutein and β-carotene levels in their leaves compared to the WT. Mutants 220 and 221 had similar lutein content in the leaves, but had significantly lower β-carotene content in the leaves compared to the WT. Mutant 227-1 had no changes in the carotenoid profiles of leaves, but had significantly higher levels of all the carotenoids in the seeds. Similarly, mutants 231 and 232 had significantly lower levels of lutein, β-carotene and violaxanthin in leaves, but had significantly higher levels of the same carotenoids in the seed. In contrast, mutant 227-5 did not show any change in the seed carotenoid levels, but had significantly lower levels of lutein, β-carotene and violaxanthin in leaves. Mutant 203 consistently had significantly lower levels of β-carotene in both leaves and seeds and was selected for further analysis and reported in this chapter.

Figure 4-2: Selection of norflurazon-resistant mutants. The figure shows a 10-day old norflurazon resistant mutant seedling KN203 among the susceptible lines, when grown in ½ strength Murashige and Skoog (MS) media containing 0.5 µM norflurazon.

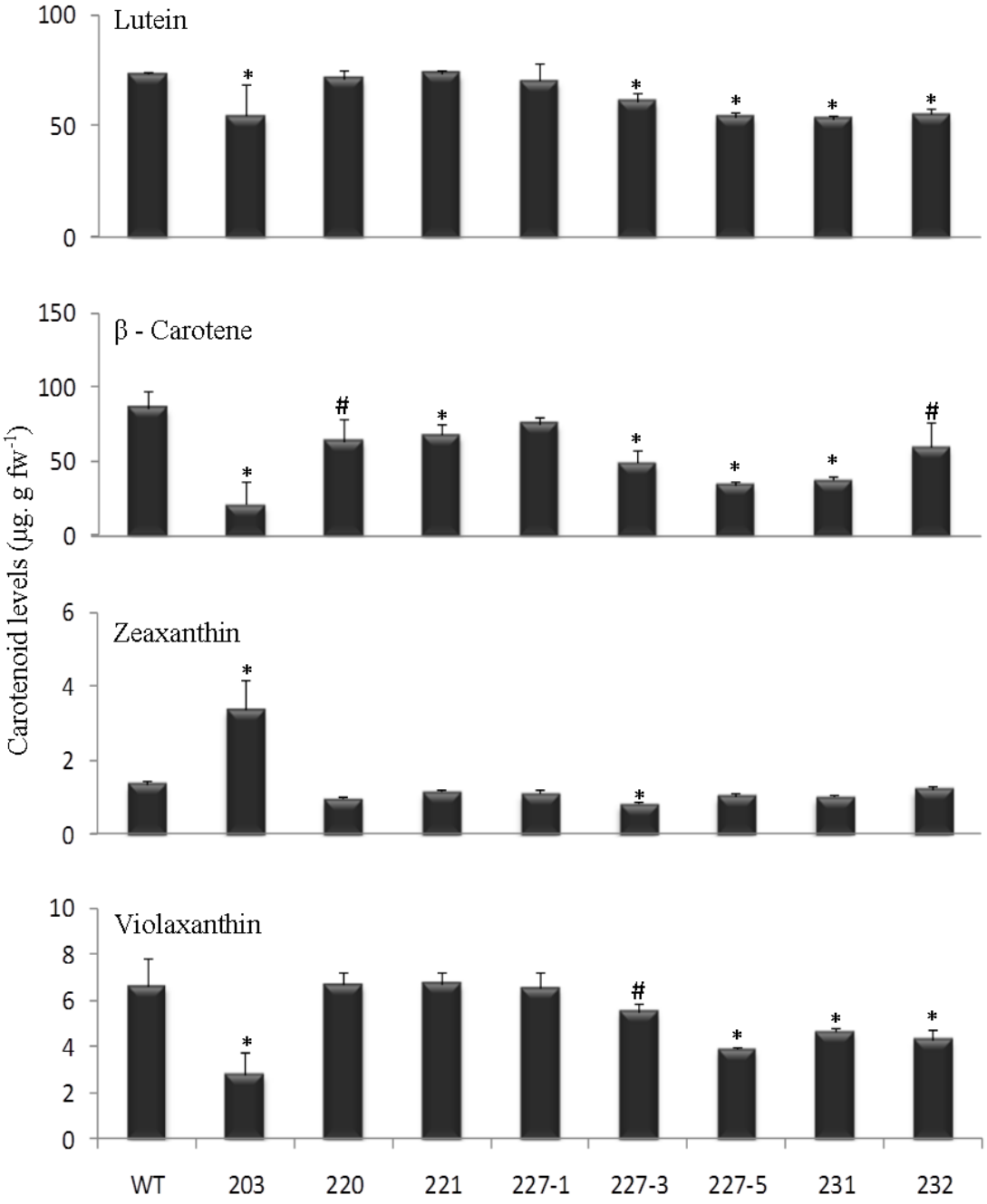

Figure 4-3: Carotenoid composition in 2-week-old (mature leaves) of WT Arabidopsis and norflurazon resistant mutants. The plants were grown in the absence of norflurazon. Values represent means ± SD (n = 3) and are expressed on a fresh weight (fw) basis. Different symbols within each panel indicate statistical significance at $p < 0.05$ (*) or $p < 0.1$ (#). fw, fresh weight.

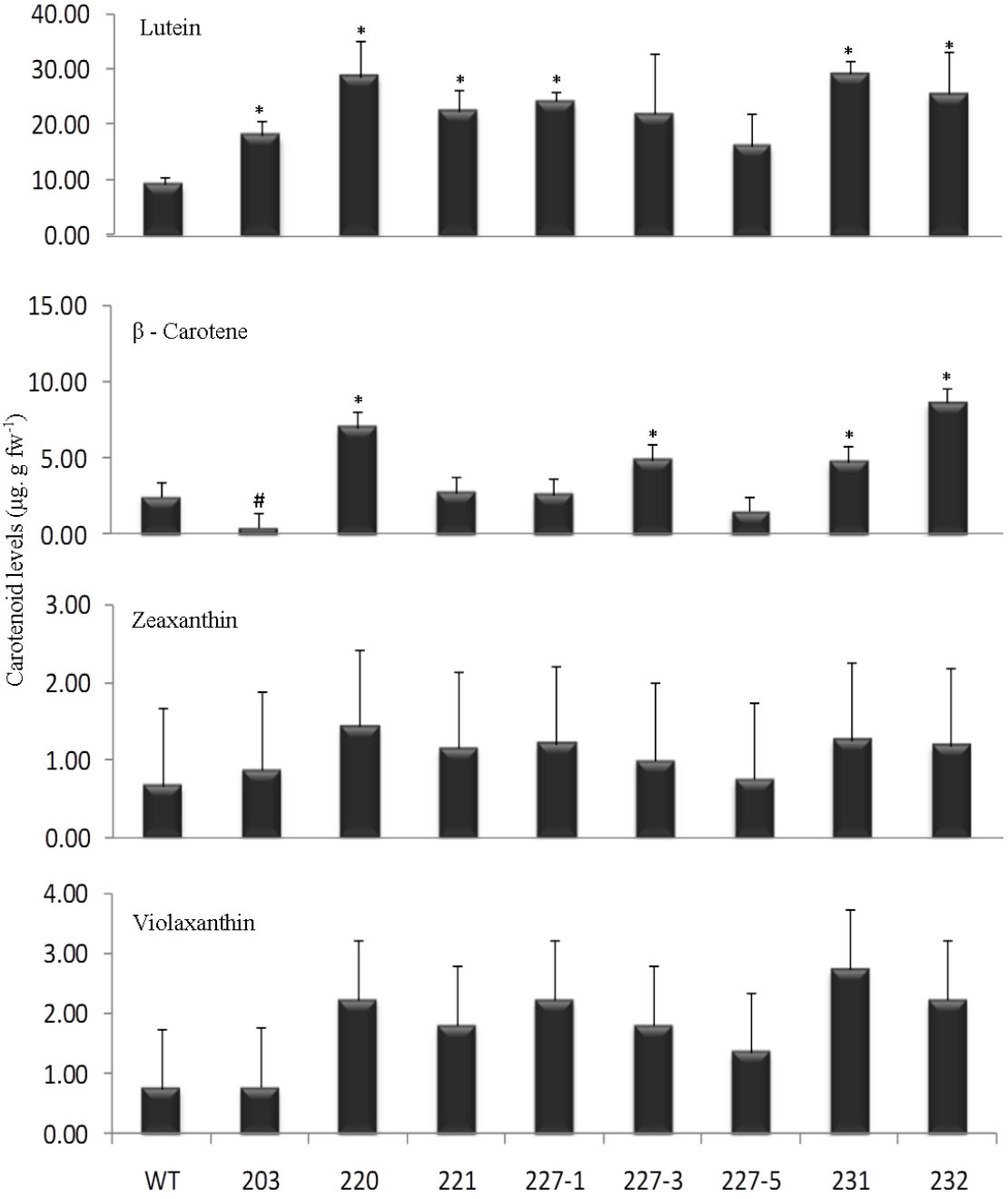

Figure 4-4: Carotenoid composition in mature seeds of WT Arabidopsis and norflurazon resistant mutants. The plants were grown in the absence of norflurazon. Values represent means ± SD (n = 3) and are expressed on a fresh weight (fw) basis. Different symbols within each panel indicate statistical significance at $p < 0.05$ (*) or $p < 0.1$ (#). fw, fresh weight.

4.3.2 Arabidopsis mutants selected for norflurazon resistance

Based on their resistance to norflurazon and their leaf and seed carotenoid profiles, five lines 203, 227-3, 227-5, 231 and 232 were selected for preliminary analysis. Two mutants, 203 and 231, were selected for additional analysis and renamed to KN203 and KN231, respectively. The details of characterization of mutant KN203 is given in this chapter, while the mutant KN231 characterization is detailed in chapter 5.

The mutant KN203 did not show any observable phenotypic changes when grown without norflurazon in the greenhouse compared to the WT (data not shown), but accumulated significantly lower levels of lutein, β-carotene, and violaxanthin in the leaves (Figure 4-3) and significantly higher levels of lutein in the mature seeds (Figure 4-4). The seedling leaf carotenoid was inconsistent with the green "resistance" like phenotype that KN203 portrayed under norflurazon selection in the screening phase.

To determine the effect of norflurazon on mutant KN203 in a greater detail, both mutant KN203 and WT were grown in a ½ × MS medium supplemented with varying norflurazon concentrations (0, 0.13, 0.25, 0.5, 0.75 and 1 μM) and the carotenoid levels were determined. The results indicated that seedling growth of mutant KN203 displayed an albino phenotype at norflurazon concentrations above 0.25 μM, while the WT displayed an albino phenotype at norflurazon concentration above 0.5 μM. Carotenoid analysis on the norflurazon-treated seedlings indicated up to 50% reduction in the carotenoid levels, with both lines responding to norflurazon treatment in a concentration dependent manner (Figure 4-5). The significant reduction in measured carotenoids levels in the mutant compared to the WT indicate that the increased susceptibility of KN203 to norflurazon was due to lower levels of carotenoids in the seedlings (Figure 4-5). Once again this contrasted with the resistance to norflurazon that enabled the selection of this mutant in the initial screening experiment. The mutant displayed a significant reduction in the leaf carotenoid levels and therefore further characterization of the affected gene was performed to gain insight into the regulation of carotenoids in Arabidopsis.

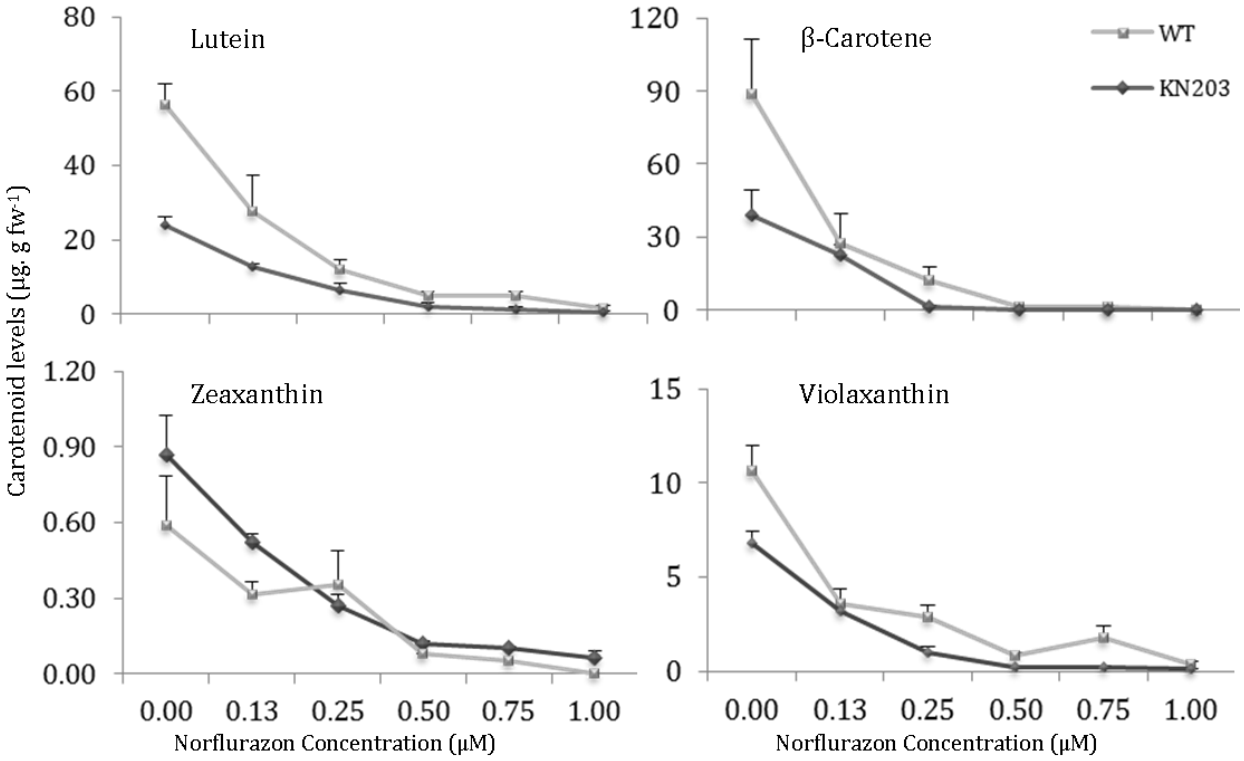

Figure 4-5: Effects of norflurazon treatment on carotenoid composition in 10-day-old seedlings of WT Arabidopsis and mutant KN203. Values represent means ± SD (n = 3) and are expressed on a fresh weight (fw) basis.

4.3.3 Molecular characterization of KN203

Southern hybridization was performed to determine the T-DNA copy numbers in the mutant KN203. The results indicated that when the mutant genomic DNA was digested using restriction enzymes *Eco*RI and *Hin*dIII (harboring a single restriction site inside the T-DNA), two bands were present (Figure 4-6A). On the other hand, when the genomic DNA was digested with the restriction enzymes *Nco*I, *Pac*I, *Pme*I and *Swa*I (having no restriction site inside the T-DNA), only a single band (> 15 kb) appeared for each enzyme (Figure 4-6A). Furthermore, one band of the two bands observed upon digestion with *Eco*RI and *Hind*III was about 6.7 kb, which is the size of the full length T-DNA. BLAST analysis from four independent sequences obtained from the Genome Walker analysis determined the presence of the T-DNA insertion in the promoter region 153 bp upstream of the start codon of the gene At5g04530 encoding β-keto acyl CoA synthase 19 (KCS 19). The enzyme is a member of the 3-ketoacyl-CoA synthase family involved in the biosynthesis of very long chain fatty acids (VLCFA) with a putative acyltransferase

activity (transferring acyl groups other than amino-acyl groups) (Figure 4-6B). Furthermore, to determine the effect of the T-DNA insertion on the neighboring loci, gene expression analysis was performed for genes upstream and downstream of the T-DNA insertion site spanning about 40 kb. The results indicated that six genes (At5g04480, At5g04490, At5g04500, At5g04540, At5g04550, At5g04590) had significantly increased expression, but the increase did not exceed 1.5-fold indicating that they are not unduly influenced by the proximity of the 35S promoter/enhancer in the T-DNA(Figure 4-6C). However, the T-DNA insertion event reduced the expression of At5g04530 by 90% which in turn may affect KCS19 enzyme levels in mutant KN203.

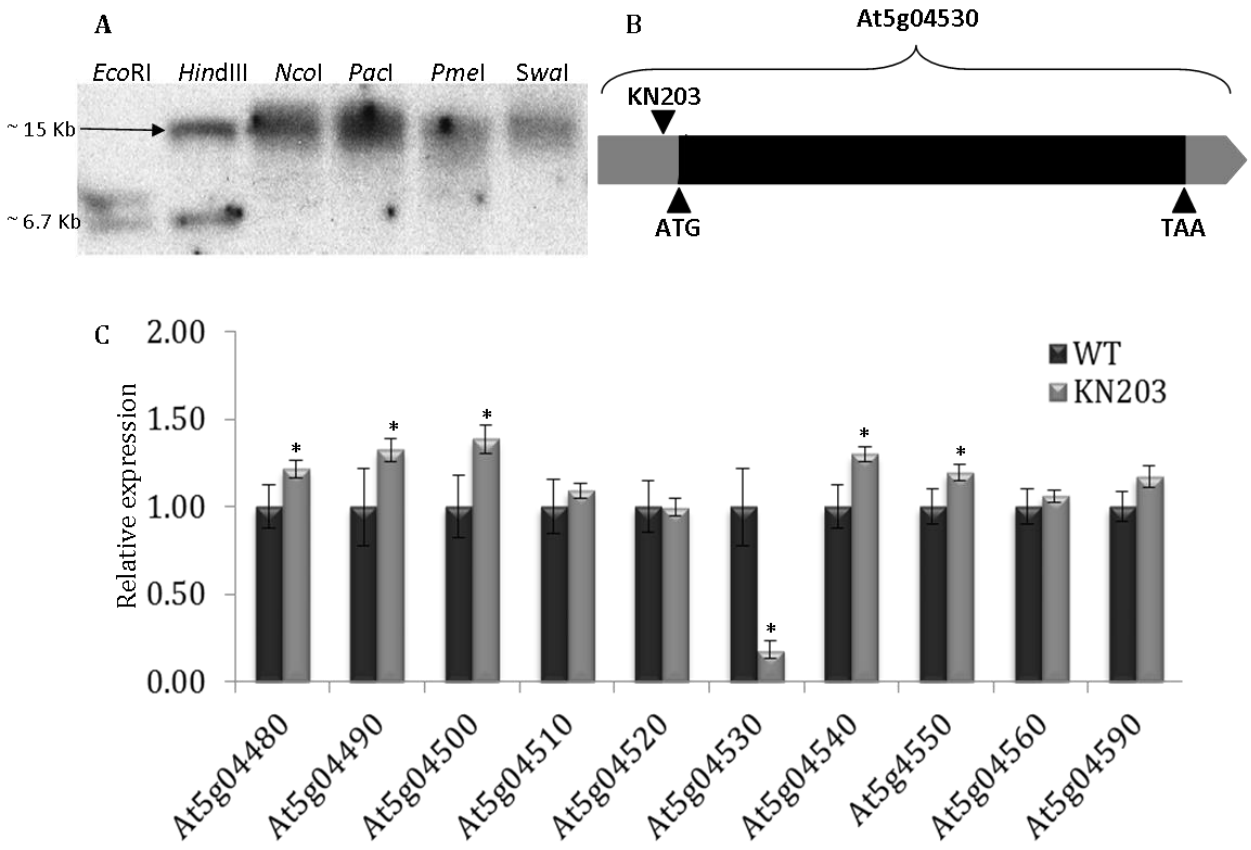

Figure 4-6: Characterization of mutant KN203. A) Southern hybridization of KN203 using genomic DNA digested with various restriction enzymes to determine T-DNA copy number. B) Gene organization of At5g04530 (*KCS19*) and T-DNA insertion position. Black inverted triangle represents T-DNA insertion in KN203 determined at 153 bp upstream of start codon, grey areas represent 5' and 3' UTRs and the black area represents the open reading frame. C) Gene expression analysis of five upstream (At5g04480 – At5g04520) and five downstream genes (At5g04530 – At5g04590) from the T-DNA insertion site in mutant KN203. The expression levels are normalized to the reference gene *PEX4* and relative to the WT set to a value of 1. Values represent means ± SD (n = 3). The "*" indicates statistical significance at $p < 0.05$.

4.3.4 Fatty acid profiling in mutant KN203

Fatty acid analysis was performed to determine if there were any changes in the fatty acid profile in mature seeds of mutant KN203. The analysis indicated that no significant changes were present in the levels of major fatty acids ranging from C16 to C24 (Figure 4-7). This indicates that the mutation in the *KCS19* gene did not affect medium to long chain fatty acids in seeds.

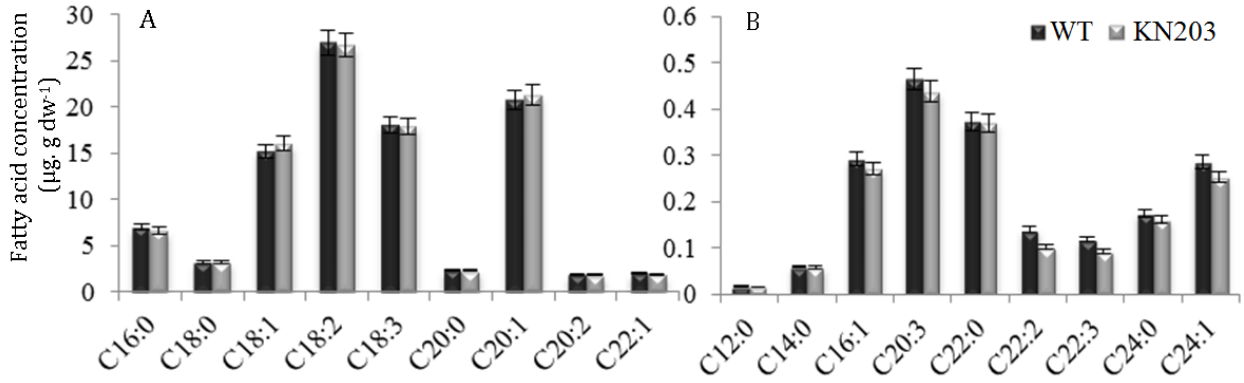

Figure 4-7: Major (A) and minor (B) fatty acid composition in mature seeds of WT Arabidopsis type and mutant KN203. Values represent means ± SD (n = 4) and are expressed on a dry weight (dw) basis. Statistical analysis ($p < 0.05$) indicated no significant difference between the WT and mutant KN203. dw, dry weight.

Since very long chain fatty acid synthesis could also be affected, lipidomics analysis was conducted on T_4 mature leaves and seeds of the mutant KN203 and WT. The analysis determined that the monoglactosyl diacyl glycerol (MGDG) content, but not the diglactosyl diacyl glycerol DGDG, was significantly lower in the mutant seedlings when compared to the WT (Figure 4-8A). Phospholipid content analyzed, namely PG, PC, PE, PI, PS and PA, did not change significantly between the mutant and the WT seedlings (Figure 4-8B, C). Conversely, the levels of PL breakdown species (lyso-PG , lyso-PC and lyso-PE) were significantly higher in the mutant compared to the WT and were increased by up to 63%, 88% and 84%, respectively (Figure 4-8D). Among the various MGDG fatty acid species profiled, the levels of fatty acids C34:6, C38:5 and C38:6 were significantly reduced in the mutant (Figure 4-8E, F). The levels of C34:6, 38:5 and C38:6 were reduced by about 25%, 52% and 58% in the mutant seedlings, respectively, when compared to the WT seedlings.

The lipid profiles in the mature seeds of mutant KN203 were compared with the WT and the results are given in Figure 4-9. The results indicate a trend towards increased DGDG levels in the mutant ($p < 0.1$) when compared to the WT. The MGDG levels did not change significantly between the mutant and the WT (Figure 4-9A). The results also indicated a significant increase in the levels of PS and a trend ($p < 0.1$) towards a reduction in the levels of PA (Figure 4-9B). A significant reduction in the levels of PC and PE and their breakdown products, *lyso-PC and lyso-PE,* were also observed in the mature seeds of mutant compared to the WT (Figure 4-9C, D). The levels of PG and lyso-PG did not change significantly in the mutant.

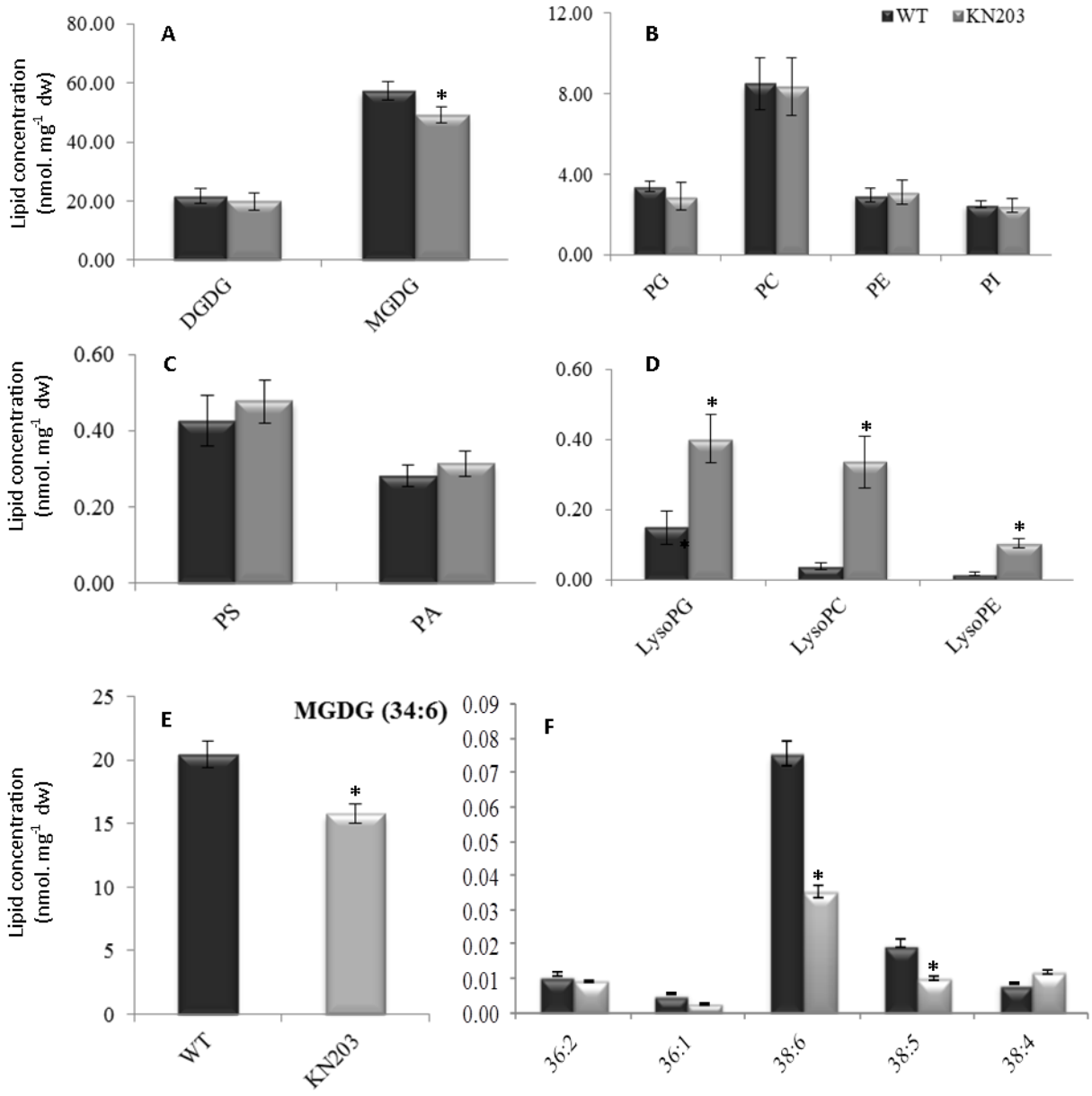

Figure 4-8: Lipid profiling of 14 –day old leaves of WT and mutant KN203 (T4). Panels A to D show concentations of major lipid classes of MGDG, DGDG and Phospholipids, while panels E and F show MGDG fatty acid species. Values represent means ± SD (n = 4). The "*" within each panel indicates statistical significance at $p < 0.05$. DGDG, diglactosyl diacyl glycerol; MGDG, monoglactosyl diacyl glycerol; PG, phosphotidylglycerol ; PC, phosphotidylcholine; PE, phosphotidylethanolamine; PI, phosphotidylionositol; PS, phosphotidylserine; PA, phosphotidic acid; LysoPG, lysophosphotidyl glycerol; LysoPC, lysophosphotidyl choline; LysoPE, lysophosphotidyl ethanolamine. The concentrations are given in nmol per mg dw (dry weight).

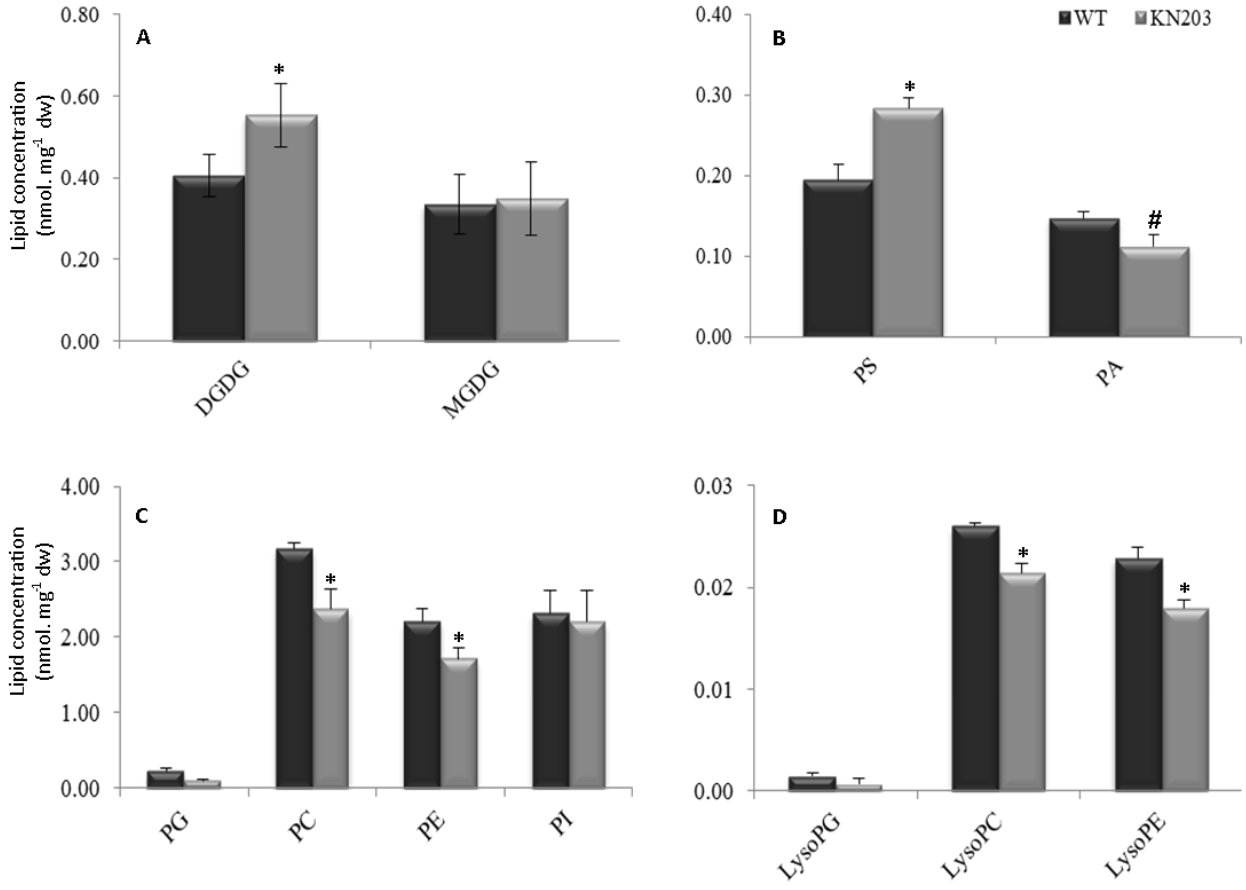

Figure 4-9: Lipid profiling of mature seeds in WT Arabidopsis and mutant KN203 (T_4). Values represent means ± SD (n = 4). The "*" within each panel indicates statistical significance at $p < 0.05$. DGDG, diglactosyl diacyl glycerol; MGDG, monoglactosyl diacyl glycerol; PG, phosphotidylglycerol ; PC, phosphotidylcholine; PE, phosphotidylethanolamine; PI, phosphotidylionositol; PS, phosphotidylserine; PA, phosphotidic acid; LysoPG, lysophosphotidyl glycerol; LysoPC, lysophosphotidyl choline; LysoPE, lysophosphotidyl ethanolamine. the concentrations are given in nmol per mg dw (dry weight).

4.3.5 Complementation of KN203 with a functional *KCS19*

Floral buds of mutant KN203 (T_4) were transformed with a functional *KCS19* gene. A total of six transformed mutant KN203 lines were obtained after screening for resistance to hygromycin and kanamycin. The complemented transformed mutant KN203 lines were named 203-C-1 to 203-C-6. Heterozygous complemented lines were grown in the greenhouse and expression of *KCS19* was determined in 10-day-old seedlings. One complemented line, 203-C-2, had 30% the expression of *KCS19* in the WT, while the levels of *KCS19* in the other five complemented lines were similar to the WT (Figure 4-10). Since the native promoter was used to

drive functional *KCS19* gene expression in the transformation construct, the expression levels did not increase to several fold above WT levels as is often noted with expression from the 35S promoter.

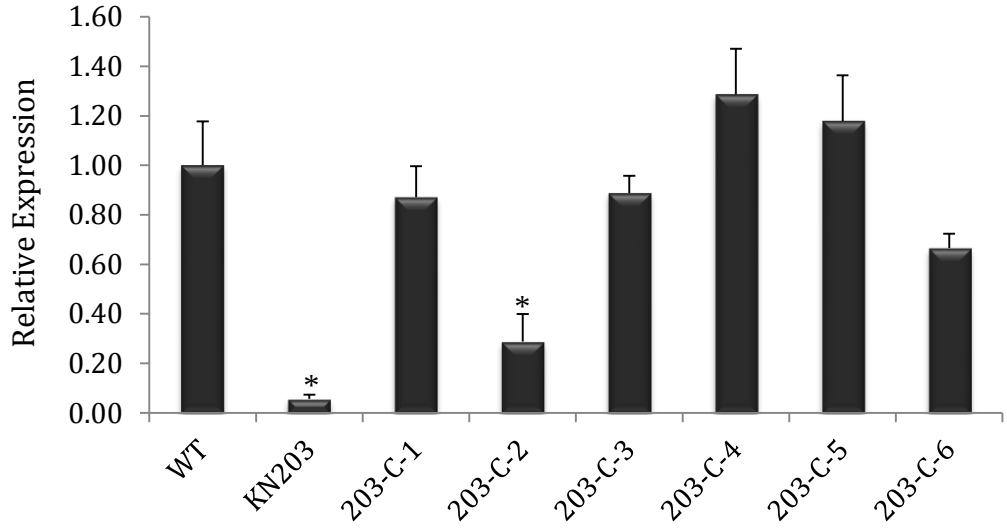

Figure 4-10: Expression levels of the *KCS19* gene in 10-day-old seedlings seedlings of WT Arabidopsis, mutant KN203 (T_4) and its complemented lines (T_1). The expression levels are normalized to the reference gene *PEX4* and relative to the WT set to a value of 1. Values represent means ± SD (n = 3). The "*" indicates statistical significance at $p < 0.05$.

4.3.6 Carotenoid analysis of complemented KN203 lines

Carotenoid content was examined in 10-day-old seedlings and the mature seeds of the WT, mutant KN203 (T_4) and the six complemented lines (Figure 4-11 and Figure 4-12), respectively. The analysis showed that the transformation with a functional *KCS19* reinstated the carotenoid levels to those of the WT. The lutein, β-carotene, zeaxanthin and violaxanthin levels in the seedlings were increased in the complemented lines compared to the native mutant and were similar to WT levels (Figure 4-11). Similarly, the lutein and β-carotene levels in the mature seeds were decreased to WT levels. These results indicate that complementation of the KN203 mutant with functional *KCS19* gene reversed the effects of the initial mutation.

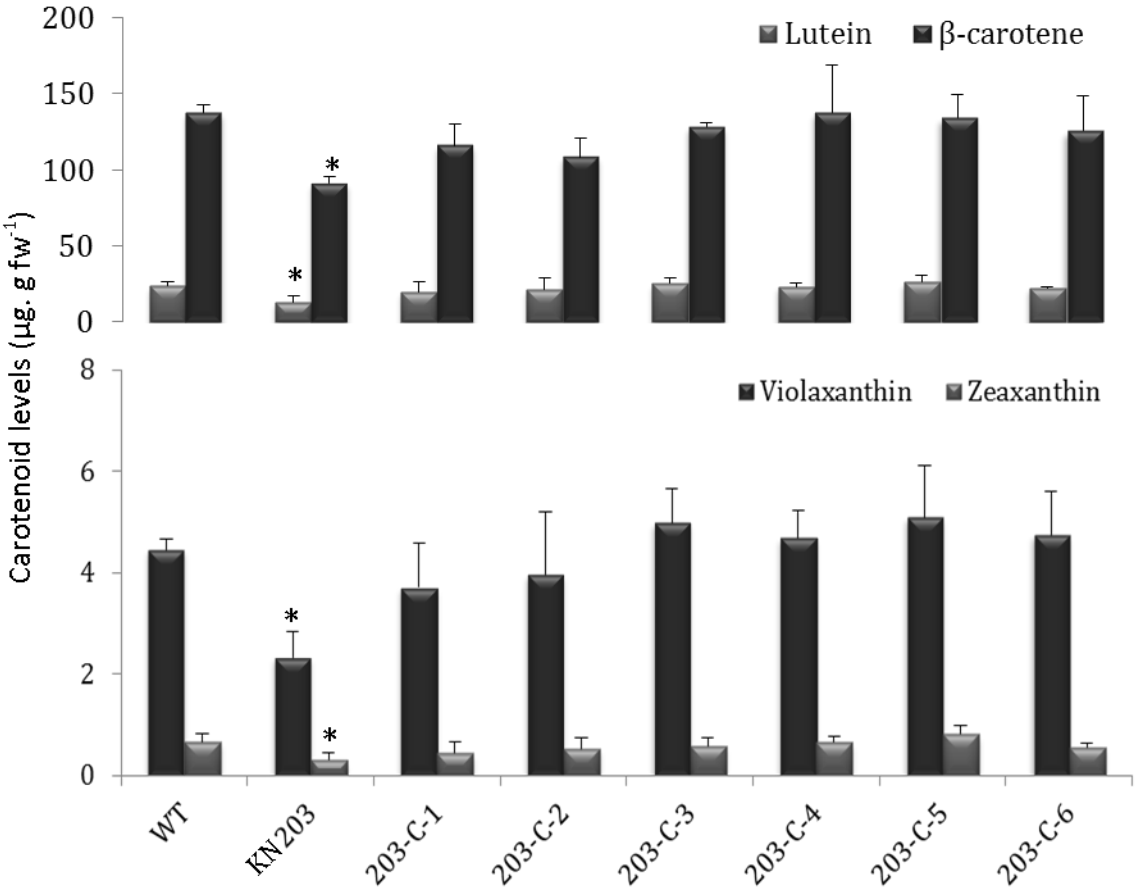

Figure 4-11: Carotenoid composition in 10-day-old seedlings of WT Arabidopsis, mutant KN203 (T_4) and its complemented lines (T_1). Values represent means ± SD (n = 3) and are expressed on a fresh weight (fw) basis. The "*" within each panel indicates statistical significance at $p < 0.05$. fw, fresh weight.

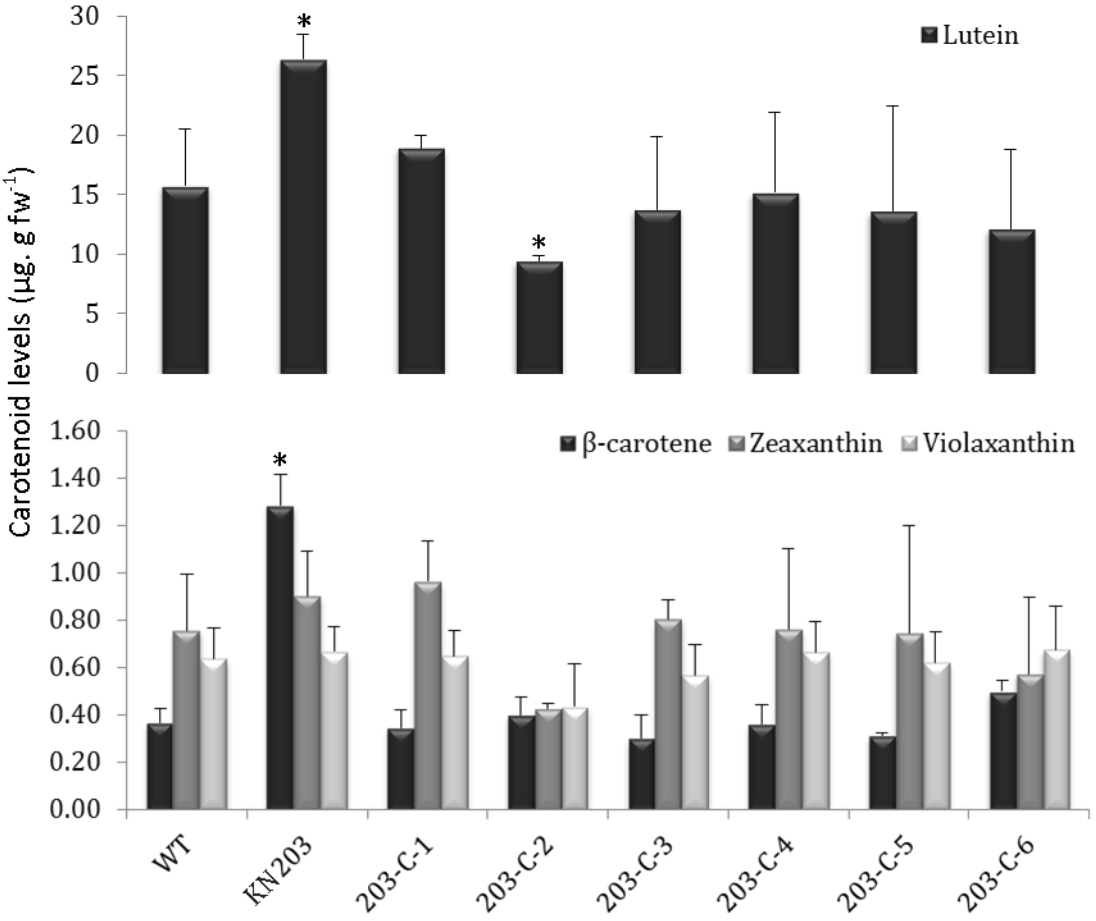

Figure 4-12: Carotenoid composition in mature seed of WT Arabidopsis, mutant KN203 (T_4) and its complemented lines (T_1). Values represent means ± SD (n = 3) and are expressed on a fresh weight (fw) basis. The "*" within each panel indicates statistical significance at $p < 0.05$. fw, fresh weight.

4.3.7 Carotenoid gene expression profiles in mutant KN203

The expression profile of genes encoding enzymes involved in carotenoid biosynthesis in the mutant KN203 was performed to determine the effect of *KCS19* suppression on the carotenoid pathway. The gene expression analysis was performed in both 10-day-old seedlings and mature seeds and their results are given in Figure 4-13 and Figure 4-14, respectively. The gene expression profiles indicate that the level of *βLYC* and *ZEP* was reduced significantly by about 50% in the mutant when compared to the WT (Figure 4-13). In contrast the gene expression levels in the mature seeds were increased significantly for most of the carotenoid genes except for *εLYC* (Figure 4-14).

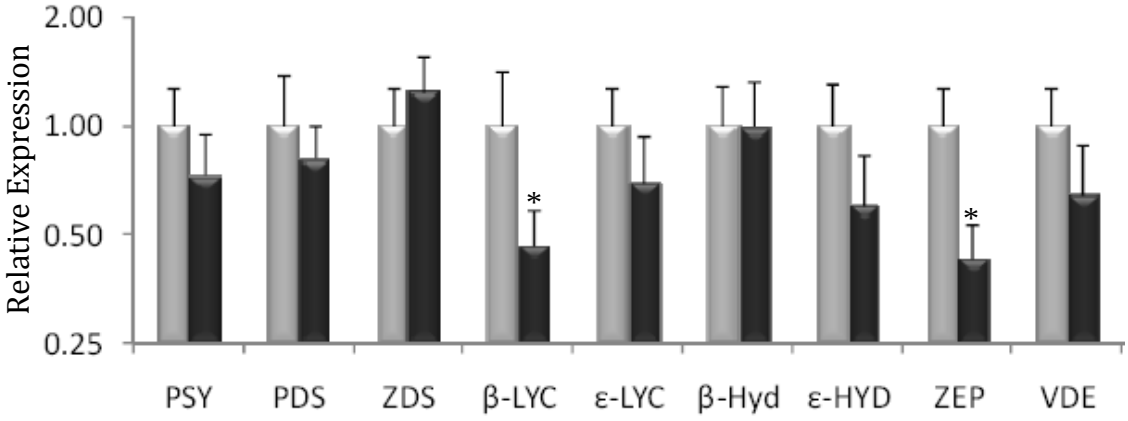

Figure 4-13: Expression profile of carotenoid biosynthetic genes in 10-days-old seedlings of WT (grey bar) Arabidopsis and mutant KN203 (T_4) (black bar). The expression levels are normalized to the reference gene *PEX4* and relative to the WT set to a value of 1. Values represent means ± SD (n = 3). The "*" indicates statistical significance at $p < 0.05$. *PSY*, phytoene synthase; *PDS*, phytoene desaturase; *ZDS*, ζ-carotene desaturase; *βLYC*, β-lycopene cyclase; *εLYC*, ε-lycopene cyclase; *βHYD*, β-ring hydroxylase; *εHYD*, ε-ring hydroxylase; *ZEP*, zeaxanthin epoxidase; *VDE*, violaxanthin de-epoxidase.

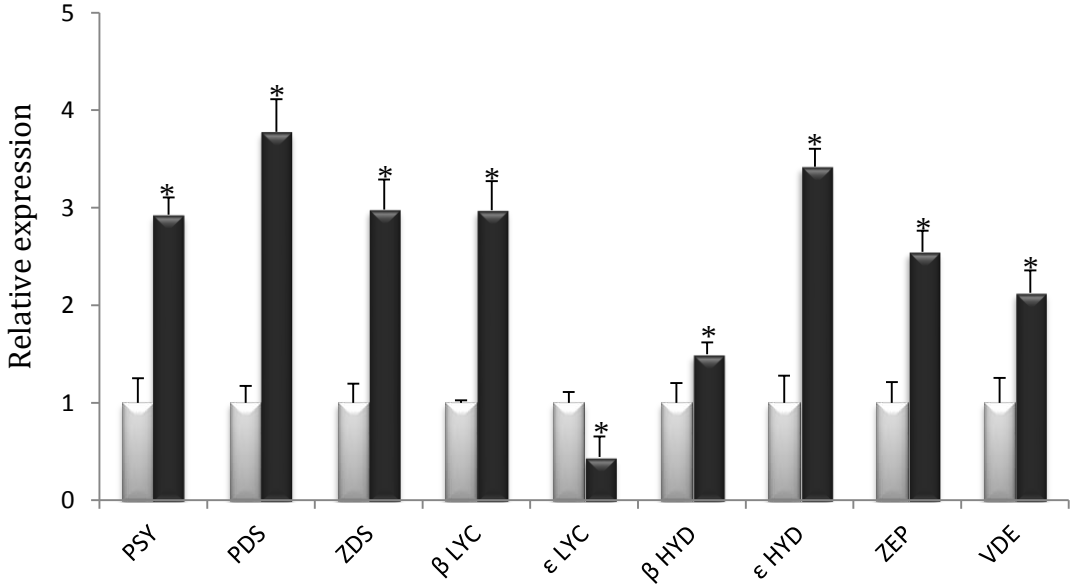

Figure 4-14: Expression profile of carotenoid biosynthetic genes in mature seeds of WT (grey bar) Arabidopsis and mutant KN203 (T_4) (black bar). The expression levels are normalized to the reference gene *PEX4* and relative to the WT set to a value of 1. Values represent means ± SD (n = 3). The "*" indicates statistical significance at $p < 0.05$. *PSY*, phytoene synthase; *PDS*, phytoene desaturase; *ZDS*, ζ-carotene desaturase; *βLYC*, β-lycopene cyclase; *εLYC*, ε-lycopene cyclase; *βHYD*, β-ring hydroxylase; *εHYD*, ε-ring hydroxylase; *ZEP*, zeaxanthin epoxidase; *VDE*, violaxanthin de-epoxidase.

4.3.8 Expression of *KCS19* in various plant organs

To determine the expression profile of *KCS19* across plant developmental stages, a developmental map microarray data set for *KCS19* (AT5g04530) was imported from the Arabidopsis eFP browser (http://bar.utoronto.ca/efp_arabidopsis/cgi-bin/efpWeb.cgi) and the values were charted in Figure 4-15. The data set indicates that the *KCS19* is expressed in all plant tissues. Its expression levels are substantially higher during silique and seed development, specifically stages 4 to 7 (Figure 4-15). In order to confirm the Arabidopsis eFP data, the developing siliques of WT Arabidopsis growing in greenhouse were harvested at different time intervals after pollination to determine *KCS19* expression analysis relative to mature rosette leaf expression levels (Figure 4-16). The results indicated that the *KCS19* gene expression in siliques harvested during 1-3 DAP increased significantly up to 5-fold compared to mature seed levels. The maximum expression level of 20- and 15-fold increase was observed at 4-6 DAP and 7-9 DAP, respectively.

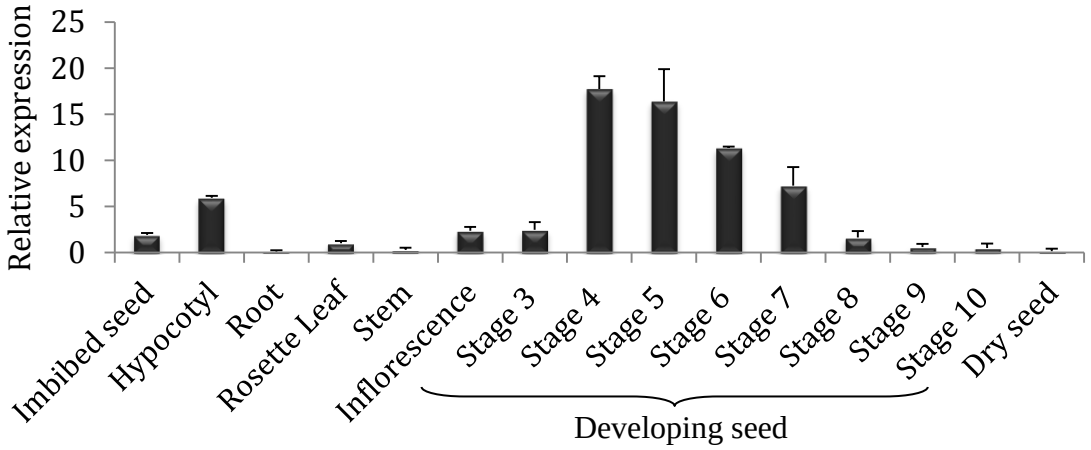

Figure 4-15: *In silico* expression profile of *KCS19* in WT Arabidopsis organs and seed development stages. The expression levels are relative to the rosette leaf set to a value of 1. The error bars indicate SD. The data was extracted from the Arabidopsis eFP browser at bar.utoronto.ca. The developing seed stages given are not indicative of the seed development stages given in Figure 4-16.

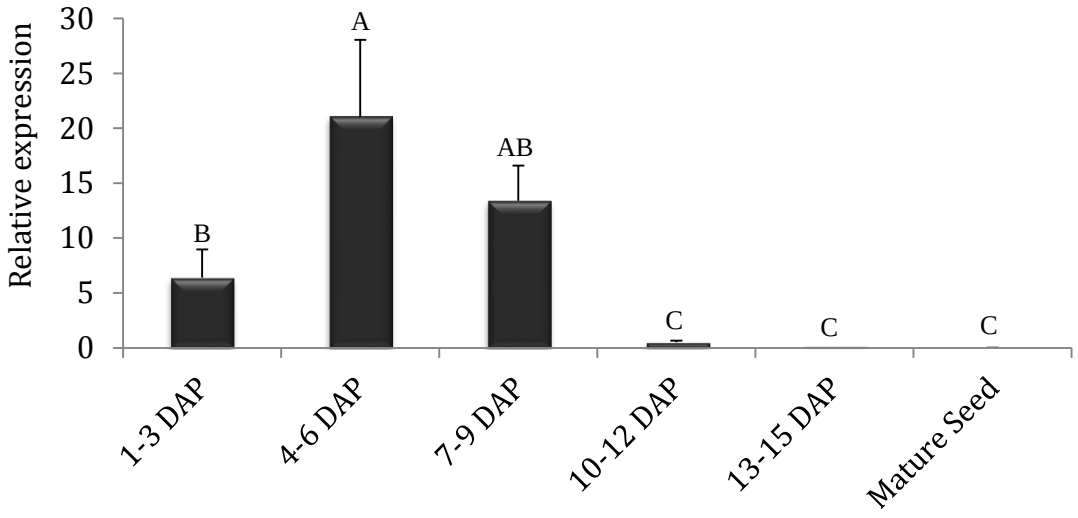

Figure 4-16: Expression profile of *KCS19* in WT Arabidopsis during seed development. The expression levels are normalized to the reference gene *PEX4* and relative to the WT leaf expression (data given in Figure 4-17) set to a value of 1. Values represent means ± SD (n = 3). Different letters indicate statistical significance at $p < 0.05$. Stage 1, 1-3 days after pollination (DAP); Stage 2, 4-6 DAP; Stage 3, 7-9 DAP; Stage 4, 10-12 DAP; Stage 5, 13-15 DAP.

4.3.9 Expression of other *KCS* genes in KN203 mutant

KCS19 belongs to a multigene family of 3-keto acyl CoA synthases. The family has 21 members involved in the elongation of fatty acid chain length (Blacklock and Jaworski, 2006). It has been reported that each member of the family has specific substrate specificity and some members could complement or duplicate activities of other members (Blacklock and Jaworski, 2006). It has also been reported that the expression of the *KCS* gene family members are affected by abiotic stress (Joubes et al., 2008). Therefore, the expression levels of other KCS family genes were determined in the mutant KN203 to investigate the relationship of *KCS19* among other genes of the *KCS* gene family (Figure 4-17). The result indicated a significant increase in the expression levels of *KCS8, KCS9* and *KCS15* up to 8-, 3- and 4-fold, respectively. Furthermore, the expression of four genes *KCS5, KCS7, KCS20* and *KCS21* were significantly increased up to two-fold in the mutant. The other 13 genes of the *KCS* family did not show significant changes in their expression levels when compared to the WT.

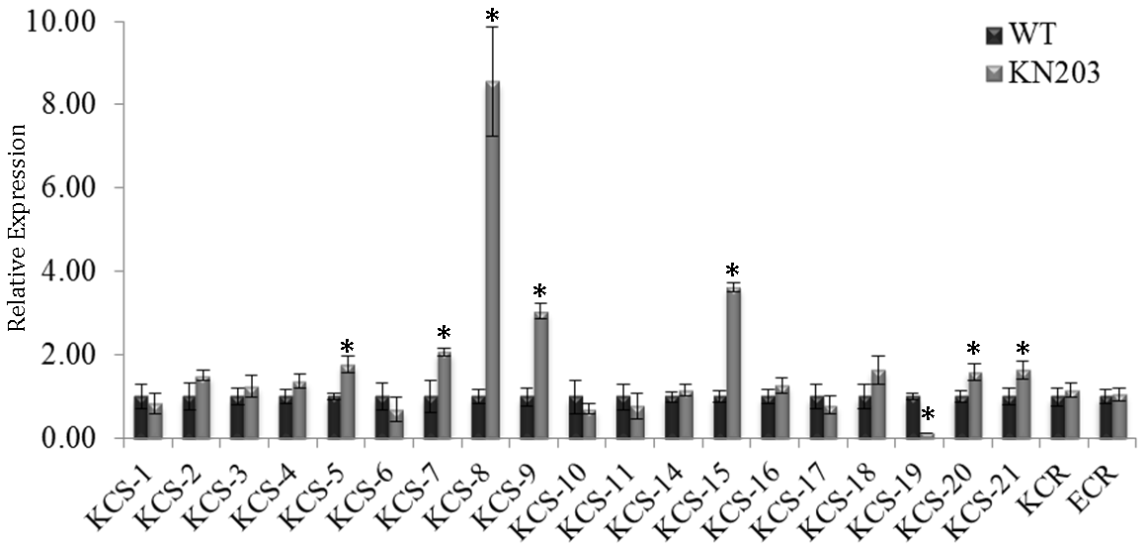

Figure 4-17: Expression profile of genes belonging to the *KCS* multigene family in 10-day-old seedlings of WT Arabidopsis and mutant KN203 (T_4). The expression levels are normalized to the reference gene *PEX4* and relative to the WT set to a value of 1. Values represent means ± SD (n = 3). The "*" indicates statistical significance at $p < 0.05$.

4.3.10 Effect of cerulenin on WT and mutant KN203

To determine the relation of fatty acids in the regulation of major carotenoids in Arabidopsis, WT and mutant KN203 T_4 generation seedlings were grown in various concentrations (0, 1, 5 and 10 μM) of cerulenin, a β-keto acyl synthase specific inhibitor that inhibits the elongation of fatty acids. The carotenoid content in the treated seedlings was determined and shown in Figure 4-18. The lutein, β-carotene and violaxanthin levels display a concentration dependent decrease in the WT as a function of increased cerulenin concentrations up to 5 μM. However at 10 μM concentration of cerulenin, only lutein displayed significant decrease compared to the lutein levels at 5 μM cerulenin concentration in the WT. This observation indicates that cerulenin affects carotenoids levels in the WT.

The lutein level in KN203 was significantly lower than WT in the absence of cerulenin, however, upon treatment with cerulenin the lutein levels in KN203 seemed to be less affected as the lutein levels were similar to the WT levels at 1 and 5 μM cerulenin concentrations. At 10 μM cerulenin concentration, the mutant KN203 lutein levels were significantly higher than that of the WT. This observation indicates that the lutein levels in the mutant KN203 was less responsive to the cerulenin treatment. The β-carotene levels in the WT were reduced in a

concentration dependent manner upon treatment with cerulenin. The β-carotene levels in the WT rapidly declined by 3-fold to reach the β-carotene level of mutant KN203 at 10 µM concentration. Violaxanthin levels also followed the pattern exhibited by the major carotenoids, with their WT violaxanthin levels gradually reduced to the violaxanthin levels of the mutant at 1 µM and 5 µM concentrations. At 10 µM concentration the mutant violaxanthin level was significantly higher than the WT treated at similar cerulenin concentration. Interestingly, the zeaxanthin levels were significantly lower in WT when compared to mutant KN203 in the absence of cerulenin and at 1 µM concentration. However at higher concentrations of cerulenin at 5 µM and 10 µM, the zeaxanthin levels did not change significantly between the WT and mutant KN203.

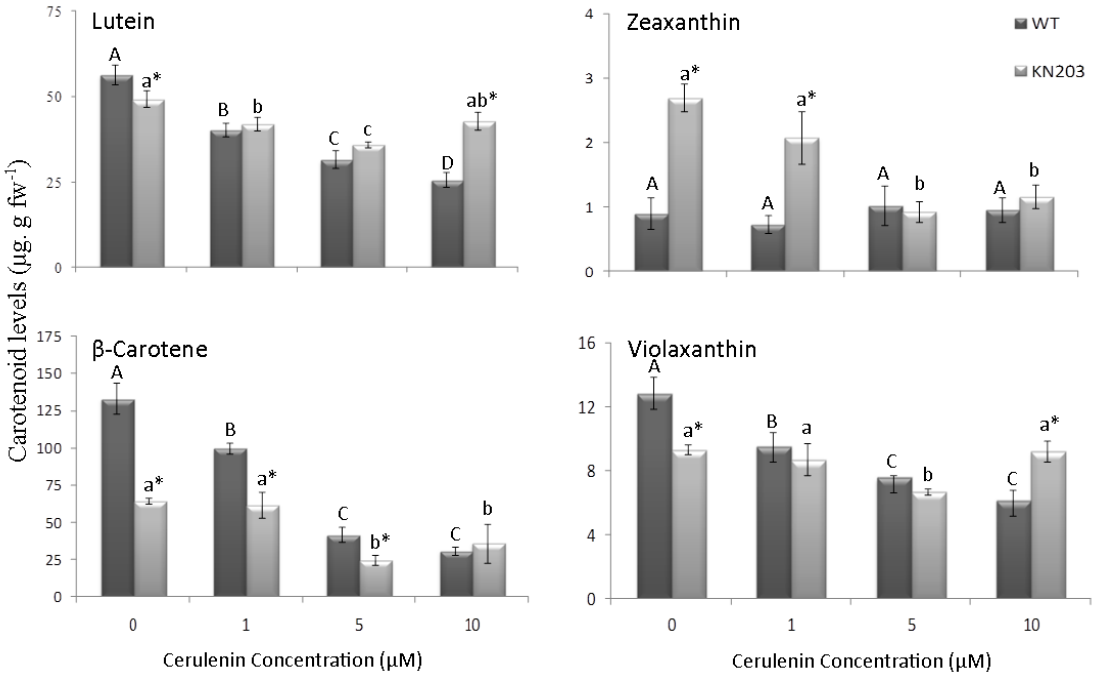

Figure 4-18: Effects of cerulenin treatment on carotenoid composition in 10-day-old seedlings of WT Arabidopsis and mutant KN203 (T_4). Values represent means ± SD (n = 3) and are expressed on a fresh weight (fw) basis. Different letters within each panel (uppercase for WT; lower case for KN203) indicate statistical significance at $p < 0.05$ among the treatments. The "*" indicates statistical significance at $p < 0.05$ between WT and KN203. fw, fresh weight.

4.3.11 Expression of carotenoid genes in cerulenin treated WT

To determine whether cerulenin treatment affects carotenoid gene expression similar to that observed in the mutant KN203, expression profiles of carotenoid genes in the WT 10-day-old seedlings treated with 10 μM cerulenin were determined and compared to the untreated WT seedlings (Figure 4-19). The expression profile indicated that *PSY* and *ε-LYC* transcripts were significantly higher in the cerulenin-treated seedlings compared to the untreated seedlings. The *β-LYC* expression was significantly lower in the cerulenin treated seedlings compared to the untreated seedlings. All the other carotenoid genes displayed statistically similar expression levels between the cerulenin-treated and un-treated seedlings WT.

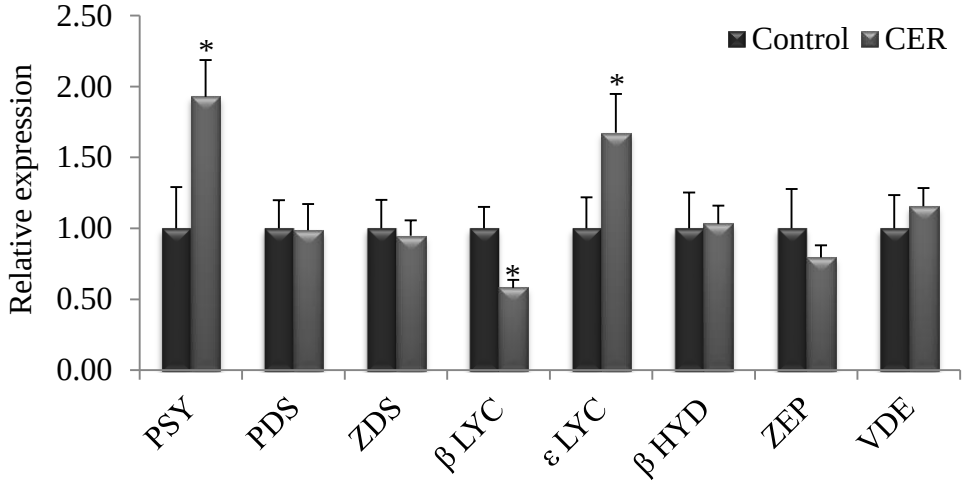

Figure 4-19: Effects of cerulenin on the expression of carotenoid biosynthetic genes in 10-day-old seedlings of WT Arabidopsis . Plants were treated with 10 μM cerulenin (CER). The expression levels are normalized to the reference gene *PEX4* and relative to the WT set to a value of 1. Values represent means ± SD (n = 3). The "*" indicates statistical significance at $p < 0.05$. *PSY*, phytoene synthase; *PDS*, phytoene desaturase; *ZDS*, ζ-carotene desaturase; *βLYC*, β-lycopene cyclase; *εLYC*, ε-lycopene cyclase; *βHYD*, β-ring hydroxylase; *ZEP*, zeaxanthin epoxidase; *VDE*, violaxanthin de-epoxidase.

4.4 Discussion

4.4.1 Norflurazon Screening

In this study, SK activation-tagged *A. thaliana* mutants were identified that were resistant to norflurazon, a phenylpyridazinone herbicide. Norflurazon leads to the accumulation of colourless carotenoid precursors, thereby reducing carotenoid biosynthesis and plant growth (Bartels and Watson, 1978). The inhibition site of norflurazon was determined initially in a cell-free carotenogenic enzyme system from a mutant strain of *Phycomyces blakesleeanus* (Mucoraceae) in which the presence of norflurazon resulted in reduced incorporation of [2-^{14}C]mevalonic acid into phytoene (7,8,11,12,7′,8′,11′,12′-octahydro-ψ,ψ-carotene) and β-carotene (β,β-carotene) (Sandmann et al., 1980). Similar carotenoid inhibitory studies were performed on other plant species, such as wheat (Wilkinson, 1987, 1989), barley (Bolychevtseva et al., 1995; Yurina and Kloppstech, 2001), and cucumber (Jung et al., 2000). Initially, it was thought that the norflurazon affects carotenoid biosynthesis by binding directly to PDS (Chamovitz et al., 1991). However, it was later revealed that norflurazon binds to a co-factor of PDS, plastoquinone, that is involved in the electron transport chain of photosystem II (Norris et al., 1995; Breitenbach et al., 2001).

Screening for carotenoid mutants using norflurazon has been reported in few studies in bacterial, algae and plant systems. Norflurazon-resistant mutants have been obtained from the blue green algae *Synechococcus* (Linden et al., 1990), *Haematococcus pluvialis* (Chen et al., 2003) and *Clamydomonas* (Vartak and Bhargava, 1997). Norflurazon screening was also used in tomato cell lines to select lines that accumulated the most phytoene or phytofluene (Engelmann et al., 2010). A few carotenoid mutants were also selected using various screening methods. The *pds* 1, 2 and 3 mutants of Arabidopsis were identified from an activation-tagged mutant population for mutants segregating for pigment defects (Albino, yellow or pale green) using visual screening (Norris et al., 1995).

Tan and coworkers screened 88 rice cultivars using HPLC to identify 19 unpolished rice lines that accumulated high levels of β-carotene to be used as parental lines (Tan et al., 2005). In sorghum, 8 putative carotenoid mutants were initially identified by their yellow kernels and displayed altered carotenoid profiles when examined using HPLC (Kean et al., 2007). In this study, eight mutant lines with altered carotenoid profiles were identified from 20,000 individual

activation-tagged *A. thaliana* mutant lines (2000 T_2 seed pools) using by screening for resistance to norflurazon. This corresponds to about 0.04% probability of a mutant to be resistant to norflurazon and with an altered carotenoid profile. Therefore, this observation implies that norflurazon based screening could prove to be an effective screening method to identify carotenoid mutants. It can be used simultaneously with other methods such as visual and HPLC based screening to increase the probability of obtaining mutants with altered carotenoid phenotypes. It was interesting to note that most of the mutants identified in this study had significantly lower levels of lutein, β-caotene, zeaxanthin and violaxanthin in the leaf tissues. However, significantly higher levels of lutein and β-caotene were observed in the mature seeds of several mutants showing resistance to norflurazon. The reason behind this observation remains unclear. Therefore, further experiments involving carotenoid analysis in the tissues of germinating seeds and seedlings could provide more insights on the carotenoid metabolism during germination.

4.4.2 KN203 is a norflurazon-sensitive mutant

Mutant KN203 was selected from the activation tagged population of *A. thaliana* for resistance to 0.5 µM norflurazon . The growth and development of the mutant KN203 were similar to the WT in the absence of norflurazon. However, the mutant displayed sensitivity to norflurazon in a concentration dependent manner although it was initially selected as a norflurazon resistant mutant. The reason behind this is not clear. The mutant seedlings were recovered upon transplanting from medium containing norflurazon to non-treated greenhouse growth conditions. The mutant had significantly lower levels of lutein and β-carotene in the seedlings compared to the WT. However, the mature seeds of the mutant KN203 had significantly higher levels of lutein and β-carotene. The sensitivity of the mutant to norflurazon could be attributed to the lower levels of the major carotenoids in the seedlings.

The molecular characterization of the mutant indicated a concatamer type T-DNA insertion into the promoter region of *KCS19* gene encoding β-Keto acyl CoA synthase. The T-DNA insertion reduced the expression of the *KCS19* by about 90% compared to the WT. However, the T-DNA insertion did not increase the expression profiles of neighboring upstream and downstream genes by more than 1.5 fold. Introduction of a functional *KCS19* to KN203 mutant

complemented the mutation and restored WT carotenoid levels to both complemented seedlings and mature seeds. This indicates that *KCS19* is directly or indirectly involved in carotenoid accumulation in Arabidopsis. Similarly the complemented lines were not sensitive to norflurazon. An attempt to recreate the mutant using antisense of the *KCS19* led to lethality in all transformation assays. Furthermore, no knockout mutant lines for the *KCS19* are available from TAIR. The embryo-lethal mutants are common in T-DNA tagging, about 233 mutants representing 159 genes (19% of the genes) that exhibited either seedling phenotypes or embryo-lethal phenotypes have been reported (Myouga et al., 2010). Some of the genes involved in the fatty acid biosynthesis are important and a loss of function mutant lead to embryo lethal phenotype, analyses of insertional mutants in *AtKCR1* and *AtKCR2* encoding *β*-ketoacyl reductase (KCR) revealed that loss of AtKCR1 function resulting in embryo lethality, which cannot be rescued by *AtKCR2* expression using the *AtKCR1* promoter. Similarly, *KCS19* seems to be a vital gene and that the plant needs at least some expression of functional *KCS19* expression for plant growth and development as in the case of KN203 mutant.

4.4.3 Expression of *KCS19* in *A. thaliana*

Gene expression profiling of *KCS19* in *A. thaliana* indicated that the gene is expressed in abundance during the initial stages of seed development. The highest level of *KCS19* expression was observed at 4-6 DAP. The expression profile also indicated that the levels decreased significantly from 9 DAP until there were no detectable transcripts of *KCS19* in the dry mature seeds. In mutant KN203, lutein and β-carotene levels were significantly increased in the mature seeds when compared to the WT and their levels restored to WT levels in the complemented lines of mutant KN203. In addition, the expression of all the major carotenoid genes, except *ε-LYC*, was significantly increased in the mature seeds of KN203 when compared to the WT seeds. In a microarray study conducted in *B. napus* to compare genes regulated in developing seeds 20 DAP and 35 DAP, an increase in the transcripts of *KCS5* was observed; this gene encodes another β-Keto acyl CoA synthase leading to carotenoid accumulation during seed development (Yu et al., 2010). In this study, a 2-fold increase in the *KCS5* gene in the 10 days-old seedlings was observed in mutant KN203 followed by significant increase in lutein and β-carotene levels in mature seeds. Therefore, it is postulated that the increase in the lutein and β-carotene in mature

seeds could be attributed to increased *KCS5* expression affected due to the disruption of *KCS19* expression.

4.4.4 Cross talk between fatty acid and carotenoids metabolism

Few studies have discussed the cross talk occurring between the fatty acid and carotenoid metabolism (Rabbani et al., 1998; Aronsson et al., 2008; Ye et al., 2008; Schaller et al). Unique biochemical machinery is present in the chloroplast envelope membranes (Joyard et al., 1991). The chloroplast envelope is the site of specific biosynthetic functions such as synthesis of plastid membrane components (glycerolipids, pigments, prenylquinones), chlorophyll breakdown, synthesis of lipid-derived signaling molecules (fatty acid hydroperoxydes, growth regulators, or chlorophyll precursors), and participates in the coordination of the expression of nuclear and plastid genes (Joyard et al., 1991). The chloroplast outer envelope membrane contains ~20% MGDG, the only Hexagonal–II-phase forming lipid present in this membrane as DGDG is a bilayer-forming lipid (Joyard et al., 1991). An *in vitro* study reported that in the presence of high concentrations of DGDG or PC, where a diadinoxanthin and violaxanthin are completely solubilized, a strongly inhibited diadinoxanthin de-epoxidation was observed, while violaxanthin de-epoxidation by VDE was completely absent. This indicates that the inverted hexagonal phase domains provided by lipid MGDG or PE is essential for de-epoxidase activity (Goss et al., 2005). Especially the interactions with MGDG are of greatest interest because MGDG is able to form membrane structures, which are thought to be involved in the protein import processes (van't Hof et al., 1991). In the mutant KN203, the MGDG levels were reduced by 30% and this could have led to the reduction in the carotenoid levels in the seedlings. Furthermore, the very long chain fatty acid species such as C34:6, C38:6 and C38:5 were also significantly reduced in the mutant. The fatty acid degradation products such as the lysoPG, lysoPC and lysoPE were significantly increased in the mutant. These results indicate that the reduction of carotenoid levels could be attributed to the structural changes in the chloroplast membrane fatty acid compositions.

It was reported that the carotenoids form complexes with lipids and specific carotenoid binding proteins, therefore it was postulated that these lipoprotein complexes are formed to sequester the carotenoids away from other structures to avoid possible harmful effects (Deruere et al., 1994). Treatment of spinach leaves with cerulenin significantly reduced the rate of

accumulation of MGDG, PC and PI (Laskay et al., 1985). To further evaluate the cross talk between fatty acid synthesis and carotenoid metabolism, the mutant and WT plants were treated with cerulenin, a fatty acid synthesis inhibitor. The seedlings of both mutant and the WT were grown in the media containing 0, 1, 5 or 10 μM concentrations of cerulenin. The lutein, β-carotene and violaxanthin levels in the WT seedlings were reduced in a concentration dependent manner, when compared to mutant KN203 treated with similar concentration of cerulenin. This observation indicates that WT seedlings are highly sensitive to cerulenin and the mutant KN203 seems to be less sensitive to cerulenin treatments.

Further investigation, such as electron microscopy to study the membrane structure in the mutant and the distribution of oil bodies in the chloroplast will help to determine the relationship between MGDG and carotenoid reduction. Similarly, lipid profiling on the complemented lines needs to performed to confirm the relationship between the MGDG levels and carotenoid biosynthesis regulation. Studies involving subcellular localization of KCS19 would provide more information on its mechanism of action.

5 NORFLURAZON TOLERANT ARABIDOPSIS MUTANT REVEALS THE ROLE OF *RBP47C* IN REGULATING CAROTENOID ACCUMULATION

5.1 Introduction

RBPs are present in all organisms from bacteria to animals. The plant RBPs, in addition to their involvement in various developmental processes, are also involved in adaptation of plants to various environmental conditions (Lorkovic, 2009). They are known to act by regulating pre-mRNA splicing, polyadenylation, RNA stability and RNA export, as well as by influencing chromatin modification (Lorkovic, 2009). RBPs are present in chloroplasts where they are involved in RNA editing, intron splicing and 3' end processing of chloroplast (Maris et al., 2005) and mitochondria transcripts (Vermel et al., 2002). However, the chloroplast genome does not encode for any RBPs; all the RBPs present in the chloroplast are nuclear-encoded and transported into chloroplasts (Ruwe et al., 2011). A survey of the Arabidopsis genome for RNA-binding proteins revealed more than 200 RRM- and 26 KH-containing proteins (Lorkovic and Barta, 2002). Both forward and reverse genetic approaches have been used to characterize proteins that have roles in RNA metabolism in plant development (Cheng and Chen, 2004).

The RNA binding protein, RB47, was found to be transported to chloroplasts of *Clamidomonas reinhardtii* where it binds to the 5'UTR of the *PSBA* encoding the D1 protein (Yohn et al., 1998). The proteins encoded by the Arabidopsis *ABH1* and *SAD1* genes involved in ABA signaling are homologous to highly conserved eukaryotic RNA-binding proteins (Kmieciak et al., 2002). The *ABH1* encodes the Arabidopsis homolog of CB80, one of the two proteins comprising the eukaryotic nuclear cap-binding complex (CBC) (Kmieciak et al., 2002). The *sad1* mutant shows defects associated with both the production and the perception of ABA (Xiong et al., 2001). The SAD1 protein is an ortholog of the yeast Lsm5 protein, which was originally identified as a subunit of the U6 small nuclear ribo nuclear protein (snRNP) complex is involved in nuclear RNA processing (Bouveret et al., 2000). RBP47 belongs to the oligouridylate-specific RRM proteins along with RBP45, UBP1, UBA1 and UBA2. Generally, these proteins contain three RRMs and a glutamine rich amino terminus. These proteins are known for their oligouridylate specificity (Lorkovic and Barta, 2002). Preliminary analysis determined that both RBP45 and RBP47 are localized in the nucleus and at least two RRMs are required for

their binding specificity (Lorkovic et al., 2000). It was also reported that RBP45 and RBP47 proteins are not involved in alternative splicing, but displayed high affinity for poly (U) oligonucleotides (Lorkovic et al., 2000).

Many Arabidopsis RBPs are known to be involved in the regulation of plant-specific processes or are involved in plant responses to changing environmental conditions. The mechanisms of how plant RBPs contribute to these processes are, however, largely unknown. More detailed characterization of more RBPs in plants would be beneficial in providing evidence for the steps of mRNA processing and how these are affected by individual proteins. In this study, the KN231 mutant with a defective At1g47490 gene encoding an RBP47C (AtRBP47c) was characterized for its involvement in the accumulation of carotenoids in the seed tissues and norflurazon resistance.

5.2 Materials and methods

5.2.1 Plant material and growth conditions

The mutant KN231 was identified from a T_3 population of activation-tagged Arabidopsis mutant lines as described in Chapter 4. Two Salk lines with T-DNA insertions in the same locus as KN231 (At1g47490) were obtained from the Arabidopsis Biological Resource Center (ABRC). These two Salk mutants, SALK_064691 and SALK_035654, were renamed S4 and S8 respectively. All plants (WT and mutants) were grown from seed under greenhouse conditions as described in section 2.2.1 The KN231 mutant was transferred to the greenhouse for seed increase as described in section 4.2.1 and then grown again to the T_3 generation as described in section 4.2.1 for subsequent analyses.

5.2.2 Carotenoid extraction and determination

Carotenoid extraction and HPLC analyses from two-week-old leaf tissues and mature seed was carried out as described in sections 2.2.2 and 2.2.3 respectively.

5.2.3 Estimation of T-DNA insertions and determination of T-DNA flanking regions

The T-DNA insertion copy number was determined by Southern hybridization as described in section 4.2.5 while the flanking regions of the T-DNA were identified using the Genome Walker kit (BD Biosciences) as described in section 4.2.6.

5.2.4 Total RNA extraction and cDNA synthesis

The extraction of total RNA from leaf and other tissues of Arabidopsis occurred as described in sections 2.2.6 and 4.2.7, respectively. cDNA synthesis occurred as described in section 2.2.6.

5.2.5 qPCR

Relative expression levels of carotenoid biosynthetic genes were determined using the gene-specific primers described in Table 3-1. The sequence similarity and homology between

RBP47C and *RBP47C*' made designing primers unique to each gene challenging. This was overcome by using the sequence differences in the untranslated regions of the two genes. Gene-specific primers (Table 5-1) were selected using Primer3 software (http://bioinfo.ut.ee/primer3/; Untergasser et al., 2012). The location of the selected primers to selectively amplify *RBP47C* or *RBP47C'* is given in Figure 5-2. qPCR and determination of relative expression levels occurred as described in section 4.2.5.

Table 5-1: Primers used in this study for sqPCR, and qPCR

Primer name	AGI Code	Forward (5'to 3')	Reverse (5' to 3")
FL1	At1g47490	CACCAGCAATCACTTCACATCACAAAAC	
FL2	At1g47500	CACCAATCTCTCACATCACATAAACAAT	
FL3	At1g47490 & At1g47500		CAAGGAGAGACAAGAAGCCAAC
RT1	At1g47490	ACGCGCCGCCGCCGTTCCCACCT	
RT2	At1g47500	GATGTACGCGCCGCCGCCACCGAT	
RT3	At1g47490 & At1g47500		ATAAGCCTCATCCATCCAGTGA

5.2.6 Cloning of RBP47C and over-expression studies

A full length cDNA of *RBP47C* (At1g47490) was amplified from WT Arabidopsis cDNA using gene-specific primers (Table 5-1). Specific methodologies for cloning, plant transformation and subsequent selection are described in detail in sections 4.2.9, 4.2.10 and 4.2.11 respectively. The Gateway destination vector pMDC32 (Figure 4.1B), containing a 2X 35S promoter was selected for these complementation studies, as the At1g47490 gene fragment contained only the open reading frame (ORF) and did not contain the endogenous promoter.

5.2.7 Bioinformatic analysis

For pairwise alignment of RBP47C and RBP47C', initially cDNA nucleotide sequences were obtained from TAIR (www.arabidopsis.org) and converted to FASTA format. The nucleotide sequences were entered into the Pairwise Sequence Alignment tool available online (http://www.ebi.ac.uk/Tools/psa/emboss_needle/nucleotide.html). The alignment was performed using default parameters (Rice et al., 2000).

For phylogenetic analysis, initially the protein sequences for the 11 RBPs were obtained from NCBI and then assembled using the SeqMan suite (DNASTAR, WI, USA). The phylogenetic analysis on the assembled Arabidopsis RBP was performed using MegAlign suite (DNASTAR, WI, USA). ClustalW algorithm with default parameters was used and the statistical analysis on the alignment was performed using bootstrapping technique using 1000 iterations. Similarly, a pairwise alignment of the two proteins RBP47C and RVP47C' was also performed in the same software using MegAlign suite (DNASTAR, WI, USA).

To determine chloroplast localization of proteins *in-silico*, the principal component logistic regression (PCLR) chloroplast localization prediction online tool available at http://www.andrewschein.com/cgi-bin/pclr/pclr.cgi was used. The protein sequence for RBP47C was used and RBP47C' were obtained from NCBI. The sequence was entered into the tool for prediction using default parameters (Schein et al., 2001). A score of more than 0.6 indicates a potential candidate for chloroplast localization.

5.2.8 Experimental design and statistical analyses

Sampling for carotenoid determination and qPCR, as well as statistical analyses of the data occurred as described in section 3.2.8.

5.3 Results

5.3.1 Identification of mutant KN231

Mutant KN231 was selected from the screening an activation-tagged mutant population grown on ½ × MS agar medium supplemented with 0.5 µM norflurazon (Figure 5-1A). The Southern hybridization results indicated the mutant KN231 had a single copy insertion (Figure 5-1B) and the Genome Walker results identified the T-DNA insertion in the first intron of the gene At1g47490 (RBP47C) that encodes a putative RBP. Another variant of At1g47490, At1g47500 (RBP47C'), was also identified during the BLAST search. The percentage identity of the Genome Walker fragment matched 100% to At1g47490 indicating that the T-DNA insertion was in AT1g47490 and not At1g47500. Two Salk mutants with a T-DNA insertion in the At1g47490 gene, SALK_064691 (S4) and SALK_035654 (S8) (Figure 5-1C), were obtained from ABRC. No Salk mutants were available for the At1g47500 gene.

All the mutants analyzed in the study, KN231 and the two Salk knock-out lines (S4 and S8) displayed tolerance to norflurazon at a concentration of 0.5 µM. The norflurazon treatment affected the WT and the mutant seedlings similarly until the 10th day of incubation, during which time the seedlings turned purple. However, after 10 days, the leaves in the mutants turned translucent and then displayed vigorous growth followed by greening of the leaves and normal growth (Figure 5-1A). Conversely, the WT plants displayed an albino phenotype and did not recover to the phenotype of the untreated control.

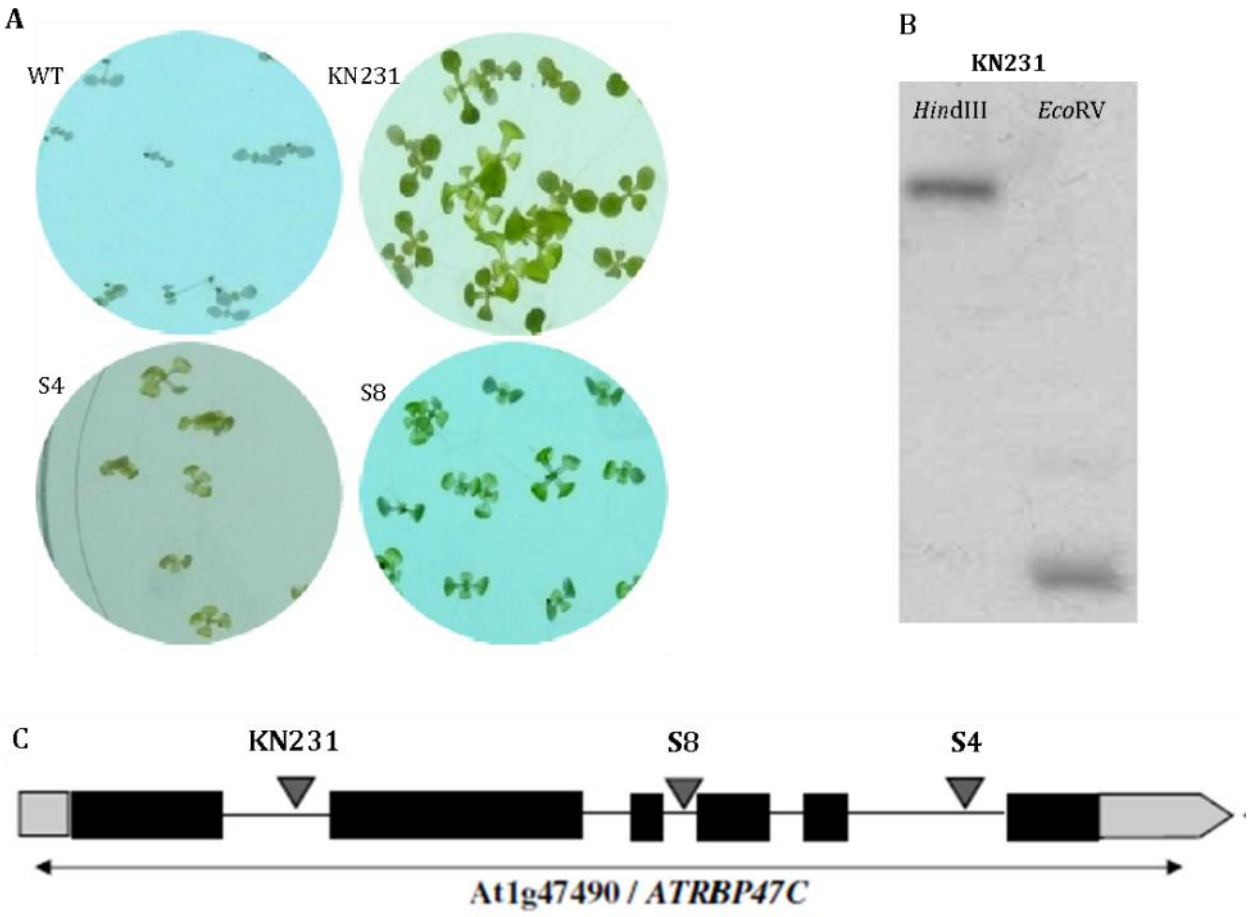

Figure 5-1: Identificaton of mutant KN231. A) 10-day-old seedlings of WT, mutant KN231 and Salk mutants S4 and S8 grown in ½ × MS media supplemented with 0.5 µM norflurazon. B) Southern hybridization of KN231 using genomic DNA digested with various restriction enzymes to determine T-DNA copy number. C) Genomic organization of At1g47490 and the T-DNA insertion sites of mutants KN231, S4 and S8; grey blocks indicate untranslated regions, black blocks indicate exons, lines indicate introns, and inverted triangles indicate the site of T-DNA insertion in the mutants KN231, S4 and S8.

5.3.2 Nucleotide and amino acid sequence alignment studies

The two genes *RBP47C* and *RBP47C'* had high sequence homology with up to 88.3% identity at the nucleotide level. There were only 120 gaps accounting to only 6.7% between the two genes (Figure 5-2). Also, most of the gaps were found in the 5' untranslated region and the first exon. Therefore, this region was used to design primers that selectively amplified *RBP47C* or *RBP47C'* sequences. The T-DNA insertions for KN231, S8 and S4 are present in the first, third and fifth introns, respectively, (Figure 5-1C). The primers that amplify full length *RBP47C* and *RBP47C'* were used to confirm the effect of T-DNA insertion at the *RBP47C* locus in the mutants. Similarly another region within the first exon that had increased number of variations between *RBP47C* and *RBP47C'* was used to design primers for qPCR analysis (Figure 5-2).

The pairwise alignment of protein sequences of RBP47C and RBP47C' indicated a 90.37% identity between the two proteins (Figure 5-3). There were a total of 6 amino acid gaps occurring within the first 75 amino acids between the two proteins (RBP47C and RBP47C'). There were a total of 36 amino acid substitutions between RBP47C and RBP47C'. Out of the 36 substitutions, ~30% of the substitutions occurred in the first 50 amino acids. This result mirrors the high level of variability observed between the *RBP47C* and *RBP47C'* nucleotide sequences within the first 150 bp.

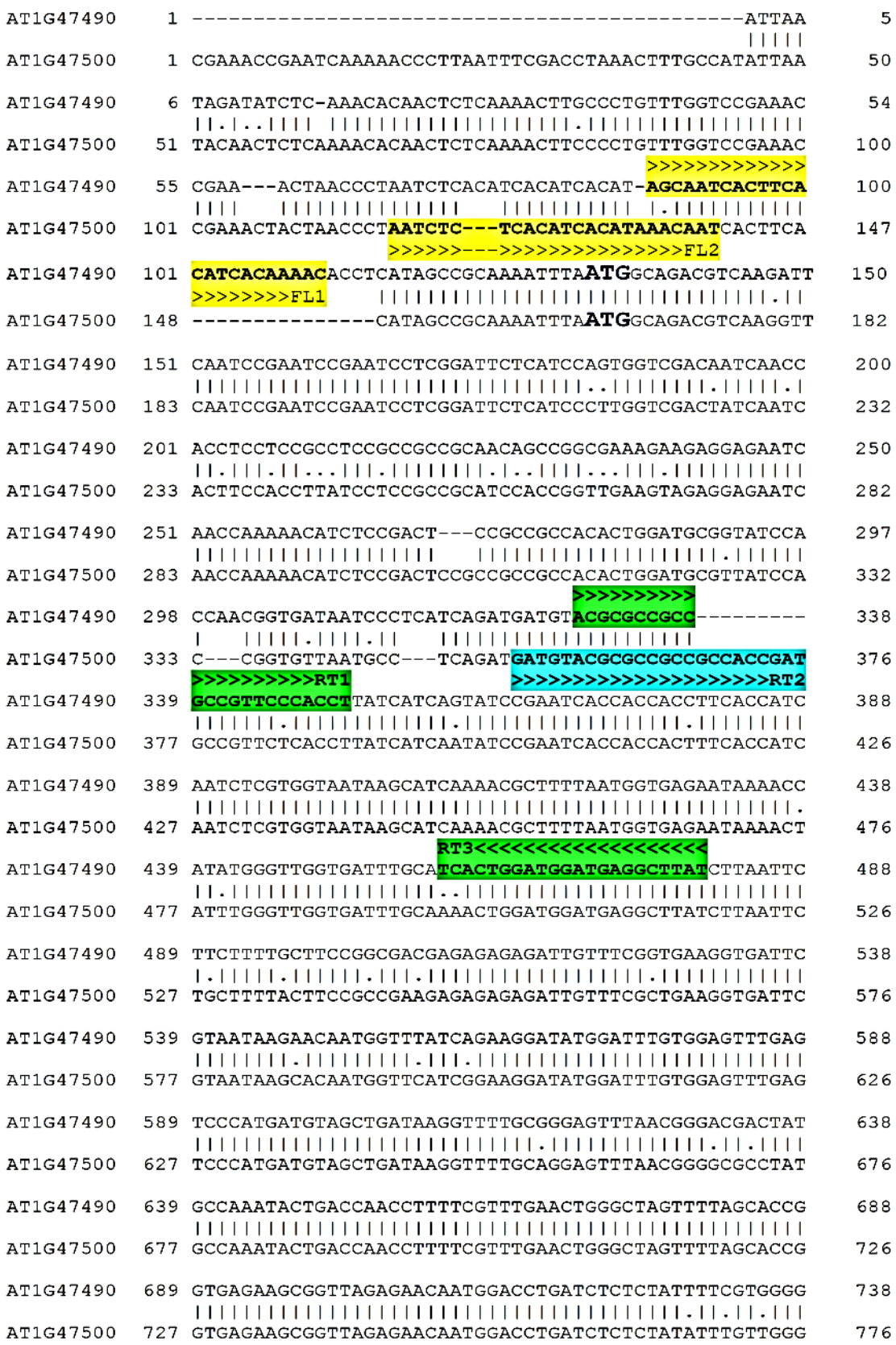
AT1G47490 1 ATTAA 5
AT1G47500 1 CGAAACCGAATCAAAAACCCTTAATTTCGACCTAAACTTTGCCATATTAA 50
AT1G47490 6 TAGATATCTC-AAACACAACTCTCAAAACTTGCCCTGTTTGGTCCGAAAC 54
AT1G47500 51 TACAACTCTCAAAACACAACTCTCAAAACTTCCCCTGTTTGGTCCGAAAC 100
AT1G47490 55 CGAA---ACTAACCCTAATCTCACATCACATCACAT-AGCAATCACTTCA 100
AT1G47500 101 CGAAACTACTAACCCTAATCTC---TCACATCACATAAACAATCACTTCA 147
>>>>>>>>>>>>>
>>>>>>---->>>>>>>>>>>>>>>>>FL2
AT1G47490 101 CATCACAAAACACCTCATAGCCGCAAAATTTAATGGCAGACGTCAAGATT 150
>>>>>>>>FL1
AT1G47500 148 ----------CATAGCCGCAAAATTTAATGGCAGACGTCAAGGTT 182
AT1G47490 151 CAATCCGAATCCGAATCCTCGGATTCTCATCCAGTGGTCGACAATCAACC 200
AT1G47500 183 CAATCCGAATCCGAATCCTCGGATTCTCATCCCTTGGTCGACTATCAATC 232
AT1G47490 201 ACCTCCTCCGCCTCCGCCGCCGCAACAGCCGGCGAAAGAAGAGGAGAATC 250
AT1G47500 233 ACTTCCACCTTATCCTCCGCCGCATCCACCGGTTGAAGTAGAGGAGAATC 282
AT1G47490 251 AACCAAAAACATCTCCGACT---CCGCCGCCACACTGGATGCGGTATCCA 297
AT1G47500 283 AACCAAAAACATCTCCGACTCCGCCGCCGCCACACTGGATGCGTTATCCA 332
>>>>>>>>>>
AT1G47490 298 CCAACGGTGATAATCCCTCATCAGATGATGTACGCGCCGCC---------- 338
AT1G47500 333 C---CGGTGTTAATGCC---TCAGATGATGTACGCGCCGCCGCCACCGAT 376
>>>>>>>>>>RT1
>>>>>>>>>>>>>>>>>>>>>>RT2
AT1G47490 339 GCCGTTCCCACCTTATCATCAGTATCCGAATCACCACCACCTTCACCATC 388
AT1G47500 377 GCCGTTCTCACCTTATCATCAATATCCGAATCACCACCACTTTCACCATC 426
AT1G47490 389 AATCTCGTGGTAATAAGCATCAAAACGCTTTTAATGGTGAGAATAAAACC 438
AT1G47500 427 AATCTCGTGGTAATAAGCATCAAAACGCTTTTAATGGTGAGAATAAAACT 476
RT3<<<<<<<<<<<<<<<<<<<<
AT1G47490 439 ATATGGGTTGGTGATTTGCATCACTGGATGGATGAGGCTTATCTTAATTC 488
AT1G47500 477 ATTTGGGTTGGTGATTTGCAAAACTGGATGGATGAGGCTTATCTTAATTC 526
AT1G47490 489 TTCTTTTGCTTCCGGCGACGAGAGAGAGATTGTTTCGGTGAAGGTGATTC 538
AT1G47500 527 TGCTTTTACTTCCGCCGAAGAGAGAGAGATTGTTTCGCTGAAGGTGATTC 576
AT1G47490 539 GTAATAAGAACAATGGTTTATCAGAAGGATATGGATTTGTGGAGTTTGAG 588
AT1G47500 577 GTAATAAGCACAATGGTTCATCGGAAGGATATGGATTTGTGGAGTTTGAG 626
AT1G47490 589 TCCCATGATGTAGCTGATAAGGTTTTGCGGGAGTTTAACGGGACGACTAT 638
AT1G47500 627 TCCCATGATGTAGCTGATAAGGTTTTGCAGGAGTTTAACGGGGCGCCTAT 676
AT1G47490 639 GCCAAATACTGACCAACCTTTTCGTTTGAACTGGGCTAGTTTTAGCACCG 688
AT1G47500 677 GCCAAATACTGACCAACCTTTTCGTTTGAACTGGGCTAGTTTTAGCACCG 726
AT1G47490 689 GTGAGAAGCGGTTAGAGAACAATGGACCTGATCTCTCTATTTTCGTGGGG 738
AT1G47500 727 GTGAGAAGCGGTTAGAGAACAATGGACCTGATCTCTCTATATTTGTTGGG 776

```
AT1G47490   739 GATTTGTCACCAGATGTTTCGGATAATTTGTTGCACGAGACCTTCTCTGA    788
              |||||||.|.|||||||||||||||..|||||||||||||||||||||||||
AT1G47500   777 GATTTGGCGCCAGATGTTTCGGATGCTTTGTTGCACGAGACCTTCTCTGA    826

AT1G47490   789 GAAGTATCCGTCGGTTAAAGCTGCGAAAGTTGTCCTTGATGCTAATACTG    838
              |||||||||||||||||||||||||.|||||||||||||||||||||||||
AT1G47500   827 GAAGTATCCGTCGGTTAAAGCTGCCAAAGTTGTCCTTGATGCTAATACTG    876

AT1G47490   839 GTAGGTCAAAGGGGTATGGGTTTGTGAGGTTTGGTGATGAGAATGAAAGG    888
              |||||.|||||||||||||||||||||||||||||.|||||||||||||||
AT1G47500   877 GTAGATCAAAGGGGTATGGGTTTGTGAGGTTTGGAGATGAGAATGAAAGG    926

AT1G47490   889 ACCAAAGCAATGACTGAGATGAATGGTGTTAAATGTTCTAGTAGAGCTAT    938
              |||||||||||||||||||||||||||||||||||||.|||||||||||||||
AT1G47500   927 ACCAAAGCAATGACTGAGATGAATGGTGTTAAATGCTCTAGTAGAGCTAT    976

AT1G47490   939 GCGCATCGGTCCTGCTACCCCGAGGAAGACTAATGGTTATCAACAACAAG    988
              |||.|||||||||||||||||.|||||.|||||||||||||||||||||||||
AT1G47500   977 GCGTATCGGTCCTGCTACCCCAAGGAAAACTAATGGTTATCAACAACAAG   1026

AT1G47490   989 GTGGATACATGCCGAATGGTACCTTGACGCGTCCTGAAGGGGACATAATG   1038
              ||||||||||||||||.|||||.|||||.|||||||.|||||||||||||.|||.
AT1G47500  1027 GTGGATACATGCCGAGTGGTGCCTTTACGCGTTCTGAAGGGGACACAATC   1076

AT1G47490  1039 AACACAACAATATTTGTTGGAGGGCTTGACTCTAGTGTCACTGATGAAGA   1088
              ||||||||||||||||||||||||||||||||||||||||||||||||||||||||
AT1G47500  1077 AACACAACAATATTTGTTGGAGGGCTTGACTCTAGTGTCACTGATGAAGA   1126

AT1G47490  1089 CTTAAAGCAACCTTTCAATGAATTCGGGGAAATAGTCTCTGTCAAGATTC   1138
              ||||||||||||||||..||||||||||||||||||.||||||||||||||
AT1G47500  1127 CTTAAAGCAACCTTTCTCTGAATTCGGGGAAATAGTGTCTGTCAAGATTC   1176

AT1G47490  1139 CTGTTGGTAAAGGATGCGGATTTGTTCAGTTTGTTAACAGACCAAATGCA   1188
              ||||||||||||||||||||||||||||||||||||||||||||||||||||||||
AT1G47500  1177 CTGTTGGTAAAGGATGCGGATTTGTTCAGTTTGTTAACAGACCAAATGCA   1226

AT1G47490  1189 GAGGAGGCTTTGGAGAAACTAAATGGGACTGTAATTGGAAAACAAACAGT   1238
              |||||||||||||||.|||||.||||||||||||||||.||||||||||||
AT1G47500  1227 GAGGAGGCTTTGGAAAAACTCAATGGGACTGTAATTGGCAAACAAACAGT   1276

AT1G47490  1239 TCGGCTTTCTTGGGGACGTAATCCCGCCAATAAGCAGCCTAGAGATAAGT   1288
              .|||||||||||||||.||||||||.|||||||||||||||||||||||||||
AT1G47500  1277 CCGGCTTTCTTGGGGCCGTAATCCAGCCAATAAGCAGCCTAGAGATAAGT   1326

AT1G47490  1289 ATGGAAACCAATGGGTTGATCCGTACTATGGAGGACAGTTTTACAATGGG   1338
              ||||||||||||||||||||||||||||||||||||||||||||||||||||||||
AT1G47500  1327 ATGGAAACCAATGGGTTGATCCGTACTATGGAGGACAGTTTTACAATGGG   1376

AT1G47490  1339 TATGGATACATGGTACCTCAACCTGACCCGAGAATGTATCCCGCTGCACC   1388
              ||||||||||||||||||||||||||||||||||||||||||||.||||||||
AT1G47500  1377 TATGGATACATGGTACCTCAACCTGACCCGAGAATGTATCCTGCTGCACC   1426

AT1G47490  1389 TTACTATCCAATGTACGGTGGTCATCAGCAACAAGTTAGCTGAGGAAACT   1438
              ||||||||||||||||||||||||||||||||||||||||||||||||||||||||
AT1G47500  1427 TTACTATCCAATGTACGGTGGTCATCAGCAACAAGTTAGCTGAGGAAACT   1476

AT1G47490  1439 AAAAGCTTAATCTGAGCATCTATCTATAGGACAACAAAAACTCACTCAGG   1488
              ||||||||||||||||||||||||||||||||||||||||||||||||||||||||
AT1G47500  1477 AAAAGCTTAATCTGAGCATCTATCTATAGGACAACAAAAACTCACTCAGG   1526
```

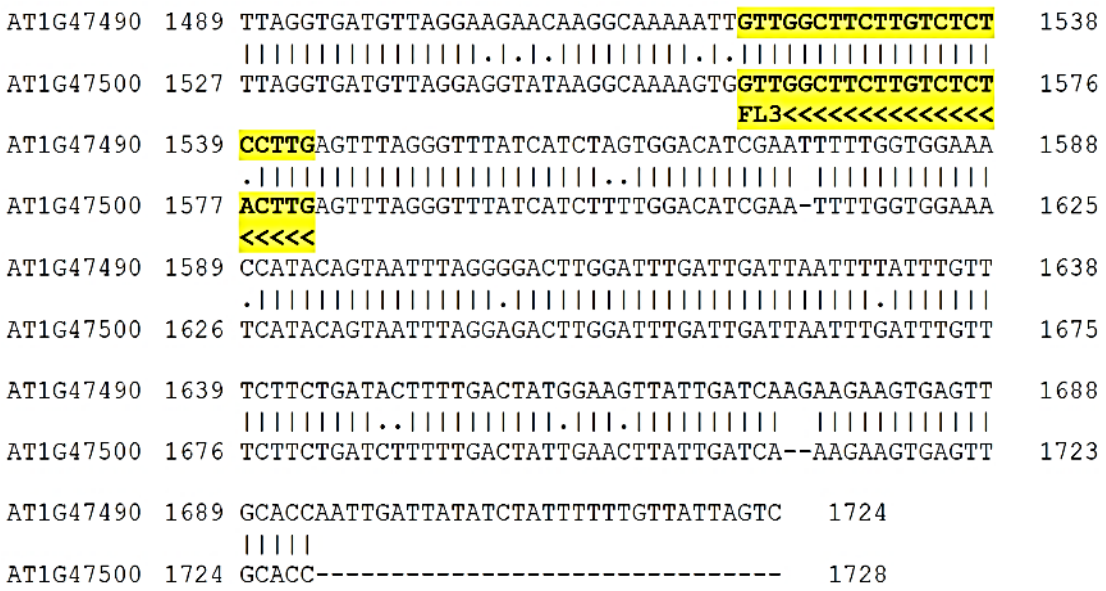

Figure 5-2: Pairwise alignment of nucleotide sequences of At1g47490 (*RBP47C*) and At1g47500 (*RBP47C'*). The nucleotide similarities between the two genes are indicated by vertical lines, dissimilarities are indicated by dots and the gaps indicated by dashes. The figure also shows the location of start codon ATG and stop codon TGA for both genes. The yellow highlighted regions indicate the positions where primers were designed to amplify the fragment containing 45 bp 5' UTR, open reading frame, and 112 bp 3'UTR. Primer pairs FL1 and FL3 were used to amplify *RBP47C* specific fragment for overexpression studies; FL2 and FL3 were used to amplify *RBP47C'* specific fragment. The green (RT1) and cyan (RT2) highlighted regions indicate the position where qPCR forward primers were chosen to differentiate gene expression levels between *RBP47C* and *RBP47C',* respectively. Reverse primer RT3 was used in common along with gene specific forward primers for gene expression analysis.

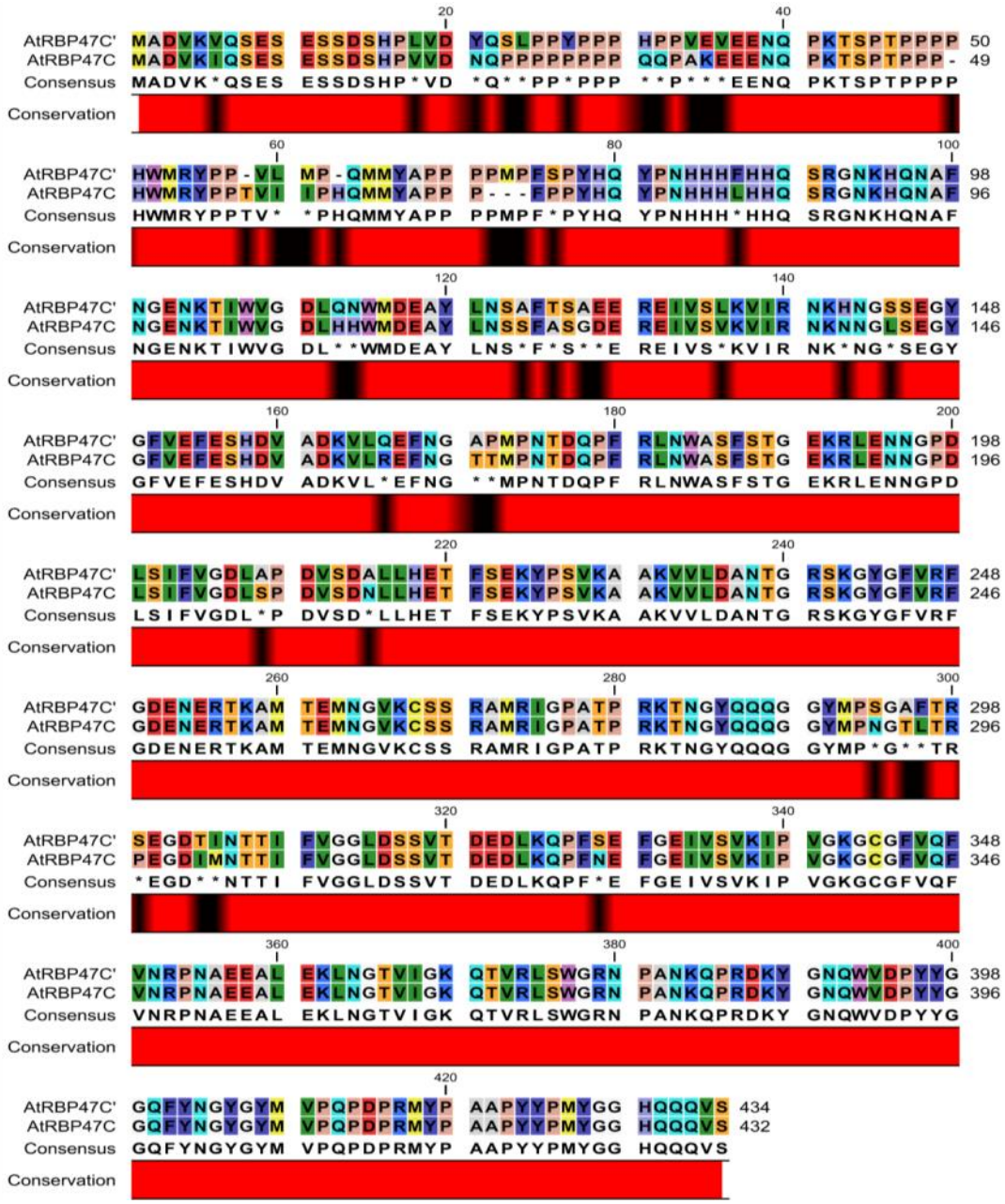

Figure 5-3: Pairwise alignment of amino acid sequences of AtRBP47C' (RBP47C') and AtRBP47C (RBP47C). The amino acid similarities between RBP47C' and RBP47C are indicated by the same color residues, corresponding amino acid residue in the consensus and red band in the conserved region. Dissimilarities are indicated by different amino acid reside colors and * in the consensus region. The gaps are indicated by dashes in the consensus region. Black bands in conserved region indicate dissimilar amino acids or gaps.

5.3.3 Characterization of KN231

The sqPCR results confirmed that the *RBP47C* expression was affected in the mutants (Figure 5-4A). The expression of *RBP47C'* was not affected in the mutants as the gene was found to be amplified from the cDNAs of the mutants (Figure 5-4B).

Leaf and seed carotenoid levels in the mutants KN231, S4 and S8 were determined and compared with WT (Figure 5-5). The levels of two major carotenoids lutein and β-carotene, did not change significantly in the leaf tissues when compared against WT. The level of violaxanthin in the leaf tissues was significantly increased in all three mutants when compared to the WT. However, no significant changes in the leaf tissues were observed in zeaxanthin levels between the three mutants and WT. All the four carotenoids measured in the mature seed of three mutants were significantly higher when compared to the WT. Each carotenoid in three mutants was increased two-fold in comparison to the WT carotenoid levels.

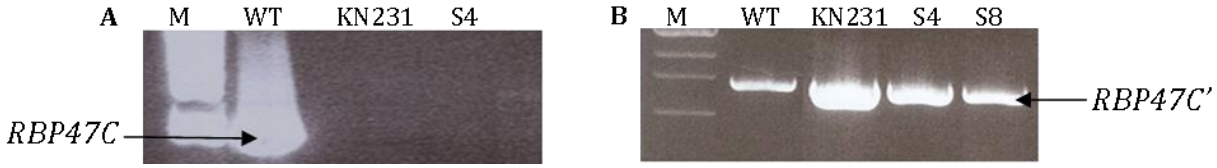

Figure 5-4: Confirmation of *RBP47C* knockout in the Arabidopsis mutants KN231, S4 and S8. A) *RBP47C* specific band visible in the WT but absent in the mutants. The gel was overexposed to confirm absence of *RBP47C* expression in the mutants. B) *RBP47C'* is expressed in the leaf tissues of WT and all mutants, indicating its gene expression was not affected. M, 100 bp ladder; WT, wild-type.

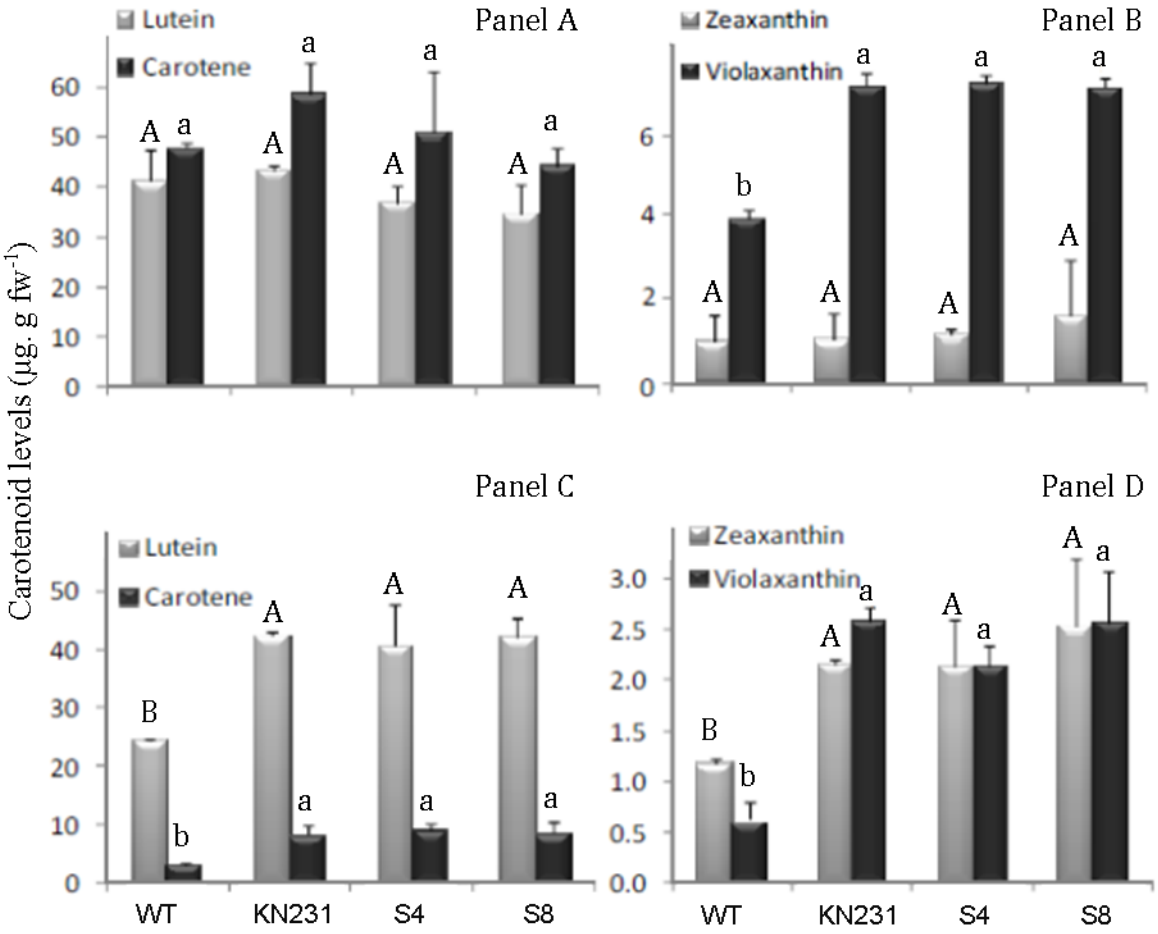

Figure 5-5: Carotenoid composition of WT Arabidopsis and mutant lines KN231, S4 and S8. Carotenoids were determined in 2-week-old leaves (A, B) and mature seeds (C, D). Values represent means ± SD (n = 3) and are expressed on a fresh weight (fw) basis. Different letters within each panel (uppercase for lutein and zeaxanthin; lower case for β-carotene and violaxanthin) indicate statistical significance at $p < 0.05$.

5.3.4 Expression of carotenoid biosynthetic genes in leaves and seeds of mutants

To examine changes in carotenoid levels observed in leaves and seeds of the three mutants, the expression profile of genes involved in carotenoid biosynthesis was determined (Figure 5-6 and Figure 5-7). The qPCR results with the leaves indicated a significant increase in the expression of genes encoding, *ZDS*, *βLYC* in all three mutants compared to the WT. The increase in the *βLYC* transcripts in the three mutants, KN231, S4 and S8, was 3.5-, 2.2- and 2.2-fold, respectively, compared to the WT. The increase in *ZDS* transcript levels in three mutants,

KN231, S4 and S8, was 1.8-, 2.5- and 1.8-fold, respectively. Excluding *ZDS* and *βLYC*, each mutant had a unique expression profile for other carotenoid genes. Mutant KN231 had significantly increased levels of genes *PDS* and *ZEP* and mutant S4 had significantly reduced expression levels of genes *εLYC*, *εHYD* and *VDE*, while mutant S8 displayed a significant increase in the transcript levels of *ZEP* when compared to the WT.

The expression profile of carotenoid biosynthetic genes in mature seeds of the mutants and the WT showed that the expression of two genes namely, *ZDS* and *εLYC*, were increased significantly. However, each mutant line had an independent expression profile for other carotenoid genes when compared with the WT. Mutant KN231 had significantly decreased levels of *βHYD* compared, while mutant S4 displayed significantly increased levels of *βLYC*, *βHYD*, *εHYD* and *VDE* compared to the WT. Mutant S8 displayed significantly lower expression levels for genes *PSY*, and *βHYD* and significantly increased expression for genes *PDS* and *εHYD* when compared to the WT.

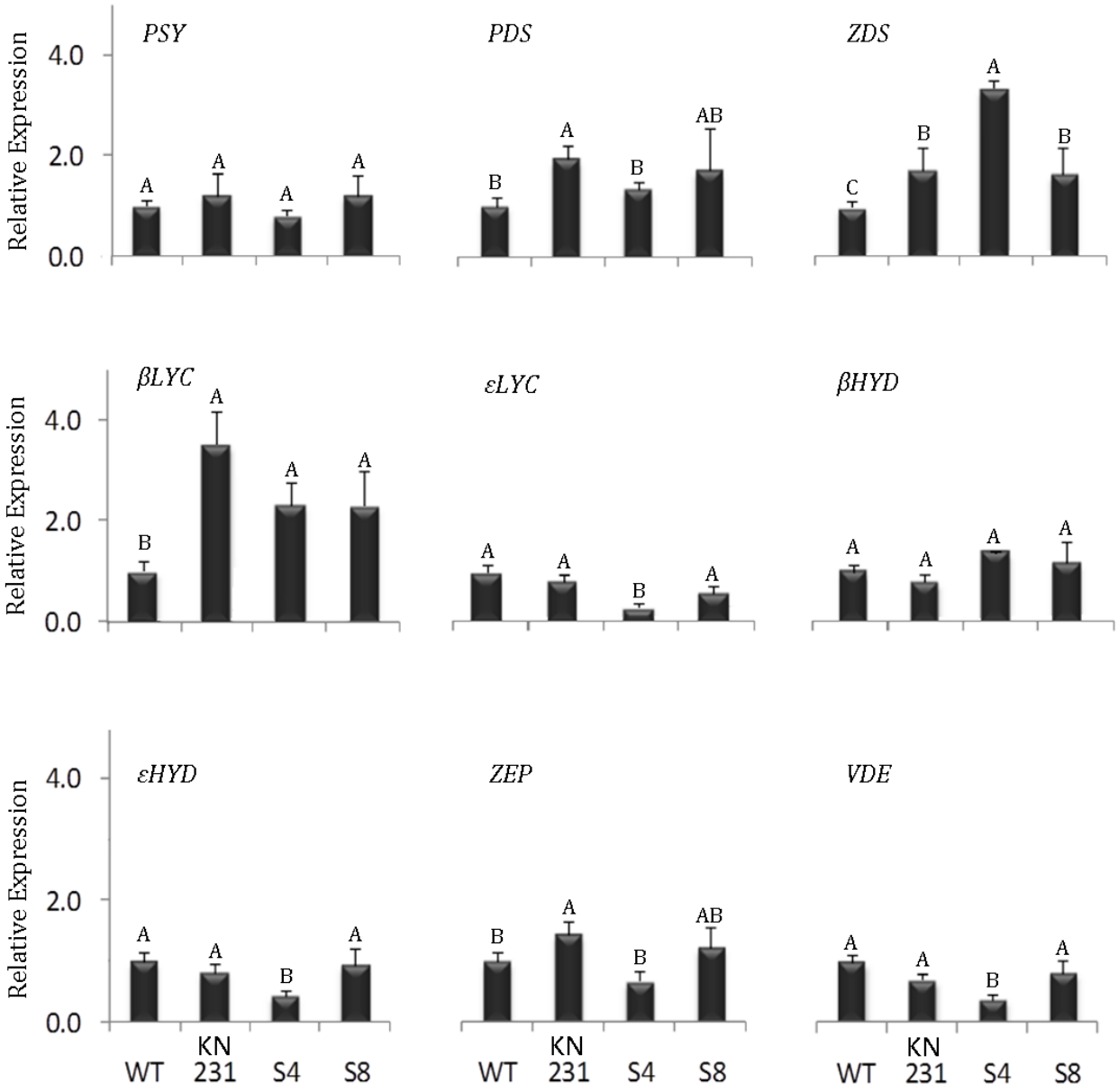

Figure 5-6: Expression of carotenoid biosynthetic genes in 2-week-old leaves of WT Arabidopsis and mutant lines KN231, S4 and S8. The expression levels are normalized to the reference gene *PEX4* and relative to the WT set to a value of 1. Values represent means ± SD (n = 3). Different letters within genes indicate statistical significance at $p < 0.05$. *PSY*, phytoene synthase; *PDS*, phytoene desaturase; *ZDS*, ζ-carotene desaturase; *βLYC*, β-lycopene cyclase; *εLYC*, ε-lycopene cyclase; *βHYD*, β-ring hydroxylase; *εHYD*, ε-ring hydroxylase; *ZEP*, zeaxanthin epoxidase; *VDE*, violaxanthin de-epoxidase.

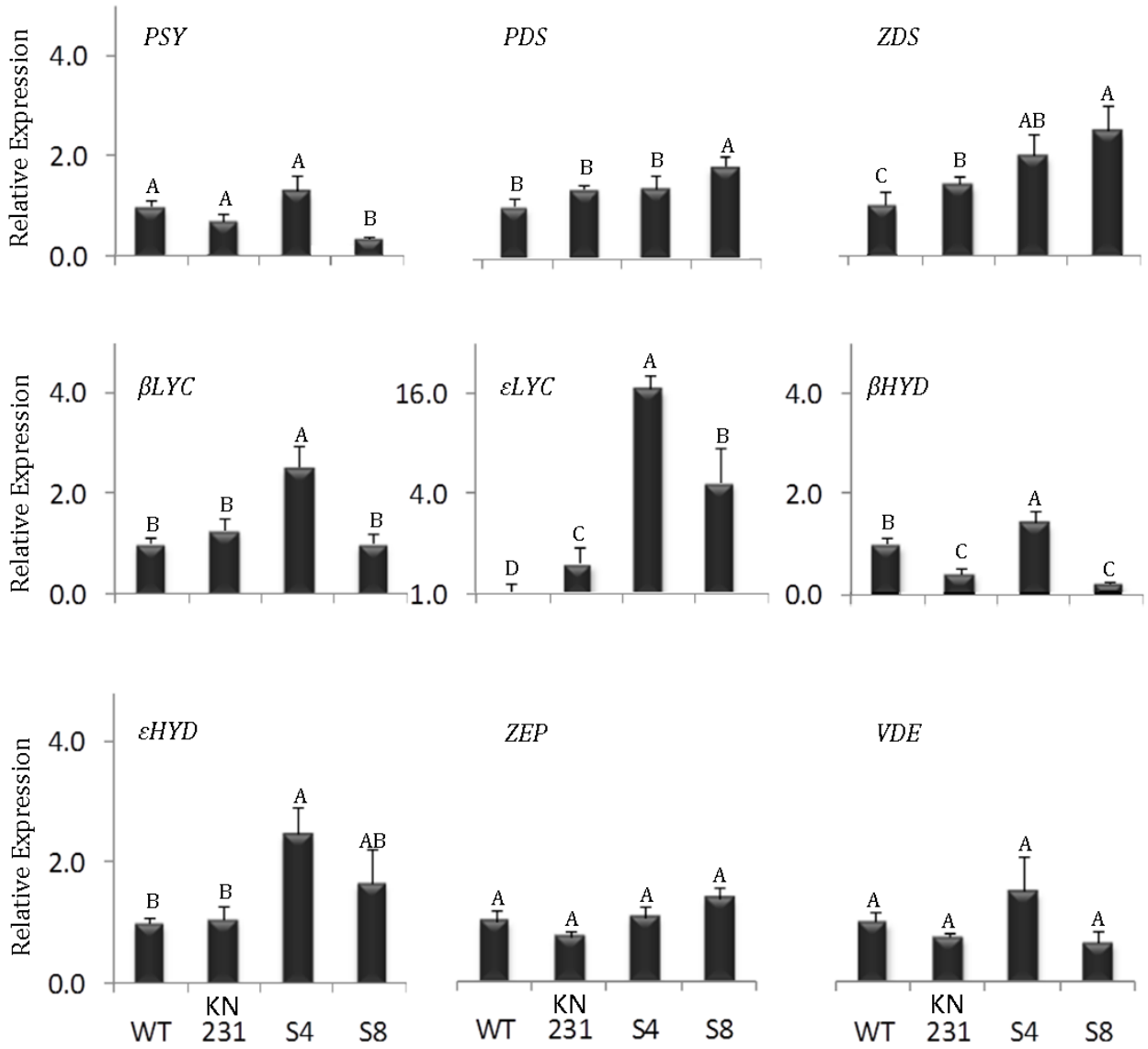

Figure 5-7: Expression of carotenoid biosynthetic genes in mature seeds of WT Arabidopsis and mutant lines KN231, S4 and S8. The expression levels are normalized to the reference gene *PEX4* and relative to the WT set to a value of 1. Values represent means ± SD (n = 3). Different letters within genes indicate statistical significance at $p < 0.05$. *PSY*, phytoene synthase; *PDS*, phytoene desaturase; *ZDS*, ζ-carotene desaturase; *βLYC*, β-lycopene cyclase; *εLYC*, ε-lycopene cyclase; *βHYD*, β-ring hydroxylase; *εHYD*, ε-ring hydroxylase; *ZEP*, zeaxanthin epoxidase; *VDE*, violaxanthin de-epoxidase.

5.3.5 Expression of *RBP47C* and *RBP47C'* in Arabidopsis tissues

To determine the expression profile of *RBP47C* across seed developmental stages, a developmental map microarray data set for At1g47490 was imported from the Arabidopsis eFP browser (http://bar.utoronto.ca/efp_arabidopsis/cgi-bin/efpWeb.cgi) and the values were charted in Figure 5-8. The data set indicates that the *RBP47C* is expressed in all seed development stages. The data set indicated the highest level of *RBP47C* gene expression was found in 24 h imbibed seed followed by mature seed. However, its expression levels are substantially lower at stage 7 of the seed development just before maturation of the seed. Furthermore, the data set represents a microarray analysis therefore, the *RBP47C* transcripts could be contaminated by the *RBP47C'* transcripts.

In order to confirm the microarray data set and determine the individual transcripts levels for both *RBP47C* and *RBP47C'*, qPCR analysis using unique primer pairs was performed (Figure 5-9). The qPCR results indicated that both genes were expressed in all tissues analyzed, except in stems. Mature seeds had the highest level of *RBP47C* transcripts and the highest transcript level for *RBP47C*' transcripts were observed in stage 4 (10-12 DAP) seed development. The expression level for both genes was similar in leaves, flower buds, and flowers. *RBP47C* expression was significantly higher in the roots compared to other vegetative tissues and flowers. However, the expression level of *RBP47C*' in roots was similar to other vegetative tissues and flowers. The transcripts of *RBP47C* and *RBP47C*' generally increased in siliques during seed development. The transcripts of *RBP47C* and *RBP47C*' in the siliques increased gradually until stage 4 (10-12 DAP). Interestingly, during stage 5 (13-15 DAP) the transcript levels of *RBP47C* and *RBP47C*' reduced rapidly to the levels of stage1 (1-3 DAP) siliques just before seed maturation. *RBP47C* transcript levels were 16-fold higher in mature seeds compared to the leaves. Similarly expression of *RBP47C*' reached 16-fold in stage 4 (10-12 DAP) siliques compared to the leaf tissue. The reason behind the sudden reduction in the gene expression or transcripts of *RBP47C* and *RBP47C*' in the stage 5 siliques needs further investigation.

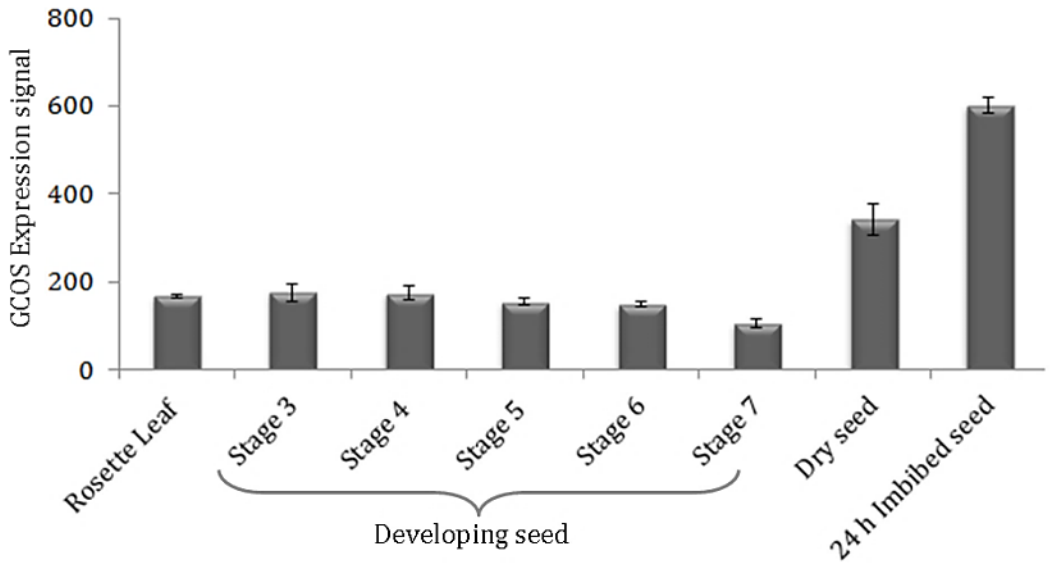

Figure 5-8: *In silico* expression profile of *RBP47C* in WT Arabidopsis tissues and seed development stages. The expression levels are relative to the rosette leaf set to a value of 1. The error bars indicate SD. The data was extracted from the Arabidopsis eFP browser at bar.utoronto.ca. The developing seed stages given are not indicative of the seed development stages given in Figure 5-9.

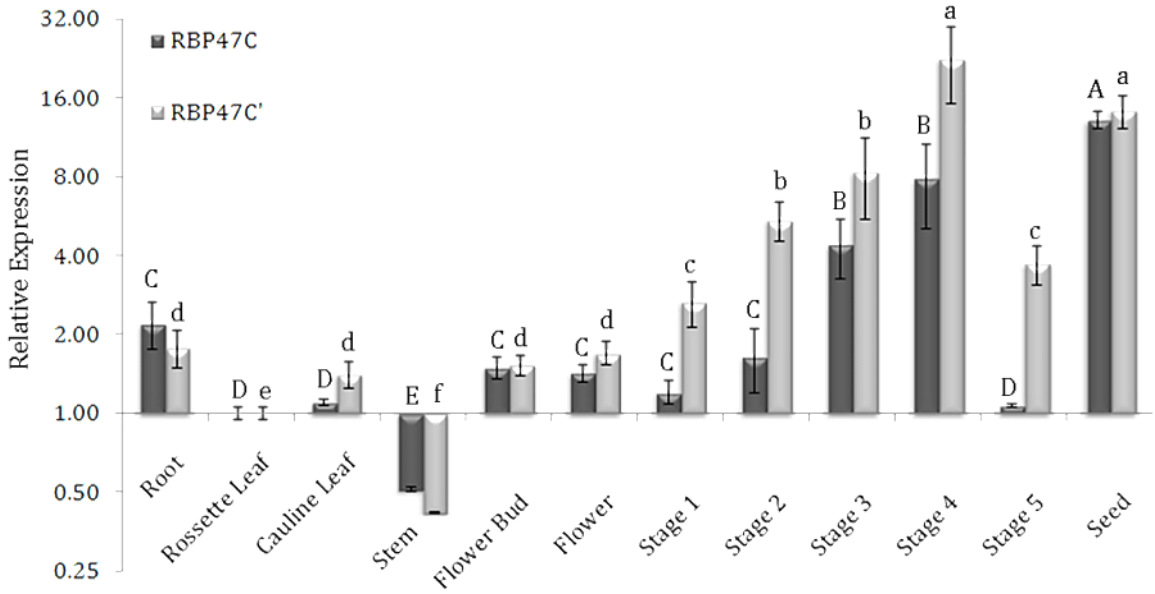

Figure 5-9: Expression profile of *RBP47C* and *RBP47C'* in Arabidopsis tissues and seed developmental stages. The expression levels are normalized to the reference gene *PEX4* and relative to the rosette leaf set to a value of 1. Values represent means ± SD (n = 3). Different letters (uppercase for *RBP47C*; lowercase for *RBP47C'*) indicate statistical significance at $p < 0.05$.Stage 1, 1-3 DAP; Stage 2, 4-6 DAP; Stage 3, 7-9 DAP; Stage 4, 10-12 DAP; Stage 5, 13-15 DAP.

5.3.6 Carotenoid biosynthetic gene expression in WT siliques

RBP47C and *RBP47C'* are expressed at higher levels in the siliques and mature seeds than vegetative tissues. Initial carotenoid biosynthetic gene expression analysis on KN231 and its allelic Salk mutants indicated that *ZDS*, and *βLYC* transcriptswere significantly increased in the leaf tissues of mutants. Similarly, *ZDS* and *εLYC* expressions were significantly increased in the mature seeds of mutants. The *RBP47C* expression during seed development displayed significantly lower expressions between stage 1 and stage 5 compared to stages 3 and 4 (Figure 5-9). As the tissues being relatively similar and distinct changes in the *RBP47C* expression was observed, the expression of carotenoid biosynthetic genes in various siliques stages were determined (Figure 5-10).

The expression of carotenoid genes did not change significantly among stage 2, 3 and 4 siliques. The seed developmental stages 1 and 5 and mature seeds displayed varying expression profiles. *PSY* and *εLYC* expression increased significantly in stage 1 and stage 5 siliques compared to other siliques stages and mature seeds, while expression of *PSY* and *εLYC* was significantly reduced in the mature seed tissue compared to all silique tissues analyzed. Similarly, *PDS* and *εHYD* expression was increased significantly in both stage 1 and stage 5 siliques when compared to siliques in other stages and mature seeds.

The expression of *βLYC* was similar among the silique stages 1, 5 and the mature seeds, however was significantly higher compared to the other silique stages. The expression profile of *βHYD* showed the highest expression in the stage 1 siliques and its transcripts levels were significantly lower in the mature seed stage when compared to the other silique stages. The expression of *ZEP* was significantly increased in the stage 5 and mature seed compared to other silique stages.

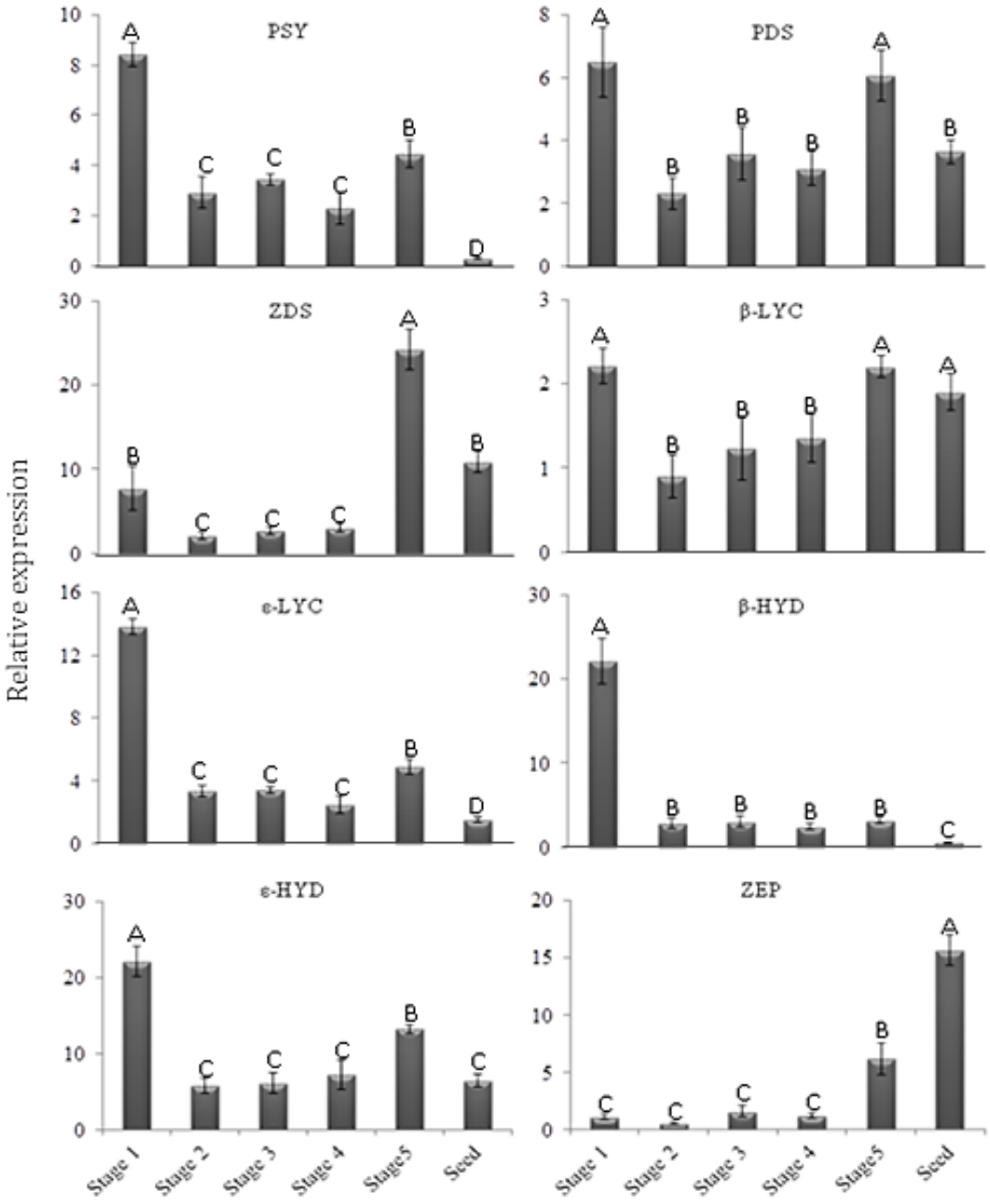

Figure 5-10: Expression of carotenoid biosynthetic genes in Arabidopsis silique developmental stages. The expression levels are normalized to the reference gene *PEX4* and relative to the WT leaf (data shown in Figure 5-9) set to a value of 1. Values represent means ± SD (n = 3). Different letters within panels indicate statistical significance at $p < 0.05$. Stage 1, 1-3 DAP; Stage 2, 4-6 DAP; Stage 3, 7-9 DAP; Stage 4, 10-12 DAP; Stage 5, 13-15 DAP; *PSY*, phytoene synthase; *PDS*, phytoene desaturase; *ZDS*, ζ-carotene desaturase; *βLYC*, β-lycopene cyclase; *εLYC*, ε-lycopene cyclase; *βHYD*, β-ring hydroxylase; *εHYD*, ε-ring hydroxylase; *ZEP*, zeaxanthin epoxidase.

5.3.7 Overexpression of *RBP47C* in mutants KN231, S4 and S8

The mutant KN231 and allelic Salk mutant lines S4 and S8 were transformed with an *RBP47C* open reading frame driven by the CaMV 35S promoter. The CaMV 35S promoter was selected due to the high sequence similarities in the promoter regions of *RBP47C* and *RBP47C'*. Six lines were obtained upon transformation of mutant KN231 line, eight for Salk mutant S4 and ten for Salk mutant S8. The growth characteristics of the overexpression lines did not have observable changes or phenotypes compared to WT or non-transformed lines.

The expression profile of *RBP47C* in the overexpression lines of mutants KN231, S4 and S8 were determined using qPCR (Figure 5-11). The expression of *RBP47C* in the overexpression mutant 231-C-1 was significantly lower compared to the WT. The overexpression mutants 231-C-2, 231-C-5 and 231-C-6 had significant increase in *RBP47C* expression. The overexpression lines of mutant S4 had *RBP47C* expression similar to that of WT in the case of S4-C-5 and significantly increased expression ranging from 4 to 64 fold in other overexpression lines. Similarly, the *RBP47C* expression was also higher in 8 out of 10 overexpression lines of S8. One overexpression mutant S8-C-5 had significantly lower *RBP47C* expression and S8-C-9 *RBP47C* expression was similar to the WT. Together the expression profile indicates a wide range of expression profile among the overexpression mutants of KN231, S4 and S8. This increased fold expression of *RBP47C* could be due to the constitutive CaMV 35S promoter. The analysis was done using qPCR using primers from the first exon; therefore, a possibility of the amplicons from the non-functional copy of the mutant *RBP47C* gene might also be present. Additionally, the overexpression mutants displaying *RBP47C* expression similar to WT levels could be due to post- transcriptional silencing mechanism as observed in 231-C-1 and S8-C-5.

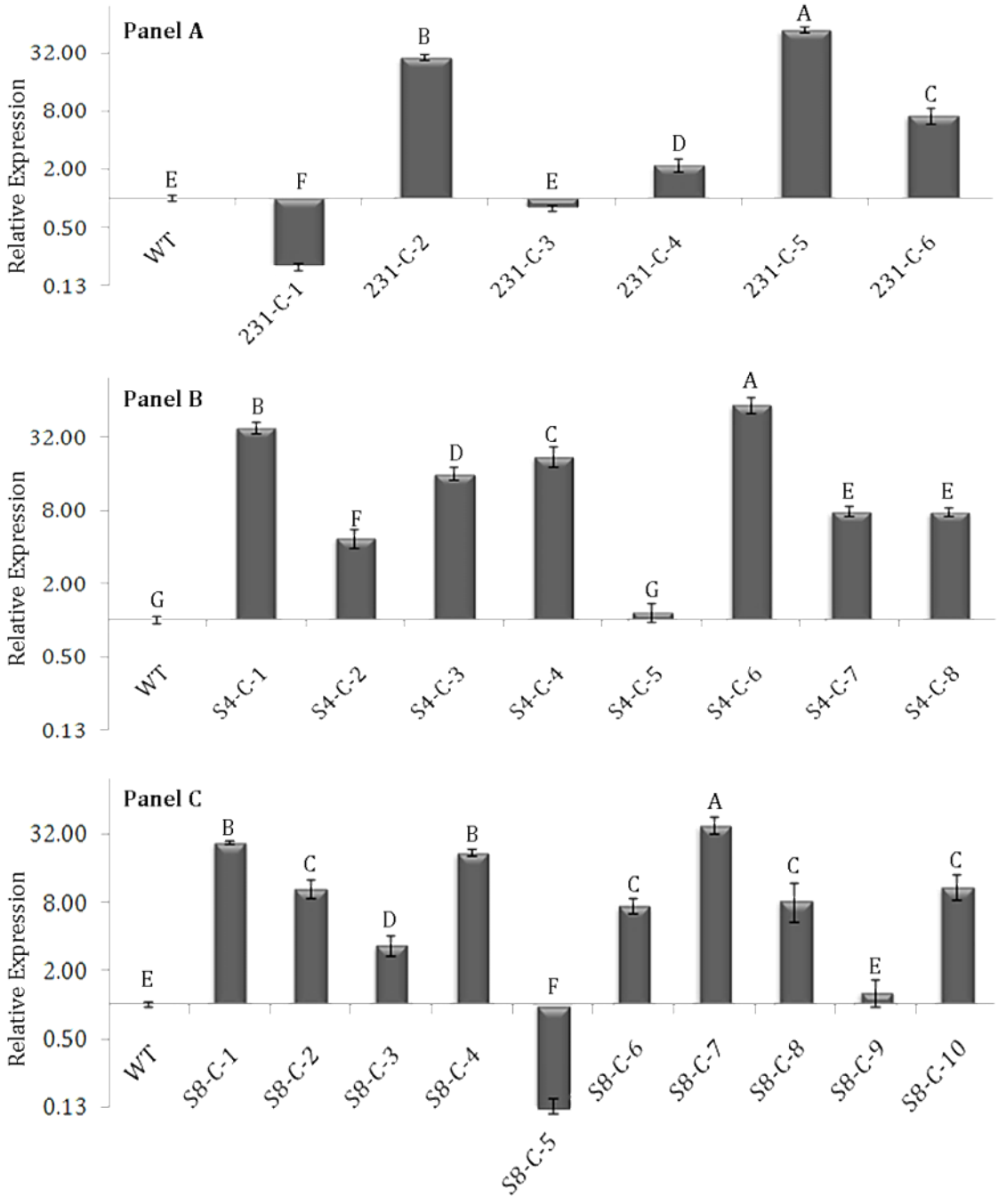

Figure 5-11: Expression of *RBP47C* in 14-day-old leaves of Arabidopsis WT and overexpression mutant lines KN231 (A), S4 (B) and S8 (C). The expression levels are normalized to the reference gene *PEX4* and relative to the WT set to a value of 1. Values represent means ± SD (n = 3). Different letters within panels indicate statistical significance at $p < 0.05$.

5.3.8 Carotenoid analysis of overexpression mutant lines of KN231, S4 and S8

Leaf and seed carotenoid analysis for the mutant KN231 and the overexpression lines is shown in Figure 5-12 and Figure 5-13, respectively. The leaf carotenoid analysis indicates that overexpression lines 231-C-2 and 231-C-5 had the lowest lutein, β-carotene and violaxanthin levels compared to the WT and the mutant KN231. These two lines also showed the highest levels of *RBP47C* expression in the overexpression lines. The overexpression mutant 231-C-1 had the highest level of β-carotene but significantly lower zeaxanthin content compared to the other lines. The expression of *RBP47C* in the 231-C-1 mimicked that of the mutant with affected *RBP47C* expression (Figure 5-11). The mutants 231-C-3 and 231-C-4 had similar levels of carotenoids between them, however was significantly lower than WT and mutant KN231. The overexpression line 231-C-3 had *RBP47C* expression levels similar to that of WT; however it should be noted that the qPCR primers are located in the first exon and therefore the expression observed could be leaky expression from the mutant (Figure 5-1C).

The seed carotenoid analysis indicated that the mutant KN231 had significantly higher levels of lutein, β-carotene, violaxanthin and zeaxanthin compared to the WT (Figure 5-13). The overexpression mutants 231-C-1 and 231-C-3 displayed similar levels of lutein, violaxanthin and zeaxanthin compared to the mutant KN231. The other three lines 231-C-2, 231-C-5 and 231-C-6 had similar levels of lutein and violaxanthin compared to the WT. The lutein and violaxanthin levels were similar to WT in three of four overexpression mutants. The β-carotene levels were significantly lower in four of five overexpression mutants. The zeaxanthin levels were similar to the mutant in three of five overexpression mutants. The carotenoid analysis indicated that at least three overexpression mutants 231-C-2, 231-C-5 and 231-C-6 have been reverted very close to the WT seed carotenoid phenotype.

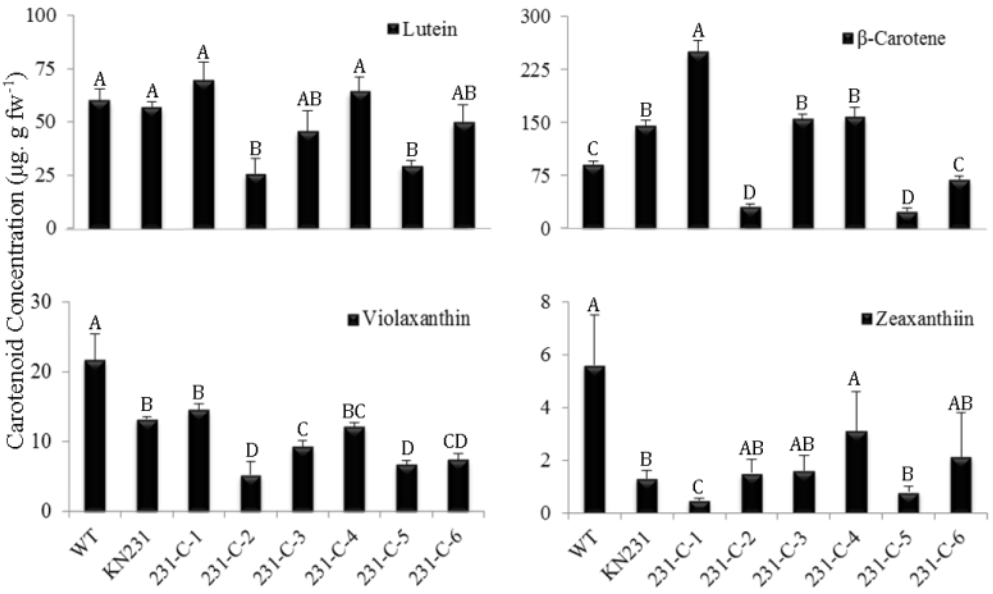

Figure 5-12: Carotenoid composition in 14-day-old leaves of WT Arabidopsis, mutant KN231 and its overexpression lines. Values represent means ± SD (n = 3) and are expressed on a fresh weight (fw) basis. Different letters within each panel indicate statistical significance at $p < 0.05$.

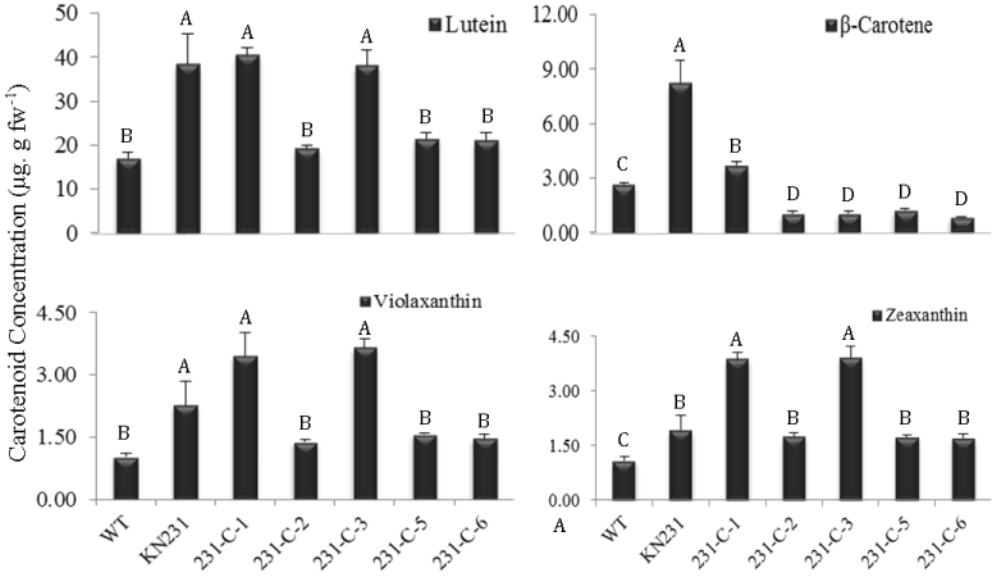

Figure 5-13: Carotenoid composition in mature seed of WT Arabidopsis, mutant KN231 and its overexpression lines. Values represent means ± SD (n = 3) and are expressed on a fresh weight (fw) basis. Different letters within each panel indicate statistical significance at $p < 0.05$.

Eight overexpression S4 mutants were successfully recovered after transformation of mutant S4 with a constitutively expressed *RBP47C* gene. The carotenoid analysis on leaves (Figure 5-14) and mature seeds (Figure 5-15) were performed to determine the effect of complementation on carotenoid levels. The leaf carotenoid analysis indicated that two overexpression mutants S4-C-7 and S4-C-8 had significantly higher levels of lutein, β-carotene and zeaxanthin compared to WT and S4 (Figure 5-14). Another overexpression mutant S4-C-1 had significantly lower levels of lutein compared to WT and S4. However, seven of eight overexpression lines, except for S4-C-1, displayed significantly higher levels of β-carotene compared to the WT and S4. Similarly six of eight overexpression lines except for S4-C-5 and S4-C-7 had significantly lower levels of zeaxanthin compared to the WT and the mutant. The violaxanthin levels in the overexpression lines did not change significantly when compared with WT or the mutant S4, but five lines were closer to WT levels (Figure 5-14).

The mature seed carotenoid analysis indicated that the mutant S4 had significantly higher levels of lutein, β-carotene and violaxanthin. Two complementary lines S4-C-1 and S4-C-2 had similar lutein levels to the mutant S4 (Figure 5-15). Five of eight overexpression lines had lutein levels significantly lower than the WT except for one overexpression mutant S4-C-8, which has similar levels of lutein compared to WT and the mutant S4. The β-carotene level in the mutant S4 was significantly higher compared to the WT. All the overexpression lines displayed significantly lower levels of β-carotene compared to both the WT and the mutant S4 (Figure 5-15). No significant difference in the zeaxanthin levels were determined between the mutant S4 and the WT due to high variability, but six overexpression lines had WT levels of zeaxanthin. The violaxanthin levels were significantly higher in the mutant S4 compared to the WT. Similarly two complementary mutants S4-C-1 and S4-C-2 also had significantly higher violaxanthin levels compared to WT. The other overexpression lines did not have significant difference in their violaxanthin levels compared to the WT, however were significantly lower compared to the S4 mutant (Figure 5-15).

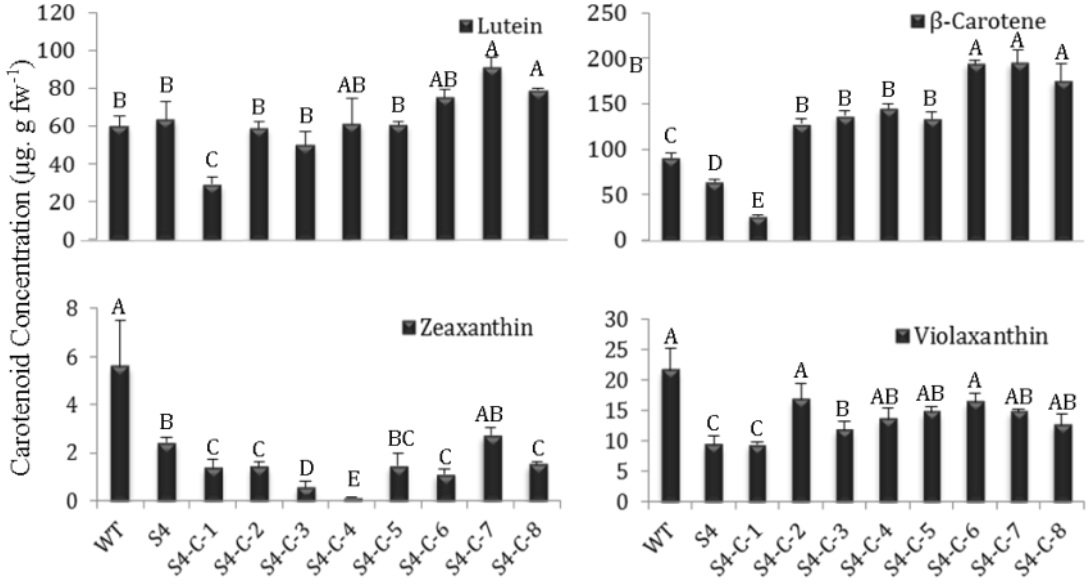

Figure 5-14: Carotenoid composition in 14-day-old leaves of WT Arabidopsis, mutant S4 and its overexpression lines. Values represent means ± SD (n = 3) and are expressed on a fresh weight (fw) basis. Different letters within each panel indicate statistical significance at $p < 0.05$.

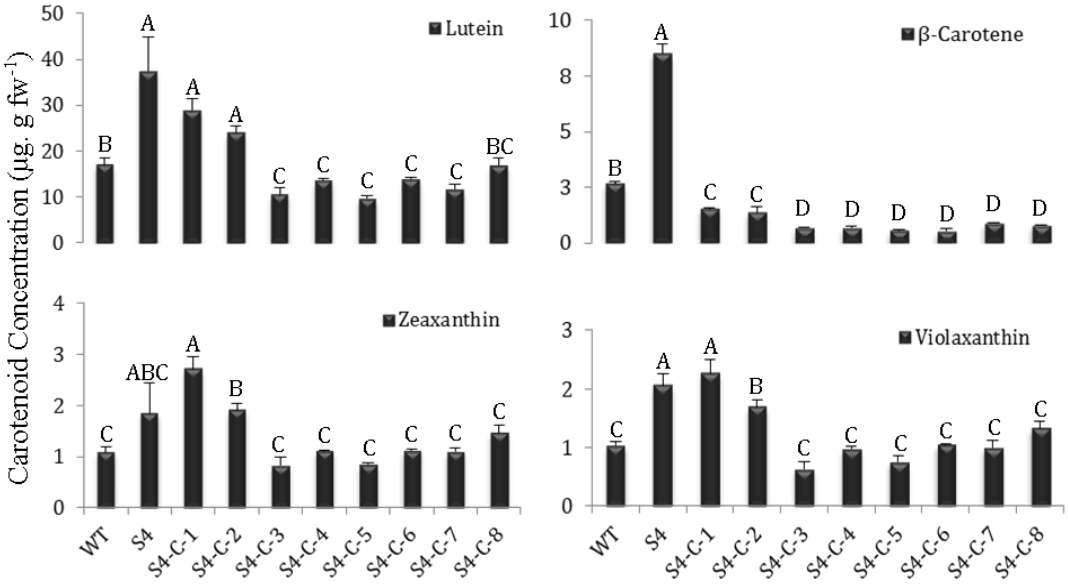

Figure 5-15: Carotenoid composition in mature seed of WT Arabidopsis, mutant S4 and its overexpression lines. Values represent means ± SD (n = 3) and are expressed on a fresh weight (fw) basis. Different letters within each panel indicate statistical significance at $p < 0.05$.

Ten complimented lines were recovered from *Agrobacterium*-mediated transformation of mutant S8 with a T-DNA containing the constitutively expressed *RBP47C* gene driven by a 35S promoter. The carotenoid analyses on the leaf and seed tissues were performed to determine the reversal of the carotenoid phenotype in the overexpression mutant lines due to the functional *RBP47C* gene. The leaf and seed carotenoid analysis results are given in Figure 5-16 and

Figure 5-17, respectively. The results obtained were then statistically compared with S8 and WT.

The leaf carotenoid analysis indicated that S8 and WT had similar levels of lutein, β-carotene, and zeaxanthin. Eight of ten overexpression lines had significantly higher lutein levels, except for S8-C-9 and S8-C-10 which had lutein levels similar to WT and the mutant S8. Nine out of ten overexpression lines also had significantly higher levels of β-carotene compared to the WT and mutant S8. Only S8-C-10 overexpression mutant alone had β-carotene levels similar to the WT and mutant S8. The zeaxanthin levels in the overexpression lines indicated that seven of ten lines had significantly lower zeaxanthin levels compared to the WT and mutant S8. Two overexpression mutants S8-C-3 and S8-C-8 had zeaxanthin levels similar to WT and significantly higher than the mutant S8. The overexpression mutants S8-C-9 had zeaxanthin levels intermediate to the mutant S8 and the other overexpression mutants. The violaxanthin level in the mutant S8 was significantly lower compared to the WT. Seven of ten overexpression lines had violaxanthin levels similar to the WT and significantly higher than mutant S8. One overexpression mutant S8-C-8 had significantly higher levels of violaxanthin compared to the WT and the mutant S8. Another overexpression mutant S8-C-9 had violaxanthin levels similar to both WT and mutant S8. The final mutant S8-C-10 had violaxanthin levels similar to the mutant S8.

The mature seed carotenoid analysis indicated that the mutant S8 had significantly higher levels of lutein, β-carotene, and violaxanthin. Only eight of the ten overexpression lines could grow to full maturity to produce enough seeds for carotenoid analysis. Four of eight overexpression mutant lines had significantly higher levels of lutein compared to the WT, but similar to mutant S8. Two overexpression lines S8-C-5 and S8-C-9 had significantly higher levels of lutein compared to mutant S8 and WT. The RBP47C expression in the complementary line S8-C-5 was significantly lower than WT levels mimicking the mutant and another line S8-C-9 had RBP47C expression levels similar to WT. However, due to the nature of the qPCR primers

the levels may not represent the overexpression construct. The remaining two overexpression lines S8-C-2 and S8-C-3 had lutein levels significantly lower compared to S8 but significantly higher than WT lutein levels. The β-carotene levels in the overexpression lines were significantly lower compared to the mutant S8. However, only four of eight overexpression lines had β-carotene levels similar to the WT. Two overexpression mutants S8-C-1 and S8-C-7 had β-carotene levels significantly lower compared to the WT. The other two overexpression mutants S8-C-5 and S8-C-9 had significantly higher β-carotene levels compared to the WT but significantly lower than the mutant S8. The zeaxanthin levels in the overexpression lines did not change significantly compared to the mutant S8 and WT except for S8-C-5 and S8-C-9 which had significantly higher zeaxanthin levels compared to both S8 and WT. The violaxanthin levels in the complementary lines mirrored that of the zeaxanthin profile, with overexpression lines S8-C-5 and S8-C-9 having violaxanthin levels significantly higher than both S8 and the WT.

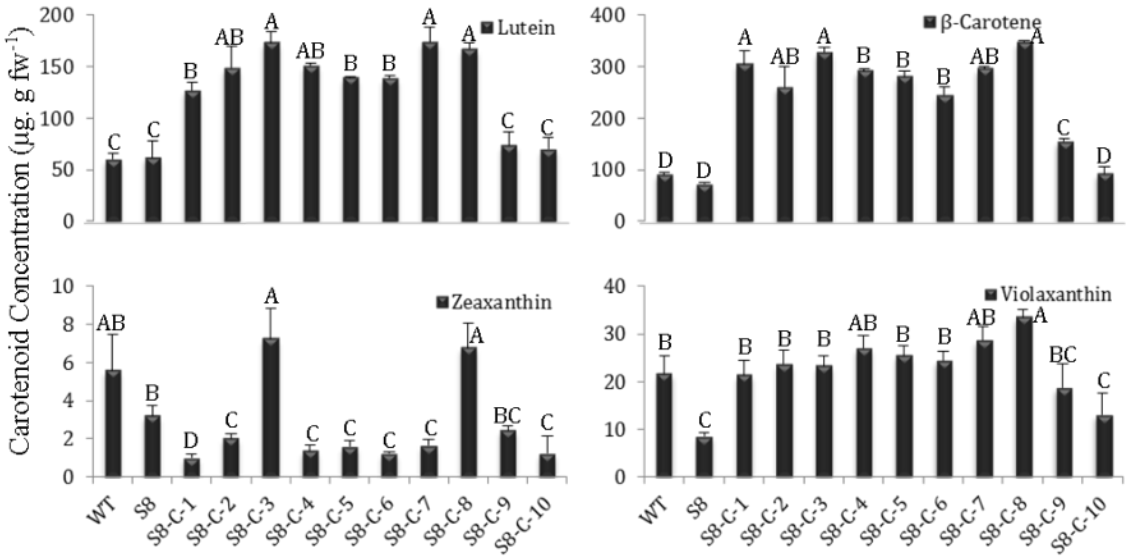

Figure 5-16: Carotenoid composition in 14-day-old leaves of WT Arabidopsis, mutant S8 and its overexpression lines. Values represent means ± SD (n = 3) and are expressed on a fresh weight (fw) basis. Different letters within each panel indicate statistical significance at $p < 0.05$.

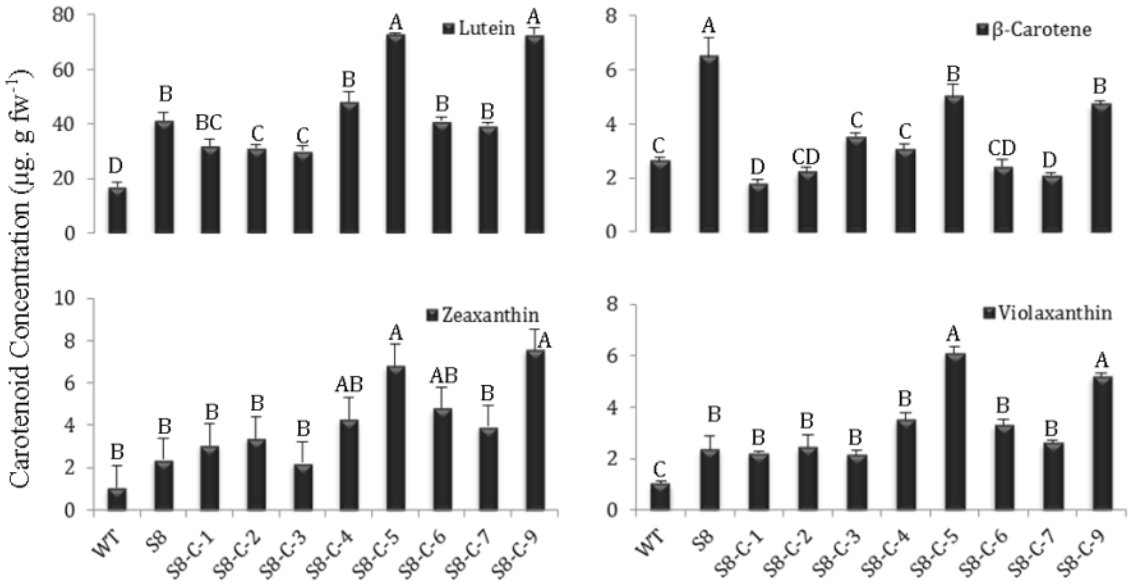

Figure 5-17: Carotenoid composition in mature seed of WT Arabidopsis, mutant S8 and its overexpression lines. Values represent means ± SD (n = 3) and are expressed on a fresh weight (fw) basis. Different letters within each panel indicate statistical significance at $p < 0.05$.

5.3.9 Bioinformatic analysis of RNA binding proteins in Arabidopsis

A search in National Center for Biotechnology Information (NCBI) and ABRC databases was performed to identify putative RNA binding proteins (RBPs) similar to RBP47C in the Arabidopsis genome. A total of 11 genes harboring more than one RNA recognition motifs (RRM) similar to RBP47C were identified. The genes encoding the 11 RBPs are spread across the genome, and at least one is present on 4 chromosomes, except chromosome 2 (Figure 5-18). Chromosome 1 contained five RBPs and three of them belonged to the ATRBP47 class proteins. No RBP gene was found in the genomes of mitochondria or chloroplast; this indicates that RBP encoding genes are nucleus-specific.

To determine the evolutionary relationship of the various RBPs in Arabidopsis, bootstrap cluster analysis was performed using DNA STAR. The tree indicated that the RBPs arose by duplication of a common progenitor that gave rise to AtRBP45 and another ancestral gene that through subsequent duplications and neo-functionalization events gave rise to the group that expanded to form the main cluster. (Figure 5-19A). The tree also indicates three different classes of RBPs exist, one class that includes the AtRBP47 class of proteins, a second class containing proteins related to AtRBP45 and third class containing RBPs with 2 RRMs (AtRBP1, AtRBP31 and AtRBP37). The third class was also the most phylogenetically distant compared to other groups suggesting that they may have a different functional role than other closely related RBPs. The tandem repeats At1g47490 and At1g47500 showed the highest homology at 90.37% and lowest number of amino acid gaps when compared among other RBPs (Figure 5-19B). The high homogeneity between the two genes indicates that they could have similar function in Arabidopsis.

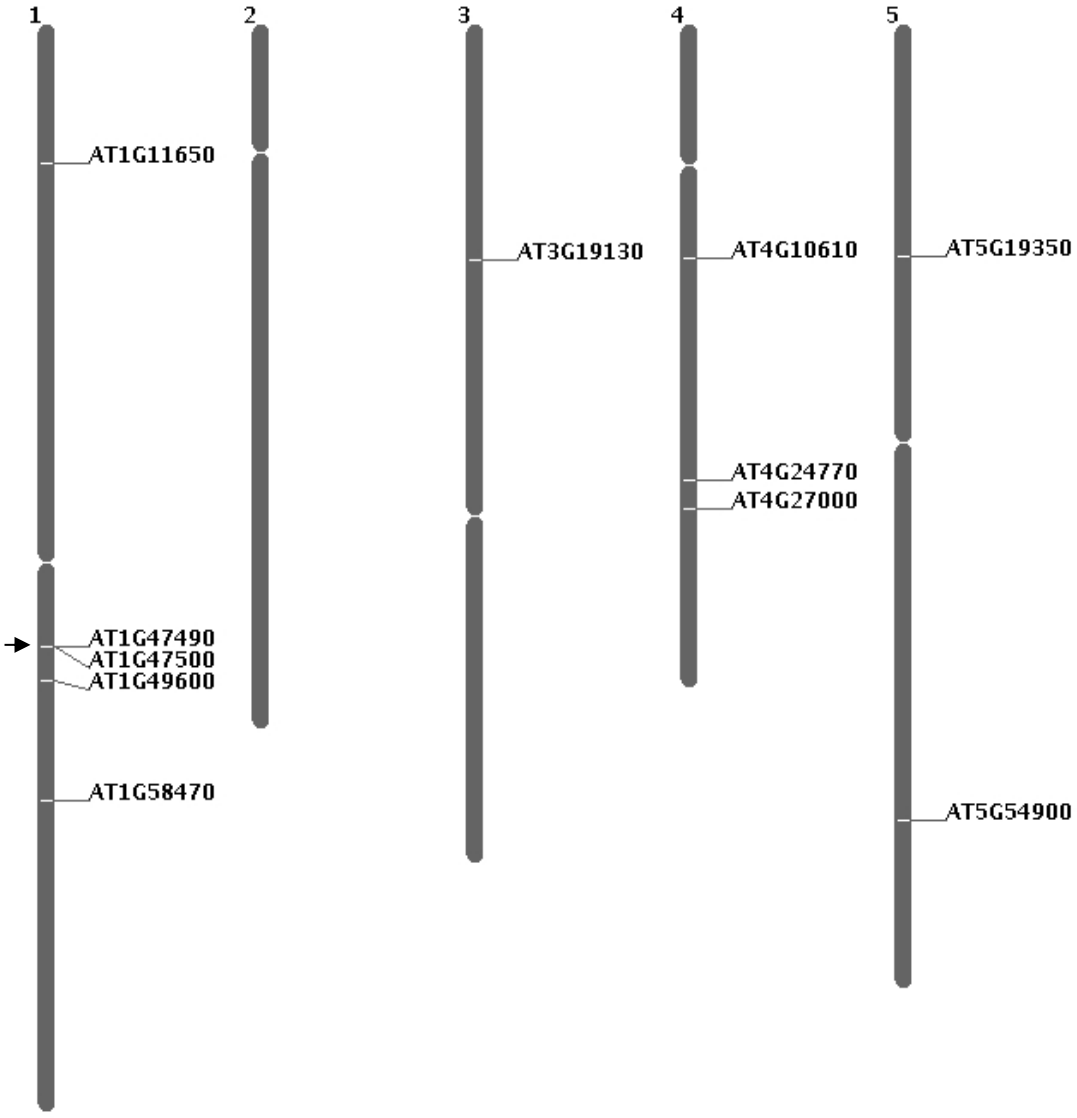

Figure 5-18: Occurrences of RBP genes in the five chromosomes of Arabidopsis. The numbers beside the vertical bars indicate respective chromosome numbers. The horizontal lines on the right indicate the RBP genes in the Arabidopsis genome. The arrow indicates a tandem duplication event in the case of At1g47490 and At1g47500. At1g11650 (RBP45B); At1g47490 (RBP47C); At1g47500 (RBP47C'); At1g49600 (RBP47A); At1g58470 (RBP1); At3g19130 (RBP47B); At4g10610 (RBP37); At4g24770 (RBP31); At4g27000 (RBP45C); At5g19350 (RBP45); At5g54900 (RBP45A)

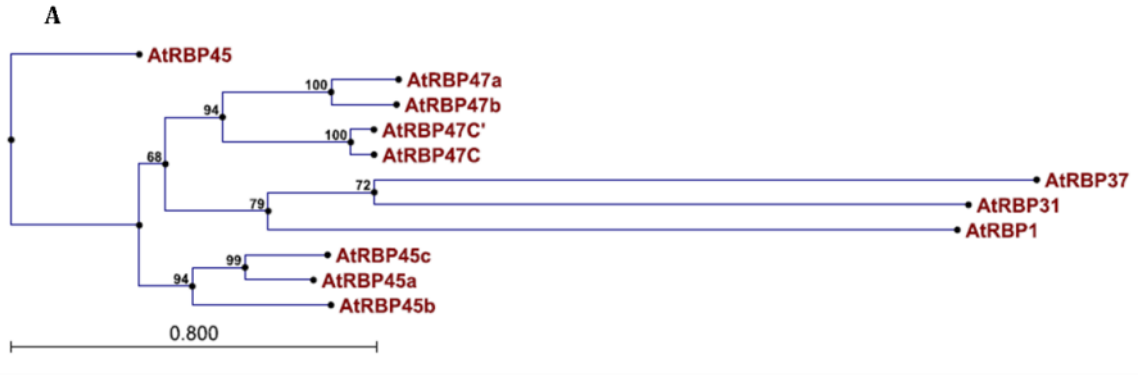

B

Percentage similarities

		1	2	3	4	5	6	7	8	9	10	11
AtRBP47C	1		90.37	48.73	51.39	43.14	41.39	40.99	35.63	14.11	13.84	12.82
AtRBP47C'	2	6		48.21	50.85	43.81	41.83	42.09	35.69	13.44	14.41	12.97
AtRBP47b	3	77	81		74.95	40.91	38.82	38.08	33.46	14.85	13.84	13.11
AtRBP47a	4	61	65	30		41.63	38.95	37.97	33.21	14.15	13.61	12.83
AtRBP45a	5	85	83	102	100		72.08	55.56	39.32	14.22	14.38	14.25
AtRBP45c	6	71	69	98	90	36		57.18	38.09	14.11	12.82	14.71
AtRBP45b	7	95	97	116	114	54	44		39.87	13.67	13.95	12.88
AtRBP45	8	159	161	180	184	134	142	108		14.38	12.40	10.39
AtRBP1	9	186	188	215	227	153	175	157	147		10.09	7.52
AtRBP31	10	193	195	190	196	188	208	198	214	203		10.26
AtRBP37	11	194	196	215	211	185	211	201	231	192	125	

Number of Gaps

Figure 5-19: Phylogenetic analysis of RNA binding proteins in Arabidopsis. A) Rooted phylogenetic tree for AtRBP protein sequences. B) Comparison plot indicating percentage sequence similarities (upper-right half) and number of amino acid gaps (lower-left half) among the AtRBP proteins analyzed.

Based on the number of RRMs present in the protein, the 11 RBPs can be divided into two groups; RBP1, RBP31 and RBP37 that contain only two RRMs while the other eight RBPs contain three RRMs (Table 5-2). Each RRM consisted of 65 to 75 amino acids and their location in the proteins also seems highly conserved. The PCLR chloroplast localization analysis revealed that 3 of 11 RBPs namely RBP31, RBP45B and RBP47C seem to be potential candidates for chloroplast localization, with the prediction score of 0.994, 0.703 and 0.758, respectively (Table

5-2). It was determined that the homologue of RBP47C, RBP47C' with a score of 0.558 did not seem to be a chloroplast localization candidate. It is interesting to note that RBP31 had the highest score among other RBPs tested and also had the most distant relationship or least amino acid similarities when compared to RBP45B and RBP47C. Furthermore, RBP31 contained only two RRM domains while the other two proteins predicted to be localized to the chloroplast contained three RRM domains.

Table 5-2: The location and number of the RNA Recognition Motifs in various Arabidopsis RNA binding proteins.

RNA binding proteins	AGI ID	Location		RRM Domains	Chloroplast localization score[#]
		Start	End		
RBP1	At1g58470	8	77	2	0.010
		122	192		
RBP31	At4g24770	152	223	2	0.994*
		246	317		
RBP37	At4g10610	152	220	2	0.144
		249	318		
RBP45	At5g19350	26	97	3	0.013
		118	190		
		239	304		
RBP45A	At5g54900	62	133	3	0.108
		156	228		
		262	327		
RBP45B	At1g11650	64	135	3	0.703*
		157	229		
		263	328		
RBP45C	At4g27000	82	153	3	0.165
		175	247		
		280	345		
RBP47A	At1g49600	121	192	3	0.347
		215	287		
		329	394		
RBP47B	At3g19130	110	181	3	0.259
		204	276		
		323	388		
RBP47C	At1g47490	103	176	3	0.758*
		199	271		
		306	371		
RBP47C'	At1g47500	105	178	3	0.558
		201	273		
		308	373		

# indicates score determined by PCLR chloroplast localization analysis. * Indicates proteins that are predicted by PCLR chloroplast localization software to be localized in the chloroplast.

5.4 Discussion

5.4.1 Mutation in *RBP47C* gene provides resistance to norflurazon

The mutant KN231 was screened from an activation-tagged population of Arabidopsis using growth media supplemented with 0.5 µM norflurazon. Southern hybridization of mutant KN231 indicated T-DNA insertion at a single locus. Genome Walker analysis indicated that the T-DNA was inserted in the first intron of At1g47490 encoding a putative RNA binding protein and affected the expression of the full length *RBP47C* gene. Two allelic Salk knockout mutant lines, S4 and S8, were identified that had T-DNA insertions in the fifth and third introns of *RBP47C*, respectively. The two Salk lines also displayed resistance to norflurazon at 0.5 µM similar to the KN231. These results indicate that norflurazon resistance is due to the defective At1g47490 gene.

Tolerance to norflurazon by increased carotenoid levels and/or enhanced or mutated *PDS* has been reported in plants. Increased levels of carotenoids in transgenic *Erwinia uredovora* due to overexpression of bacterial *PSY* led to norflurazon tolerance (Misawa et al., 1993). Similarly, Arabidopsis mutants, *aba-1*, with increased levels of a carotenoid by-product ABA in the seeds were reported to display norflurazon tolerance (Ezhova et al., 1997). One non-segregating Arabidopsis line, carrying *Hydrilla* PDS with the *Thr* mutation, was resistant to 3 µM norflurazon and 200 nM fluridone (Arias et al., 2006). Similarly, Some A. thaliana lines transformed with *His* and *Cys* mutations of Hydrilla PDS also survived 3 µM norflurazon treatments (Wagner et al., 2002).

It has been determined that norflurazon binds to plastoquinone molecules (Breitenbach et al., 2001), thereby affecting the desaturase reactions that are coupled with plastoquinone redox reactions and carotenoid biosynthesis (Carol and Kuntz, 2001). Electrons from carotenoid desaturation reactions are converted to oxygen via photo-respiration to terminate the reduction of molecular oxygen through the oxidation of plastoquinol (Bennoun, 2001). The Arabidopsis variegated mutant, *immutans* contains lesions in a plastid-targeted alternative oxidase (PTOX) required for desaturase activity, thereby linking desaturation to chloroplast electron transport (Yu et al., 2007). Similarly in *C. reinhardtii*, enhanced *PDS* expression assisted in the prevention of $^1O_2$ formation under high light stress conditions (Chang et al., 2013). In the same study, it was

proposed that *C. reinhardtii* cells generated H_2O_2 under high light stress in defense against photo-oxidative stress via enhancing carotenoid-mediated $^1O_2$ scavenging ability through the activation of PDS-catalyzed carotenoid synthesis (Chang et al., 2013). Similarly in this study, significantly increased expression of both *PDS* and *ZDS* involved in the carotenoid desaturation reactions was observed in mutant KN231 leaves, as were the expression of several other carotenoid genes such as *βLYC* and *ZEP* which could have led to the increased violaxanthin content in the leaves. In addition, the *ZDS* expression was significantly increased in the leaf tissues of Salk mutants S4 and S8 compared to the WT. These results indicate that the tolerance to norflurazon is related to the increase in the expression of genes encoding the desaturase enzymes of the carotenoid biosynthetic pathway.

5.4.2 *RBP47C* affects carotenoid accumulation in mature seeds of Arabidopsis

Most leaf carotenoid levels, except for violaxanthin, did not change significantly between the mutants (KN231, S4 and S8) and the WT. However, seed carotenoid levels in the mutants KN231, S4 and S8 with a defective *RBP47C* gene were significantly higher compared to the WT. Furthermore, the majority of the complemented lines overexpressing the functional *RBP47C* gene in the mutants KN231, S4 and S8 had decreased lutein and β-carotene levels in the seeds that reached WT seed levels or significantly lower than WT seed levels. The complemented lines 231-C-1 and S8-C-5 mimicked the seed carotenoid levels of the mutants KN231 and S8, respectively with significantly higher levels of lutein and β-carotene compared to the WT. Gene expression analysis in 231-C-1 and S8-C-5 lines indicated that the *RBP47C* gene was significantly reduced in these lines. From these results it can be inferred that *RBP47C* gene plays an important in accumulation of carotenoid in seeds.

Carotenoid synthesis and accumulation occur throughout seed development in Arabidopsis. Carotenoid accumulation is also developmentally-regulated in *B. napus* seeds, with the highest levels of carotenoids detectable later in seed maturation at 35–40 DAP (Yu et al., 2010) Similarly in this study, significant accumulation of carotenoids in the mature seeds could be attributed to increased carotenoid biosynthesis during the silique developmental stages. In this study, expression of both the *RBP47C* genes and many genes involved in carotenoid biosynthesis were found to be expressed during the silique/seed developmental stages. This is the first study

to report the pattern of RBP47C expression in various silique/seed development stages. *RBP47C* transcripts were significantly higher in the mature seeds followed by stage 3 and 4 representing 7-9 and 10-12 DAP, respectively. Interestingly stage 1 (1-3 DAP) and 5 (13-15 DAP) had significantly lower levels of *RBP47C* gene transcripts. In contrast, carotenoid gene expression analysis during silique development indicated significantly higher transcript levels of *PSY*, *PDS*, *εLYC* and *εHYD* in stage 1 and 5 siliques. Although, there seems to be a negative correlation between the expression of *RBP47C* and some carotenoid genes in the developing siliques, further experiments involving RNAi and/or overexpression studies are required to confirm the involvement of *RBP47C* in the regulation of carotenoid genes.

5.4.3 RBP47C and RBP47C' potentially differ in their localization

The two genes *RBP47C* and *RBP47C*' both share about 90.37% homology at the amino acid base level. The gene *RBP47C* encodes a putative RNA binding protein and a homology search of the gene indicated that the *RBP47C* gene belonged to a multi-gene family consisting of 11 members. The 11 genes are characterized by the presence of the RRM. The 11 genes span across four of the five chromosomes of Arabidopsis except for the 2nd chromosome due to duplication events on an evolutionary scale. One tandem duplication event of *RBP47C* resulted in its homologue *RBP47C*'. Tandem duplication is very common in Arabidopsis. Many of the R genes responsible for resistance against plant pathogens are reported to be evolved due to tandem duplication and recombination (Leister, 2004). Tandemly duplicated Arabidopsis sesquiterpene synthase genes At4g13280 and At4g13300 was characterized and both the genes were reported to encode a root-specific and wound-inducible (Z)-γ-bisabolene synthases (Auldridge et al., 2006). Similarly, in this study both *RBP47C* and *RBP47C*' were found to be expressed in Arabidopsis. The expression profile of the two genes *RBP47C* and *RBP47C*' indicate that both the genes are expressed in all the analyzed tissues of Arabidopsis except for stem tissues. Both the genes had increased expression during silique development. The highest levels of transcripts were found in Stage 4 (10-12 DAP) and mature seeds for both genes. Analysis of the amino acid sequence *in-silico* using PCLR Chloroplast Localization Prediction (Schein et al., 2001) indicated that RBP47C to be a highly probable candidate with chloroplast targeting function with the score of 0.745 compared to RBP47C' with a score of 0.558. Furthermore, in mutants KN231, S4 and S8 the *RBP47C*' is expressed, but could not compensate for the functions of *RBP47C*.

Additionally, complementation of mutants with a functional copy of *RBP47C* aided some mutants to revert to WT phenotype. These results indicate that the genes *RBP47C* and *RBP47C*' have a common expression profile, but different functions or target organelles. Further studies, involving *in vivo* localization of potential RBP candidates would provide much needed information on their function in the chloroplast. Protein-RNA interaction studies would also help in determining the role of RBP47C and also provide insights on its substrate specificity.

6 GENERAL DISCUSSION

Carotenoids are localized on membranes of plastids, and plastids are known to be the site of carotenoid biosynthesis. However, plastids are architecturally unique, dynamic organelles that go through a developmental program altering the ultrastructure, chemistry, and structural aspects of the carotenoid biosynthesis machinery. The carotenoid biosynthesis pathway has been extensively studied, and most of the genes involved in the pathways are now available. Although the biochemistry of carotenogenesis has been well-established over the past decades, little is known about its gene regulation. There might be more unknown connections of carotenogenesis to other metabolic pathways, which should be revealed and considered to understand the full scope of carotenoid deposition and to improve the potential for future engineering of carotenoid biosynthesis. Therefore, the onus of this thesis was to discover novel regulatory mechanisms involved in carotenoid metabolism by identifying new Arabidopsis mutants with altered carotenoid levels.

Screening for plant mutants based on tissue color is not unusual. Mutants that show altered color profiles are often related to changes in the carotenoid profiles. Some of the common examples include *cara cara*, a spontaneous mutant of navel orange leading to bright red pulp due to the accumulation of lycopene (Tao et al., 2007; Alquezar et al., 2008) and the mutant, *pinalate*, derived from the orange (*Citrus sinensis* L. Osbeck) variety Navelate (Rodrigo and Zacarias, 2007). This latter mutant produces distinctive yellow fruits instead of the typical bright orange coloration and has been shown to accumulate linear carotenoids, such as phytoene, phytofluene and ζ- carotene. The regulation of carotenogenesis in chromoplasts has been extensively studied using the color changes from green to red that occur in tomato mutants (Hirschberg, 2001). In the *delta* mutants of tomato, the accumulation of δ-carotene was correlated with increased levels of ε-LYC gene expression and orange colored flesh (Ronen et al., 1999; Lewinsohn et al., 2005). Similarly in the *beta* mutants, the lycopene β-LYC gene was up-regulated leading to accumulation of β-carotene and, therefore, bright orange flesh (Ronen et al., 2000; Lewinsohn et al., 2005).

The red seed coat screening method was successful in obtaining 14 Arabidopsis mutants with altered carotenoid profiles. However, red seed coat mutants identified did not have single T-

DNA insertion and the seed coat phenotype could be due to other pigmentations in the seed coat. The seed coat is a multifunctional organ that aids in embryo nutrition during seed development and protection against detrimental agents from the environment (Mohamed-Yasseen et al., 1994). The seed coat exerts dormancy on the seed mainly by being impermeable to water and/or oxygen, and by its mechanical resistance to radicle protrusion. These properties have been positively correlated with seed coat color due to phenolic compounds or other secondary metabolites that accumulate in the seed. The red seeds of charlock (*Sinapis arvensis* L.) exhibit reduced dormancy compared with black seeds (Duran and Retamal, 1989). In faba beans, white seeds lacking tannins imbibe more rapidly and germinate earlier than colored seeds, while white seeds suffer greater damage due to imbibition, higher solute leakage, and reduced vigor and viability (Kantar et al., 1996). In wheat, the strongest dormancy is associated with a red seed coat color, whereas lines with white seed coats are non-dormant or weakly dormant and therefore are susceptible to pre-harvest sprouting damage (Torada and Amano, 2002). Dark seeds of proso millet (*Panicum miliaceum*L.) have heavier seed coats, imbibe and germinate more slowly, suffer less imbibition damage, and therefore persist longer in soil than light-colored seed (Khan et al., 1997). Additionally, the pale yellow color of Arabidopsis *tt4* seeds that are devoid of any colored flavonoids is likely due to the localization of carotenoids in the aleurone layer and the embryo (Debeaujon et al., 2000). These findings suggest that the carotenoid precursors required for ABA synthesis are present in the seed coat.

The second objective of this thesis was to determine light-mediated regulation of carotenoid biosynthesis and to screen the Arabidopsis population for mutants with norflurazon tolerance. The light/dark-adaptation and redox regulation of carotenoid biosynthesis was studied with respect to the expression profiles of carotenoid genes during dark adaptation and upon treatment with photosynthetic inhibitors DCMU and DBMIB in chapter 3. The understanding paved the way for norflurazon screening and the identification of eight mutants showing tolerance to norflurazon. Two out of the eight mutants identified were characterized in detail. Previously norflurazon screening identified mutants that are directly related to the carotenoid biosynthetic pathway as it affects the carotenoid desaturation reactions. However, two mutants, KN203 and KN231 identified in this thesis using norflurazon screening were characterised, respectively did not elucidate a direct relationship to the carotenoid biosynthetic pathway. Instead, they

highlighted the complex regulatory mechanisms that are involved in carotenoid biosynthesis. One mutant KN203 was found to have a defective *KCS19* and later was found to actually be sensitive to norflurazon. Another mutant KN231 displaying tolerance to norflurazon significantly accumulated lutein and β-carotene in mature seeds was defective in a gene encoding a RBP.

This thesis identified that several genes involved in the carotenoid biosynthetic pathway are regulated by light and/or the plastoquinone redox pool. Another novel regulatory aspect was the demonstration of a connection between the expression levels of genes responsible for carotene desaturation and changes in photosynthetic electron transport (ET). Both carotenoid desaturation and ET processes share the thylakoid plastoquinone pool. Under high light stress or DBMIB treatment, the pool of plastoquinone is mainly oxidized, which facilitates carotene desaturation. This thesis showed that *PSY* and *PDS* expression is modified by changes in the plastoquinone redox pool, while *ZDS* seems to be expressed when the plastoquinol concentration increases during high-light stress conditions or DBMIB treatment. *βLYC* expression was affected by the treatment of photosynthetic inhibitors.

This thesis identified the cross-talk between very long chain fatty acids and carotenoid biosynthesis, a finding which has not been described before. The "cross talk" was identified using the mutant KN203 screened for altered carotenoid profile, but found to be norflurazon sensitive, cerulenin insensitive, and having a defective KCS19 gene encoding Keto acyl CoA synthase 19. This mutant had very low expression of KCS19 gene, but enough for Arabidopsis to survive, as many attempts to recreate mutant phenotype using RNAi methods led to an embryo lethal phenotype. The cerulenin treatment mimicking the effect of the KN203 mutant had *βLYC* expression affected in WT seedlings. Furthermore, the mutant KN203 with the defective *KCS19* gene involved in very long chain fatty acids and also had significantly lower lever levels of βLYC transcripts in the mutant seedlings compared to the WT.

This thesis also identified a norflurazon resistant mutant (KN231) with increased seed carotenoid levels using norflurazon screening. Characterization of this mutant revealed that RNA binding protein RBP47C affected carotenoid accumulation during silique/seed development. The accumulation of lutein and β-carotene in the seeds of mutants defective in *RBP47C* has been proved using allelic Salk mutants and complementation studies. A tandem repeat homologue of

RBP47C, *RBP47C'*, was identified in this thesis. Although the tandem repeat was expressed in all the tissues similar to its counterpart, *RBP47C'* expression alone was not able to compensate for the phenotype (norflurazon resistance) observed. Moreover, based on bioinformatics analysis RBP47C is a potential candidate to be localized to the chloroplast whereas, AtRBP47C' is not. This observation indicated that even with 90% homology and being tandem repeats the genes can have varying functions in plant cells and may be differentially localized.

This thesis has provided valuable insights on the relationship between carotenoid biosynthesis and other metabolic pathways (very long chain fatty acid synthesis and RNA binding). However, a comprehensive understanding of their mechanisms of action requires further investigation. Although there are more than 600 species of carotenoids present in plants, very few carotenoids belong to groups with major concentrations. All the studies in this thesis characterized the levels of only four major carotenoids; namely, lutein, β-carotene, zeaxanthin and violaxanthin. However, the levels of other major carotenoids such as phytoene, lycopene and neoxanthin were not measured due to limitations in the HPLC techniques as they cannot identify compounds with similar retention time. New techniques such as mass spectroscopy could be tested to detect all major carotenoids in plants. This would provide better understanding on the pattern of accumulation of carotenoids in Arabidopsis tissues.

Quantitative gene expression studies were used in this thesis to determine the expression profiles of various genes involved in carotenoid biosynthesis and mutant genes in Arabidopsis tissues. Quantitative gene expression methodologies are limited to providing information on the steady state levels of the transcripts at the time period when tissue samples are harvested. They do not indicate a complete depiction of gene expression patterns or other levels of regulation. Therefore, correlation of gene expression pattern with carotenoids or any chemical product needs further supporting evidence from enzyme activity or protein product accumulation for the genes under investigation. Furthermore, post-transcriptional changes and post-translational changes occurring in the plant cells are unaccounted for in this thesis. Therefore, protein or enzyme kinetic studies are required to confirm the relationship between the gene expression and the corresponding carotenoid concentration. Additionally, subcellular localization experiments for the proteins affected in the two mutants KN203 and KN231 would provide much needed understanding of their role in carotenoid biosynthesis and accumulation.

The involvement of carotenoids in protecting the photosynthetic machinery from oxidative and high light stress has been discussed in this thesis. Furthermore, carotenoids in plants are also precursors for the synthesis of the stress hormone ABA. This thesis provided a better understanding on the carotenoid biosynthesis genes during light/redox stress. Other environmental factors such as cold, freezing, drought and pathogens also cause stress in plants. Therefore, future research on the expression profiles of various carotenoid genes in the two mutants KN203 and KN231 under a range of environmental stress conditions would aid in deducing additional mechanisms of action for the *KCS19* and *RBP47C* in Arabidopsis.

In KN231, the defective RBP47C increased the carotenoid content of Arabidopsis seeds and also imparted norflurazon resistance to seedlings. Therefore, it may be fruitful to develop RNAi or antisense *RBP47C* mutant lines in *B. napus* to enhance carotenoid levels in canola seeds and also at the same time provide herbicide tolerance for norflurazon –like herbicides.

7 REFERENCES

Abdel-Aal ESM, Akhtar MH (2006) Recent advances in the analyses of carotenoids and their role in human health. Current Pharmaceutical Analysis **2:** 195-204

Abrous-Belbachir O, De Paepe R, Trémolières A, Mathieu C, Aïd F, Benhassaine-Kesri G (2009) Evidence that norflurazon affects chloroplast lipid unsaturation in Soybean leaves (*Glycine max* L.). Journal of Agricultural and Food Chemistry **57:** 11434-11440

Abrous O, Benhassaine-Kesri G, Tremolieres A, Mazliak P (1998) Effect of norflurazon on lipid metabolism in soya seedlings. Phytochemistry **49:** 979-985

Alfonso M, Perewoska I, Kirilovsky D (2000) Redox Control of psbA Gene Expression in the *Cyanobacterium Synechocystis* PCC 6803. Involvement of the Cytochrome *b6/f* Complex. Plant physiology **122:** 505-516

Alquezar B, Rodrigo MJ, Zacarías L (2008) Regulation of carotenoid biosynthesis during fruit maturation in the red-fleshed orange mutant Cara Cara. Phytochemistry **69:** 1997-2007

Alves-Rodrigues A, Shao A (2004) The science behind lutein. Toxicology Letters **150:** 57-83

Arias RS, Dayan FE, Michel A, Howell J, Scheffler BE (2006) Characterization of a higher plant herbicide-resistant phytoene desaturase and its use as a selectable marker. Plant Biotechnology Journal **4:** 263-273

Armstrong GA, Hearst JE (1996) Carotenoids 2: Genetics and molecular biology of carotenoid pigment biosynthesis. The Federation of American Societies for Experimental Biology Journal **10:** 228-237

Aronsson H, Schuttler MA, Kelly AlA, Sundqvist C, Durmann P, Karim S, Jarvis P (2008) Monogalactosyldiacylglycerol deficiency in arabidopsis affects pigment composition in the prolamellar body and impairs thylakoid membrane energization and photoprotection in leaves. Plant Physiology **148:** 580-592

Auldridge ME, Block A, Vogel JT, Dabney-Smith C, Mila I, Bouzayen M, Magallanes-Lundback M, DellaPenna D, McCarty DR, Klee HJ (2006) Characterization of three members of the Arabidopsis carotenoid cleavage dioxygenase family demonstrates the divergent roles of this multifunctional enzyme family. The Plant Journal **45:** 982-993

Ayala MB, Gorgé JL, Lachica M, Sandmann G (1992) Changes in carotenoids and fatty acids in photosystem II of Cudeficient pea plants. Physiologia Plantarum **84:** 1-5

Baroli I, Do AD, Yamane T, Niyogi KK (2003) Zeaxanthin accumulation in the absence of a functional xanthophyll cycle protects *Chlamydomonas reinhardtii* from photooxidative stress. Plant Cell **15:** 992-1008

Barrero JM, Piqueras P, Gonzalez-Guzman M, Serrano R, Rodriguez PL, Ponce MR, Micol JL (2005) A mutational analysis of the *ABA1* gene of *Arabidopsis thaliana* highlights the involvement of ABA in vegetative development. Journal of Experimental Botany **56:** 2071-2083

Bartels PG, Watson CW (1978) Inhibition of carotenoid synthesis by fluridone and norflurazon. Weed Science **26:** 198-203

Ben-Dor A, Steiner M, Gheber L, Danilenko M, Dubi N, Linnewiel K, Zick A, Sharoni Y, Levy J (2005) Carotenoids activate the antioxidant response element transcription system. Molecular Cancer Therapy **4:** 177-186

Bennoun P (2001) Chlororespiration and the process of carotenoid biosynthesis. Biochimica et Biophysica Acta - Bioenergetics **1506:** 133-142

Biehler E, Bohn T (2010) Methods for assessing aspects of carotenoid bioavailability. Current Nutrition and Food Science **6:** 44-69

Blacklock BJ, Jaworski JG (2006) Substrate specificity of Arabidopsis 3-ketoacyl-CoA synthases. Biochemical and Biophysical Research Communications **346:** 583-590

Bohne F, Linden H (2002) Regulation of carotenoid biosynthesis genes in response to light in *Chlamydomonas reinhardtii*. Biochimica et Biophysica Acta - Gene Structure and Expression **1579:** 26-34

Bolychevtseva YV, Rakhimberdieva MG, Karapetyan NV, Popov VI, Moskalenko AA, Kuznetsova NY (1995) The development of carotenoid-deficient membranes in plastids of barley seedlings treated with norflurazon. Journal of Photochemistry and Photobiology B: Biology **27:** 153-160

Bouveret E, Rigaut G, Shevchenko A, Wilm M, Seraphin B (2000) A Sm-like protein complex that participates in mRNA degradation. European Molecular Biology Organiation Journal **19:** 1661-1671

Bouvier F, Keller Y, D'Harlingue A, Camara B (1998) Xanthophyll biosynthesis: molecular and functional characterization of carotenoid hydroxylases from pepper fruits (*Capsicum annuum* L.). Biochimica et Biophysica Acta **1391:** 320-328

Bouvier F, Suire C, Mutterer J, Camara B (2003) Oxidative remodeling of chromoplast carotenoids: identification of the carotenoid dioxygenase *CsCCD* and *CsZCD* genes involved in Crocus secondary metabolite biogenesis. Plant Cell **15:** 47-62

Bramley PM (2002) Regulation of carotenoid formation during tomato fruit ripening and development. Journal of Experimental Botany **53:** 2107-2113

Bratt CE, Arvidsson P-O, Carlsson M, Åkerlund H-E (1995) Regulation of violaxanthin de-epoxidase activity by pH and ascorbate concentration. Photosynthesis Research **45:** 169-175

Breitenbach Jr, Zhu C, Sandmann G (2001) Bleaching herbicide norflurazon inhibits phytoene desaturase by competition with the cofactors. Journal of Agricultural and Food Chemistry **49:** 5270-5272

Britton G, Liaaen-Jensen S, Pfander H (2004) Carotenoids handbook. Birkhauser Verlag

Brügger B, Erben G, Sandhoff R, Wieland FT, Lehmann WD (1997) Quantitative analysis of biological membrane lipids at the low picomole level by nano-electrospray ionization tandem mass spectrometry. Proceedings of the National Academy of Sciences **94:** 2339-2344

Burd CG, Dreyfuss G (1994) Conserved structures and diversity of functions of RNA-binding proteins. Science **265:** 615-621

Calucci L, Capocchi A, Galleschi L, Ghiringhelli S, Pinzino C (2004) Antioxidants, free radicals, storage proteins, puroindolines, and proteolytic activities in bread wheat (*Triticum aestivum*) seeds during accelerated aging. Journal of Agricultural and Food Chemistry **52:** 4274-4281

Carey M, Smale ST (2000) Transcriptional regulation in eukaryotes :concepts, strategies, and techniques. Cold Spring Harbor Laboratory Press, Cold Spring Harbor, NY

Carol P, Kuntz M (2001) A plastid terminal oxidase comes to light: implications for carotenoid biosynthesis and chlororespiration. Trends in Plant Science **6:** 31-36

Castenmiller JJM, West CE (1997) Bioavailability of carotenoids. Pure and Applied Chemistry **69:** 2145-2150

Cazzonelli CI, Cuttriss AJ, Cossetto SB, Pye W, Crisp P, Whelan J, Finnegan EJ, Turnbull C, Pogson BJ (2009) Regulation of carotenoid composition and shoot branching in Arabidopsis by a chromatin modifying histone methyltransferase, SDG8. Plant Cell **21:** 39-53

Cazzonelli CI, Pogson BJ (2010) Source to sink: regulation of carotenoid biosynthesis in plants. Trends in Plant Science **15:** 266-274

Cazzonelli CI, Roberts AC, Carmody ME, Pogson BJ (2010) Transcriptional control of set domain group 8 and carotenoid isomerase during arabidopsis development. Molecular Plant **3:** 174-191

Chamovitz D, Pecker I, Hirschberg J (1991) The molecular basis of resistance to the herbicide norflurazon. Plant Molecular Biology **16:** 967-974

Chang H-L, Kang C-Y, Lee T-M (2013) Hydrogen peroxide production protects *Chlamydomonas reinhardtii* against light-induced cell death by preventing singlet oxygen accumulation through enhanced carotenoid synthesis. Journal of Plant Physiology **170:** 976-986

Chaudhary N, Nijhawan A, Khurana J, Khurana P (2010) Carotenoid biosynthesis genes in rice: structural analysis, genome-wide expression profiling and phylogenetic analysis. Molecular Genetics and Genomics **283:** 13-33

Chen Y, Li D, Lu W, Xing J, Hui B, Han Y (2003) Screening and characterization of astaxanthin-hyperproducing mutants of *Haematococcus pluvialis*. Biotechnology Letters **25:** 527-529

Cheng Q (2006) Structural diversity and functional novelty of new carotenoid biosynthesis genes. Journal of Industrial Microbiology and Biotechnology **33:** 552-559

Cheng Y, Chen X (2004) Post-transcriptional control of plant development. Current Opinion in Plant Biology **7:** 20-25

Choi Y, Gehring M, Johnson L, Hannon M, Harada JJ, Goldberg RB, Jacobsen SE, Fischer RL (2002) DEMETER, a DNA glycosylase domain protein, is required for embryo gene imprinting and seed viability in arabidopsis. Cell **110:** 33-42

Christensen SK, Dagenais N, Chory J, Weigel D (2000) Regulation of Auxin Response by the Protein Kinase PINOID. Cell **100:** 469-478

Clough SJ, Bent AF (1998) Floral dip: a simplified method forAgrobacterium-mediated transformation of *Arabidopsis thaliana*. The Plant Journal **16:** 735-743

Corona V, Aracri B, Kosturkova G, Bartley GE, Pitto L, Giorgetti L, Scolnik PA, Giuliano G (1996) Regulation of a carotenoid biosynthesis gene promoter during plant development. The Plant Journal **9:** 505-512

Crowell DN, Packard CE, Pierson CA, Giner J-L, Downes BP, Chary SN (2003) Identification of an allele of CLA1 associated with variegation in *Arabidopsis thaliana.* Physiologia Plantarum **118:** 29-37

Cunningham F, Gantt E (2001) One ring or two? Determination of ring number in carotenoids by lycopene epsilon-cyclases. Proceedings of the National Academy of Sciences of the United States of America **98:** 2905-2910

Cunningham FX, Gantt E (1998) Genes and enzymes of carotenoid biosynthesis in plants. Annual Review of Plant Physiology and Plant Molecular Biology **49:** 557-583

Cunningham FX, Gantt E (2005) A study in scarlet: Enzymes of ketocarotenoid biosynthesis in the flowers of *Adonis aestivalis*. The Plant Journal **41:** 478-492

Curl AL, Bailey GF (1954) Orange carotenoids, polyoxygen carotenoids of valencia orange juice. Journal of Agricultural and Food Chemistry **2:** 685-690

Czechowski T, Stitt M, Altmann T, Udvardi MK, Scheible W-R (2005) Genome-wide identification and testing of superior reference genes for transcript normalization in Arabidopsis. Plant Physiology. **139:** 5-17

Czeczuga B (1987) Carotenoid contents in leaves grown under various light intensities. Biochemical Systematics and Ecology **15:** 523-527

Dahnhardt D, Falk J, Appel J, van der Kooij TA, Schulz-Friedrich R, Krupinska K (2002) The hydroxyphenylpyruvate dioxygenase from *Synechocystis* sp. PCC 6803 is not required for plastoquinone biosynthesis. FEBS Letters **523:** 177

Dall'osto L, Fiore A, Cazzaniga S, Giuliano G, Bassi R (2007) Different roles of alpha- and beta-branch xanthophylls in photosystem assembly and photoprotection. Journal of Biological Chemistry **282:** 35056-35068

Dall'Osto L, Piques M, Ronzani M, Molesini B, Alboresi A, Cazzaniga S, Bassi R (2013) The Arabidopsis *nox* mutant lacking carotene hydroxylase activity reveals a critical role for xanthophylls in photosystem I biogenesis. The Plant Cell Online **25:** 591-608

Davuluri GR, van Tuinen A, Fraser PD, Manfredonia A, Newman R, Burgess D, Brummell DA, King SR, Palys J, Uhlig J, Bramley PM, Pennings HMJ, Bowler C (2005) Fruit-specific RNAi-mediated suppression of DET1 enhances carotenoid and flavonoid content in tomatoes. Nature Biotechnology **23:** 890-895

Davuluri GR, Van Tuinen A, Mustilli AC, Manfredonia A, Newman R, Burgess D, Brummell DA, King SR, Palys J, Uhlig J, Pennings HMJ, Bowler C (2004) Manipulation of DET1 expression in tomato results in photomorphogenic phenotypes caused by post-transcriptional gene silencing. Plant Journal **40:** 344-354

De Spirt S, Lutter K, Stahl W (2010) Carotenoids in photooxidative stress. Current Nutrition and Food Science **6:** 36-43

Debeaujon I, Laon-Kloosterziel KM, Koornneef M (2000) Influence of the testa on seed dormancy, germination, and longevity in Arabidopsis. Plant Physiology **122:** 403-414

DellaPenna D (1999) Carotenoid synthesis and function in plants: Insights from mutant studies in Aradopsis. Pure Applied Chemistry **71:** 2205-2212

Demmig-Adams B, Cohu M C, Adams WII, W (2012) Dealing with the hazards of harnessing sunlight. Nature Education Knowledge **4:** 18-23

Demmig-Adams B, Adams WII, W (2002) Antioxidants in Photosynthesis and Human Nutrition. Science **298:** 2149-2153

Deruere J, Romer S, Dharlingue A, Backhaus RA, Kuntz M, Camara B (1994) Fibril assembly and carotenoid overaccumulation in chromoplasts: a model for supramolecular lipoprotein structures. Plant Cell **6:** 119-133

Desfeux C, Clough SJ, Bent AF (2000) Female reproductive tissues are the primary target of agrobacterium-mediated transformation by the Arabidopsis floral-dip method. Plant Physiology **123:** 895-904

Diretto G, Welsch R, Tavazza R, Mourgues F, Pizzichini D, Beyer P, Giuliano G (2007) Silencing of beta-carotene hydroxylase increases total carotenoid and beta-carotene levels in potato tubers. BMC Plant Biology **7:** 11, doi: 10.1186/1471-2229-7-11

Dong H, Deng Y, Mu J, Lu Q, Wang Y, Xu Y, Chu C, Chong K, Lu C, Zuo J (2007) The Arabidopsis spontaneous cell death1 gene, encoding a -carotene desaturase essential for carotenoid biosynthesis, is involved in chloroplast development, photoprotection and retrograde signaling. Cell Research **17:** 458-470

Duran JM, Retamal N (1989) Coat structure and regulation of dormancy in *Sinapis arvensis* L. seeds. Journal of Plant Physiology **135:** 218-222

Eguchi S, Takano H, Ono K, Takio S (2002) Photosynthetic electron transport regulates the stability of the transcript for the protochlorophyllide oxidoreductase gene in the Liverwort, *Marchantia paleacea* var. diptera. Plant Cell Physiology **43:** 573-577

Eisenreich W, Bacher A, Arigoni D, Rohdich F (2004) Biosynthesis of isoprenoids via the non-mevalonate pathway. Cellular and Molecular Life Sciences **61:** 1401-1426

Engelmann NJ, Campbell JK, Rogers RB, Rupassara SI, Garlick PJ, Lila MA, Erdman JW (2010) Screening and selection of high carotenoid producing *in vitro* tomato cell culture lines for [13C]-carotenoid production. Journal of Agricultural and Food Chemistry **58:** 9979-9987

Ezhova TA, Soldatova OP, Ondar UN, Mamanova LB, Radyukina NL, Sof'in AV, Romanov VI, Shestakov SV (1997) Norflurazon-tolerant dwarf mutants of Arabidopsis as a model for studying plant resistance to oxidative stress. Russian Journal of Plant Physiology **44:** 575-579

Farré G, Sanahuja G, Naqvi S, Bai C, Capell T, Zhu C, Christou P (2010) Travel advice on the road to carotenoids in plants. Plant Science **179:** 28-48

Farrell R, Jr. (2007) The regulation of gene expression in plants and animals. *In* C Bassett, ed, Regulation of Gene Expression in Plants. Springer US, pp 1-38

Fiore A, Dall'osto L, Fraser PD, Bassi R, Giuliano G (2006) Elucidation of the beta-carotene hydroxylation pathway in *Arabidopsis thaliana*. FEBS Letters **580:** 4718 - 4722

Foudree A, Putarjunan A, Kambakam S, Nolan T, Fussell J, Pogorelko G, Rodermel S (2012) The mechanism of variegation in *immutans* provides insight into chloroplast biogenesis. Frontiers in Plant Science **3:** 1-10

Frechijia S, Zhu J, Talbott LD, Zeiger E (1999) Stomata from *npq1*, a zeaxanthin-less Arabidopsis mutant, lack a specific response to blue light. Plant Cell Physiology **40:** 949-954

Frey A, Audran C, Marin E, Sotta B, Marion-Poll A (1999) Engineering seed dormancy by the modification of zeaxanthin epoxidase gene expression. Plant Molecular Biology **39:** 1267-1274

Frey A, Godin B, Bonnet M, Sotta B, Marion-Poll A (2004) Maternal synthesis of abscisic acid controls seed development and yield in *Nicotiana plumbaginifolia*. Planta **218:** 958-964

Galleschi L, Capocchi A, Ghiringhelli S, Saviozzi F, Calucci L, Pinzino C, Zandomeneghi M (2002) Antioxidants, free radicals, storage proteins, and proteolytic activities in Wheat (*Triticum durum*) seeds during accelerated aging. Journal of Agricultural and Food Chemistry **50:** 5450-5457

Galpaz N, Ronen G, Khalfa Z, Zamir D, Hirschberg J (2006) A chromoplast-specific carotenoid biosynthesis pathway is revealed by cloning of the tomato white-flower locus. Plant Cell **18:** 1947 - 1960

Goss R, Lohr M, Latowski D, Grzyb J, Vieler A, Wilhelm C, Strzalka K (2005) Role of hexagonal structure-forming lipids in diadinoxanthin and violaxanthin solubilization and de-epoxidation. Biochemistry **44:** 4028-4036

Gupta R, Webster C, Gray J (1998) Characterisation and promoter analysis of the Arabidopsis gene encoding high-mobility-group protein HMG-I/Y. Plant Molecular Biology **36:** 897-907

Gyula P, Schäfer E, Nagy F (2003) Light perception and signalling in higher plants. Current Opinion in Plant Biology **6:** 446-452

Hagve T-A, Christophersen B, Boger P (1985) Norflurazon-An inhibitor of essential fatty acid desaturation in isolated liver cells. Lipids **20:** 719-722

Hannoufa A, Hossain Z (2012) Regulation of carotenoid accumulation in plants. Biocatalysis and Agricultural Biotechnology **1:** 198-202

Hannoufa A, McNevin J, Lemieux B (1993) Epicuticular waxes of eceriferum mutants of *Arabidopsis thaliana*. Phytochemistry **33:** 851-855

Harwood JL (1997) Plant Lipid Metabolism. *In* PM Dey, JB Harborne, eds, Plant Biochemistry. Academic Press, London, pp 237-272

Havaux M (1998) Carotenoids as membrane stabilizers in chloroplasts. Trends in Plant Science **3:** 147-151

Havaux M, Dall'Osto L, Bassi R (2007) Zeaxanthin has enhanced antioxidant capacity with respect to all other xanthophylls in Arabidopsis leaves and functions independent of binding to PSII antennae. Plant Physiology. **145:** 1506-1520

Hayashi H, Czaja I, Lubenow H, Schell J, Walden R (1992) Activation of a plant gene by T-DNA tagging: auxin-independent growth *in vitro*. Science **258:** 1350-1353

Heinzel T, Lavinsky RM, Mullen T-M, Soderstrom M, Laherty CD, Torchia J, Yang W-M, Brard G, D N, R D, Seto E, Eisenman RN, Rose DW, Glass CK, Rosenfeld MG (1997) A complex containing N-CoR, mSln3 and histone deacetylase mediates transcriptional repression. Nature **387:** 43-48

Hirschberg J (2001) Carotenoid biosynthesis in flowering plants. Current Opinion in Plant Biology **4:** 210-218

Hobbs SL, Kpodar P, DeLong CM (1990) The effect of T-DNA copy number, position and methylation on reporter gene expression in tobacco transformants. Plant Molecular Biology **15:** 851 - 864

Holbrook LA, Magus JR, Taylor DC (1992) Abscisic acid induction of elongase activity, biosynthesis and accumulation of very long chain monounsaturated fatty acids and oil body proteins in microspore-derived embryos of *Brassica napus* L. cv Reston. Plant Science **84:** 99-115

Horn R, Paulsen H (2004) Early steps in the assembly of light-harvesting chlorophyll a/b complex: Time-resolved fluorescence measurements. Journal of Biological Chemistry **279:** 44400-44406

Horváth G, Kissimon J, Faludi-Dániel Á (1972) Effect of light intensity on the formation of carotenoids in normal and mutant maize leaves. Phytochemistry **11:** 183-187

Howitt CA, Pogson BJ (2006) Carotenoid accumulation and function in seeds and non-green tissues. Plant, Cell and Environment **29:** 435-445

Hsieh JJD, Zhou S, Chen L, Young DB, Hayward SD (1999) CIR, a corepressor linking the DNA binding factor CBF1 to the histone deacetylase complex. Proceedings of the National Academy of Sciences of the United States of America **96:** 23-28

Hsieh M-H, Goodman H (2006) Functional evidence for the involvement of Arabidopsis *IspF* homolog in the nonmevalonate pathway of plastid isoprenoid biosynthesis. Planta **223:** 1-6

Huang X, Kadonaga JT (2001) Biochemical analysis of transcriptional repression by Drosophila histone deacetylase. Journal of Biological Chemistry **276:** 12497-12500

Ito K, Barnes PJ, Adcock IM (2000) Glucocorticoid receptor recruitment of histone deacetylase 2 inhibits interleukin-1beta -induced histone h4 acetylation on lysines 8 and 12. Molecular and Cellular Biology **20:** 6891-6903

Jacob F, Monod J (1961) Genetic regulatory mechanisms in the synthesis of proteins. Journal of Molecular Biology **3:** 318-356

Jahns P, Holzwarth AR (2012) The role of the xanthophyll cycle and of lutein in photoprotection of photosystem II. Biochimica et Biophysica Acta - Bioenergetics **1817:** 182-193

James D J (2009) Do carotenoids serve as transmembrane radical channels? Free Radical Biology and Medicine **47:** 321-323

Janick-Buckner D, Hammock JD, Johnson JM, Osborn JM, Buckner B (1999) Biochemical and ultrastructural analysis of the *y10* mutant of maize. Journal of Heredity **90:** 507

Jeon J-S, An G (2001) Gene tagging in rice: a high throughput system for functional genomics. Plant Science **161:** 211-219

Jiang C, Kim SY, Suh D-Y (2008) Divergent evolution of the thiolase superfamily and chalcone synthase family. Molecular Phylogenetics and Evolution **49:** 691-701

Johansen LK, Carrington JC (2001) Silencing on the Spot. Induction and Suppression of RNA Silencing in the Agrobacterium-Mediated Transient Expression System. Plant Physiology **126:** 930-938

Johnson MP, Havaux M, Triantaphylides C, Ksas B, Pascal AA, Robert B, Davison PA, Ruban AV, Horton P (2007) Elevated zeaxanthin bound to oligomeric lhcii enhances the resistance of Arabidopsis to photooxidative stress by a lipid-protective, antioxidant mechanism. Journal of Biolological Chemistry **282:** 22605-22618

Joubes J, Raffaele S, Bourdenx B, Garcia C, Laroche-Traineau J, Moreau P, Domergue F, Lessire R (2008) The VLCFA elongase gene family in Arabidopsis thaliana: phylogenetic analysis, 3D modelling and expression profiling. Plant Molecular Biology **67:** 547-566

Journet E-P, Douce R (1985) Enzymic capacities of purified cauliflower bud plastids for lipid synthesis and carbohydrate metabolism. Plant Physiology **79:** 458-467

Joyard J, Block MA, Douce R (1991) Molecular aspects of plastid envelope biochemistry. European Journal of Biochemistry **199:** 489-509

Jung S, Kim JS, Cho KY, Tae GS, Kang BG (2000) Antioxidant responses of cucumber (*Cucumis sativus*) to photoinhibition and oxidative stress induced by norflurazon under high and low PPFDs. Plant Science **153:** 145-154

Kang H-G, Kim J, Kim B, Jeong H, Choi SH, Kim EK, Lee H-Y, Lim PO (2011) Overexpression of *FTL1/DDF1*, an AP2 transcription factor, enhances tolerance to cold, drought, and heat stresses in *Arabidopsis thaliana*. Plant Science **180:** 634-641

Kantar F, Pilbeam CJ, Hebblethwaite PD (1996) Effect of tannin content of faba bean (*Vicia faba*) seed on seed vigour, germination and field emergence. Annals of Applied Biology **128:** 85-93

Karssen CM, Brinkhorst-van der Swan DLC, Breekland AE, Koornneef M (1983) Induction of dormancy during seed development by endogenous abscisic acid: studies on abscisic acid deficient genotypes *Arabidopsis thaliana* (L.). Planta **157:** 158-165

Kean EG, Ejeta G, Hamaker BR, Ferruzzi MG (2007) Characterization of carotenoid pigments in mature and developing kernels of selected yellow-embryo Sorghum varieties. Journal of Agricultural and Food Chemistry **55:** 2619-2626

Khan M, Cavers PB, Kane M, Thompson K (1997) Role of the pigmented seed coat of proso millet (*Panicum miliaceum* L.) in imbibition, germination and seed persistence. Seed Science Research **7:** 21-26

Kieselbach T, Hagman Å, Andersson B, Schröder WP (1998) The Thylakoid Lumen of Chloroplasts: Isolation and characterization. Journal of Biological Chemistry **273:** 6710-6716

Kim B-H, Malec P, Waloszek A, Arnim A (2012) Arabidopsis BPG2: a phytochrome-regulated gene whose protein product binds to plastid ribosomal RNAs. Planta **236:** 677-690

Kim T, Pfeiffer SE (1999) Myelin glycosphingolipid/cholesterol-enriched microdomains selectively sequester the non-compact myelin proteins CNP and MOG. Journal of Neurocytology **28:** 281-293

King RW (1976) Abscisic acid in developing wheat grains and its relationship to grain growth and maturation. Planta **132:** 43-51

Kmieciak M, Simpson CG, Lewandowska D, Brown JWS, Jarmolowski A (2002) Cloning and characterization of two subunits of *Arabidopsis thaliana* nuclear cap-binding complex. Gene **283:** 171-183

Komatsu T, Kawaide H, Saito C, Yamagami A, Shimada S, Nakazawa M, Matsui M, Nakano A, Tsujimoto M, Natsume M, Abe H, Asami T, Nakano T (2010) The chloroplast protein BPG2 functions in brassinosteroid-mediated post-transcriptional accumulation of chloroplast rRNA. The Plant Journal **61:** 409-422

Kong K-W, Khoo H-E, Prasad KN, Ismail A, Tan C-P, Rajab NF (2010) Revealing the power of the natural red pigment lycopene. Molecules **15:** 959-987

Krol M, Spangfort MD, Huner N, Oquist G, Gustafsson P, Jansson S (1995) Chlorophyll a/b-binding proteins, pigment conversions, and early light-induced proteins in a chlorophyll b-less Barley mutant. Plant physiology **107:** 873-883

Lamers PP, Janssen M, De Vos RCH, Bino RJ, Wijffels RH (2008) Exploring and exploiting carotenoid accumulation in *Dunaliella salina* for cell-factory applications. Trends in Biotechnology **26:** 631-638

Lamers PP, van de Laak CCW, Kaasenbrood PS, Lorier J, Janssen M, De Vos RCH, Bino RJ, Wijffels RH (2010) Carotenoid and fatty acid metabolism in light-stressed *Dunaliella salina*. Biotechnology and Bioengineering **106:** 638-648

Laskay G, Farkas T, Lehoczki E (1985) Cerulenin-induced changes in lipid and fatty acid content of chloroplasts in detached greening Barley leaves. Journal of Plant Physiology **118:** 267-275

Lauria M, Rossi V (2011) Epigenetic control of gene regulation in plants. Biochimica et Biophysica Acta - Gene Regulatory Mechanisms **1809:** 369-378

Leister D (2004) Tandem and segmental gene duplication and recombination in the evolution of plant disease resistance genes. Trends in Genetics **20:** 116-122

Lemoine Y, Schoefs B (2010) Secondary ketocarotenoid astaxanthin biosynthesis in algae: a multifunctional response to stress. Photosynthesis Research **106:** 155-177

Leóna R, Cousoa I, Fernándezb E (2007) Metabolic engineering of ketocarotenoids biosynthesis in the unicelullar microalga *Chlamydomonas reinhardtii*. Journal of Biotechnology **130:** 143-152

Lewinsohn E, Sitrit Y, Bar E, Azulay Y, Meir A, Zamir D, Tadmor Y (2005) Carotenoid Pigmentation affects the volatile composition of tomato and watermelon fruits, as revealed by comparative genetic analyses. Jouranl of Agricultural and Food Chemistry **53:** 3142-3148

Li F, Murillo C, Wurtzel ET (2007) Maize Y9 encodes a product essential for 15-cis-zeta-carotene isomerization. Plant Physiology **144:** 1181-1189

Li L, Paolillo DJ, Parthasarathy MV, DiMuzio EM, Garvin DF (2001) A novel gene mutation that confers abnormal patterns of beta;-carotene accumulation in cauliflower (*Brassica oleracea* var. botrytis). The Plant Journal **26:** 59-67

Li Z, Ahn TK, Avenson TJ, Ballottari M, Cruz JA, Kramer DM, Bassi R, Fleming GR, Keasling JD, Niyogi KK (2009) Lutein accumulation in the absence of zeaxanthin restores nonphotochemical quenching in the *Arabidopsis thaliana npq1* Mutant. The Plant Cell Online **21:** 1798-1812

Linden H, Sandmann G, Chamovitz D, Hirschberg J, Boger P (1990) Biochemical characterization of *Synechococcus* mutants selected against the bleaching herbicide norflurazon. Pesticide Biochemistry and Physiology **36:** 46-51

Lindgren LO, Stalberg KG, Hoglund A-S (2003) Seed-specific overexpression of an endogenous Arabidopsis phytoene synthase gene results in delayed germination and increased levels of carotenoids, chlorophyll, and abscisic acid. Plant Physiology **132:** 779-785

Liu Z, Yan H, Wang K, Kuang T, Zhang J, Gui L, An X, Chang W (2004) Crystal structure of spinach major light-harvesting complex at 2.72Å resolution. Nature **428:** 287-292

Lois LM, Rodríguez-Concepción M, Gallego F, Campos N, Boronat A (2000) Carotenoid biosynthesis during tomato fruit development: regulatory role of 1-deoxy-D-xylulose 5-phosphate synthase. The Plant Journal **22:** 503-513

Lorkovic ZJ (2009) Role of plant RNA-binding proteins in development, stress response and genome organization. Trends in Plant Science **14:** 229-236

Lorkovic ZJ, Barta A (2002) Genome analysis: RNA recognition motif (RRM) and K homology (KH) domain RNA-binding proteins from the flowering plant *Arabidopsis thaliana*. Nucleic Acids Research **30:** 623-635

Lorkovic ZJ, Wieczorek Kirk DA, Klahre U, Hemmings-Mieszczak M, Filipowicz W (2000) RBP45 and RBP47, two oligouridylate-specific hnRNP-like proteins interacting with poly(A)+ RNA in nuclei of plant cells. RNA **6:** 1610-1624

Ma L, Lin XM (2010) Effects of lutein and zeaxanthin on aspects of eye health. Journal of the Science of Food and Agriculture **90:** 2-12

Macko S, Wehner A, Jahns P (2002) Comparison of violaxanthin de-epoxidation from the stroma and lumen sides of isolated thylakoid membranes from Arabidopsis: implications for the mechanism of de-epoxidation. Planta **216:** 309-314

Mandel MA, Feldmann KA, Herrera-Estrella L, Rocha-Sosa M, León P (1996) CLA1, a novel gene required for chloroplast development, is highly conserved in evolution. The Plant Journal **9:** 649-658

Maoka T (2009) Recent progress in structural studies of carotenoids in animals and plants. Archives of Biochemistry and Biophysics **483:** 191-195

Maris C, Dominguez C, Allain FHT (2005) The RNA recognition motif, a plastic RNA-binding platform to regulate post-transcriptional gene expression. FEBS Journal **272:** 2118-2131

Matsuno T (2001) Aquatic animal carotenoids. Fisheries Science **67:** 771-783

Matus Z, Molnar P, Szabo LG (1993) Main carotenoids in pressed seeds (*Cucurbitae semen*) of oil pumpkin (*Cucurbita pepo* convar. pepo var. styriaca). Acta pharmaceutica Hungarica **63:** 247-256

Mayfield S, Taylor W (1984) The appearance of photosynthetic proteins in developing maize leaves. Planta **161:** 481-486

McElver J, Tzafrir I, Aux G, Rogers R, Ashby C, Smith K, Thomas C, Schetter A, Zhou Q, Cushman MA, Tossberg J, Nickle T, Levin JZ, Law M, Meinke D, Patton D (2001) Insertional mutagenesis of genes required for seed development in *Arabidopsis thaliana*. Genetics **159:** 1751-1763

McGraw KJ (2005) Interspecific variation in dietary carotenoid assimilation in birds: Links to phylogeny and color ornamentation. Comparative Biochemistry and Physiology Part B: Biochemistry and Molecular Biology **142:** 245-250

McGraw KJ, Hill GE, Stradi R, Parker RS (2001) The influence of carotenoid acquisition and utilization on the maintenance of species-typical plumage pigmentation in male American goldfinches (*Carduelis tristis*) and northern cardinals (*Cardinalis cardinalis*). Physiological and Biochemical Zoology **74:** 843–852

McNevin Jp WWHAFKLB (1993) Isolation and characterization of eceriferum (cer) mutants induced by T-DNA insertions in *Arabidopsis thaliana.* Genome **36:** 610-618

Michel A, Arias RS, Scheffler BE, Duke SO, Netherland M, Dayan FE (2004) Somatic mutation-mediated evolution of herbicide resistance in the nonindigenous invasive plant hydrilla (*Hydrilla verticillata*). Molecular Ecology **13:** 3229-3237

Millar AA, Jacobsen JV, Ross JJ, Helliwell CA, Poole AT, Scofield G, Reid JB, Gubler F (2006) Seed dormancy and ABA metabolism in Arabidopsis and Barley: the role of ABA 8'-hydroxylase. The Plant Journal **45:** 942-954

Misawa N, Masamoto K, Hori T, Ohtani T, Böger P, Sandmann G (1994) Expression of an Erwinia phytoene desaturase gene not only confers multiple resistance to herbicides interfering with carotenoid biosynthesis but also alters xanthophyll metabolism in transgenic plants. The Plant Journal **6:** 481-489

Misawa N, Yamano S, Linden H, de Felipe MR, Lucas M, Ikenaga H, Sandmann G (1993) Functional expression of the *Erwinia uredovora* carotenoid biosynthesis gene crtl in transgenic plants showing an increase of β-carotene biosynthesis activity and resistance to the bleaching herbicide norflurazon. The Plant Journal **4:** 833-840

Moehs CP, Tian L, Osteryoung KW, DellaPenna D (2001) Analysis of carotenoid biosynthetic gene expression during marigold petal development. Plant Molecular Biology **45:** 281-293

Mohamed-Yasseen Y, Barringer S, Splittstoesser W, Costanza S (1994) The role of seed coats in seed viability. The Botanical Review **60:** 426-439

Mozzo M, Passarini F, Bassi R, van Amerongen H, Croce R (2008) Photoprotection in higher plants: The putative quenching site is conserved in all outer light-harvesting complexes of Photosystem II. Biochimica et Biophysica Acta - Bioenergetics **1777:** 1263-1267

Müller-Moulé P, Conklin PL, Niyogi KK (2002) Ascorbate deficiency can limit violaxanthin de-epoxidase activity *in vivo*. Plant Physiology **128:** 970-977

Murphy DJ (2006) The extracellular pollen coat in members of the Brassicaceae: composition, biosynthesis, and functions in pollination. Protoplasma **228:** 31-39

Myouga F, Akiyama K, Motohashi R, Kuromori T, Ito T, Iizumi H, Ryusui R, Sakurai T, Shinozaki K (2010) The chloroplast function database: a large-scale collection of Arabidopsis Ds/Spm- or T-DNA-tagged homozygous lines for nuclear-encoded chloroplast proteins, and their systematic phenotype analysis. The Plant Journal **61:** 529-542

Myśliwa-Kurdziel B, Jemioła-Rzemińska M, Strzałka ETK, Malec P (2012) Variations in xanthophyll composition in etiolated seedlings of *Arabidopsis thaliana* correlate with protochlorophyllide accumulation. Acta Biochimica Polonica **59:** 57-60

Nakazawa M, Ichikawa T, Ishikawa A, Kobayashi H, Tsuhara Y, Kawashima M, Suzuki K, Muto S, Matsui M (2003) Activation tagging, a novel tool to dissect the functions of a gene family. The Plant Journal **34:** 741-750

Niyogi KK, Grossman AR, Bjorkman O (1998) Arabidopsis mutants define a central role for the xanthophyll cycle in the regulation of photosynthetic energy conversion. Plant Cell **10:** 1121-1134

Norris SR, Barrette TR, DellaPenna D (1995) Genetic dissection of carotenoid synthesis in arabidopsis defines plastoquinone as an essential component of phytoene desaturation. Plant Cell **7:** 2139-2149

North HM, Frey A, Boutin J-P, Sotta B, Marion-Poll A (2005) Analysis of xanthophyll cycle gene expression during the adaptation of Arabidopsis to excess light and drought stress: Changes in RNA steady-state levels do not contribute to short-term responses. Plant Science **169:** 115-124

Nowicka B, Strzalka W, Strzalka K (2009) New transgenic line of *Arabidopsis thaliana* with partly disabled zeaxanthin epoxidase activity displays changed carotenoid composition, xanthophyll cycle activity and non-photochemical quenching kinetics. Journal of Plant Physiology **166:** 1045-1056

Oelze M-L, Kandlbinder A, Dietz K-J (2008) Redox regulation and overreduction control in the photosynthesizing cell: Complexity in redox regulatory networks. Biochimica et Biophysica Acta - General Subjects **1780:** 1261-1272

Olson JA (1989) Provitamin A function of carotenoids: the conversion of beta-carotene into vitamin A. The Journal of Nutrition **119:** 105-108

Osorio S, Alba R, Damasceno CMB, Lopez-Casado G, Lohse M, Zanor MI, Tohge T, Usadel B, Rose JKC, Fei Z, Giovannoni JJ, Fernie AR (2011) Systems biology of tomato fruit development: combined transcript, protein, and metabolite analysis of tomato transcription factor (nor, rin) and ethylene receptor (nr) mutants reveals novel regulatory interactions. Plant Physiology **157:** 405-425

Ouyang M, Ma J, Zou M, Guo J, Wang L, Lu C, Zhang L (2010) The photosensitive *phs1* mutant is impaired in the riboflavin biogenesis pathway. Journal of Plant Physiology **167:** 1466-1476

Palsdottir H, Hunte C (2004) Lipids in membrane protein structures. Biochimica et Biophysica Acta - Biomembranes **1666:** 2-18

Peers G, Truong TB, Ostendorf E, Busch A, Elrad D, Grossman AR, Hippler M, Niyogi KK (2009) An ancient light-harvesting protein is critical for the regulation of algal photosynthesis. Nature **462:** 518-521

Perez-Martin J (1999) Chromatin and transcription in *Saccharomyces cerevisiae*. FEMS Microbiology Reviews **23:** 503-523

Pfannschmidt T (2003) Chloroplast redox signals: how photosynthesis controls its own genes. Trends in Plant Science **8:** 33-41

Pfannschmidt T, Allen JF, Oelmüller R (2001) Principles of redox control in photosynthesis gene expression. Physiologia Plantarum **112:** 1-9

Pfannschmidt T, Schutze K, Fey V, Sherameti I, Oelmuller R (2003) Chloroplast redox control of nuclear gene expression: A new class of plastid signals in interorganellar communication. Antioxidants and Redox Signaling **5:** 95-101

Pfannschmidt T, Schütze K, Brost M, Oelmüller R (2001) A novel mechanism of nuclear photosynthesis gene regulation by redox signals from the chloroplast during photosystem stoichiometry adjustment. Journal of Biological Chemistry **276:** 36125-36130

Pogson BJ, Niyogi KK, Bjorkman O, DellaPenna D (1998) Altered xanthophyll compositions adversely affect chlorophyll accumulation and nonphotochemical quenching in Arabidopsis mutants. Proceedings of the National Academy of Sciences of the United States of America **95:** 13324

Qin G, Gu H, Ma L, Peng Y, Deng XW, Chen Z, Qu LJ (2007) Disruption of phytoene desaturase gene results in albino and dwarf phenotypes in Arabidopsis by impairing chlorophyll, carotenoid, and gibberellin biosynthesis. Cell Research **17:** 471-482

Rabbani S, Beyer P, Lintig Jv, Hugueney P, Kleinig H (1998) Induced β-Carotene synthesis driven by triacylglycerol deposition in the unicellular alga *Dunaliella bardawil*. Plant Physiology **116:** 1239-1248

Reinhold C, Niczyporuk S, Beran KC, Jahns P (2008) Short-term down-regulation of zeaxanthin epoxidation in *Arabidopsis thaliana* in response to photo-oxidative stress conditions. Biochimica et Biophysica Acta - Bioenergetics **1777:** 462-469

Rice P, Longden I, Bleasby A (2000) EMBOSS: The European Molecular Biology open software suite. Trends in genetics **16:** 276-277

Riso P, Brusamolino A, Scalfi L, Porrini M (2004) Bioavailability of carotenoids from spinach and tomatoes. Nutrition, Metabolism and Cardiovascular Diseases **14:** 150-156

Roberts AG, Bowman MK, Kramer DM (2004) The inhibitor dbmib provides insight into the functional architecture of the Q_o site in the cytochrome *b6f* complex. Biochemistry **43:** 7707-7716

Robinson S, Tang L, Mooney B, McKay S, Clarke W, Links M, Karcz S, Regan S, Wu Y-Y, Gruber M, Cui D, Yu M, Parkin I (2009) An archived activation tagged population of *Arabidopsis thaliana* to facilitate forward genetics approaches. BMC Plant Biology **9:** 101, doi: 10.1186/1471-2229-9-101

Rodrigo MJ, Zacarias L (2007) Effect of postharvest ethylene treatment on carotenoid accumulation and the expression of carotenoid biosynthetic genes in the flavedo of orange (*Citrus sinensis* L. Osbeck) fruit. Postharvest Biology and Technology **43:** 14-22

Ronen G, Carmel-Goren L, Zamir D, Hirschberg J (2000) An alternative pathway to beta - carotene formation in plant chromoplasts discovered by map-based cloning of Beta and old-gold color mutations in tomato. Proceedings of the National Academy of Sciences of the United States of America **97:** 11102-11107

Ronen G, Cohen M, Zamir D, Hirschberg J (1999) Regulation of carotenoid biosynthesis during tomato fruit development: expression of the gene for lycopene epsilon-cyclase is down-regulated during ripening and is elevated in the mutant Delta. The Plant Journal **17:** 341-351

Rossel JB, Wilson IW, Pogson BJ (2002) Global changes in gene expression in response to high light in Arabidopsis. Plant Physiology **130:** 1109-1120

Rostoks N, Schmierer D, Mudie S, Drader T, Brueggeman R, Caldwell DG, Waugh R, Kleinhofs A (2006) Barley necrotic locus *nec1* encodes the cyclic nucleotide-gated ion channel 4 homologous to the Arabidopsis *HLM1*. Molecular Genetics and Genomics **275:** 159-168

Rowland O, Zheng H, Hepworth SR, Lam P, Jetter R, Kunst L (2006) CER4 encodes an alcohol-forming fatty acyl-coenzyme a reductase involved in cuticular wax production in Arabidopsis. Plant Physiology **142:** 866-877

Ruwe H, Kupsch C, Teubner M, Schmitz-Linneweber C (2011) The RNA-recognition motif in chloroplasts. Journal of Plant Physiology **168:** 1361-1371

Sagar AD, Horwitz BA, Elliott RC, Thompson WF, Briggs WR (1988) Light effects on several chloroplast components in norflurazon-treated pea seedlings. Plant Physiology **88:** 340-347

Sambrook J, Russell DW (2001) Molecular cloning: a laboratory manual, Ed 3rd. Cold Spring Harbor Laboratory Press, Cold Spring Harbor, N.Y.

Sandmann G, Bramley PM, Boeger P (1980) The inhibitory mode of action of the pyridazinone herbicide norflurazon on a cell-free carotenogenic enzyme system. Pesticide Biochemistry and Physiology **14:** 185-191

Schaller S, Latowski D, Jemiola-Rzeminska M, Wilhelm C, Strzalka K, Goss R (2010) The main thylakoid membrane lipid monogalactosyldiacylglycerol (MGDG) promotes the de-epoxidation of violaxanthin associated with the light-harvesting complex of photosystem II. Biochimica et Biophysica Acta - Bioenergetics **1797:** 414-424

Schein AI, Kissinger JC, Ungar LH (2001) Chloroplast transit peptide prediction: a peek inside the black box. Nucleic Acids Research **29:** 82-89

Scholes GD, Fleming GR, Olaya-Castro A, van Grondelle R (2011) Lessons from nature about solar light harvesting. Nature Chemistry **3:** 763-774

Schwertner HA, Biale JB (1973) Lipid composition of plant mitochondria and of chloroplasts. Journal of Lipid Research **14:** 235-242

Shewmaker CK, Sheehy JA, Daley M, Colburn S, Ke DY (1999) Seed-specific overexpression of phytoene synthase: increase in carotenoids and other metabolic effects. The Plant Journal **20:** 401-412

Shimakata T, Stumpf PK (1982) Isolation and function of spinach leaf β-ketoacyl-[acyl-carrier-protein] synthases. Proceedings of the National Academy of Sciences of the United States of America **79:** 5808-5812

Siggaard-Andersen M, Kauppinen S, von Wettstein-Knowles P (1991) Primary structure of a cerulenin-binding beta-ketoacyl-[acyl carrier protein] synthase from barley chloroplasts. Proceedings of the National Academy of Sciences of the United States of America **88:** 4114-4118

Sloan DB, Moran NA (2012) Endosymbiotic bacteria as a source of carotenoids in whiteflies. Biology Letters **8:** 986-989

Steiger S, Schäfer L, Sandmann G (1999) High-light-dependent upregulation of carotenoids and their antioxidative properties in the cyanobacterium *Synechocystis* PCC 6803. Journal of Photochemistry and Photobiology B: Biology **52:** 14-18

Steinbrenner J, Linden H (2001) Regulation of two carotenoid biosynthesis genes coding for phytoene synthase and carotenoid hydroxylase during stress-induced astaxanthin formation in the green alga *Haematococcus pluvialis*. Plant physiology **125:** 810-817

Steinbrenner J, Sandmann G (2006) Transformation of the green alga *Haematococcus pluvialis* with a phytoene desaturase for accelerated astaxanthin biosynthesis. Applied and Environmental Microbiology **72:** 7477-7484

Sun Z, Gantt E, Cunningham FX, Jr. (1996) Cloning and functional analysis of the beta-carotene hydroxylase of *Arabidopsis thaliana*. Journal of Biological Chemistry **271:** 24349-24352

Suzuki Y, Kawazu T, and Koyama H (2004) RNA isolation from siliques, dry seeeds, and other tissues of *Arabidopsis thaliana*. BioTechniques **37 (4):** 542-544

Takayama S, Shiba H, Iwano M, Shimosato H, Che F-S, Kai N, Watanabe M, Suzuki G, Hinata K, Isogai A (2000) The pollen determinant of self-incompatibility in *Brassica campestris*. Proceedings of the National Academy of Sciences of the United States of America **97:** 1920-1925

Tan BC, Schwartz SH, Zeevaart JAD, McCarty DR (1997) Genetic control of abscisic acid biosynthesis in Maize. Proceedings of the National Academy of Sciences of the United States of America **94:** 12235-12240

Tan J, Baisakh N, Oliva N, Parkhi V, Rai M, Torrizo L, Datta K, Datta SK (2005) The screening of rice germplasm, including those transgenic rice lines which accumulate β-

carotene in their polished seeds, for their carotenoid profile. International Journal of Food Science and Technology **40:** 563-569

Tanaka Y, Sasaki N, Ohmiya A (2008) Biosynthesis of plant pigments: Anthocyanins, betalains and carotenoids. Plant Journal **54:** 733-749

Tao N, Hu Z, Liu Q, Xu J, Cheng Y, Guo L, Guo W, Deng X (2007) Expression of phytoene synthase gene is enhanced during fruit ripening of Cara Cara navel orange (*Citrus sinensis* Osbeck). Plant Cell Reports **26:** 837-843

Tian L, Magallanes-Lundback M, V M, DellaPenna D (2003) Functional analysis of β- and ε-Ring carotenoid hydroxylases in Arabidopsis. Plant Cell **15:** 1320-1332

Tian L, Musetti V, Kim J, Magallanes-Lundback M, DellaPenna D (2004) The Arabidopsis *LUT1* locus encodes a member of the cytochrome P450 family that is required for carotenoid {epsilon}-ring hydroxylation activity. Proceedings of the National Academy of Sciences of the United States of America **101:** 402-407

Torada A, Amano Y (2002) Effect of seed coat color on seed dormancy in different environments. Euphytica **126:** 99-105

Torrissen OJ, Naevdal G (1988) Pigmentation of salmonids-Variation in flesh carotenoids of Atlantic salmon. Aquaculture **68:** 305-310

Untergasser A, Cutcutache I, Koressaar T, Ye J, Faircloth BC, Remm M, Rozen SG (2012) Primer3-new capabilities and interfaces. Nucleic Acids Research **40:** 115-120

van't Hof R, Demel RA, Keegstra K, de Kruijff B (1991) Lipid—peptide interactions between fragments of the transit peptide of ribulose-1,5-bisphosphate carboxylase/oxygenase and chloroplast membrane lipids. FEBS Letters **291:** 350-354

Vanin EF (1985) Processed Pseudogenes: Characteristics and Evolution. Annual Review of Genetics **19:** 253-272

Vartak V, Bhargava S (1997) Characterization of a norflurazon-resistant mutant of *Chlamydomonas reinhardtii*. Weed Science **45:** 374-377

Vermel M, Guermann B, Delage L, Grienenberger JM, Maréchal-Drouard L, Gualberto JM (2002) A family of RRM-type RNA-binding proteins specific to plant mitochondria. Proceedings of the National Academy of Sciences of the United States of America **99:** 5866-5871

Vidhyavathi R, Sarada R, Ravishankar GA (2009) Expression of carotenogenic genes and carotenoid production in *Haematococcus pluvialis* under the influence of carotenoid and fatty acid synthesis inhibitors. Enzyme and Microbial Technology **45:** 88-93

Vishnevetsky M, Ovadis M, Vainstein A (1999) Carotenoid sequestration in plants: the role of carotenoid-associated proteins. Trends Plant Science. **4:** 232

von Lintig J, Welsch R, Bonk M, Giuliano G, Batschauer A, Kleinig H (1997) Light-dependent regulation of carotenoid biosynthesis occurs at the level of phytoene synthase expression and is mediated by phytochrome in *Sinapis alba* and *Arabidopsis thaliana* seedlings. The Plant Journal **12:** 625-634

Wackenroder HWF (1831) Ueber die Möhrenwurzel (Rad. *Dauci Carotae* L.); von Prof. Dr. Wackenroder in Jena. (On the carrot root (*Daucus Carota* L.) by Prof. Dr. Wackenroder in Jena.), Vol 1

Wagner T, Windhovel U, Romer S (2002) Transformation of tobacco with a mutated cyanobacterial phytoene desaturase gene confers resistance to bleaching herbicides. Zeitschrift Fur Naturforschung C-a Journal of Biosciences **57:** 671-679

Wei S, Gruber M, Yu B, Gao M-J, Khachatourians G, Hegedus D, Parkin I, Hannoufa A (2012) Arabidopsis mutant sk156 reveals complex regulation of SPL15 in a miR156-controlled gene network. BMC Plant Biology **12:** 169

Wei S, Li X, Gruber MY, Li R, Zhou R, Zebarjadi A, Hannoufa A (2009) RNAi-mediated suppression of DET1 alters the levels of carotenoids and sinapate esters in seeds of *Brassica napus*. Journal of Agricultural and Food Chemistry **57:** 5326-5333

Wei S, Yu B, Gruber MY, Khachatourians GG, Hegedus DD, Hannoufa A (2010) Enhanced seed carotenoid levels and branching in transgenic *Brassica napus* expressing the Arabidopsis *miR156b* gene. Journal of Agricultural and Food Chemistry **58:** 9572-9578

Weigel D, Ahn JH, BlÃ¡zquez MA, Borevitz JO, Christensen SK, Fankhauser C, Ferrnandiz C, Kardailsky I, Malancharuvil EJ, Neff MM, Nguyen JT, Sato S, Wang Z-Y, Xia Y, Dixon RA, Harrison MJ, Lamb CJ, Yanofsky MF, Chory J (2000) Activation tagging in Arabidopsis. Plant physiology **122:** 1003-1014

Welsch R, Beyer P, Hugueney P, Kleinig H, von Lintig J (2000) Regulation and activation of phytoene synthase, a key enzyme in carotenoid biosynthesis, during photomorphogenesis. Planta **211:** 846-854

Welti R, Li W, Li M, Sang Y, Biesiada H, Zhou H-E, Rajashekar CB, Williams TD, Wang X (2002) Profiling membrane lipids in plant stress responses: Role of phospholipase Dα in freezing-induced lipid changes in Arabidopsis. Journal of Biological Chemistry **277:** 31994-32002

Weng H, Pan A, Yang L, Zhang C, Liu Z, Zhang D (2004) Estimating number of transgene copies in transgenic rapeseed by real-time PCR assay with HMG I/Y as an endogenous reference gene. Plant Molecular Biology Reporter **22:** 289-300

Wilkinson RE (1987) Reversal of norflurazon carotenogenesis inhibition by isomers. Pesticide Biochemistry and Physiology **28:** 381-388

Wilkinson RE (1989) EPTC-reversed carotenogenic inhibition by norflurazon. Pesticide Biochemistry and Physiology **33:** 257-263

Wise R (2006) The Diversity of Plastid Form and Function. *In* R Wise, JK Hoober, eds, The Structure and Function of Plastids, Vol 23. Springer Netherlands, pp 3-26

Woitsch S, Romer S (2003) Expression of xanthophyll biosynthetic genes during light-dependent chloroplast differentiation. Plant Physiology **132:** 1508-1517

Wurtzel ET, Luo R, Yatou O (2001) A simple approach to identify the first rice mutants blocked in carotenoid biosynthesis. Journal of Experimental Botany **52:** 161-166

Xiong L, Gong Z, Rock CD, Subramanian S, Guo Y, Xu W, Galbraith D, Zhu JK (2001) Modulation of abscisic acid signal transduction and biosynthesis by an Sm-like protein in Arabidopsis. Developmental Cell **1:** 771-781

Xiong L, Lee H, Ishitani M, Zhu J-K (2002) Regulation of osmotic stress-responsive gene expression by the *LOS6/ABA1* locus in Arabidopsis. Journal of Biological Chemistry **277:** 8588-8596

Xu Y, Skinner DJ, Wu H, Palacios-Rojas N, Araus JL, Yan J, Gao S, Warburton ML, Crouch JH (2009) Advances in Maize genomics and their value for enhancing genetic gains from breeding. International Journal of Plant Genomics **Article ID# 957602:** 1-30

Yaish MW, El-kereamy A, Zhu T, Beatty PH, Good AG, Bi Y-M, Rothstein SJ (2010) The APETALA-2-like transcription factor OsAP2-39 controls key interactions between abscisic acid and gibberellin in Rice. PLoS Genetics **6(9):** e1001098. doi:10.1371 /journal.pgen.1001098

Ye Z-W, Jiang J-G, Wu G-H (2008) Biosynthesis and regulation of carotenoids in Dunaliella: Progresses and prospects. Biotechnology Advances **26:** 352-360

Yohn CB, Cohen A, Danon A, Mayfield SP (1998) A poly(A) binding protein functions in the chloroplast as a message-specific translation factor. Proceedings of the National Academy of Sciences of the United States of America **95:** 2238-2243

Yu B, Gruber M, Khachatourians GG, Hegedus DD, Hannoufa A (2010) Gene expression profiling of developing *Brassica napus* seed in relation to changes in major storage compounds. Plant Science **178:** 381-389

Yu B, Gruber MY, Khachatourians GG, Zhou R, Epp DJ, Hegedus DD, Parkin IAP, Welsch R, Hannoufa A (2012) Arabidopsis cpSRP54 regulates carotenoid accumulation in Arabidopsis and *Brassica napus*. Journal of Experimental Botany **63:** 5189-5202

Yu B, Lydiate DJ, Schafer UA, Hannoufa A (2007) Characterization of a beta-carotene hydroxylase of *Adonis aestivalis* and its expression in *Arabidopsis thaliana*. Planta **226:** 181-192

Yu FEI, Fu A, Aluru M, Park S, Xu Y, Liu H, Liu X, Foudree A, Nambogga M, Rodermel S (2007) Variegation mutants and mechanisms of chloroplast biogenesis. Plant, Cell and Environment **30:** 350-365

Yurina NP, Kloppstech K (2001) Accumulation of plastid protein precursors under norflurazon-induced carotenoid deficiency and oxidative stress in barley. Plant Physiology and Biochemistry **39:** 807-814

Zhekisheva M, Zarka A, Khozin-Goldberg I, Cohen Z, Boussiba S (2005) Inhibition of astaxanthin synthesis under high irradiance does not abolish triacylglycerol accumulation in the green alga *Haematococcus pluvialis* (chlorophyceae). Journal of Phycology **41:** 819-826